Newcastle University

MODELLING OF POLLUTANT ADSORPTION BY ACTIVATED CARBON AND BIOCHAR WITH AND WITHOUT MAGNETITE IMPREGNATION FOR THE TREATMENT OF REFINERY AND OTHER WASTEWATERS

A thesis submitted to Newcastle University in partial fulfilment of the requirement for the degree of Doctor of Philosophy in the Faculty of Science, Agriculture and Engineering

Badruddeen Saulawa SANI

B.Engr, MSc

School of Civil Engineering and Geosciences

Newcastle University, UK

January, 2017

DECLARATION

I declare that this thesis has been composed solely by myself and that it has not been submitted, in whole or in part, in any previous application for a degree. Except where stated otherwise by reference or acknowledgment, the work presented is entirely my own.

Badruddeen Saulawa SANI, January, 2017

ABSTRACT

This study evaluated the application of magnetised powdered activated carbons and biochars, in the removal of typical pollutants encountered in refinery and other wastewaters. Phenol, pharmaceuticals and heavy metals were chosen as representatives of priority pollutants, organic micropollutants and metals.

In the sorption of the organics, there existed a strong correlation (Pearson correlation R up to 0.9990) between isotherm models' capacity parameters and sorbents' capacity influencing properties. In the case of the metals, the sorbents' capacities are not dependent upon surface area and micropore volume. In some instances, the biochars have on the average about 20.45 % higher uptake of the metals than the activated carbons.

A general decrease in phenol uptake on the biochars with increase in pH was recorded, due to electrostatic repulsion between like charged surface and sorbates. For the activated carbons, peak phenol sorption was found within the vicinity of the pKa and point of zero charge when there is maximum electrostatic attraction between the opposite charged surface and sorbates. For the micropollutants, ibuprofen was negatively affected by an increase in pH while diclofenac sorption was not sensitive to changes in pH. Sorption of metals was found to increase with an increase in pH.

Synthetic wastewater (SWW) did not have a significant impact on the sorption of the phenol and heavy metals. In the case of phenol, the highest impact, an average of just 6.15 % for all sorbents was recorded. For the micropollutants, according to the linear model, there is, on the other hand, about 92 and 96 % less uptake of diclofenac and ibuprofen respectively due to competition. Finally, in an equimolar solution, due to its high solubility, Zn^{2+} was outcompeted by Cu^{2+} and Pb^{2+} for binding to available sorption sites.

ACKNOWLEDGEMENTS

In the course of the PhD, I cherish your contributions and suggestions on how best to strategize to win the contest. My soul mates in the battle; Maria Valdivia, Tarric Igun, Aizat Mohd Taib, Kasim Muhammad, Sani Makarfi (RIP), Abdul'azeez Al-Shareedah, Edmond Ndam, George Mangse and Alero Arenyeka

I received terrific companionship whilst I was undertaking the PhD. Hence, I must express my genuine appreciation to those that made me find home away from home here in the UK; Auwal Aliyu, Misbahu Muhammad, Ahmad Adamu, Michael Henderson, Muhammad Alhaji, Abdullahi Bello, Abdul Gambo, Maimuna Saleh, Agatha Okeke, Bashir Abdulkadir, Abubakar Imam, Abubakar Bature, Sadiq Bawa & his family, Salisu Alfa, Mansur Yahaya, Buhari Dahiru, Abdurrazak Lamidi, Abbas Umar, Abdulwasiu (Abu Abdulbasit), Ibrahim Eldidi, Salihu Ayala Portella and the entire members of NMFUK Newcastle Chapter. Thank you for making my stay in Newcastle upon Tyne a memorable one. Equally, I must appreciate those that helped back home, ensuring my interests are protected even while am away, Nuruddeen Yusuf, Umar Shehu and Auwal Kasim and Gaminana Jimoh

To my family –the best ever. I find your unflinching support and encouragement in specific, special, and unique ways valueless and that has kept the hope alive in me. My loving parents Alh Sani and Haj Hadiza B. Saulawa, who started it all and my all siblings; particularly Ihtisham, Fatima, Babangida and Abudurrahman – you have been the strongest fortress one could ever have. Prof Abubakar Ismail, indeed I am grateful for your unwavering assistance. My wife Zainab for your patience, endurance and the time you've diligently devoted in helping me to maintain a fabulous home and for never complaining of my perpetual absence or for the difficulties we've encountered in the course of my programme. To my lovely daughters Rukayya, Maryam and little Asiya for giving me all the reasons to be happy however tough the condition was. I love you all and am truly grateful that you have always been there as strong as ever.

The list of nice people that have helped in providing the conducive environment required to surmount the challenges of a PhD is inexhaustive. I can't mention everyone but I believe you can understand and I'll reiterate that I am deeply glad that your contributions have not gone in vein and indeed none of it will ever be forgotten. WE DID IT!!!

How could I ever appreciate you all with words befitting your contributions. You have time and time again helped in putting me back in one whole, when am shattered in pieces due to the turbulence of life and the overwhelming challenges associated with such a daunting task, studying a PhD. May God Almighty reward you in ways that best befit His generosity and majesty. Thank you all.

TABLE OF CONTENTS

LIST OF FIGURES

LIST OF TABLES

GLOSSARY OF ABBREVIATIONS AND ACRONYMS

AC(s)	Activated carbon(s)
ARE	Average Relative Error
A_S	Surface area
ASE	Average sum of error
BAT	Best Available Technology
BET	Brunauer–Emmett–Teller
BC(s)	Biochar(s)
Bio-1	Woodchip based biochar
BOD	Biochemical oxygen demand
BPT	Best Practicable Technology
ca.	Approximately
CEC(s)	Contaminats or Compounds of Emerging Concern
CoAC	Coconut shell based activated carbon
CoalAC	Coal based activated carbon
COD	Chemical oxygen demand
CoD	Coefficient of determination
DA	Dubinin-Ashtakov model
DOC	Dissolved organic carbon
DOM	Dissolved organic matter
EABS	Sum of absolute errors
EC	European Commission
EPA	Envvironmental Protection Agency, US
ERSSQ	Error Sum of Squares
FREU	Freundlich model
FR_L	Linear transformed Freundlich model
GAC	Granular activated carbon
H+	Hydrogen proton

HPLC	High-Performance Liquid Chromatography
HYBRID	Error function similar to Chi-square
IUPAC	International Union of Pure and Applied Chemistry
LANG	Langmuir model
LANG_L	Linear transformed Langmuir model
LogK$_{OW}$	logarithm of octanol-water partition coefficient
LTFM	Linear transformed model
MAC(s)	Magnetic activated carbon(s)
MBC(s)	Magnetic biochar(s)
MBio-1	Magnetic woodchip based biochar
MBio-1$_{norm}$	Mass normalised magnetic woodchip based biochar
MCoAC	Magnetic coconut shell based activated carbon
MCoAC$_{norm}$	Mass normalised magnetic coconut shell based activated carbon
MCoalAC	Magnetic coal based activated carbon
MCoalAC$_{norm}$	Mass normalised magnetic coal based activated carbon
Me^{2+}	Hypothetical bivalent metal
MOrgBio	Magnetic organic biochar
MOrgBio$_{norm}$	Mass normalised magnetic organic biochar
MPSD	Marquardt's Percentage Standard Deviation
MSC	Model selection criteria
NSAIDs	Nonsteroidal anti-inflammatory drugs
OrgBio	Organic biochar
PAC	Powdered activated carbon
PDM	Polanyi-Dubinin-Manes model
pH$_{PZC}$	Point of net zero charge
pKa	Compound's dissociassion constant
PNP	p-nitrophenol
PTFE	Polytetrafluoroethylene
RED-PET	Redlich-Peterson model
RP_L	Linear transformed Redlich-Peterson model

RIP	Rest in peace
SAW	Salallahu alaihi wasallam
SEM	Scanning electron microscope
SWW	Synthetic wastewater
TSS	Total suspended solids
TDS	Total dissolved salts
UHQ	Ultra High Quality
UPLC	Ultrahigh-Performance Liquid Chromatography
v/v	volumeby volume
V_{MP}	Volume of micropores
V_P	Volume of pores
w/w	weight by weight
WWTP	Wastewater treatment plant
WWTPE	Wastewater treatment plant effluent
XRD	X-ray diffraction

CHAPTER 1.   INTRODUCTION

1.1   HISTORY OF CARBON ADSORPTION AS A WATER TREATMENT PROCESS

The binding forces on the surfaces of solid materials interact in similar yet specific ways with different compounds. This makes it possible for them to preferentially attract and accumulate many compounds from solution onto their surface in what is known as adsorption. There is seemingly an endless array of possible outcomes due to this difference in the level of interaction for any given pair of sorbent and sorbate in a sorption system. The difference in nature of interactions can be controlled to enable the utilisation of adsorption process to serve many specific purposes. This application can be traced almost throughout history, or in the least, carbon adsorption has been in use for centuries before biblical times. The description of carbon adsorption has been found on ancient manuscripts dating 1550 BC. Ancient Hindus were known to have used charcoal to filter their water. However, it was not until in the late 18th century that the phenomenon was first scientifically documented (Dąbrowski, 2001; Hung *et al.*, 2012). The earliest applications of carbon adsorption processes was in the industries, where it has been used for the purification or separation of compounds (Çeçen and Aktas, 2011), as a catalyst or catalyst support (Dąbrowski, 2001). The application of carbon adsorption has ever since been utilised to serve the separation of solutes from solutions and as a result, many purification purposes were made possible. With the advent of more stringent environmental regulations since the early '70s, the interest in carbon adsorption has received genuine attention for application in pollution prevention and control (Cheremisinoff, 2002; Çeçen and Aktas, 2011).

To date, carbon adsorption has remained a reliable technological option; in the treatment of potable water and wastewaters to meet regulatory requirements, in environmental pollution clean-ups and in amendment of contaminated soils and sediments. In the agricultural fields, it has been found that when added to soils, charcoal (or biochar) whose main composition is carbon, helps to maintain or enhance soil fertility (Chan *et al.*, 2007; Atkinson *et al.*, 2010; Agegnehu *et al.*, 2015), facilitate root development, improve soil moisture retention potentials

(Jones *et al.*, 2012), prevent the leaching of nutrients and contaminants from the soil (Xu *et al.*, 2012), reduces the dissipation of herbicides and the emission of greenhouse gasses from the soil (Spokas *et al.*, 2009).

1.2 DEFINITION OF TERMS

1.2.1 CHARCOAL, BIOCHAR OR ACTIVATED CARBON?

These terms are sometimes used interchangeably (Lehmann and Joseph, 2009; Spokas and Reicosky, 2009), because the materials they refer to are much related. Therefore, for the purpose of this work, there is a need to establish proper definitions for the two types of carbon sorbents used in this research; i.e. activated carbon and biochar to avoid ambiguity.

To begin with, any organic material that is subjected to incomplete combustion in an oxygen deficient condition will produce a solid charred material that is composed mostly of carbon. Charcoal, biochar and activated carbon are all related in this way. What differentiate them is the processes that they are made to undergo before obtaining the final product and the purpose it is meant to serve (Lehmann and Joseph, 2009). With this in mind, the following applies;

Charcoal: Is obtained when for all purpose and intent, organic biomass material is charred to obtain a carbon rich material that is to be used as a fuel.

Biochar: Is obtained when for all purpose and intent, modern (i.e. non-fossil) organic biomass material is charred to obtain a carbon rich material that is to be used for pollutants removal or carbon sequestration or conditioning of soil.

Activated carbon: Is obtained when carbon rich material obtained from the charring of organic biomass is subjected to further chemical and/or heat treatment or processes by which its surface area and pore structure is amplified. It is mainly used for water and wastewater treatment, environmental pollution control and purification of industrial products.

1.2.2 SORPTION, SORBATE AND SORBENT,

Sorption (also termed adsorption) is a phenomenon by which a sorbate (the solute in a solution) is transferred from an aqueous or gaseous phase to attach and accumulate onto a sorbent (solid body or solid phase).

The constituent that undergoes adsorption onto a surface is called the adsorbate, and the solid onto which the constituent is adsorbed is called the adsorbent.

1.3 PRACTICAL USE OF ACTIVATED CARBON IN WASTEWATER TREATMENT.

Activated carbon adsorption is used in wastewater treatment usually as a polishing stage to achieve higher effluent qualities (Bush, 1980; Ranade and Bhandari, 2014). A typical arrangement for industrial wastewater treatment is shown in Figure 1.1. The effectiveness of the adsorption process can be impaired in the presence of competing materials i.e. suspended and dissolved matter (Ratnayaka *et al.*, 2009; Chowdhury *et al.*, 2013). Therefore, to maximise the efficacy of this process, it is usually employed at the tail end of the treatment train i.e after clarification and/or filtration, just before the final disposal of the treated wastewater (IPIECA, 2010; Çeçen and Aktas, 2011). The two most common forms of activated carbon used in wastewater treatment are the granular activated carbon (GAC) and powdered activated carbon (PAC).
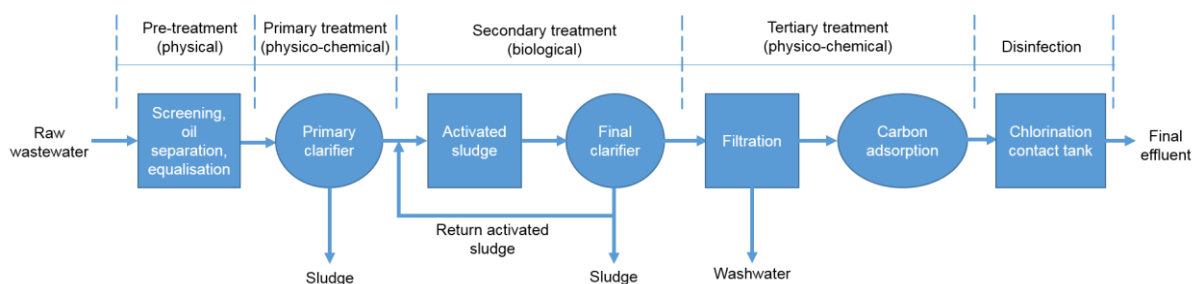
Figure 1.1:   Typical flow diagram for wastewater treatment system. Adapted from (Sundstrom and Klei, 1979; Metcalf et al., 1991)

1.3.1 GAC BED

GAC is normally contacted with wastewater in the form of filtration type fixed bed arrangement, whereby the wastewater to be treated flows through the GAC

bed (Chowdhury *et al.*, 2013). As the wastewater flows through the carbon bed, contaminants are removed by adsorption within the mass transfer zone. With time the MTZ is saturated and it continually moves downward through the column until breakthrough is attained i.e. when a predetermined concentration of contaminants is detected in the effluent. The bed is then exhausted and the carbon is removed for regeneration and is replaced with fresh or reactivated GAC (Çeçen and Aktas, 2011).
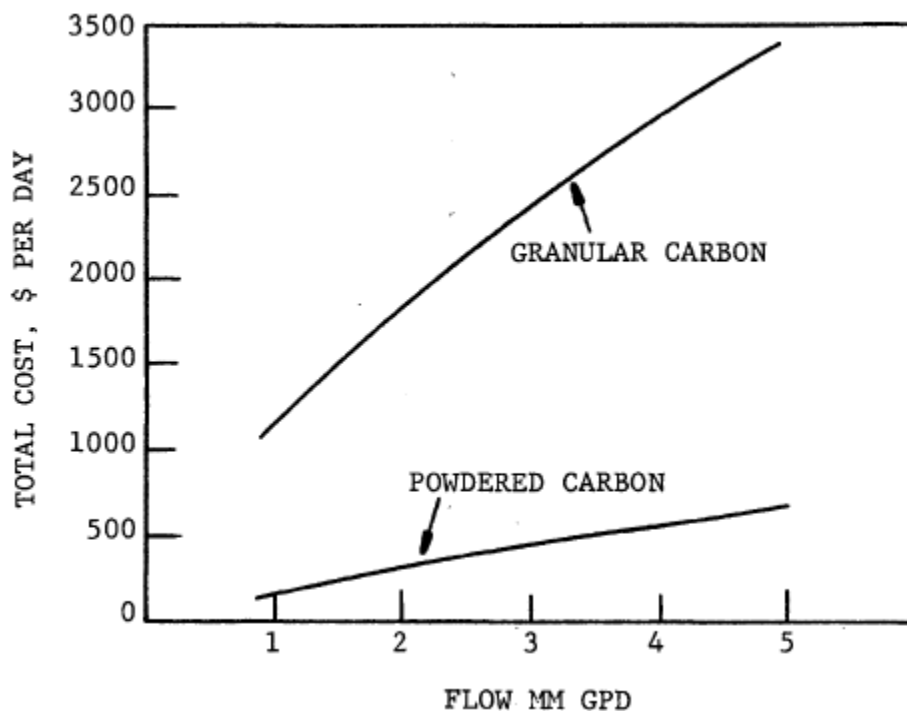
Figure 1.2:   Comparison of estimated carbon costs: Source (EPA, 1979)

1.3.2 PAC

PAC is usually contacted with the wastewater in the form of slurry to adsorb contaminants and is removed with other particles in solid management (Ratnayaka *et al.*, 2009). Its low capital cost together with the ability to apply PAC seasonally to address periodic spikes in target contaminants gives it an inherent advantage. However, the regeneration of PAC is rather difficult because it cannot be separated easily from treated wastewater (Newcombe, 2008; Chowdhury *et al.*, 2013).

1.3.3 SEPARATION OF PAC

The particles of PAC are too fine to settle by gravity within the practicable treatment detention times that are normally adopted. They are usually removed through coagulation/flocculation or membrane filtration. Alternatively, magnetised form of PAC can be used and easily separated using principles of magnetism. Numerous studies have proven the efficacy of using magnetic materials in the adsorption of different pollutants from water and wastewaters (Bitton *et al.*, 1976; Bolto, 1990; Šafařík *et al.*, 1997; Hu *et al.*, 2005; Girginova *et al.*, 2010; Fan *et al.*, 2012). These magnetic materials have been reported to be separated from the treatment medium using magnetic attraction to a permanent magnet or induced magnetic field (van Velsen *et al.*, 1991; Mikhailovsky and Radovenchik, 1996)
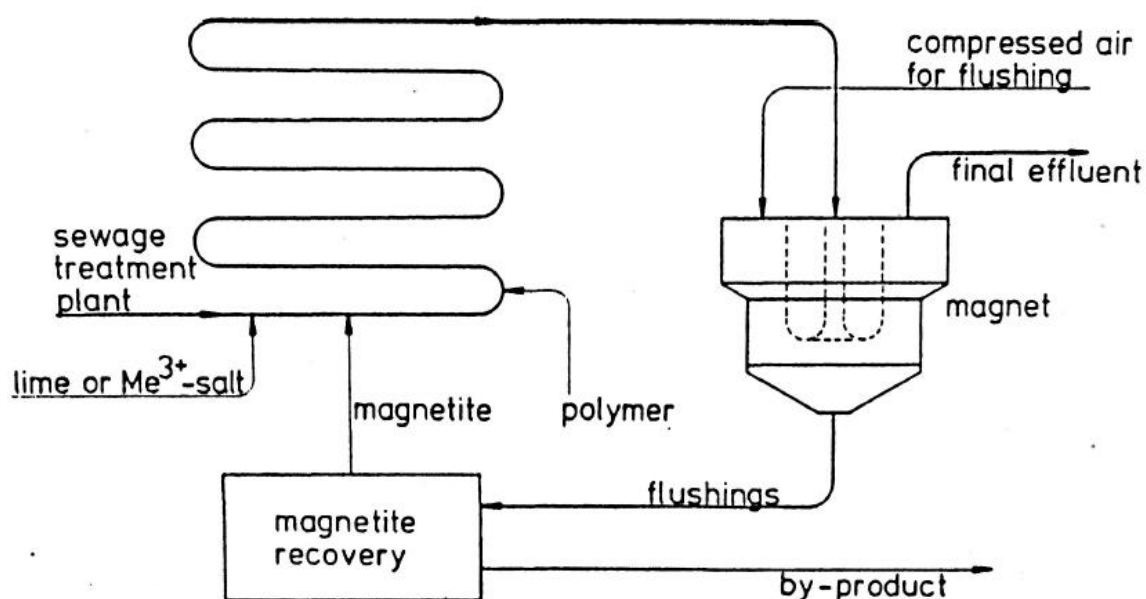
Figure 1.3: Schematic diagram of high gradient magnetic separation technique. Adopted form (van Velsen *et al.*, 1991)

The magnetite materials can be separated from the treatment medium using magnetic drum separator, cleaned by means of shear forces generated e.g. by ultrasonic agitation and regenerated using appropriate solvents. The magnetic separation procedure has been used successfully in the separation of magnetic materials that are used for the treatment of water and wastewater at industrial scale (Sundstrom and Klei, 1979; Booker *et al.*, 1991; van Velsen *et al.*, 1991;

Carlos *et al.*, 2013). The schematic diagram of one such system is shown in Figure 1.3

1.4   REFINERY WASTEWATER

Each refinery is uniquely configured, depending on the type of crude refined and desired products. Generally refineries consume large quantities of water and as a result they generate high volumes of wastewater. Different units within the refinery generate different volumes of wastewater with varying degree of contamination (Al-Zarooni and Elshorbagy, 2006; Coelho *et al.*, 2006; Diya'uddeen *et al.*, 2011). Typical composition of effluents from some units of the refinery are shown in Table 1.1. Refinery wastewater usually includes cooling tower blowdown, boiler blowdown, oily process water, stripper effluent, residential sewage and contaminated runoff. Water that has not been in contact with hydrocarbons may require no treatment and can be discharged, recycled or reused within the refinery to minimise water consumption. Otherwise, highly contaminated water require comprehensive treatment before being released to the environment (IPIECA, 2010).

Table 1.1:   Typical concentrations of pollutants found in effluents of some refinery units (IPIECA, 2010)

Contaminant	Desalter	Stripped sour water	Crude tank bottom sediment
COD (mg/L)	400 to 1000	600 to 1200	400 to 1000
Free hydrocarbons, (mg/L)	Up to 1000	< 10	Up to 1000
Suspended solids, (mg/L)	Up to 500	< 10	Up to 500
Phenol, (mg/L)	10 to 100	Up to 200	
Benzene, (mg/L)	5 to 15	0	
Sulphides, (mg/L)	Up to 100	< 10	Up to 100
Ammonia, (mg/L)	Up to 100	< 100	

In general, wastewater from refineries is composed of wide variety of contaminants that includes; hydrocarbons, dissolved and suspended solids, organics, inorganics and bacteria (Hale *et al.*, 1979; WORLD BANK GROUP, 1998; Lahcen and Jean-Luc, 2011). Therefore except for slight modifications of the pre-treatment stage, refinery effluents are treated by similar processes used in the treatment of conventional domestic sewage and industrial wastewaters. Consequently, a refinery wastewater treatment plant is also comprised of

preliminary, primary, secondary and tertiary treatment stages (as shown in Figure 1.1). Ultimately, carbon adsorption has been used effectively as a tertiary treatment to remove residual organics after the wastewater has received secondary treatment processes (Bush, 1980; IPIECA, 2010).

1.5 STATEMENT OF PROBLEM AND JUSTIFICATION OF STUDY

Numerous studies have been conducted in the area of wastewater treatment using carbon adsorption. Notwithstanding, the basic principles behind this process is still not completely understood. This study is conceived in this light, with the hope of providing additional understanding of the application of adsorption process in wastewater treatment. Especially after advancements in analytical technologies made it possible to discover more pollutants that are difficult to treat using conventional methods. This brings about an urgent need for the redesigning and upgrading of existing water and wastewater treatment plants to achieve removal levels required with respect to pollutants that have hitherto remained recalcitrant to existing treatment technologies. This calls for researches to be conducted at fundamental levels so as to have a better understanding of processes involved in the removal of these pollutants. Those processes that are found to be ineffective can be evaluated to further understand their shortcomings and possibly proffer solutions as to how they can be modified to make them effective. Other processes that appear to be effective need also to be studied, to have an in-depth understanding of the principles that make them work in order to make them even more efficient. The need to be innovative in attending to the needs of environmental pollution and control is too conspicuous to be ignored.

The following problems have been identified to be the focus of this study and they are discussed in more detail in chapter 2.

1. Proliferation of pollutants that could escape conventional, biological processes. Adsorption has been shown to be a reliable wastewater polishing process that can handle the removal of these pollutants.

2. Understand and improving upon the limitation of adsorption process to increase its acceptability as a reliable treatment option; this is to address difficulties such as

i.   Separation of the adsorbent in its most effective, fine particulate form, from treatment medium

ii.   Custom made process to attend to different types of pollutants

iii.   Unknown sorption outcomes especially for magnetised sorbents.

3.   Possibility of arriving at wrong judgements due to application of linear model fitting methods in the analysis of sorption data during mathematical modelling.

1.6   RESEARCH QUESTIONS

1.   How does magnetisation affect the physicochemical properties of activated carbons (ACs) and biochars (BCs)?

2.   What is the effect of magnetisation on the sorption of organic contaminants and heavy metals by activated carbons and biochars?

3.   What sorption mechanisms are relevant for the binding of different types of pollutants by the magnetic activated carbons and biochars?

4.   How do solution properties such as pH or dissolved organic carbon contents influence the sorption of organic contaminant and heavy metals on magnetic activated carbons (MACs) and biochars (MBCs), and how does the influence compare to that on nonmagnetic sorbent?

1.7   HYPOTHESES

1.   The presence of precipitated magnetic iron oxides on the surface of the magnetised ACs and BCs, will reduce their surface area and porosity. Magnetisation will also alter other surface properties of the sorbents.

2.   Due to the decrease in surface area and porosity, the sorption capacities of the magnetised sorbents will be lower than those of their corresponding pristine pairs. Therefore, the magnetised sorbents will have reduced removal of organic contaminants and heavy metals from wastewater.

3.   The magnetic sorbents will have different sorption mechanisms from their nonmagnetic pairs. Thus they will differ in terms of their sorption kinetics and responses to pH changes.

4. The influence of competing compounds on the sorption of organic contaminants and heavy metals on magnetic and nonmagnetic sorbents will be comparable.

1.8   AIMS AND OBJECTIVES

The aim of this research is to study the effect of magnetisation on the sorption properties of activated carbon and biochar in the sorption of typical organic pollutants and heavy metals from aqueous solutions using batch experiments in an attempt to have a better understanding of the possible application of magnetic activated carbon and magnetic biochars in the treatment of refinery and other wastewaters.

The objectives of the research are as follows;

1. To produce magnetic activated carbon and magnetic biochar using a wet co-precipitation method.
2. To assess the effect of magnetisation on the sorption characteristics of MACs and MBCs in the sorption of typical organic contaminants and heavy metals from aqueous solutions using batch methods. This will be achieved using mathematical models to evaluate the following;
   i.   Sorption isotherms,
   ii.   Sorption capacities,
   iii. Nature of surface coverage of sorbate on sorbent,
   iv.   Sorption kinetics,
   v.   Sorption energies.
3. To compare the quality of results obtained from the modelling of experimental data using linear and nonlinear fitting methods.
4. To evaluate the effect of external factors such as pH, temperature and presence of competitors in the sorption of the selected pollutants on MAC and MBC.

1.9   SCOPE AND LIMITATION

It is not the interest of the work to produce any carbonaceous sorbent from feedstock materials. All sorbents will be used as obtained from suppliers except for their being modified to have magnetic properties. The data on the sorbents'

characterisation was obtained as part of a research collaboration with a second party (Dr Zhantao Han). Therefore, the procedures to measure these properties are not presented in this study.

Real wastewater from refineries could not be sourced for use in this study. However, wastewaters generally consist of similar types of contaminants which include, dissolved and suspended solids, organic and inorganic compounds and microorganisms. Furthermore, it is practically impossible to examine all types of compounds present in such wastewaters. Therefore this study focused on typical compounds found in refineries, industrial and domestic sewage. To measure the effect of competition from other adsorbable compounds other than the target pollutants, the study was conducted using $CaCl_2$, synthetic wastewater and domestic wastewater as background solutions.

1.10 THESIS STRUCTURE

Chapter 1: General introduction and background

This chapter is intended to give a brief overview of the study, why it is conducted, what it hopes to achieve, the area it covers and the format by which it is presented.

Chapter 2: Literature review

This chapter gives an overview of research activities conducted that are both specifically and generally related to the scope of this research. This is to have a better understanding of the research topic so as to help in developing appropriate concepts and procedures that can be adopted towards attaining the objectives of the study.

Chapter 3: Materials and methods

This chapter presents the sorbents and sorbates used in this study and why they are chosen. It also discusses about the methods adopted in the analysis of experimental data.

Chapter 4: Adsorption of phenol

This chapter forms the baseline study of the research. Phenol is used as the probe pollutant to derive preliminary insights into the sorption potentials of the

selected sorbents. Results from this chapter are used to develop the procedures that are used in the proceeding chapters.

Chapter 5:   Adsorption of pharmaceuticals.

Micropollutants are especially more difficult to treat than heavier organic pollutants using carbon adsorption. This chapter is intended to consolidate the findings of the previous chapter as regards the sorption of organic pollutants.

Chapter 6:   Adsorption of heavy metals

This chapter evaluated the sorption of heavy metals on the sorbents to enable the coverage of an additional category of pollutants whose sorption characteristics differ from those of organic pollutants.

Chapter 7:   Summary and conclusion

This chapter gives a summarised discussion of the findings obtained in the preceding three chapters and suggestion for future work.

CHAPTER 2.   LITERATURE REVIEW

2.1   POLLUTANTS FROM WASTEWATER

The world is witnessing a continuous trend of population increase which results in a similar trend in the need for constant exploration, exploitation and procession of all manners of resources in large quantities (Kundzewicz, 2007). At the background of all these activities is a constant demand for energy and water. These trends are presented in Figure 2.1.
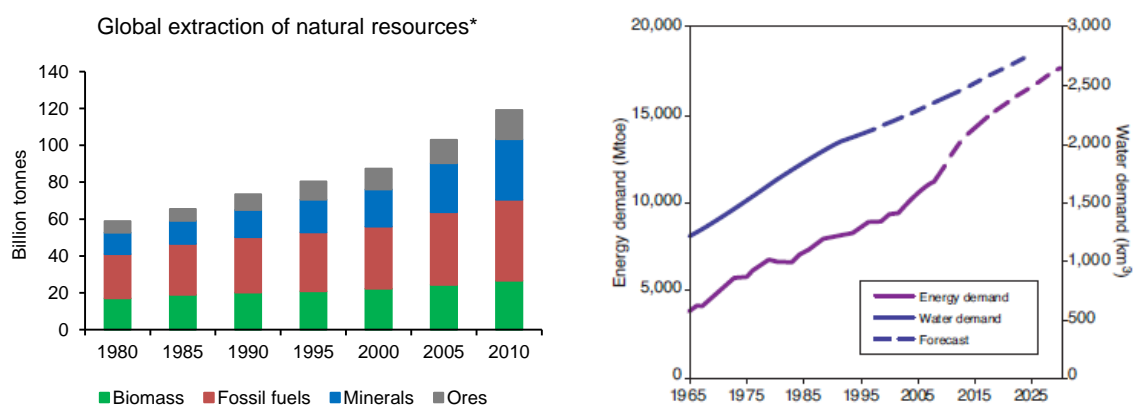
Figure 2.1:   Global extraction of natural resources, (Nabzar, 2011; *SERI and WU Vienna database: Visualising Global Material Flows*, 2014)

The nature of utilisation or consumption of these resources differs but they contribute in the release of parent pollutants and their by-products to the environment through countless pathways. For instance, crude oil refining requires significant amounts of energy and large volumes of water. It has been estimated that on the average, at global level, to produce a litre of oil, 3 – 5 litres of wastewater is generated (Nabzar, 2011). Wastewater from refineries is associated with biochemical oxygen demand (BOD) and chemical oxygen demand (COD) levels of approximately 150–250 milligrams per litre (mg/L) and 300–600 mg/L, respectively; it may also contain, bacteria, suspended particles (TSS), dissolved salts (TDS), phenol levels of 20–200 mg/L; oil levels of 100–300 mg/L in desalter water and up to 5,000 mg/L in tank bottoms; benzene levels of 1–100 mg/L; benzo(a)pyrene levels of less than 1 to 100 mg/L; heavy metals levels of 0.1–100 mg/L for chrome and 0.2–10 mg/L for lead; and other pollutants including radioactive metals, dissolved organic products especially hydrocarbons

such as toluene, ethylbenzene, xylene polycyclic aromatic hydrocarbons, and naphthalenes (Hale *et al.*, 1979; WORLD BANK GROUP, 1998; Lahcen and Jean-Luc, 2011). Some of these compounds are toxic, recalcitrant to degradation and capable of bioaccumulation when they enter the food chain, posing serious threat to the ecosystem and human health (Onwumere and Oladimeji, 1990; Sandrin and Maier, 2003; Chuah *et al.*, 2005; Marrot *et al.*, 2006; Indu *et al.*, 2008; Song *et al.*, 2012). Furthermore, they are less likely to be removed completely by conventional biologic treatment units. Phenol in particular, has been reported to be observed in concentrations higher than permissible levels even after biological treatment (Al-Zarooni and Elshorbagy, 2006; Otokunefor and Obiukwu, 2005). The human history, since the ancient times has been littered with incidences of environmental pollution resulting in adverse effects on human health and fatal consequences on the ecosystems sometimes leading to loss of biodiversity (Nriagu, 1988; Nriagu, 1996; Makra and Brimblecombe, 2004).

2.1.1 PRIORITY POLLUTANTS

The priority pollutants are listed in regulations such as section 307(a)(1) of the Clean Water Act 1977 (EPA, 2002) and Article 16(2) of Directive 2000/60/EC (European Commission, 2000). The inclusion of a substance on this list requires it to pose a threat to human health or to the aquatic environment. This can be through acute or chronic toxicity to receptor organism, accumulation in the ecosystem and losses to habitats and biodiversity. Accordingly, guidelines and standards have been developed that will enable adequate monitoring to ensure their production and utilisation conform to approved best practices and available technology. It is necessary that these pollutants conveyed in wastewaters are not released at levels that could harm or pose a threat to the environment. For instance, in compliance to the European Union recommendation, the limits for phenol have been set as follows; in potable and mineral waters it is 0.5 µg/l, while the limits for wastewater emissions are 0.5 mg/l, for surface waters and 1 mg/l for the sewerage system (Busca *et al.*, 2008). In Germany, a phenol index of ≤ 0.15 mg/L has been set for wastewater before mixture with other waste water for the production of hydrocarbons and oil processing. In the UK, a non-statutory environmental quality standard recommends 300 µg/L as maximum allowable phenol concentration (JRC, 2006). Also, the annual mean concentration set

environmental quality standards limits of 10 µg/L for copper and lead, and 75 µg/L for zinc in England and Wales (Gray, 2004). In the US, EPA regulation "40 CFR Part 419" has set effluent limits for various industries. According to the "best practicable control technology currently available (BPT)" criteria, the maximum effluent limit for phenolic compounds for any one day from any category of point sources discharge from petroleum refining ranges between 0.168 to 0.40 kg/1000 m^3 of feedstock (EPA, 2013). Likewise, EPA regulation "40 CFR Part 439" has set the maximum daily limit for effluents COD from different categories of point sources in pharmaceutical industries at 228 to 1675 mg/L. While phenol has been set at 0.05 mg/L according to the "best available technology economically achievable (BAT)" criteria (EPA, 2015). The list of EPA regulations for various industries can be found in (Federation, 2008). Depending on the processes involved, wastewater treatment offers reliable effluent qualities within approved guidelines. Conventional wastewater treatment plants do not always provide 100 % removal of these pollutants (Sonune and Ghate, 2004). For instance, it has been reported that phenol contents of effluents of biological wastewater purification plants can be as high as 48 mg/L (JRC, 2006).

Since the industrial revolution, the mining and smelting, transportation, electroplating and petroleum refining industries continue to be the main sources from which heavy metals are released into the environment (Mohammed *et al.*, 2011). Furthermore, heavy metals are not degraded and sometimes even toxic to microorganisms in biological wastewater treatment process (Ochoa-Herrera *et al.*, 2011). Consequently, they have become persistent and widespread in the environment at levels that have since raised concerns. Exposure to some of these metals -even at trace levels- are reported to have an adverse effect on the human health or the environment. For instance, kidney damage and renal failure may be due to exposure to cadmium (Järup *et al.*, 2000; Mohammed *et al.*, 2011), copper has been associated with Wilson disease (Bull *et al.*, 1993; Thomas *et al.*, 1995), exposure to lead can cause damage to the brain, kidney and central nervous system, (Lanphear *et al.*, 2005; Tchounwou *et al.*, 2012), and zinc has been implicated in the pathogenesis and progression of prostate malignancy (Plum *et al.*, 2010). Already measures have been taken to minimise the release of heavy metals and so far, their levels have been on the decline, especially in developed countries (Järup, 2003). Nevertheless, they are still encountered in aquatic and

soil environments that are used in the disposal of industrial and domestic wastewaters (Audry *et al.*, 2004). Treatment of wastewaters has for long been a reliable means by which the proliferation of heavy metals in the environment is controlled. The removal of heavy metals from wastewater can be achieved by many processes that include; ion exchange, chemical precipitation, membrane filtration and adsorption (Srivastava and Majumder, 2008). Of these processes, adsorption by carbon has been found to be one of the most reliable, due to the following reasons; its low energy requirement and as a result lower operational cost, abundance of raw materials for the production of the sorbents, ability to regenerate spent carbon and recover metals for reuse and the absence of otherwise highly contaminated sludge which is difficult and expensive to handle and dispose of.

2.1.2 POLLUTANTS OF EMERGING CONCERNS

While the focus of environmental regulation has so far been mainly on priority pollutants, there exist also in the background an ever increasing hazard posed by yet to be prioritised compounds. Also known as compounds or contaminants of emerging concern (CECs), their occurrence in the environment is drawing increasing attention (Luo *et al.*, 2014). These CECs can be broadly classified into six categories as; pharmaceuticals, personal care products, hormones, steroids, industrial chemicals, surfactants and pesticides (Daughton and Ternes, 1999; Çeçen and Aktas, 2011). These group of emerging pollutants potentially pose at least an equivalent impact to the environment in the long run as do the priority pollutants (Rivera-Utrilla *et al.*, 2013). These anthropogenic compounds follow many pathways to enter the environment including, the discharge of improperly treated industrial and domestic wastewater, improper disposal of unused drugs and daily usages of personal care products (Boxall, 2004). In the case of administered drugs, some fraction is excreted as unmetabolised parent compound or as active metabolites (Zuccato *et al.*, 2000; Schwaiger *et al.*, 2004). These compounds find their way to the wastewater treatment plant where their removal varies depending on the treatment process involved (Stumpf *et al.*, 1999; Ellis, 2006; Rivera-Utrilla *et al.*, 2013). In some instances, they are released into receiving water because conventional treatment plants are not designed to eliminate most of these compounds from wastewater

(Lindqvist *et al.*, 2005; Nakada *et al.*, 2006; Cabrita *et al.*, 2010; Sotelo *et al.*, 2013; Mailler *et al.*, 2016). Another way by which these compounds are released into the environment is through the use of; excreta from farm animals, improperly treated biosolids and wastewater for agricultural purposes (Boxall, 2004). Recent advancements in analytical methods have made the detection of numerous of these compounds possible even when at low levels in the environment. Therefore, a large number of them are detected in trace levels in receiving water bodies (Ahrer *et al.*, 2001; Blair *et al.*, 2013). This has as a result brought to lime light the existence of an additional frontier of environmental pollution which hitherto has gone undetected (Daughton and Ternes, 1999). Consequently, a lot of these compounds are yet to be regulated or at best are undergoing regulatory processes. Individually, they may not pose serious ecological hazard at the trace concentration levels they are detected. However, a cocktail of these compounds could have inductive or synergetic effects that may pose serious threat to the aquatic organisms (Hernando *et al.*, 2006). Furthermore, these compounds are pseudo persistent due to their continuous discharge. There is thus the uncertainty of their effect due to long term exposure on aquatic organism, especially over many generations (Ferrari *et al.*, 2003).

Hazardous compounds such as pesticides, pharmaceuticals, polychlorinated biphenyls, flame retardants, dioxins and many others can contaminate the soil matrix (Kinney *et al.*, 2006; Elskens *et al.*, 2013; Fairbairn *et al.*, 2015) thereby making it a long-lasting source of many of these chemicals. Especially persistent compounds have become ubiquitous in soil because they are resistant to biological and chemical degradation (Sotelo *et al.*, 2013). Studies have found that the use of reclaimed water can cause the accumulation of pharmaceuticals in the soil, with the potentials of leaching into deeper soil layers (Kinney *et al.*, 2006; Li *et al.*, 2013). Some of these contaminants remain bio-available, and lipophile, persistent compounds may bio-accumulate and bio-magnify to concentrations that can cause harmful effects along the food chain (Eichbaum *et al.*, 2014).

2.2 WASTEWATER TREATMENT

To make it less harmful to the environment, numerous treatment processes are employed to treat wastewater, usually in combination to have final

effluent with pollutants' concentration below threshold levels that poses hazard to the environment. Treatment processes of choice include, oxidation ponds, activated sludge, trickling filters, rotating biological contactors, ion exchange, carbon adsorption and reverse osmosis (Escwa, 2010; Ramalho, 2012). Hardly is any one process adequate in meeting this requirement and more so, each treatment process has its peculiarity (Belhateche, 1995). Hence the selection of a treatment process is influenced by many factors such as efficiency in the removal of target pollutants, cost, flexibility in terms of its integration with other processes, adaptability in terms of land and climatic constraints, and importantly in the final fate of the treated pollutants (Metcalf & Eddy Inc *et al.*, 2003; Muga and Mihelcic, 2008). Most processes produce substantial volumes of sludge that is usually heavily contaminated and requires special handling and perhaps further treatment before its disposal (Stover *et al.*, 1976; Kelessidis and Stasinakis, 2012). Not only emerging pollutants, but also relatively recalcitrant, water-soluble compounds such as phenols, or heavy metals are not just resistant to conventional treatment processes but also toxic (Çeçen and Aktas, 2011). Thus they can have an adverse effect on microorganisms that are responsible for biological processes. This leads to the release of partially treated wastewater leading to the accumulation of toxic pollutants in receiving waters. Some processes have been rated high in the treatment of these and other pollutants based on reduction in the concentration of target compounds (Mailler *et al.*, 2016). This may be misleading because, in some cases the reduction in concentration of a target pollutant simply result from decrease in the concentration of the parent compound when in reality it is simply transformed to a substituted compound at the background continuing to pose a similar degree of hazard (Luo *et al.*, 2014). Carbon adsorption has received wide acceptability as a process that can eliminate these compounds from wastewater (Jusoh *et al.*, 2007; Schneider *et al.*, 2007; Piero, 2009b; Aghav *et al.*, 2011; Figueiredo *et al.*, 2011; Zhuang *et al.*, 2011). Furthermore, adsorption process does not result in the production of by-products of pollutants which pose perhaps at least an equal environmental hazard as does the parent compound (Rivera-Utrilla *et al.*, 2013). Finally, since adsorption utilizes a completely different mechanism than conventional, biological wastewater treatment, it may be ideally suited for the polishing of effluents from biological wastewater treatment plants.

2.3 APPLICATION OF ADSORPTION IN ENVIRONMENTAL POLLUTION AND CONTROL

Over many years, adsorption processes using activated carbon or biochars have demonstrated promising outcomes in the removal of such contaminants from wastewater and, more recently as amendments of such contaminated soils and sediments to minimize the transfer of pollutant into the aquatic or terrestrial food chains (Pelekani and Snoeyink, 2000; Le Cloirec and Faur-Brasquet, 2008; Yu *et al.*, 2009; Cabrita *et al.*, 2010; Ghosh *et al.*, 2011; Han *et al.*, 2013a).

2.3.1 REMOVAL FROM AQUEOUS SOLUTIONS

The application of as little as 10 to 20 mg/L of PAC resulted in the removal of a wide range of micropollutants by over 80% from wastewater in a large scale pilot treatment plant (Margot *et al.*, 2013). PAC adsorption is flexible and can be conveniently used in conjunction with other treatment processes. Combined use of PAC with the coagulation process facilitated the removal of micropollutants from wastewater treatment plant effluent by up to > 90%, especially after sufficient contact time (Altmann *et al.*, 2015). A study by Secondes *et al.* (2014), used a hybrid process that involves a combination of membrane ultrafiltration, activated carbon adsorption and ultrasound irradiation. This hybrid process was able to achieve well above 99% removal of emerging contaminants (ECs) with adsorption being the main removal mechanism. In another work, Mailler *et al.* (2015), studied a pilot scale use of fluidised PAC at a dosage of 10 mg/L, as a tertiary treatment process. The process was observed to have resulted in an average removal of 72 – 80% of total of wide range of emerging and priority micropollutants from wastewater treatment plant effluents.

2.3.2 SOIL AMENDMENT

For the in-situ use of sorbents, it has been reported (Cho *et al.*, 2012), that the uptake of polychlorinated biphenyls (PCBs) by passive samplers in sediments amended with just 3.7 dry wt% activated carbon dose was decreased by up to 73% over a period of 5 years. Wang *et al.* (2012), have demonstrated that, amendment of agricultural soils with biochar enhances and also dominates the

sorption of pesticides, such that, a remarkable reduction in the uptake of pesticide by earthworms was observed. In another study by Yu *et al.* (2009), the amendment of soil with just 1% by weight of biochar was observed to be capable of sequestering pesticide residue and as a result, a remarkable reduction in its uptake by plants was recorded. These and similar studies have further demonstrated the ability of biochar amendment in the immobilisation of contaminants in the soils and sediments. It has however been reported (Zhang *et al.*, 2010a) that the effect of ageing can cause a substantial decrease in the sorption ability of the biochar. This decrease is influenced by competition with other compounds, especially soil dissolved organic matter, for the available sorption sites (Yang and Sheng, 2003). Therefore, it is theoretically possible that with time, the added biochar becomes less effective in providing continuous protection against possible future recontaminations.

2.4   WASTEWATER TREATMENT BY ADSORPTION

Of the treatment processes, carbon adsorption appears to be promising in the removal of otherwise difficult to treat pollutants (Ahmaruzzaman and Sharma, 2005; Schneider *et al.*, 2007; Cabrita *et al.*, 2010; El-Naas *et al.*, 2010). Although wastewater treatment by activated carbon adsorption has been extensively studied over the years, the need to have a better understanding of its application on the removal of micropollutants cannot be ignored (Ebie *et al.*, 2001; Yu *et al.*, 2008). Especially within conditions that closely resemble real scenarios under which it will eventually be applied. For instance, in batch treatment process, the smaller the size of the sorbent, the better the kinetics and the shorter the time required for treatment objective to be met (Jain *et al.*, 2003; Özacar and Şengil, 2003; Roostaei and Tezel, 2004). However, in real scenario, there is always the need for powdered activated carbon (PAC) to be separated from the wastewater stream before discharge, ideally for reuse in another batch, for regeneration or permanent disposal. However, smaller particles are often difficult to be separated from the treated wastewater (Weber, 1974; Kim *et al.*, 2010; Çeçen and Aktas, 2011) and are usually removed with the addition of a coagulant as part of the sludge. The sludge produced under such arrangement will be heavily contaminated because it contains in addition to a lot of water, the coagulant, the added sorbent and all the pollutants it has sorbed. Separation of the sorbent from

the sludge is practically impossible making it more difficult to handle and dispose (Snoeyink and Summers, 1999; Chowdhury *et al.*, 2013). Separation of fine particles from water can be achieved by the membrane filtration technology which requires a lot of energy to create high pressures necessary to force the water through the membrane (Côté *et al.*, 1997; Šostar-Turk *et al.*, 2005). Alternatively, separate sorption process unit can be used; which can incorporate for instance, coagulation process (Margot *et al.*, 2013; Altmann *et al.*, 2015), but this will add to the overall detention time of the wastewater treatment plant as it typically requires flocculation and sludge settling tanks and often also sand filter units. Consequently, leading to higher overall cost of construction, operation and maintenance of the treatment plant. An alternative is either to use granular activated carbon (GAC) in fixed bed column operation or by magnetising PAC to enable easy separation from treatment units using magnetic principles (Wang *et al.*, 2015a).

The use of more expensive GAC with larger particles but slower kinetics than PAC in a fixed bed column adsorption is usually the favoured solution (Li *et al.*, 2003; Kim *et al.*, 2010). With this, the treatment objective can be met in a shorter period and there is no need for the provision of additional treatment units for the separation of exhausted sorbents from wastewater. However, utilisation of the sorbent's full sorption capacity is often not achieved because the contact is for a short period and slower kinetics of larger sorbent particles prevent the achievement of sorption equilibrium (Weber, 1974; Al-Degs *et al.*, 2009); such that at breakthrough point, only partial sorption capacity is utilised (Snoeyink and Summers, 1999; Worch, 2012).

2.4.1 NEED FOR MAGNETISATION OF SORBENTS

By using magnetic separation techniques, fine sized magnetic sorbents can be readily separated from treated wastewater within the same treatment unit used to contact wastewater with sorbent. This is easier than separation by membrane filtration which requires more energy (Côté *et al.*, 1997; Šostar-Turk *et al.*, 2005). This will ensure full utilisation of sorbents' sorption capacities as compared to contact using GAC in fixed bed where partial utilisation is achieved. Furthermore, because the sorbent is recovered without being enmeshed in floc

particles aggregated with the coagulant, it can be more readily disposed of or regenerated.

Although several works have been conducted on the use of activated carbons and biochars in the adsorption of several pollutants (Lijuan *et al.*, 2011; Maher *et al.*, 2012; Mandu *et al.*, 2012; Muhtab *et al.*, 2012), the process of magnetisation may change the surface characteristics of the carbon. This can have an influence on the sorption properties of the magnetised sorbent such that in the overall, their sorption behaviour may differ substantially from the pristine sorbent. Additionally, the magnetisation can be achieved using different methods each resulting to a sorbent with unique sorption properties (Šafařík *et al.*, 1997; Nguyen *et al.*, 2011; Jiang *et al.*, 2015). At the moment, there is limited literature coverage on the effect of magnetisation on the sorption properties of sorbents and their application in control of environmental pollution. Therefore, there is the need to assess the effect of the modification and the possible trade-off between the necessity of magnetisation and altered sorption properties.

2.5   ACTIVATED CARBON

Biochars and activated carbon (also called active carbon, activated charcoal, or activated coal) are obtained by the pyrolysis of carbonaceous materials to obtain a material that is composed mainly of carbon atoms. Activated carbon can be prepared from many materials such as coal, peat, wood, sawdust, coconut shell, petroleum based residues and almost any material with a high carbon content (Cameron Carbon Incorporated, 2006). The production of activated carbon involves two stages; carbonisation and activation. During carbonisation, the carbonaceous feedstock is pyrolysed at high temperatures under oxygen deficient conditions. The carbonised product (coal or biochar) – which consist basically of carbon as most of the other elements are eliminated as volatile gaseous species- has pores that are not well developed therefore has a rather small surface area. In thermal activation, the charred material is further heated in an atmosphere of air, carbon dioxide or steam at temperatures in the range of 800°C to 900°C. In chemical activation, the original feedstock is impregnated with chemicals that include; phosphoric acid, potassium hydroxide and zinc chloride. The activation process result in a product that is extremely porous with a highly amplified surface area (Çeçen and Aktas, 2011).

2.5.1 TYPES

Activated carbon can be classified based on the parent material from which it was produced and for which they can be named as coconut shell, coal, wood, peat, petroleum based activated carbon activated carbon etc. (Cameron Carbon Incorporated, 2006). Classification can also be based on shape of material such as fibrous activated carbon and activated carbon cloth or based on additives used in its production such as impregnated activated carbon. However, the main classification is based on the particle size where it can either be granular activated carbon (GAC) if it has particle size within 0.1 to 4.0mm or powdered activated carbon (PAC) if the particle size is within 0.001 to 0.25mm (Metcalf & Eddy Inc *et al.*, 2003; Roop and Meenakshi, 2005; Norit Americas Inc., 2012).

2.5.2 STRUCTURE

Activated carbon consist of microcrystallite structure which closely approximate the structure of an ideal graphite (Snoeyink and Weber, 1967; Coughlin and Ezra, 1968; Çeçen and Aktas, 2011). Based on the ideal graphite structure, the microcrystallite structure of activated carbon is assumed to be composed of infinite layers of fused hexagonal rings of carbon atoms. Typical graphite crystal is shown in Figure 2.2.

(a)   (b)
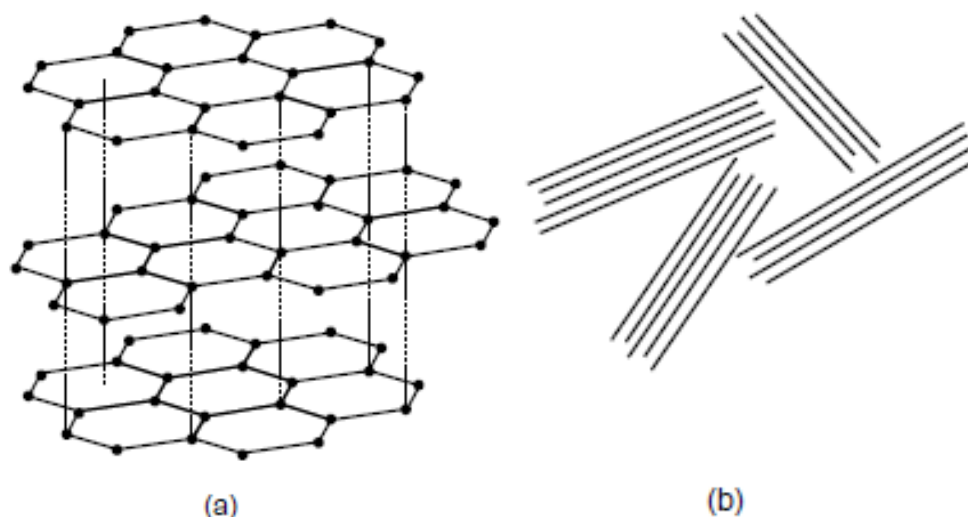
Figure 2.2:   Structural elements of activated carbons: (a) graphite structure, (b) randomly oriented graphite microcrystallites (Worch, 2012)

Three of the carbon's four electrons are localised and they participate in regular covalent bonds with neighbouring atoms. The fourth electron (usually

called the π electron) resonates between several valence-bond structures, giving each carbon-carbon bond a one-third double-bond character (Walker, 1962; Snoeyink and Weber, 1967). In a more recent study, Harris *et al.* (2008) used aberration-corrected transmission electron microscopy imaging to show evidence that activated carbon is made up of a highly disordered structure consisting mostly of hexagonal and a few pentagonal rings of carbon atoms. Adsorption on the microcrystallite planes are normally due to the effect of van der Waals forces (Roop and Meenakshi, 2005; Çeçen and Aktas, 2011).

2.5.3 PROPERTIES

With reference to sorption, the behaviour of an activated carbon may depend on the precursor organic material and the process used in its production. Variation in any of these would result in differences in behaviour or properties of an activated carbon sample. The properties that influence the sorption characteristics of AC include; surface area, porosity, particle size, surface functional groups and surface charges.

2.5.3.1 *Surface Area:*

Because adsorption is a surface phenomenon, adsorption capacities are usually proportional to the surface area (Weber, 1974). Therefore, large surface area is a significant property of activated carbon that makes them sorbents of choice in water and wastewater treatment. Typical ACs have surface area within the range 500 – 1500 m^2/g (Çeçen and Aktas, 2011; Worch, 2012; Chowdhury *et al.*, 2013), although surface area as high as 2500 m^2/g has been reported (Snoeyink and Weber, 1967; Roop and Meenakshi, 2005). The total surface area of the AC consists of internal and external surface areas. The external area arises due to bulges and cavities that have greater width than depth and they serve as conduits for the conveyance of sorbates to sorption sites. The internal surface area -which arises due to activation process where the porosity of the coal is amplified and developed even further- consists of pores of different sizes. Hence, it takes the largest fraction of the total surface area (Worch, 2012) and as a result determines the sorption capacity of activated carbon (Roop and Meenakshi, 2005). In the case of metal cations, the surface area does not directly dictate the

sorption capacity, rather the surface chemistry is more important (Leyva Ramos *et al.*, 2002).

2.5.3.2   Porosity

The IUPAC classification, developed by (Everett, 1972), classified pores based on their sizes into the following three types; macropore (> 50 nm) mesopore (between 20 and 50 nm) and micropore (< 2 nm). The macropore and mesopore here also facilitate mass transfer of sorbates to the interior of the sorbent particle. Generally the macropores contribute little to the total surface area and sorption capacity of activated carbons (Weber, 1974). The micropores constitute about 95% of the total surface area of the activated carbon and therefore determines its sorption capacity. This is particularly true if the sorbate molecules are small enough to access the micropores (Roop and Meenakshi, 2005). Walker and Weatherley (2001), studied the sorption of acid dyes on solid adsorbent, they found that much of the specific surface area was left redundant due to molecular weight aggregation. For ACs having similar surface area and micropore volume, larger mesopore volume also contribute to the sorption capacity of the activated carbon especially for larger adsorbates (Hsieh and Teng, 2000). Also, sorbates with molecules having similar sizes will compete equally for the available sorption sites either within the micropore or mesopore accordingly (Pelekani and Snoeyink, 1999). In the same vein, loss of sorption capacity for smaller sized sorbates due to pore blockage by competing larger sized sorbates can be minimised if micropore size distribution is adjusted to include a significant volume of secondary micropores (Pelekani and Snoeyink, 2001). It is therefore essential to select sorbents that have compatible porosity with respect to the size and nature of the sorbate to adsorb to ensure efficient utilisation of its sorption capacity (Gergova *et al.*, 1994). Pore size also influences the sorption intensity. Sorbate molecules tend to have more contact with the surface of the sorbent as the pore size decreases, leading to increase in sorption intensity. Also, sorption potential between opposite pore walls begin to overlap once the pore size is less than twice the diameter of the sorbate molecule (Li *et al.*, 2002).

2.5.3.3   Surface Chemistry

Compounds are able to adsorb on the surface of carbon sorbents mainly due to action of intermolecular interaction that results from van der Waals forces, electrostatic attractions and π interactions (Worch, 2012). The aromatic sheets have edges due to limited dimensions, defects, dislocations and discontinuities. The atoms at the edges are rich in potential energy and are thus highly reactive because they have impaired electrons and unsaturated valencies. These constitute the active sites on carbon surfaces and they exercise a profound influence on the sorption capacity of carbon sorbents (Coughlin and Ezra, 1968; Roop and Meenakshi, 2005). Heteroatoms such as oxygen, hydrogen, nitrogen and sulphur can interact with the adsorption sites at the edges to form surface functional groups carbon (Mattson *et al.*, 1969; Li *et al.*, 2002; Dąbrowski *et al.*, 2005). The carbon-oxygen surface groups are the most important functional groups that influence the surface characteristics of carbon sorbents. The presence and relative concentration of these function groups goes a long way in determining the sorption behaviour of activated carbon (Roop and Meenakshi, 2005; Çeçen and Aktas, 2011).

Because the carbon atoms on the planar surface of AC are involved in covalent bonding with neighbouring carbon atoms, adsorption on the basal plane is usually due to the action of van der Waals forces and π coordination with compatible sorbates (Snoeyink and Weber, 1967). The delocalised π electron facilitates the sorption of a multiplicity of sorbates through π interactions. This type of interaction is stronger for molecules having more than two double and triple bonds or poly-nuclear aromatics (Heibati *et al.*, 2015).

The surface of carbon sorbents has a net charge density, depending on the pH of the solution it interacts with. At low pH it has a positive charge, at high pH a negative charge and a neutral charge in between. The pH at which the surface has a zero net charge density is called the point of zero charge (pH_{PZC}). This behaviour is due to the protonation and deprotonation of surface -OH groups (Worch, 2012). The pH_{PZC} can be determined using methods such as suspension effect; electrophoretic mobility; change of pH by adding of adsorbent to solution; titration with acid and alkali (Tschapek *et al.*, 1974)

2.5.3.4   Particle Size

The particle size influences the rate at which adsorption progresses, as it determines the length that a sorbate must travel to reach a sorption site. Under same conditions therefore, the smaller the particle size the faster sorption progresses. Therefore, the particle size determines the mode of AC sorption method that can be applied; either in batch or fixed bed continuous flow reactors. While smaller size yields faster kinetics, in fixed bed reactors, particle sizes that practical flow conditions allow are chosen (Weber, 1974). Below this limit excessive pressures would be required to force wastewater through the bed resulting to higher energy demand. Thus PAC application is limited to batch process where the AC is added to the wastewater to be treated in the form of slurry (Chowdhury *et al.*, 2013). On the other hand, larger particle sizes as in GAC results in slower kinetics, hence there is practical limitation in the size of AC to use in a batch process. The use of GAC in batch process is not economical as it would require longer detention time or provision of larger reactors before treatment objectives can be achieved. GAC is more expensive than PAC, but the former can easily be recovered and regenerated for repeated use (Roop and Meenakshi, 2005).

2.6   MAGNETISED SORBENTS

Sorbents are modified in order to facilitate their separation from a medium or matrix (Šafařík *et al.*, 1997; Oliveira *et al.*, 2002; Zhang *et al.*, 2007; Chen *et al.*, 2011a; Han *et al.*, 2015a; Han *et al.*, 2015b), or to provide a support for catalysts to enhance decomposition and degradation of organic compounds in aqueous medium and photocatalytic disinfection (Roop and Meenakshi, 2005; Castro *et al.*, 2009; Nguyen *et al.*, 2011; Gamage McEvoy and Zhang, 2014). Numerous lab based simple procedures have been adopted to achieve the magnetisation of activated carbon and biochars. These include;

i)   Chemical co-precipitation technique alone at low temperature (Šafařík *et al.*, 1997; Oliveira *et al.*, 2002)

$CuCl_2$, $FeCl_3$ and NaOH (Zhang *et al.*, 2007), $FeCl_3$, $FeSO_4$ and NaOH (Oliveira *et al.*, 2002) $FeSO_4 \cdot 7H_2O$ and NaOH, (Šafařík *et al.*, 1997); $FeSO_4 \cdot 7H_2O$ and $FeCl_3 \cdot 6H_2O$ and NaOH (Han *et al.*, 2015a; Han *et al.*, 2015b)

ii)   Chemical co-precipitation of iron salts on biomass then pyrolysis at elevated temperature (Chen *et al.*, 2011a)

$FeCl_2$, $FeCl_3$ and $NaOH$ (Chen *et al.*, 2011a)

iii) Chemical impregnation of activated carbon followed by heat treatment at elevated temperature $Fe(NO_3)_3•9H_2O$ and HNO_3 or $Fe(NO_3)_3•9H_2O$ and $MnSO_4•H_2O$ (Nguyen *et al.*, 2011)

iv)   Hydrothermal synthetic method

$NiSO_4•6H_2O$, $FeCl_3•6H_2O$ and $NaOH$ mixed at low temperature, then diluted with water and heated at 435 K for 10 hours (Jiang *et al.*, 2015).

These methods produce unique magnetised sorbents whose properties are changed either for better or for worse compared to the original sorbents from which they are synthesised. For instance, Castro *et al.* (2009), recorded reduction in BET surface area and micropore volume with increase in iron oxide content. SEM micrography of the magnetised AC reveals well-dispersed iron oxide particles covering the surface of the activated carbon for higher iron oxide content, while much of the surface is exposed when the iron content is lower. XRD analysis suggests the presence in the composite of only goethite, although the presence of maghemite or magnetite and small amounts of goethite, were seen in the pure iron oxide. Using a different method, Nguyen *et al.* (2011) recorded improvement in surface area and porosity were improvement despite the presence of iron oxides within the sorbent particles -in the case of impregnation without $MnSO_4·H_2O$; which they attributed to further activation action of Fe(III) salt. Impregnation with $MnSO_4·H_2O$ did not affect the surface area and porosity significantly. XRD indicated the presence of metal oxides in the form of ferrite and manganese ferrite spinels. SEM shows that the porous nature of the magnetic particle deposits on the carbon surface could be the reason for the maintenance of high surface area and porosity of the activated carbon even after magnetisation. The magnetisation however increased the pH_{PZC} slightly from 8.0 to 9.0

Various magnetic sorbents have been tested in the removal of different compounds that include volatile organic compounds (phenol, chloroform and chlorobenzene) from aqueous solutions (Oliveira *et al.*, 2002), hydrophobic organic compounds (p-nitrotoluene and naphthalene) and phosphate (Chen *et al.*, 2011a), water soluble organic dyes (Šafařík *et al.*, 1997) acid orange II dye

(Zhang *et al.*, 2007). In general, the sorption of the magnetised sorbents has been shown to depend on the organic carbon content while the magnetic iron oxide contribution is negligible or almost nothing (Šafařík *et al.*, 1997; Chen *et al.*, 2011a). Sorption of organic compounds show slight reduction in sorption capacities due to small surface area of iron oxide, which reduces the overall surface area of the composite to about 30%. (Oliveira *et al.*, 2002). Zhang *et al.* (2007), recorded an increase in the sorption of acid orange dye due the presence of $CuFe_2O_4$ because the modified surface makes it more heterogeneous which may alter the sorption behaviour from monolayer to multilayer.

2.7   ADSORPTION OF ORGANIC COMPOUNDS

The application of adsorption process in the removal of organic compounds from aqueous solutions has been extensively studied (Damaskin *et al.*, 1971; Kim *et al.*, 1976; Šafařík *et al.*, 1997; Pelekani and Snoeyink, 1999; You *et al.*, 2002; Lazar *et al.*, 2013). Activated carbon and biochars in their pure and modified forms have been reported to be very effective in the adsorption of organic compounds (Moore *et al.*, 2010; Gupta *et al.*, 2014; Jing *et al.*, 2014; Jung *et al.*, 2015; Sun *et al.*, 2015). The sorption of organic compounds is influenced by factors that include; the surface area, surface chemistry and porosity of the sorbent, the solubility, speciation, size and molecular weight of the sorbate, the pH, temperature and presence of competing species (Roop and Meenakshi, 2005; Worch, 2012). The sorption of organic compounds onto carbon sorbents occurs according to mechanism which arise due to the interaction of the factors mentioned above. The following mechanisms have been identified; (i) sorption by electrostatic interactions, (ii) sorption by interaction of dispersive forces, (iii) sorption due to formation of complexes with surface functional groups, (iv) sorption due to hydrophobic interactions (Ahmaruzzaman and Sharma, 2005; Dąbrowski *et al.*, 2005; Kennedy *et al.*, 2007; Moreno-Castilla, 2008). Generally, the solution pH has a profound influence on the mechanism and can affect the sorption either for better or for worse. Additionally, distinction between these mechanisms is not in a strict sense since they tend to occur simultaneously.

2.7.1 SORPTION BY ELECTROSTATIC INTERACTION

This mechanism occurs due to the ability of both the sorbate and the surface of the sorbent to have net charge(s) due to the influence of the solution pH. The interaction can be attractive or repulsive depending on the ionic strength of the solution and the charge densities of the sorbent and the sorbate (Moreno-Castilla, 2008). Generally, the sorption fate of the sorbate is influenced by the position of the pH with respect to its pKa and the charge density constant of the sorbent (pH_{PZC}) as shown in Table 2.1.

At low pH, the surface of the sorbent becomes positively charged (if pH < pH_{PZC}) due to the existence of electron-rich regions acting as Lewis basic sites that accepts protons from the solution (Moreno-Castilla, 2004). At lower pH, below pKa, organic acids exist in neutral form, while the anionic specie predominates at higher pH above the pKa. The reverse is the case for bases, as such at lower pH below pKa, the protonated (cationic) specie is dominant while the neutral specie is dominant at high pH above pKa.

Table 2.1: Sorption of organic compounds by electrostatic interaction (Worch, 2012)

Sorbate character	Relative position of pH_{PZC} and pKa	pH range	Dominating sorbate charge	Dominating sorbent surface charge	Resulting electrostatic interactions
Acidic	pH_{PZC} < pKa	pH > pKa	Negative	Negative	Repulsion
	pH_{PZC} > pKa	pKa < pH < pH_{PZC}	Negative	Positive	Attraction
		pH > pH_{PZC}	Negative	Negative	Repulsion
Basic	pH_{PZC} > pKa	pH < pKa	Positive	Positive	Repulsion
	pH_{PZC} < pKa	pH_{PZC} < pH < pKa	Positive	Negative	Attraction
		pH < pH_{PZC}	Positive	Positive	Repulsion

Generally, the sorption of neutral species is relatively favoured (Limousin *et al.*, 2007), while the sorption of charged species on charged surface is influenced by electrostatic forces of attraction or repulsion. Cationic species are attracted to negatively charged surface and sorption is favoured, while their sorption is hindered on negatively charged sorbent surface due to repulsive forces. Anionic sorbate species are sorbed better on positively charged sorbent surface and their sorption is hindered on negatively charged surfaces due to repulsive forces (Leyva Ramos *et al.*, 2002). It can thus be inferred that sorption will be maximal in the pH range where the sorbate specie has an opposite charge

as the surface of the sorbent (Rodrigues *et al.*, 2011). In the case of organic acids, this is possible only when a compounds with low pKa interacts with a sorbent with high pH$_{PZC}$.

2.7.2 ADSORPTION BY COMPLEXATION:

This can be through a complex formation between surface carbonyl groups acting as donors and the aromatic hydroxyl or nitro-substituted compounds acting as electron acceptors (Weber, 1974). The ability of a sorbent to partake in the formation of a donor-acceptor complexes increases if it is processed at a higher temperature such that the number of surface oxygen groups of basic character is increased. Consequently, its sorption of organic compounds increases through electron donor-acceptor complexes, with the basic surface oxygen group as the donors and the phenol aromatic ring as the acceptor (Moreno-Castilla *et al.*, 1995; Dąbrowski *et al.*, 2005). In the other way, oxidation of the carbonyl and carboxyl groups impairs the formation of the electron donor-acceptor complex and thus adsorption decreases (Rodrigues *et al.*, 2011).

2.7.3 ADSORPTION BY HYDROPHOBIC INTERACTIONS:

The amphoteric nature of the surface of carbon materials are influenced by the type of carbon-oxygen surface groups. When oxygen surface complexes or oxygen functionalities such as carboxyls, anhydrides, lactones and phenols are the predominant functional groups, the surface has an acidic, hydrophilic and polar behaviour (Roop and Meenakshi, 2005; Foo and Hameed, 2012). At low sorbate concentrations, polar sorption sites would preferentially sorb water molecules through hydrogen bonding with carboxylic acid and phenolic hydroxyl groups (Moreno-Castilla, 2008). Eventually water clusters could form on such sites rendering the graphitic basal planes and pores inaccessible to the sorbate molecules (Moreno-Castilla, 2004; Dąbrowski *et al.*, 2005). Presence of acidic oxygen complexes on the surface of carbon increases its polarity, thus sorption of a sorbate can only occur after the stronger solvent-activated carbon bond is broken (Snoeyink and Weber, 1967; Snoeyink and Summers, 1999). If however the oxygen and nitrogen containing groups are supressed and functionalities such as carbonyl, pyrenes, ethers and chromenes predominate, then sorbent will

have a basic character and thus be capable of sorbing both hydrophobic and hydrophilic sorbates (Lopez-Ramon *et al.*, 1999; Li *et al.*, 2002). In a like manner compounds with lower solubility are preferentially sorbed over those with higher solubility (Weber, 1974).

2.7.4 SORPTION BY DISPERSIVE INTERACTIONS:

Although not a general case, the sorption of phenol is possible by the formation of hydrogen bonding between phenolic protons and the oxygen groups of basic character (Coughlin and Ezra, 1968; Li *et al.*, 2014). Another way for compounds with aromatic structure to interact, is by π- π interaction between the delocalised π electrons of the hexagonal rings on the surface of the sorbent (acting as electron donor) and that of the aromatic ring on the compound (as electron acceptor) (Moreno-Castilla, 2004). Oxidation of the sorbent results in the withdrawal of the surface π electron system leading to a decrease in sorption (Dąbrowski *et al.*, 2005; Rodrigues *et al.*, 2011). Also coordination between the aromatic ring of the sorbate and the hexagonal carbon ring on the sorbent's surface or between molecules of adjacent sorbed layers could induce dipole-dipole interaction (Lee *et al.*, 2016) leading to sorption by aromatic stacking (Kundu *et al.*, 2013).

2.8   ADSORPTION OF HEAVY METALS.

Several types of sorbents such as; activated carbon (Carrott *et al.*, 1997; Leyva Ramos *et al.*, 2002; Wang *et al.*, 2008; Cronje *et al.*, 2011), biochar (Tong *et al.*, 2011; Pellera *et al.*, 2012), agricultural residues (Ho, 2003; Chen *et al.*, 2012), nanomaterials (Boparai *et al.*, 2011; Hu and Shipley, 2013), peat (Ho and McKay, 2002), and clay (Celis *et al.*, 2000; Lukman *et al.*, 2013) have been used for the removal of heavy metals from aqueous solutions. Generally, the sorption of metals is heavily influenced by the solution pH, such that sorption has a minimum at low pH and as the pH increases, sorption increases to a maximum within a narrow pH adsorption edge (Yu *et al.*, 2000; Kula *et al.*, 2008). The sorption of metals onto carbon sorbents is governed by several factors that relate to the sorbent, sorbate and solution. The sorbent related factors include; nature and concentration of surface functional groups, pH_{PZC} and porosity; sorbate related factors include, metal speciation, ionic radius, electronegativity and

solubility; finally, solution related factors include; pH, ionic strength, presence of competing compounds and temperature (Pagnanelli *et al.*, 2003; Le Cloirec and Faur-Brasquet, 2008; Tong *et al.*, 2011; Wiwid Pranata *et al.*, 2014). The uptake of metals by carbon sorbents has been identified to progress according to four main mechanisms which are influenced by the interaction of the aforementioned factors. The mechanisms identified include; adsorption, ion exchange, formation of surface complex and surface precipitation (Kadirvelu *et al.*, 2001; Faur-Brasquet *et al.*, 2002; Inyang *et al.*, 2012; Lu *et al.*, 2012; Xu *et al.*, 2013). The heavy metals sorption capacity of a sorbent is dependent on the nature and concentration of specific sorption sites not surface area (Leyva Ramos *et al.*, 2002). Nonetheless, a sorbent with large surface area that contains sufficient specific sites is always desired in the removal of these metals.

2.8.1 UPTAKE BY ADSORPTION:

This manifests due to electrostatic and π - π interactions (Xu *et al.*, 2013). Adsorption may be due to columbic interaction between positively charged metal species and the negatively charged sorbent surface (Le Cloirec and Faur-Brasquet, 2008). This mechanism is most effective over a narrow moderate pH range (also known as the pH adsorption edge) i.e. when pH > pH_{PZC}, and the free form of the metal specie is the dominant. At low pH, the surface of the sorbent is positively charged, therefore sorption of metal is impaired due to electrostatic repulsion and competition by H^+ in solution for coordination with surface oxygen functional groups (Liu and Zhang, 2009; Pellera *et al.*, 2012). At high pH, this mechanism is less effective due to higher solubility of the hydrolysed metal specie which becomes dominant under such conditions or due to the precipitation of the metal and subsequent loss of concentration. In addition to sorption by electrostatic interaction, transition metals (especially those with exposed π-orbitals) can sorb by π - π interaction mechanism if there is sufficient energy to overcome the electrostatic repulsion forces (Leyva Ramos *et al.*, 2002; Lehmann and Joseph, 2009). Adsorption due to dispersive interactions between the surface of the sorbent and ionic species in solution is usually small (Roop and Meenakshi, 2005).

2.8.2 UPTAKE BY ION EXCHANGE:

This mechanism is manifest when heavy metal from solution replaces another in existing precipitates or complexed functional groups such as -OH and -COOH on the surface of the carbon. Because the replaced metal specie is released into the solution, Lu *et al.* (2012), detected significant concentrations of the divalent alkaline earth cations, Ca^{2+} and Mg^{2+} in supernatants following sorption of Pb^{2+} on sludge-derived biochar. Sorption by ion exchange can be associated with a decrease in final pH due to the release of H_3O^+ (Le Cloirec and Faur-Brasquet, 2008). The ion exchange potentials of the Me^{2+} species differ and one specie is preferentially removed from solution over another, essentially due to the effects of electrostatic binding strength. This depends on the radius of hydrated metal ion and the charge of the metal ion. The electrostatic binding strength increases with decrease in hydrated metal radius and increase in charge. The larger the radius the more the energy required to dehydrate the metal ion (Mohan and Singh, 2005). Therefore, selectivity increases with decrease in ionic radius of hydrated metal ion (Pehlivan and Altun, 2006).

2.8.3 UPTAKE BY COMPLEXATION WITH SURFACE FUNCTIONAL GROUPS:

This is due to the coordination of heavy metal with especially oxygen surface functional groups to form complexes (Roop and Meenakshi, 2005). The carboxyl and hydroxyl groups can act as proton donor and once deprotonated, they can coordinate with Me^{2+} forming complexes (Lu *et al.*, 2012). Therefore, uptake by formation of complexation will be favoured by an increase in pH, such that the carboxyl and hydroxyl groups get deprotonated leading to higher metal sorption (Tong *et al.*, 2011).

2.8.4 UPTAKE BY SURFACE PRECIPITATION:

This can result in the formation of a new solid or gel metal hydroxide at the surface of the sorbent when heavy metals react with negatively charged ions such as carbonate and phosphate on the surface of biochars (Le Cloirec and Faur-Brasquet, 2008; Tong *et al.*, 2011). Xu *et al.* (2013), also observed a decrease in the concentration of phosphate and carbonate in supernatant following the sorption of Cu^{2+}, Zn^{2+} and Cd^{2+} on dairy manure biochar from solution. They also

attributed this to the formation of metal phosphate and carbonate precipitates on the surface of the biochar. Using both SEM and XRD analysis, Inyang *et al.* (2012) were able to observe the presence of precipitate on the surface of biochar after the sorption of Pb^{2+}.

2.9 EVALUATION OF BATCH ADSORPTION PROCESS

The sorption of a compound from solution can be described based on sorption capacity, affinity and kinetics. The sorption capacity is influenced by the space on the sorbent that is potentially available for sorption, while sorption affinity is influenced by interaction of intermolecular forces (Yang and Xing, 2010). Sorption kinetics determines how much of the sorption capacity is utilised in a given time interval. Normally, the better the kinetics the more rapid the approach to equilibrium or attainment of treatment objectives (Weber, 1974).

Generally, sorption equilibrium can be represented by the expression

$$Q = f(C) \qquad \text{-} \qquad \text{-} \qquad \text{-} \qquad \text{-} \qquad \text{-} \qquad \text{-} \qquad \text{-} \qquad \text{-} \qquad \text{-} \qquad (2.1)$$

The solid phase sorbate concentration or amount sorbed can be computed using the mass balance equation.

$$Q_e = \frac{(C_o - C_e)}{m} V \qquad \text{-} \qquad \text{-} \qquad \text{-} \qquad \text{-} \qquad \text{-} \qquad \text{-} \qquad \text{-} \qquad \text{-} \qquad (2.2)$$

Where: Q_e is the solid phase sorbate concentration at equilibrium; (mg/g) or (mmol/g),

C_o and C_e are the initial and equilibrium liquid phase sorbate concentration respectively; (mg/L) or (mmol/L).

m is the mass of sorbent; (g)

V is the volume of solution; (L)

2.10 SORPTION ISOTHERMS

For a given sorption system at a particular temperature, the graphical plot of various corresponding pairs of Q_e against C_e gives the sorption isotherm. Isotherms can be grouped into four main groups based on the nature of the initial

part of the plot as classes C, L, H and S (Giles *et al.*, 1974; Dąbrowski *et al.*, 2005). Examples of the typical isotherms is shown in Figure 2.3.
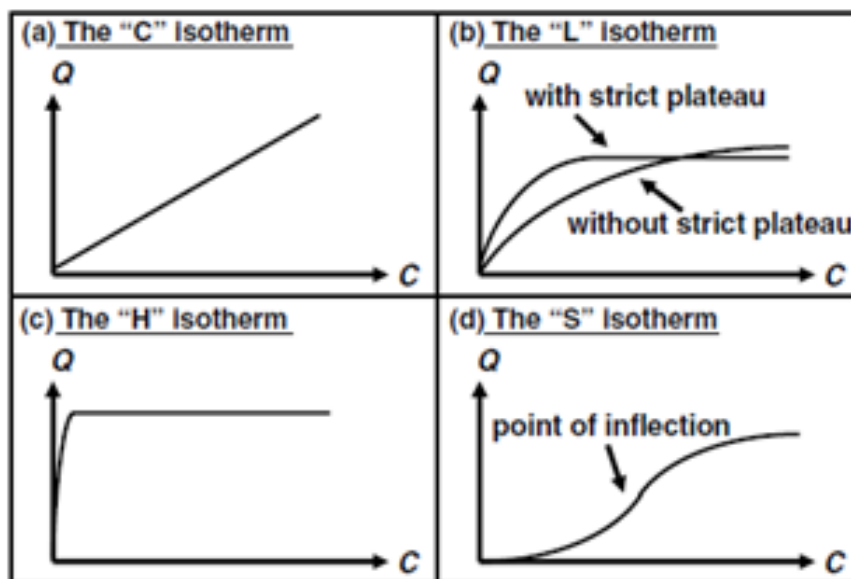
Figure 2.3:   Four main types of sorption isotherms (Limousin *et al.*, 2007)

The sorption isotherm can provide some information on the nature of the sorbent-solute interactions. With particular reference to the use of carbon based sorbents in the sorption of most wastewater pollutants, the 'L' class is mostly encountered while the 'H' class is a special type of 'L' class where the sorbate exhibits a very high affinity for the sorbent. The 'C' class is used to obtain a one-point estimate of sorbate partitioning. (Limousin *et al.*, 2007).

2.10.1   MODELLING OF ISOTHERM DATA:

Isotherm models provide a means for mathematical description of the experimental data and consequently the dependence of sorption capacity on concentration can be evaluated (Weber, 1974).

2.10.1.1   Linear Model

This is a 1-parameter model and is the simplest sorption isotherm model. It is primarily based on Henry's Law (Burwell, 1976), hence the solid phase concentration has a direct relationship with the equilibrium concentration. It can be represented by the mathematical expression;

$$Q_e = K_d C_e$$ -   -   -   -   -   -   -   -   -   (2.3)

Where: K_d is the partition or dispersion coefficient; (L/kg)

This model presents an infinite adsorption potential, but in reality it is valid over the low concentration range, in which the isotherm tends to be approximately linear (Limousin *et al.*, 2007). At higher concentration adsorption ceases to be linear and this model is not applicable. Although this model was derived empirically, it is particularly useful for modelling contaminant adsorption provided the conditions are similar to those within which the K_d value was measured (Cantrell *et al.*, 2002; Goldberg *et al.*, 2005). It can be used to estimate the sorbate partitioning preference of a given sorption system. Higher K_d values may indicate preference for the solid phase while lower K_d values may indicate preference for the liquid phase.

2.10.1.2   *Nonlinear Models*

Sorption isotherms are mostly nonlinear; therefore, their characteristics are better evaluated using one or more nonlinear models. However, each of these models was developed to explain particular properties of the sorption system based on some assumptions and limitations (Kumar *et al.*, 2008a; Liu, 2009). Consequently, no single model can comprehensively explain the nature of the isotherm (Ho *et al.*, 2002; Allen *et al.*, 2004). As a result, it has been the usual practice to use as many models as possible to complement each other in describing the sorption system (Kumar and Porkodi, 2006; Hamdaoui and Naffrechoux, 2007b; Hamdaoui and Naffrechoux, 2007a; Giraldo and Moreno-Piraján, 2014). In this study, the following two 2-parameter and three 3-parameter models were selected to evaluate the isotherms of phenol, ibuprofen, diclofenac and divalent metal cations sorption on the ACs and BCs.

A.   2- parameter models

a)   The Langmuir model (Langmuir, 1918);

Although this model was originally developed to describe the sorption of gasses, it is being applied to explain the sorption from liquids. The Langmuir model depicts a monolayer sorption on a surface containing finite number of identical sites (energetically and sterically) (Mc Kay *et al.*, 1983). Each of these sites can accommodate only one molecule of a given compound at a time and

although adsorption and desorption are reversible, there is no lateral interaction between adsorbed molecules (Roop and Meenakshi, 2005; Limousin *et al.*, 2007; Armenante, 2009a).

The Langmuir model is given as;

$$Q_e = \frac{Q_m K_L C_e}{1 + K_L C_e}$$ -   -   -   -   -   -   -   -   (2.4)

The Langmuir model can be linear transformed in at least two different ways, with each having different inherent error structure, thus yielding different estimated parameter values (Ho, 2004; Hamdaoui and Naffrechoux, 2007a; Kumar, 2007; Boulinguiez *et al.*, 2008). The constants can be determined from the slope and intercept of a linear data fit. The most common linear forms of the Langmuir model are;

Either;

Linear transformed Langmuir model type 1

$$\frac{C_e}{Q_e} = \frac{1}{Q_{m1} K_{L1}} + \frac{C_e}{Q_{m1}}$$ -   -   -   -   -   -   (2.5)

$$\text{Slope} = \frac{1}{Q_{m1}} \qquad\qquad \text{Intercept} = \frac{1}{Q_{m1} K_{L1}}$$

Or;

Linear transformed Langmuir model type 2

$$\frac{1}{Q_e} = \frac{1}{Q_{m2}} + \left(\frac{1}{K_{L2} Q_{m2}} \right) \frac{1}{C_e}$$ -   -   -   --   -   -   (2.6)

$$\text{Slope} = \frac{1}{Q_{m2} K_{L2}} \qquad\qquad \text{Intercept} = \frac{1}{Q_{m2}}$$

Where: The constants Q_{mi} and K_{Li} are the maximum monolayer adsorption capacity, (mg/g) or (mol/g) and Langmuir equilibrium constant, (L/mg) or (L/mol).

The Langmuir constant K_L is related to the energy of adsorption and it increases as the strength of adsorption bond increases. It is the ratio of sorption rate to desorption rate, thus it is a measure of sorption intensity (Armenante,

2009a). Therefore, it can be used to evaluate the favourability of the sorption by assessing a dimensionless constant known as the separation factor 'S_L' or equilibrium parameter (Hall *et al.*, 1966; Ho, 2003) expressed as;

$$S_L = \frac{1}{1+K_L C_O}$$

- - - - - - - - (2.7)

Slope of isotherm may be interpreted based on the values of S_L as

Table 2.2: Classification of isotherms according to separation factor

Separation factor	Nature of isotherm slope
$S_L > 1$	Unfavourable
$S_L = 1$	Linear
$0 < S_L < 1$	Favourable
$S_L = 0$	Irreversible

b) The Freundlich model (Freundlich, 1906)

This model depicts sorption considering heterogeneous surface energies allowing for multilayer surface coverage.

The Freundlich model is expressed as;

$$Q_e = K_F C_e^{\frac{1}{n}}$$

- - - - - - - - (2.8)

The term n is a dimensionless constant related to energetic heterogeneity describing sorption intensity, a larger $1/n$ value represents a more homogeneous adsorbent with a narrower site energy distribution (Li *et al.*, 2002). Although in principle 'n' can assume any value, it is in practice mostly greater than unity. Consequently the following can be inferred; $n = 1$ implies a linear isotherm, $n > 1$ implies favourable sorption possibility of higher loadings at low concentrations and $n < 1$ implies unfavourable sorption (Mc Kay *et al.*, 1983; Worch, 2012). The constant K_F is related to adsorbent adsorption capacity for a given adsorbent, ($mg^{1-1/n}L^{1/n}g^{-1}$).

The linearized Freundlich isotherm equation can be written as:

$$Log\, Q_e = Log\, K_f + \frac{1}{n} \times Log\, C_e$$

- - - - - (2.9)

The constants can be determined from the slope and intercept of a linear data fit.

This model lacks theoretical basis and is incapable of describing neither the low concentration linear range of the isotherm nor the saturation effect at very high concentration (Roop and Meenakshi, 2005; Worch, 2012; Chowdhury *et al.*, 2013). However, it generally agrees well with the Langmuir equation and experimental data over moderate ranges of concentration (Weber, 1974).

B   3- Parameter Models

a)   Redlich-Peterson

The model can be expressed in the form;

$$Q_e = \frac{K_R C_e}{1 + A_R C_e^{\gamma}} \qquad \text{-} \quad \text{-} \quad \text{-} \quad \text{-} \quad \text{-} \quad \text{-} \quad \text{-} \qquad (2.10)$$

The constants K_R and A_R are the Redlich-Peterson isotherm constants (L/g) and $(\text{L/mg})^{\gamma}$ respectively, while γ is an exponent that lies between 0 and 1 (Ho *et al.*, 2002; Wu *et al.*, 2010).

This model constitute both Freundlich and Langmuir characteristics (Wong *et al.*, 2004) and therefore allows the evaluation of sorption isotherm data over a wide range of concentration. It reduces to the Freundlich isotherm at low concentration and Langmuir isotherm at high concentration. Based on the exponent term, two possible special cases are possible; when $\gamma = 1$ the model becomes a special case of Langmuir model and when $\gamma = 0$ the model becomes linear (Sips, 1948; Sips, 1950; Redlich and Peterson, 1959).

In linear form it can be expressed as;

$$\ln\left(K_R \frac{C_e}{Q_e} - 1\right) = \ln A_R + \gamma \ln C_e \qquad \text{-} \qquad \text{-} \qquad \text{-} \qquad \text{-} \qquad (2.11)$$

The model parameters can be obtained from a plot of $\ln\left(K_R \frac{C_e}{Q_e} - 1\right)$ against $\ln C_e$ and using trial and error linear regression by adjusting the value of K_R to obtain the highest possible value of the coefficient of determination (R^2).

b)   Models based on Polanyi theory for potential adsorption.

This theory stipulates that a sorbate molecule within the sorption space on a sorbent surface will experience an attractive force whose strength is proportional to the distance from the surface. It defines the adsorption potential 'ε' (J/mol) as the work done by the adsorption forces in bringing a molecule from the fluid phase to an adsorption point within an adsorbed film. In essence, ε is a measure of the adsorption force of attraction (Manes and Hofer, 1969; Roop and Meenakshi, 2005; Yan et al., 2008).

$$\varepsilon = RT \ln \left({C_s}/{C_e} \right) \qquad - \quad - \quad - \quad - \quad - \quad - \qquad (2.12)$$

Where: C is the universal gas constant, T is the Kelvin temperature (K), C_s is the sorbate's water solubility (mg/L).

The theory describes the volume of an adsorption space enclosed between parallel equipotential planes and the surface of the sorbent within which the formation of adsorbed film takes place. Adsorption is thought to occur by capillary condensation of the sorbate in the sorbent pores. The relationship between the volume of the adsorption space and 'ε' for a given pair of sorbent-sorbate system is defined by the characteristic curve which is temperature-independent. The characteristic curve is usually obtained as a plot of adsorbed volume 'Q_v' against 'ε' (Manes and Hofer, 1969; Roop and Meenakshi, 2005; Sander and Pignatello, 2005). According to this theory, the isotherm obtained for a given sorbent as a plot of adsorbed volume per unit mass of sorbent 'Q_v' against the adsorption potential density 'ε/V_s' will be the same for all liquid sorbates provided there is no specific interactions between sorbates and sorbent surface (Xia and Ball, 1999).

i)   The Polanyi-Dubinin-Manes model

The most common Polanyi based sorption isotherm model is the one suggested by (Crittenden et al., 1987) and commonly referred to by many as the "Polanyi-Manes" (Xia and Ball, 1999; Yang et al., 2006b; Xu et al., 2008) or "Polanyi-Dubinin-Manes" (Long et al., 2008) model and it has been successfully adopted to describe sorption isotherms for aqueous medium.

$$\log Q_e = \log Q_o - a(\varepsilon_{sw}/V_s)^b \qquad - \quad - \quad - \quad - \quad - \qquad (2.13)$$

Where: Q_o is the sorbed mass at saturation (i.e. complete filling of volume of adsorption space); (mg/g)

a and b are fitting parameters.

V_s is the molar volume of the adsorbate (cm³/mol), which is estimated as the ratio of molecular weight (M_w) and the density of the adsorbate (ρ) in its pure form (Yan et al., 2008)

ii) The Dubinin-Ashtakov Polanyi based model

Another model describing the theory of "Volume Filling of Micropores" was proposed by (Dubinin and Astakhov, 1971). Like the Polanyi based model, its theory is based on the concept of temperature invariance of the characteristic equation which related the degree of pore filling to the differential molar work of adsorption. Here instead, the differential molar work of adsorption is determined with respect to the Gibbs loss of free energy instead of adsorption potential, in contrast to the Polanyi theory.

$$\log Q_e = \log Q_o - (\varepsilon/E)^b \qquad - \quad - \quad - \quad - \quad - \qquad (2.14)$$

Where: E is the characteristic energy of adsorption; 'J/mol'

This model has also exhibited very good fitting to sorption isotherm data for sorption in aqueous medium (Yang *et al.*, 2006a; Yang *et al.*, 2008).

2.11 MODELLING OF KINETICS DATA:

Sorption of compounds on sorbents progresses according to diffusion based and reaction based mechanisms and as such, mathematical models have been developed to describe the sorption kinetics, in terms of both mass transfer and chemisorption (Ho *et al.*, 2000). For the chemisorption, kinetic models have been presented describing the order of reaction either based on the solution concentration (for which they are termed first and second order) or based on the capacity of the sorbent (for which they are termed as pseudo first and pseudo second order). The difference between the solid phase concentration at time t

and that at equilibrium $(Q_e - Q_t)$ is the driving force governing the pseudo-first and second order models (Chiou and Li, 2002; Yang and Al-Duri, 2005). To describe the kinetics using the reaction based model, it is important to establish the sorption mechanism, since in some instances, sorption process is essentially physical in nature (Ho, 2006; Qiu *et al.*, 2009).

2.11.1 CHEMISORPTION BASED MODELS

2.11.1.1 *Pseudo First Order Model*

The earliest equation describing sorption kinetics as first order rate based on sorption capacity was presented by Lagergren (1898) for sorption of oxalic acid and malonic acid onto charcoal, (Ho and McKay, 1998; Qiu *et al.*, 2009). The equation is popularly referred to as the pseudo-first order rate equation to distinguish it from rate equation based on solution concentration (Wu *et al.*, 2001; Chen *et al.*, 2010).

$$\frac{dQ_t}{dt} = k_1(Q_e - Q_t) \qquad - \quad - \quad - \quad - \quad - \quad - \qquad (2.15)$$

Integrating this expression with the boundary conditions $Q_t = 0$ at $t = 0$ and $Q_t = Q_t$ at $t = t,$ we have the expression as presented by (Yuh-Shan, 2004; Khambhaty *et al.*, 2009);

$$Q_t = Q_e\left(1 - e^{(-k_1 t)}\right) \quad - \quad - \quad - \quad - \quad - \quad - \qquad (2.16)$$

Or in linear form as;

$$\log(Q_e - Q_t) = \log Q_e - \left(\frac{k_1}{2.303}\right)t \quad - \quad - \quad - \quad - \quad - \quad - \qquad (2.17)$$

Where: Q_t the adsorption capacity at time t (mgg^{-1}) and k_1 the pseudo-first order rate constant (min^{-1}).

The slope of the linear fit of $\log(Q_e - Q_t)$ versus t allows the determination of the value of $\left(-\frac{k_1}{2.303}\right)$. The intercept of the straight line gives the value of $\log Q_e$.

Azizian (2004), used a theoretical approach to derive the pseudo-first order model and was able to determine the conditions for using the first-order model. He eventually found that the model is applicable in cases where the initial

concentration 'C_o' is very high. In fact, k_1 is a function of 'C_o' and both sorption and desorption rate constants 'k_{ads}' and 'k_{des}' respectively.

$$k_1 = k_{ads}C_o + k_{des} \qquad \text{-} \quad \text{-} \quad \text{-} \quad \text{-} \quad \text{-} \qquad (2.18)$$

The ratio k_{ads}/k_{des} gives the equilibrium constant K 'Lmg^{-1}' and it can be computed from the slope and intercept of a linear plot of k_1 vs C_o.

The pseudo-first order model does not fit well over the whole range of contact time. It has been shown in most literature to be applicable over the initial 20 to 30 minutes of the sorption process and the equilibrium sorption capacity is normally obtained by trial and error (Ho and McKay, 1998).

2.11.1.2 Pseudo Second Order Model

The equation describing sorption kinetics as second order rate according to the sorption capacity is commonly referred to as the pseudo-second order rate equation. This model assumes that chemisorption reaction rate depends on the amount of sorbate sorbed on the surface of the sorbent at time t and that at equilibrium (Ho and McKay, 1998; Qiu et $al.$, 2009).

$$\frac{dQ_t}{dt} = k_2(Q_e - Q_t)^2 \qquad \text{-} \quad \text{-} \quad \text{-} \quad \text{-} \quad \text{-} \qquad (2.19)$$

It can be expressed as (Khambhaty et $al.$, 2009; Tonucci et $al.$, 2015);

$$Q_t = \frac{k_2 Q_e^2 t}{1 + k_2 Q_e t} \qquad \text{-} \quad \text{-} \quad \text{-} \quad \text{-} \quad \text{-} \quad \text{-} \quad \text{-} \qquad (2.20)$$

Or in linear form as (Ho and McKay, 1999);

$$\frac{t}{Q_t} = \left(\frac{1}{h}\right) + \left(\frac{1}{Q_e}\right)t \quad \text{-} \quad \text{-} \quad \text{-} \quad \text{-} \quad \text{-} \quad \text{-} \quad \text{-} \quad \text{-} \qquad (2.21)$$

Where k_2 is the pseudo-second order rate constant (g mg^{-1}min^{-1}) and $h = k_2 Q_e^2$ is the initial sorption rate (mg g^{-1} min^{-1}).

If the kinetics follows the pseudo-second order equation, a plot of $\frac{1}{Q_t}$ against t will give a straight line with $\frac{1}{Q_e}$ and $\frac{1}{h}$ as the slope and the intercept respectively.

According to Azizian (2004), k_2 is a complex function of 'C_o' and this model has a good fit for values of C_o that are not too high.

2.11.1.3 Elovich Equation.

The equation considers both chemisorption rate and desorption constant. It is suitable for describing heterogeneous sorption systems (Ho and McKay, 2002).

$$Q_t = \left(\frac{1}{\beta}\right) ln(\alpha\beta) + \left(\frac{1}{\beta}\right) ln(t) \quad - \quad - \quad - \quad - \quad - \quad - \quad (2.22)$$

Where: α is the initial chemisorption rate (mg g-1 min-1) and β is the desorption constant (g mg-1).

If sorption progresses according to the Elovich model, then, a plot of Q_t versus $ln(t)$ will be a straight line with $\left(\frac{1}{\beta}\right)$ and $\left(\frac{1}{\beta}\right)ln(\alpha\beta)$ as the slope and intercept respectively (Ho and McKay, 1998). Both constants are related to the relative concentrations of sorbate and sorbent. Ho and McKay (2002) showed that in the sorption of copper (II) on peat, increasing C_o resulted to a decrease in α and an increase in β. While increasing the sorbent dose resulted in an increase in α and a decreases in β.

2.11.2 DIFFUSION BASED MODEL

2.11.2.1 The Intraparticle Diffusion Model

This model assumes that in well mixed systems, external diffusions are negligible and the intra-particle diffusion is the controlling step (Ho *et al.*, 2000). It is based on two assumptions; (i) intra-particle diffusivity 'D' is constant and (ii) the uptake of sorbate by sorbent is small relative to the liquid phase concentration (Yang and Al-Duri, 2005). The (Weber and Morris, 1963) equation is the most widely applied in describing the intra-particle diffusion and is given as;

$$Q_t \approx k_{id}t^{0.5} - \quad - \quad - \quad - \quad - \quad - \quad - \quad - \quad - \quad (2.23)$$

Where: k_{id} (mg g^{-1} min$^{-0.5}$) is the intra-particle diffusion rate constant and is related to the intra-particle diffusivity 'D' in the following way,

$$k_{id} = \frac{6Q_e}{R} \sqrt{\frac{D}{\pi}} \qquad - \quad - \quad - \quad - \quad - \quad - \quad - \quad - \qquad (2.24)$$

Where: D (cm^2 min^{-1}) and R (cm) is the particle radius.

When sorption progresses according to the intra-particle diffusion, a plot Q_t versus $t^{0.5}$ will yield a straight line passing through the origin with k_{id} as the slope (Qiu *et al.*, 2009).

Some authors (Ho and McKay, 2002; Khambhaty *et al.*, 2009), refer to this equation as fractional power and is written in the general form expressed as

$$Q_t = k_{id} t^z \quad - \qquad - \quad - \quad - \quad - \quad - \quad - \quad - \qquad (2.25)$$

This equation can be expressed in linear form as

$$\ln Q_t = \ln k_{id} + z \ln t \qquad - \qquad - \qquad - \qquad - \qquad - \qquad - \qquad - \qquad (2.26)$$

Where: k_{id} (mg g^{-1} min^{-1}) and 'z' is usually < 1 is a constant. The product of k_{id} and z gives another constant known as the specific sorption rate at unit time, i.e. when $t = 1$. In the linear form, z and k_{id} can be determined as the slope and intercept of a linear plot of $\ln Q_t$ vs $\ln t$ respectively.

This model is usually valid at the initial stage, since sorption will not continue indefinitely, and because it is only an approximate solution of the actual intraparticle diffusion differential equation.

2.12   SORPTION THERMODYNAMICS.

Energy requirement is crucial in the successful operation of sorption process in wastewater treatment. Thus, it is essential that the process progresses without the input of energy other than what is required to move the wastewater through the treatment unit. This is possible if the process is spontaneous. To determine whether the process is spontaneous or not, it is necessary to evaluate both energy ΔH^o and entropy ΔS^o factors (Ho *et al.*, 2005a). The change Gibbs free energy (ΔG^o) is commonly used to assess the spontaneity of the process

(Lataye *et al.*, 2006; Liu and Zhang, 2009; Han *et al.*, 2013a). A more energetically favoured process is characterised by a higher negative value of ΔG^o (Dubey *et al.*, 2010). Additionally, thermodynamic details are useful in understanding the type of sorption and the mechanism governing the process. The sorption can either be of the physisorption type, if the heat evolved is in the range of heat of condensation (2.1 to 20.9 kJ/mol). Or it can be chemisorption type, if the heat evolved is high in the range of (80 to 200 kJ/mol). Sorption process can be exothermic; if the value of ΔH^o is positive otherwise it is endothermic. The value of ΔS^o is a measure of randomness, the higher the value the more the spontaneity (Liu, 2009). At equilibrium, ΔG^o is related to the sorption thermodynamic equilibrium constant (K_{eq}) in the following expression;

$$\Delta G^o = -RT \ln K_{eq} \qquad \text{-} \qquad \text{-} \qquad \text{-} \qquad \text{-} \qquad \text{-} \qquad \text{-} \qquad \text{-} \quad (2.27)$$

The mathematical expression relating the changes in Gibbs free energy, enthalpy and entropy is given as;

$$\Delta G^o = \Delta H^o - T\Delta S^o \qquad \text{-} \qquad \text{-} \qquad \text{-} \qquad \text{-} \qquad \text{-} \qquad \text{-} \qquad \text{-} \quad (2.28)$$

Finally, a combination of the above two equation yields the linear form of the Van't Hoff equation as follows;

$$\ln K_{eq} = -\frac{\Delta H^o}{RT} + \frac{\Delta S^o}{R} \qquad \text{-} \qquad \text{-} \qquad \text{-} \qquad \text{-} \qquad \text{-} \qquad \text{-} \qquad \text{-} \quad (2.29)$$

The values of ΔH^o and ΔS^o are calculated as the slope and intercept of a linear plot of $\ln K_{eq}$ vs $1/T$.

Where; ΔG^o is the change in free Gibbs energy, (kJ/mol); ΔH^o is the change in enthalpy, (kJ/mol); ΔS^o is the change in entropy, (kJ/mol/K); K_{eq} is the thermodynamic equilibrium constant and is dimensionless, T is the absolute temperature (K) and R is the gas constant (8.314x10⁻³ kJ/mol/K).

The equilibrium constant is a very important term in the estimation of the thermodynamic status of the process. Different approaches have been adopted in the estimation of K_{eq}. Commonly encountered ones include; the use of

Langmuir K_L (Han *et al.*, 2013a; García-Mateos *et al.*, 2015), the y-intercept of a plot of $\ln(Q_e/C_e)$ vs Q_e (Khan and Singh, 1987; Calvet, 1989), the slope of a plot of Q_e vs C_e (Sawalha *et al.*, 2006) or simply the K_d (Liu and Zhang, 2009) or the K_d value for very low initial concentration (Han *et al.*, 2009). These approaches eventually produce different values of K_{eq} (Milonjić, 2007; Tosun, 2012) since different standard states were adopted in expressing the units of the phase concentrations (Salvestrini *et al.*, 2014). Therefore, it becomes imperative to approach the calculation of K_{eq} with caution since the correctness of estimating the energy terms are all based on its value. With appropriate units (preferably L/mol), K_L can be used in place of K_{eq} for neutral sorbates, sorbates with very weak charge and dilute solution of charged sorbates (Liu, 2009).

CHAPTER 3.   MATERIALS AND METHODS

3.1   INTRODUCTION

This chapter presents the selection of materials used in the study. It also presents methods adopted to attain the objectives (such as production of magnetised sorbents, modelling of sorption data) that are common to the proceeding chapters. Specific methods of sorption experiments are presented at the beginning of their respective chapters for ease of reference.

3.2   SORBENTS

As has been presented in chapter 2, the sorption properties of a sorbent depend on the nature of the feedstock and the production process (Lorenc-Grabowska and Rutkowski, 2014; Mailler *et al.*, 2016). Therefore, in this study, the sorbents are selected according to their difference in feedstock, activation and magnetisation such as to evaluate the sorption variations that these differences can allow.

In terms of the differences of feedstock, two kinds of commercial activated carbon were investigated, one produced from Coconut shells by Norit (GCN 1240), labelled "CoAC", and one produced from anthracite coal by Calgon (Calgon Filtrasorb 400) and obtained from Chemviron (Lancashire, United Kingdom), labelled "CoalAC". Two kinds of commercial biochar were obtained from Romchar (Harghita, Romania) labelled "Bio-1", and Oxford Biochar Ltd. (Dorset, UK) labelled "OrgBio", respectively. According to the manufacturers, both biochars were made from mixed wood chips with a maximum pyrolysis temperature of 500 °C, and the UK biochar was described by the producer as sustainable and organic (Han *et al.*, 2015b). All sorbents were ground to a fine particle size < 212 μm before use and they were not subjected to any further pre-treatment. The characteristics of the sorbents are presented in Table 3.1.

Biochars (BCs) and activated carbons (ACs) were both assessed in order to evaluate the benefits of activation (larger surface area and enhanced porosity) in the sorption of the target pollutants from wastewater. Overall, it is expected that comparable behaviour will be recorded among the pairs of these two groups

of sorbents. Hence due to their superior surface area and porosity, it is expected that the ACs will have superior sorption capacities, at least for organic compounds. While the BCs, having not been subjected to elevated temperatures that are necessary during activation are likely to have better sorption of heavy metals, due to their higher oxygen contents.

Finally, the variation in sorbent properties due to magnetisation was assessed by producing magnetised sorbents from each of the aforementioned ACs and BCs. It is expected that due to the magnetisation (procedure presented in 3.2.1), the surface area and porosity of the magnetised sorbents will be decreased compared to those of their pristine pairs, especially for the activated carbons. The resulting difference in sorption capacities as well as, their affinity for the different types of sorbates should also be evaluated.

3.2.1 PRODUCTION OF MAGNETIC SORBENTS.

Figure 3.1: Production of magnetic sorbent

The magnetic sorbents were produced using the co-precipitation method as explained in (Han *et al.*, 2015b). Briefly, the procedure as shown in Figure 3.1, involves the continuous heating and stirring of a mixture containing 2.5 g sorbent, 3.33 g of $FeCl_3 \cdot 6H_2O$, 1.83 g of $FeSO_4 \cdot 7H_2O$ and 100 mL deionised water in a beaker to 65 °C. While still stirring, the mixture is allowed to cool to below 40 °C and then 5 M NaOH solution is added dropwise to raise the pH to 10-11 to precipitate the iron hydroxides. It is allowed to stir further for an hour and then left to settle overnight. The supernatant is carefully decanted using a pipette and the precipitate-laden sorbent is washed with deionized water into a coffee filter paper. The product is further rinsed with ethanol after the water has drained, and then

dried at 80 °C overnight. The dried composite material is then washed into a beaker and rinsed thoroughly with deionised water. The magnetic activated carbon or biochar composite is collected with magnetic rods and dried again at 80 °C overnight. The final product is a powder consisting of about 36% magnetite impregnated on the surface and in the macropores of the activated carbon or biochar. The magnetic carbon composites are labelled after their pristine pairs as MCoAC, MCoalAC, MBio-1 and MOrgBio respectively. Their characteristics are presented in Table 3.1.

Table 3.1:   Properties of sorbents (Han *et al.*, 2015b)

Sorbent	CoAC	MCoAC	CoalAC	MCoalAC	Bio-1	MBio-1	OrgBio	MOrgBio
Surface Area (m²/g)	975	643	974	659	261	219	6.1	68
Open Surface Area[a] (m²/g)	40	70	120	130	50	110	0	70
Pore Volume (cm³/g)	0.47	0.41	0.58	0.50	0.17	0.23	0.01	0.15
Micropore Volume (cm³/g)	0.43	0.26	0.40	0.24	0.10	0.05	0.00	0.00
Pore Size (Å)	37.1	91.1	52.0	67.9	52.1	66.9	304.4	91.1
Geometric mean Particle Size (μm)	7.3		6.5		7.3		25.5	
pH$_{PZC}$	10.4	6.3	9.8	9.0	9.2	9.0	8.7	7.8
Theoretical mass magnetic susceptibility [b] [10⁻⁶ m³/kg]		156.5		129.7		107.4		122.8
Measured mass magnetic susceptibility [10⁻⁶ m³/kg]		119.7		145.4		108.3		178.6

[a] Due to macropores

[b] The theoretical mass magnetic susceptibility was calculated by the mass fraction of magnetite in each material, and the mass magnetic susceptibility of magnetite (6.0 ×10⁻⁴ m³/kg, (Dearing, 1999)).

The surface areas of CoAC, CoalAC and Bio-1 were decreased by about 34.05, 32.34 and 16.09% respectively. Similarly, their micropore volumes were also reduced by about 39.53, 40.00 and 50.00% respectively. It should be noted however, that these decreases are as a result of lower carbon content in the composites. The composites contain about 36% lesser carbon content (Han *et al.*, 2015b), therefore, corresponding pairs of sorbents will have comparable values for these parameters when measured with respect to their carbon content only. On the contrary however, the surface area and micropore volumes of the OrgBio, were increased dramatically by about 1014.75 and 1400% respectively. This increase in surface area and micropore volume could be due to the dissolution of carbonate deposits in the pores of biochar during the magnetisation process, i.e. due to excessive acidic conditions, which results in the creation of

new accessible pore-space. Also, the deposition of magnetic particles on the surface of AC could result in formation of new pores as observed by Nguyen et al. (2011). The acidic conditions created during the magnetisation resulted to the lowering of the pH_{PZC} of all the sorbents after magnetisation. This will favour the sorption anionic species by electrostatic attraction, while on the other hand it will weaken the sorption of cationic species due to electrostatic repulsion.

3.2.2 SORBENT CHARACTERISATION

The properties of the sorbent presented in Table 3.1 were obtained from a collaborative research with Dr Zhantao Han and their measurement is not repeated in this study. The data has already been published, therefore detailed description of the methods can be found in (Han *et al.*, 2015b).

3.3 SORBATES

The list of priority pollutants as well as compounds of emerging concern (CEC) is vast and each of them affects the environment in a specific manner. Their compositional make up makes them have different characteristics and it is practically impossible to study them individually when evaluating the applicability of a given treatment process. Yet there is a good chance that compounds which share similar properties are more likely to behave in a similar way when subjected to the same treatment process. So a representative member of a group of pollutants can be studied in order to have an idea on the probable effectiveness of the chosen treatment process against other members of the same general group.

3.3.1 PHENOL
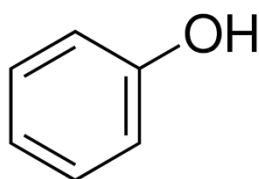
Figure 3.2:   Structure of phenol

Phenol was chosen because it is a typical, toxic organic compound with a simple structure and is also listed among priority pollutants (European Commission, 2001; EPA, 2014). It is among the organic compounds that have been reported to exist in high concentrations in effluents of biological treatment processes (Al-Zarooni and Elshorbagy, 2006; JRC, 2006; Çeçen and Aktas, 2011; Otokunefor and Obiukwu, 2005). Therefore, like in many other studies, it is chosen as an ideal exemplar compound that can be used in the evaluation of sorption characteristics of various sorbents. It is expected that sorbents with large surface area and amplified porosity will be most suitable for its removal by adsorption from wastewater.

Its chemical structure is presented in Figure 3.2 and some of its properties are presented in Table 3.2. Phenol solution (30 g/L) was obtained from VWR (Lutterworth, UK).

Table 3.2:   Properties of phenol, ibuprofen and diclofenac

Compound	Phenol	Ibuprofen	Diclofenac sodium
Molecular formula	C_6H_5OH	$C_{13}H_{18}O_2$	$C_{14}H_{10}Cl_2NO_2.Na$
Molar mass (g/mol)	94.11	206.29[c]	318.13[d]
Mass density	1.07	1.03	0.63
Molar volume (mL/mol)	87.872	200.282	504.968
Size (nm)	0.43 x 0.57[b]	1.0 x 0.6[e]	0.97 x 0.96[d]
Solubility (mg/mL)	81.68[j&k] (10°C) and 90.61[j&k] (22°C)	0.021[f]	50[i]
pKa	9.98 [b]	4.82 - 4.91[g]	4.15 – 4.18 [g]
LogK$_{ow}$	1.57 [a]	3.97[h]	4.51 [h]

[a](Schwarzenbach *et al.*, 2005) [b](Lorenc-Grabowska and Rutkowski, 2014), [c](Lindqvist *et al.*, 2005), [d](Sotelo *et al.*, 2013), [e](Narayanan, 2008), [f](Yalkowsky and Dannenfelser, 1992) [g](Lekkerkerker-Teunissen *et al.*, 2012), [h](Baccar *et al.*, 2012), [i](Fisher Scientific Ltd, Prod. no 12317163), [j](Góral *et al.*, 2011), [k](Henrigton, 1974)

3.3.2 MICROPOLLUTANTS

This category of sorbates represents contaminants of emerging concerns (CECs) that are found in wastewaters, and not readily removed in biological wastewater treatment. In many cases within a refinery, sewage from residential and administrative facilities and wastewater from refining facilities are treated

centrally (IPIECA, 2010). Pharmaceuticals are selected as representatives of micropollutants that originate from domestic sewage from within the refinery. Although they share common sorption mechanisms with other major organic pollutants such as phenol, they are larger and more complex molecules which are often less susceptible to removal from wastewater by sorption. Ibuprofen and diclofenac are chosen to represent this group. Their chemical structure is shown in Figure 3.3. Both are pharmaceuticals that belong to a group of drugs known as nonsteroidal anti-inflammatory drugs (NSAIDs), which are being extensively used in the treatment of pain, fever and rheumatic disorders (Mestre *et al.*, 2009). They are produced in large quantities with an estimated annual global production running into several kilotons for ibuprofen alone (Cleuvers, 2004; Jolliffe and Gerogiorgis, 2015). Some of their properties of interest are shown in Table 3.2.
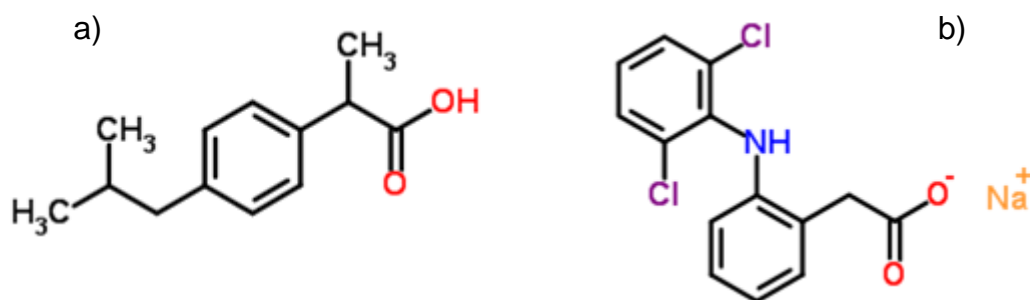
Figure 3.3:   Structure of (a) ibuprofen and (b) diclofenac (sodium salt)

Ibuprofen and diclofenac were chosen as typical pharmaceuticals because they are among the pharmaceuticals that have been detected at high concentrations in effluent of WWTP (Ellis, 2006; Verlicchi *et al.*, 2012; Margot *et al.*, 2013). Sometimes, all that conventional, biological treatment process do is to convert them to other hydrolysed or conjugate forms (Hernando *et al.*, 2006). They have been reported to be toxic to aquatic microflora and fauna, invertebrates and fish (Farré *et al.*, 2001; Ferrari *et al.*, 2003; Cleuvers, 2004). Diclofenac was reported to delay the hatching time of fish eggs, cause alterations or damage to kidney and gills of fish after prolonged exposure (Hallare *et al.*, 2004; Schwaiger *et al.*, 2004). Evidence of Ibuprofen induced liver damage, changes in the production of hormones and testosterone in freshwater fish has been reported (Han *et al.*, 2010; Islas-Flores *et al.*, 2014). Yet the overall impact of these compounds on environmental entities is still unpredictable due to the diversity of species and variations in individual communities. One thing is for sure,

their release to the environment should be minimised and if possible historical exposures be reversed. Consequently, the treatment or removal of these compound has to this day remain an essential field that demands continuous research.

Ibuprofen was purchased from Sigma-Aldrich Company Ltd, while diclofenac sodium was obtained from Fisher Scientific UK Ltd and both were in analytical purity.

3.3.3 HEAVY METALS.

This category is chosen because they do not degrade and are persistent, thereby making them ubiquitous in the environment at levels that have since raised concerns (JRC, 2010; Carlos *et al.*, 2013). Exposure to some of these metals -even at trace levels- are reported to have an adverse effect on the human health or the environment (Dabrowski and Curie, 1999; Çeçen and Aktas, 2011). The metals chosen to represent this category are Cu^{2+}, Pb^{2+} and Zn^{2+}. They are expected to share common sorption mechanism, which will be influenced by how they interact with the sorbent properties according to the differences in their properties such as the ones listed in Table 3.3. The mechanism by which they are removed by adsorption from the wastewater is different from that responsible for the removal of most organic pollutants. They are usually removed by sorption to specific, electronegative sites on the surface of the sorbents (Worch, 2012). Therefore, unlike the organic pollutants, sorbents' surface area will only be advantageous if it is associated with sufficient number of the specific sites.

Table 3.3:   Properties of heavy metals

Metal/salt	Solubility (g/100 mL)*	Effective ionic radius (pm)*	Electronegativity**
Cu^{2+}	-	73	1.93
$CuCl_2 \cdot 2H_2O$	76.4	-	-
Pb^{2+}	-	119	2.33
$Pb(NO_3)_2$	56	-	-
Zn^{2+}	-	74	1.63
$ZnCl_2$	395	-	-

*Data obtained from (Speight, 2005). ** data obtained from (Wiwid Pranata *et al.*, 2014)

3.4   WASTEWATER

Two types of wastewater sample were used in this study, one real and the other synthetic.

3.4.1 REAL WASTEWATER SAMPLE

Wastewater sample (termed WWTPE) was obtained from the effluent of Tudhoe Mill Sewage Treatment Plant, Spennymore, Durham, UK. This is a nitrifying domestic wastewater treatment plant that serves a population of about 22,000 (Neal *et al.*, 2000; Nurthumbrian Water, 2009; Brown *et al.*, 2015). The satellite image of the site is shown in Figure 3.4. The characteristic of wastewater from this plant is shown in the Table 3.4.

Figure 3.4:   Satellite image of Tudhoe Sewage Treatment Plant, UK. [Courtesy of: Imagery ©2016 Getmapping plc, Infoterra Ltd & Bluesky, Map data ©2016 Google]

The WWTPE was autoclaved at 120°C for 15 min and allowed to cool to room temperature before filtration through glass-microfiber filter FT-3-1101-070 (Sartorius stedim Biotech GmbH Goettingen, Germany). Aliquot of the filtered sample was taken for DOC measurement and the rest is stored in the dark at 4°C

until required (usually in less than a week). The DOC of the sample was 11.08 mg/L.

Table 3.4: Comparison of wastewater compositions

Parameter	Tudoe Mill wastewater treatment plant	Port Harcourt Refinery [e,f]	Refinery sour water [g]
COD (mg/L)	602[a,b]	232.1	850-1020
BOD (mg/L)	240 [a,b]	216	570
DOC(mg/L)			300-440
TSS (mg/L)	243 [a,b]		
VSS (mg/L)	206 [a,b]		
TDS (mg/L)		335.4	
SO_4^{2-} (mg/L)	6.38 [a,b]	30.31	15-23
NH_3 (mg/L)	25.1-36.8 [c,d]	26.01	5.1-21.1
TN^h (mg/L)	41.7-48 [c,d]		
Phosphate (mg/L)		15.4	
Phenol (mg/L)		69.11	98-128
Oil and grease (mg/L)		12.48	12.7
pH	7-7.7 [c,d]	8.3	8.0-8.2

[a][(Petropoulos *et al.*, 2016)], [b][Screened raw influent], [c][(Bundy *et al.*, 2017)], [d][post primary clarification], [e][(Otokunefor and Obiukwu, 2005)], [f][raw wastewater Port Harcourt Refinery Nigeria], [g][(Coelho *et al.*, 2006)], [h][TN is defined as the sum of TKN and anions-N ($NO^{-3} + NO^{-2}$)].

3.4.2 SYNTHETIC WASTEWATER

Synthetic wastewater (termed SWW) was prepared using a similar procedure adopted by (Pholchan *et al.*, 2008) which was based on the OECD test guidelines 209 protocols (OECD, 2010). Briefly, peptone (160 mg), meat extract (110 mg), urea (30 mg), NaCl (7 mg), $CaCl_2 \cdot 2H_2O$ (4 mg), $MgSO_4 \cdot 7H_2O$ (2 mg), and K_2HPO_4 (28 mg) were dissolved in 1 L of deionised water. Immediately after preparation, the stock SWW was autoclaved at 120°C for 15 min and allowed to cool to room temperature. Aliquot of the SWW sample was taken for DOC measurement and the rest is stored in the dark at 4°C until required (usually in less than a week). The DOC of the sample diluted at 1:100 was 6.45 mg/L.

3.4.3 DOC MEASUREMENT

For the DOC measurement, aliquot of the wastewater samples were treated according to the HACH LCK 385 kit procedure, using HACH LT200 dry

thermostat digester and HACH DR 1900 spectrophotometer. The kit and instruments used were all supplied by HACH LANGE United Kingdom.

3.5 SORPTION TEST

The batch process is chosen to test the sorption characteristics of the sorbents. This provides a simple and straightforward method of analysing the characteristics of a sorption system and its response to internal and external changes. Isotherms were generated using the batch process bottle point method by varying the initial concentration. This makes it possible to find the relationship between sorbent dosage, sorbate initial concentration and amount adsorbed. Also, existing isotherm models can easily be applied not just to estimate the sorption capacity, but also the nature of interaction between the sorbate and the sorbent surface and the nature of the adsorbed layer (Crini and Badot, 2008). In the same vein, the rate of the utilisation of the sorption capacity can be evaluated by using kinetic models to analyse the rate of uptake of the sorbate on the sorbent with respect to time.

3.6 MODELLING OF SORPTION DATA

Mathematical expressions will be used to evaluate the sorption data. Sorption models are many, each with unique sets of parameters that describe specific properties of the sorption system. Furthermore, since these models were developed based on different assumptions -each with inherent limitations- no single model can explain in entirety the real characteristics of the system. As a result, it is a good precaution to adopt as many sorption models as possible in the evaluation of sorption data. These models complement each other i.e. the parameters of one model can help in explaining the behaviour of another model and accordingly, a better assessment of the process becomes possible.

3.6.1 MODELLING OF ISOTHERM DATA

The following five models whose details were presented in chapter 2 were chosen to analyse the isotherm data.

i) The linear model is only applicable at low concentration. It can be used to evaluate the partitioning preference of the sorbate between the solid and aqueous phases at the lower concentration range end of the isotherm data.

ii) The Langmuir and Freundlich models are among those chosen to analyse the isotherm data, not just because of their wide acceptability but because of their simplicity and ability to simulate the experimental data. To run these models, only the basic data from isotherm experiment is required. These models are capable of estimating the sorption capacities, the nature of surface coverage, affinity or intensity of the sorbed layer and whether it is favourable or not.

iii) The Redlich-Peterson model incorporates the features of both Langmuir and Freundlich types of isotherm. Additionally, it tends to have better fitting to isotherm data over them. Therefore, it is chosen to confirm the type of isotherm, especially in cases where the decision to choose which of the two models best described the data is not straightforward.

iv) The Polanyi based models (Polanyi-Dubinin-Manes and Dubinin-Ashtakov) are chosen to help explain the mechanism of sorption of organic compounds. Either their sorption is by micropore filling or not. They also good at data fitting and can help in estimating the sorption capacities.

3.6.1.1 Choosing Among Models

The model selection criteria (MSC) can be used to choose models with consideration to degrees of freedom for a given number of model parameters and number of data points. This compensates for the bias due to overparametrisation of models, since models with higher number of parameters tend to fit experimental data better than those with lesser number of parameters (Sander and Pignatello, 2005; Yang and Xing, 2010; Worch, 2012). It is recommended that the number of fitted parameters should be kept as minimum as possible (Koeppenkastrop and De Carlo, 1993; Limousin *et al.*, 2007). The MSC is defined as follows;

$$
\text{MSC} = \ln\left(\frac{\sum_{i=1}^{\varphi} w_i \left(Q_{e,m} - \overline{Q_{e,m}}\right)_i^2}{\sum_{i=1}^{\varphi} w_i \left(Q_{e,m} - Q_{e,c}\right)_i^2}\right) - \frac{2\mu}{\varphi} \qquad - \qquad - \qquad - \qquad - \qquad (3.1)
$$

Where: $Q_{e,m}$ and $Q_{e,c}$ are the measured and model-calculated equilibrium solid phase sorbate concentration respectively,

$\overline{Q_{e,m}}$ is the average measured value of observed $Q_{e,m}$,

φ is the number of variables or data points,

μ is the number of fitted parameters,

w is the weight factor (if needed),

The model with the highest MSC value for a given experimental data set has the highest information content and is therefore assumed to be the most appropriate for describing the experimental data. In the MSC expression, w_i cancels out when measurement errors are approximately uniform (Saiers and Hornberger, 1996).

3.6.2 MODELLING OF KINETICS DATA:

Sorption of compounds on sorbents progresses according to diffusion based and reaction based mechanisms and as such, mathematical models have been developed to describe the sorption kinetics, in terms of both mass transfer and chemisorption (Ho *et al.*, 2000). The following models will be used to analyse the kinetics data to determine if the kinetics is governed by chemisorption; Pseudo first order, pseudo second order and Elovich models. The intraparticle diffusion model will be used to test for mass transfer dependence. The details of the models are presented in chapter 2.

3.7   DATA FITTING AND DETERMINATION OF MODEL PARAMETERS

The application of mathematical modelling enables the prediction of the characteristics of a sorption system under consideration. It is essential that the data is handled in such a way that simulation outputs are the closest resemblance of experimental data. In doing so, care should be taken to avoid unnecessary alterations of models so as to minimise the introduction of redundant errors which could lead to erroneous interpretations (Kumar and Sivanesan, 2005). Sorption data is usually fitted against established mathematical models which are nonlinear in nature and it has been the tradition to transform them to linear forms to enable easier fitting of experimental data. Unfortunately, linearization of these

models alters their error structure (Kinniburgh, 1986; Ho, 2004; Kumar *et al.*, 2008b), therefore, data obtained under such condition could in some instances be misleading resulting to wrong decisions taken that could undermine the success of the entire process.

3.7.1 LINEAR FITTING METHOD

With particular reference to sorption isotherm and kinetics data, it has been the most common tradition to obtain model parameters using the linear regression method, such that experimental data is fitted to linear transformed models (LTFM) (Porter *et al.*, 1999). The popular practice is to assess the conformity of a given linear model to the experimental data based on the r^2 value of its linear regression fit plot (Potgieter, 1991; Shi *et al.*, 2009; Hua *et al.*, 2012; Belaid *et al.*, 2013; Zhang *et al.*, 2013; Nekouei *et al.*, 2015). As such, the higher the value of the correlation coefficient for a given fitted model the better it is assumed to describe the experimental isotherm (Ho *et al.*, 2002). Additionally, the suitability of the model is further confirmed by the assessment of the residuals between experimental and model simulated data based on some error function (Wong *et al.*, 2004). Hence if the model is adequate, it will be able to predict the experimental data with significant accuracy (Özkaya, 2006).

On the one hand, the linear method enjoys popularity because of its simplicity and in some instances its capability of generating very precise model parameters. On the other hand, the linearization of models distorts their error structure (Porter *et al.*, 1999; Ho, 2004) and parameters obtained hence could be less precise and sometimes even misleading (Wong *et al.*, 2004; Ho *et al.*, 2005b; Foo and Hameed, 2010). For instance, the Langmuir model can be linearly transformed in at least two different ways, with each having different inherent error functions, thus yielding different estimated parameters (Ho, 2004; Hamdaoui and Naffrechoux, 2007a; Boulinguiez *et al.*, 2008). It can thus be seen that there is higher chance of choosing a less accurate set of parameters using one of the different forms of the LTFM Langmuir model.

3.7.2 NONLINEAR FITTING METHOD

In their original form, the nonlinear models conform to the nonlinear nature of the sorption isotherm and kinetics data and these models are developed based on this important consideration. A nonlinear regression method offers a mathematically rigorous way of determining model parameters using numerical approximations (Ho *et al.*, 2002; Kumar and Porkodi, 2006). Here, experimental data is fitted to mathematical models by minimising the error distribution between experimental and model simulated data using a defined error function (Ng *et al.*, 2002; Kumar *et al.*, 2008b). Several error functions have been used to evaluate the conformity of both linear and nonlinear models to experimental data. The nature of the error functions is well documented in the literature (Porter *et al.*, 1999; Allen *et al.*, 2004; Wong *et al.*, 2004; Boulinguiez *et al.*, 2008; Kumar *et al.*, 2008b). For a given model, each error function will generate a different set of parameters and a different value for that error function (e.g., for CoD = 0 < R^2 < 1). Therefore, the choice of the best model to describe the experimental data is not straightforward, necessitating the adoption of a selection criterion by which models can be compared considering the overall bias due to all error functions for each given model (Ho *et al.*, 2002).

3.7.3 ERROR FUNCTIONS

The advent of computer programming has made it possible to apply nonlinear regression method (also called nonlinear least squares) in determining model parameters. As a result, many researchers have recommended such as a better way of fitting sorption experimental data against the use of linear least square method (Kinniburgh, 1986; Porter *et al.*, 1999; Ho, 2004; Kumar, 2007). The use of error functions in the fitting of experimental sorption data has been widely accepted in contemporary literature (Ho *et al.*, 2002; Ng *et al.*, 2002; Allen *et al.*, 2004; Boulinguiez *et al.*, 2008; Davis and Di Toro, 2015; Wu *et al.*, 2016). These error functions are based on the measured squared deviations between experimental and predicted data (Kinniburgh, 1986; Kapoor and Yang, 1989). Thus a good approximation of experimental data would imply small deviation i.e. a model that best fit experimental data would have low values of error function (large R^2 value in the case of coefficient of determination).

In this study, models will be compared based on the average of the values of optimised error functions and consequently, the model that has the least average sum of error (ASE) is chosen as the best to describe the experimental data. The following six error functions were applied to solve the model equations and approximations were done using the "solver add-in function" on the Excel spreadsheet 2013 edition of Microsoft Corporation.

i) Error Sum of Squares (ERSSQ) (Porter *et al.*, 1999)

This is the primary form of error functions and its main drawback is, it biases fitting towards data obtained at high end of concentration range.

$$\text{ERSSQ} = \Sigma_{i=1}^{\varphi} \left(Q_{e,c} - Q_{e,m} \right)_i^2 \qquad - \qquad - \qquad - \qquad - \qquad - \qquad (3.2)$$

ii) Coefficient of determination (CoD) (Boulinguiez et al., 2008)

This function represents the degree (e.g. in percentage) of the variance dependent variable (predicted data) about the mean (Foo and Hameed, 2010). Its value ranges between 0 and 1. The closer to unity the value of CoD due to a fitted data the better the prediction of the variation.

$$\text{CoD} = \frac{\Sigma_{i=1}^{\varphi} \left(Q_{e,c} - \overline{Q_{e,m}} \right)^2}{\Sigma_{i=1}^{\varphi} \left(Q_{e,c} - \overline{Q_{e,m}} \right)^2 + \Sigma_{i=1}^{\varphi} \left(Q_{e,m} - Q_{e,c} \right)^2} \qquad - \qquad - \qquad - \qquad (3.3)$$

iii) HYBRID error function (Porter *et al.*, 1999)

This error function reduces the bias due to the sum of squares of error s encountered at low concentration. Here, in addition to the squared residuals being divided by the measured value, the number of degrees of freedom of the system are also considered. Thus the summed residual is ultimately divided by the dumber of degrees of freedom.

$$\text{HYBRID} = \frac{100}{\varphi - \mu} \Sigma_{i=1}^{\varphi} \left[\frac{\left(Q_{e,m} - Q_{e,c} \right)^2}{Q_{e,m}} \right]_i \qquad - \qquad - \qquad - \qquad - \qquad (3.4)$$

iv) Marquardt's Percentage Standard Deviation (MPSD) (Marquardt, 1963)

This is a modified version of geometric mean error distribution which incorporates the number of degrees of freedom (Ng *et al.*, 2002; Lataye *et al.*, 2006; Wu *et al.*, 2010).

$$\text{MPSD} = 100 \left(\sqrt{\frac{1}{\varphi-\mu} \sum_{i=1}^{\varphi} \left[\frac{(Q_{e,m}-Q_{e,c})}{Q_{e,m}} \right]_i^2} \right) \qquad - \qquad - \qquad - \qquad (3.5)$$

v)   Sum of absolute errors (EABS) (Porter *et al.*, 1999)

The isotherms predicted using this function usually have better fit towards the high concentration range. This bias is reduced if experiments are conducted using mass to volume ratio of 1 mg/mL., since both solid and liquid phase concentrations contribute equally to the error weighting criterion for the model solution.

$$\text{EABS} = \sum_{i=1}^{\varphi} |Q_{e,c} - Q_{e,m}|_i - \qquad - \qquad - \qquad - \qquad - \qquad - \qquad (3.6)$$

vi)   Average Relative Error (ARE) (Kapoor and Yang, 1989)

This function incorporates the features of the last two functions (MPSD and EABS). Instead of being squared, the absolute values of the residuals is taken and the number of data points is used as a divisor.

$$\text{ARE} = \frac{100}{\varphi} \sum_{i=1}^{\varphi} \left| \frac{(Q_{e,c}-Q_{e,m})}{Q_{e,m}} \right|_i \qquad - \qquad - \qquad - \qquad - \qquad - \qquad (3.7)$$

With this, numerical comparison can be made to understand how variations in source material and production affects the performance of the sorbents on their removal of target compounds form aqueous solution, synthetic and autoclaved real wastewater. These methods will be used to assess the sorption capacities and kinetics of the sorbents in their pristine and magnetised form. The sorption experiments conducted to achieve these objectives are presented in the continuing chapters.

CHAPTER 4.   SORPTION OF PHENOL

4.1   INTRODUCTION

This chapter investigates the effect of magnetisation on the characteristics of phenol sorption on activated carbons and biochars. Phenol is a typical organic compound with a simple chemical structure. It is the parent compound of many derivative organics and has made it to the list of priority pollutants. It is wide spread in wastewaters including refinery effluents and as a result it has been considered as an ideal probe compound that can be used in the appraisal of the sorption properties of sorbents. Phenol has been identified as one of the pollutants that have a wide range of toxic effects in humans and pose a significant threat to the environment due to its toxicity to the aquatic ecosystem (Barber *et al.*, 1995; Tišler and Zagorc-Končan, 1997; Park *et al.*, 2012). Additionally, it is capable of undermining the efficiency of some biological wastewater treatment processes due to its toxicity to the microorganisms involved in the treatment (Fang and Chan, 1997; Scully *et al.*, 2006). Phenol can be effectively removed from wastewaters using aerobic biological processes and carbon sorption process. The sorption progresses according to mechanisms that include, electrostatic interaction between charged sorbent surface and dissociated phenolate anion, hydrogen bonding between –OH groups of phenol and functional groups such as carboxylic on the surface of the carbon, π - π interaction between the hexagonal carbon rings on the sorbent surface and the aromatic ring, complexation with oxygen functional groups and hydrophobic interactions (Nevskaia *et al.*, 1999; Salame and Bandosz, 2003; Tseng *et al.*, 2003; Busca *et al.*, 2008).

4.2   EXPERIMENTAL SECTION

4.2.1   DETERMINATION OF SORPTION ISOTHERMS

To determine the sorption isotherms, experiment was conducted according to the method used by (Han *et al.*, 2015b). Briefly, 60 mg of ACs (or 100 mg of BCs) were added to 60 mL amber glass vials with a Teflon-lined screw cap supplied by VWR (Lutterworth, UK). The vial was closed using the screw cap and

the sample was autoclaved. The vial was filled with 59 mL (49 mL for BCs) of autoclaved 0.01 M $CaCl_2$ solution, then closed once again with the screw cap and agitated on a shaker (KS 4000i by IKA) at 90 rpm and room temperature overnight. The desired initial batch phenol concentrations (5-450 mg/L) were obtained by adding 1 mL of pre-diluted stock solution into the equilibrated $CaCl_2$ sorbent mixture. Blank controls containing phenol solution without sorbent were run in parallel with the samples to check for phenol degradation. The vials were then returned to the shaker and allowed to shake under the conditions stated before for 7 days at 22°C. Duplicate batches were set up for all phenol concentrations. After shaking, the samples were filtered using a 25 mm syringe filter with a 0.45 μm PTFE membrane obtained from VWR International (Lutterworth, UK). High-Performance Liquid Chromatography (HPLC) was used to determine the amount of phenol remaining in the filtrate. The amount of phenol adsorbed per unit weight of adsorbent was computed using the difference between equilibrium concentrations of treatment and control samples. The HPLC system (Shimadzu; Kyoto, Japan) consisted of an LC-10AD VP pump, SIL-10A VP autosampler, SPD-10A VP UV detector, and SCL 10 A-VP controller unit. Data were acquired and processed by CLASS-VP V 5.032 software. The stationary phase was a Gemini-NX 150 x 4.6 mm, 5μ, C18, 110 E column (Phenomenex, USA). The mobile phase consisted of acetonitrile and water (50: 50 % v/v), at an isocratic flow rate of 1 mL min^{-1}. The elution profiles were recorded at 254 nm, and the injection volume was 10 μL.

4.2.2 DETERMINATION OF INFLUENCE OF TEMPERATURE ON SORPTION

In order to evaluate the effect of temperature on the sorption of phenol, the same experiment was repeated as described in 4.2.1, under refrigeration at a temperature of 10°C.

4.2.3 DETERMINATION OF pH INFLUENCE ON SORPTION

To evaluate the influence of pH on the sorption of phenol, 60 mg of ACs (or 100 mg of BCs) were added to 60 mL amber glass vials with a Teflon-lined screw cap supplied by VWR (Lutterworth, UK). The vial was closed using the screw cap and the sample was autoclaved. The vial was then filled with 59 mL (49 mL for

BCs) of autoclaved 0.01 M CaCl$_2$ solution, then closed once again with the screw cap and agitated on a shaker (KS 4000i by IKA) at 90 rpm and room temperature overnight (22°C). The pH of the CaCl$_2$ conditioned samples were then adjusted to 3, 5, 7, 9 and 11 using aliquot of 0.01 M of HNO$_3$ or KOH. The pH was monitored over 72 hours and necessary adjustments were made to maintain target values. Thereafter, 1 mL of appropriate phenol stock solution was then added to the preconditioned sorbents to have a predetermined volume and initial phenol concentration in the order; 60 mL, 300 mg/L for activated carbon or magnetic activated carbon and 50 mL, 45 mg/L for biochar or magnetic biochar. All samples are in duplicate including control samples containing no sorbent and treated in similar manner. The vials were shaken on a constant temperature oscillator (KS 4000i by IKA) at 90 rpm for 7 days at 22 °C. After shaking, the samples were filtered using a 25 mm syringe filter with a 0.45 µm PTFE membrane obtained from VWR International (Lutterworth, UK). High-Performance Liquid Chromatography (HPLC) was used to determine the amount of phenol remaining in the filtrate. The amount of phenol adsorbed per unit weight of adsorbent was computed using the difference between equilibrium concentrations of treatment and control samples

4.2.4 DETERMINATION OF SORPTION KINETICS

To evaluate the phenol sorption kinetics, 60 mg of AC or MAC (100 mg of BC or MBC) were added to 60 mL amber glass vials with a Teflon-lined screw cap supplied by VWR (Lutterworth, UK). The vial was closed using the screw cap and the sample was autoclaved. The vials were filled with (59 and 49 mL for AC and BC samples) autoclaved 0.01 M CaCl$_2$ solution and then allowed to shake overnight at 90 rpm and room temperature. Thereafter, 1 mL of appropriate phenol stock solution was then added to the preconditioned sorbents to have a predetermined volume and initial phenol concentration in the order; 60 mL, 300 mg/L for activate carbon or magnetic activated carbon and 50 mL, 45 mg/L for biochar or magnetic biochar. All samples are in duplicate, including control samples containing no sorbent and treated in similar manner. The vials were shaken on a constant temperature oscillator (KS 4000i by IKA) at 90 rpm. Duplicate vials each from the ACs BCs and control samples were removed after 5, 15, 30 min, 1, 6, 12, 24, 48 hrs, 5 and 7 days and the samples were filtered

using a 25 mm syringe filter with a 0.45 μm PTFE membrane obtained from VWR International (Lutterworth, UK). High-Performance Liquid Chromatography (HPLC) was used to determine the amount of phenol remaining in the filtrate. The amount of phenol adsorbed per unit weight of adsorbent was computed using the difference between equilibrium concentrations of treatment and control samples.

4.2.5 DETERMINATION OF EFFECT OF FOULING ON SORPTION

In order to evaluate the effect of fouling on the sorption of phenol, synthetic wastewater (SWW) prepared according to the OECD test guidelines 209 protocols (OECD, 2010) as described in 3.4.2, was introduced to the sorption system. As a factor of safety, all materials for the experiment were autoclaved. The experiment was planned in such a way as to allow for the appraisal of the impact of the order by which the phenol (at 200 and 45 mg/L for ACs and BCs resp.) and the SWW (at 16 mg/L DOC) were contacted with the sorbents (at 1 and 2 mg/mL for ACs and BCs resp.). The following order of contact wad adopted;

4.2.5.1 Phenol Sorbed before SWW Addition (Phenol first)

In this order, phenol was given a 24-hour head start for adsorption before the SWW was introduced. The sorbents (40 and 80 mg for ACs and BCs resp.) were contacted with 39 mL of 0.01 M $CaCl_2$ in a 40 mL amber glass vials with a Teflon-lined screw cap supplied by VWR (Lutterworth, UK). The set up was allowed to shake overnight on a constant temperature oscillator (KS 4000i by IKA) at 90 rpm and room temperature. Thereafter, 1 mL of appropriate phenol stock solution was added to the preconditioned sorbents to have a predetermined initial phenol concentration as; 200 and 45 mg/L for ACs and BCs respectively. The samples were returned to shake for 24 hours and then 1 mL of appropriate SWW was added such as to have a concentration of 16 mg/L (as DOC). The vials were shaken for a further 6 days, after which they were filtered using a 25 mm syringe filter with a 0.45 μm PTFE membrane obtained from VWR International (Lutterworth, UK). All samples are in duplicate, including control samples containing no sorbent and treated in similar manner. High-Performance Liquid Chromatography (HPLC) was used to determine the amount of phenol remaining in the filtrate. The amount of phenol adsorbed per unit weight of adsorbent was

computed using the difference between equilibrium concentrations of treatment and control samples.

4.2.5.2 *Synthetic Wastewater Sorbed before Phenol Addition (SWW first)*

In this order, SWW was given a 24-hour head start before the phenol was introduced. The same procedure as in 4.1.5.1 was adopted, it should be noted that 7 days shaking was maintained after phenol was added.

4.2.5.3 *Simultaneous Contact of Phenol and SWW*

In this order, both phenol and SWW were added at the same time. The same procedure as in 4.1.5.1 was adopted, with slight modification. Sorbents were conditioned with 38 mL of $CaCl_2$ overnight before the addition of 1 mL each of the phenol and SWW stock solutions. The rest is the same.

4.3 RESULT AND DISCUSSION

4.3.1 EVALUATION OF SORPTION ISOTHERMS
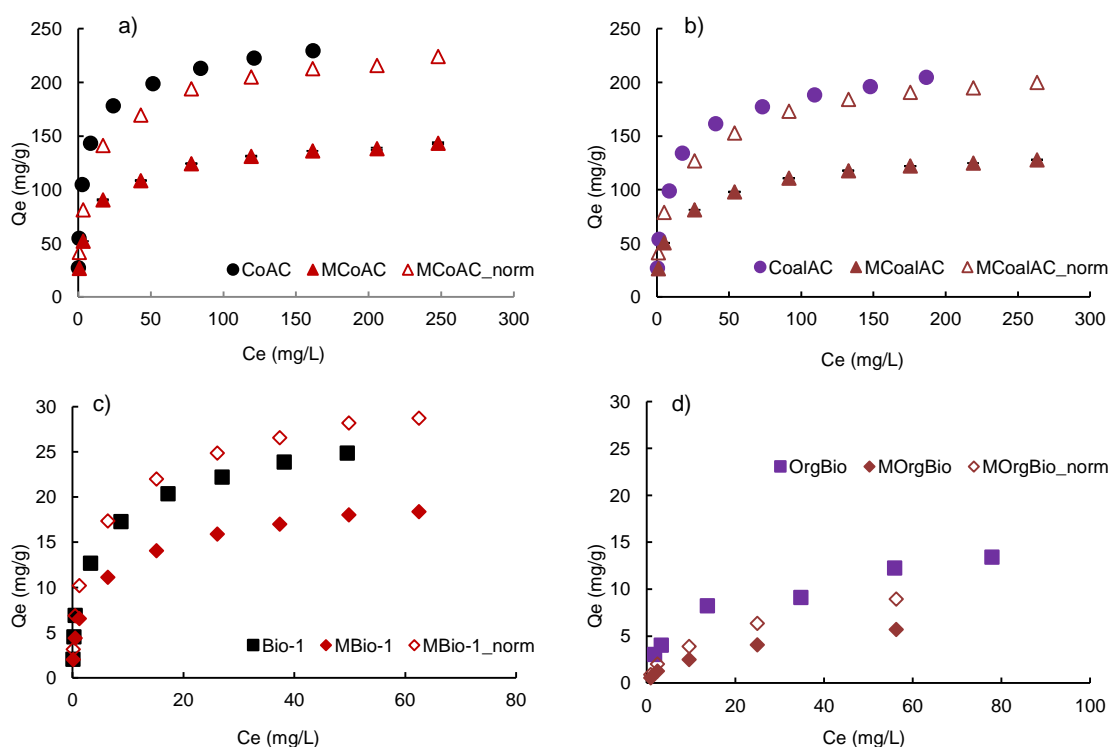
Figure 4.1: Sorption of phenol @ 22°C on (a) CoAC & MCoAC, (b) CoalAC & MCoalAC, (c) Bio-1 & MBio-1 and (d) OrgBio & MOrgBio

The sorption isotherms for the sorption of phenol on ACs and BCs is shown in Figure 4.1. The isotherms depict nonlinear curves that are very steep at low concentration. In this range, sorbent-sorbate interaction supersedes by far the sorbate-solute interaction, therefore the phenol has higher affinity to partition in the solid phase more than it does the liquid phase. As the concentration increases, the curves gradually lose steepness because the sorbent dosage is constant. Thus, at high concentration the sorption sites are almost completely occupied and the sorbent is within its saturation limit.

Phenol uptake on the ACs is within the same order of magnitude, although the coconut based activated carbon (CoAC) seem to have better phenol sorption than the coal based activated carbon (CoalAC). This can be seen that in Figure 4.1(a), the isotherm for the CoAC is steeper and corresponding C_e values are less that what is recorded for the CoalAC. As has been presented in Table 3.1, it can easily be seen that the two sorbents have equal surface area (A_S). However, CoAC has higher micropore volume (V_{MP}) value which could be the reason why it has better phenol sorption capacity. This suggests that phenol sorption is influenced by the V_{MP}. There is no doubt that V_{MP} together with A_S significantly govern the sorption capacities of the sorbents, hence the ACs –due to their superior surface area and well developed pore system– present about 2 order of magnitude higher phenol uptake as compared to the BCs. Accordingly, Bio-1, which has higher A_S and V_{MP} exhibit higher phenol uptake as compared to OrgBio.

The magnetic sorbents appear to have lower phenol uptake compared to their corresponding pristine pairs. It should be noted however, that the composites have about 36% less carbon content than their pristine pairs, because they are composites with magnetite. This by extension indicate they have in the same proportion, less A_S and V_{MP} available for phenol uptake. Therefore, when phenol sorption on the composites is normalised with respect to the mass of carbon in the composites, the isotherms almost overlap, as observed in Figure 4.1. It can therefore be deduced that, in order to have the same phenol sorption, the dosage of magnetic composites should be increased by 36 % to make up for the deficit in carbon content.

4.3.2 MODELLING OF SORPTION ISOTHERMS DATA:

For the purpose of assessment and design of sorption processes, mathematical models are used to evaluate the experimental data. The result is a summary of numerical values that are useful for direct comparison of different materials as well as the prediction of sorption behaviour in a replicated/modified conditions. This is crucial in the transfer of the process from laboratory to field application.

4.3.2.1 Linear Isotherm Model
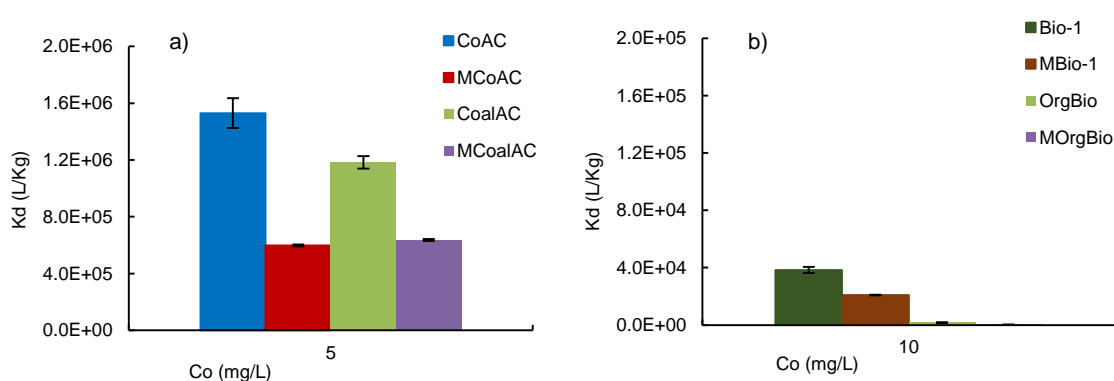
Figure 4.2:   Partitioning coefficient for sorption of phenol @ 22°C on (a) ACs and (b) BCs

The linear model is used essentially to assess the partition behaviour of phenol between the liquid and solid phases within the low concentration region (linear part) of the isotherm. Higher values of partition coefficient (K_d), is an indication of phenol's preference for the solid phase and vice versa. The K_d for the sorbents have been computed from the low concentration range of the isotherm (at Co = 5 and 10 mg/L for ACs and BCs resp.) and the result is shown in Figure 4.2.

Phenol partitions on CoAC more than it does on the other sorbents as follows CoalAC [22.69%], Bio-1 [97.49%] and OrgBio [99.89%]. Based on the K_d value, the sorbents can be ranked in the order phenol uptake as; MOrgBio < OrgBio < MBio-1 < Bio-1 < MCoAC < MCoalAC < CoalAC < CoAC. According to this model, the difference in phenol uptake between the composites and their pristine pairs is in the range of 45.4 to 62.84 % with an average of 53.85%. This difference is not proportional to that due to varied carbon content between corresponding pairs. Which is therefore an indication that at this concentration

level, the presence of iron oxide on the surface of the sorbents can somewhat reduce their phenol partition behaviour. Nonetheless, excepting the reading for OrgBio and MOrgBio, the K_d value is satisfactory for the rest of the sorbents to be used in water treatment.

4.3.2.2   Nonlinear Isotherm Models

Unlike the linear model, the nonlinear models can be used to evaluate the isotherm over the entire range of concentration considered. Another advantage of the nonlinear models is that they can give an insight into the intensity of sorbent-sorbate interaction, nature of surface coverage and mechanism of sorption.

Table 4.1:   Model parameters for sorption isotherms of phenol @ 22°C on ACs and BCs; (obtained using linear regression)

Model	Parameter	CoAC	MCoAC	CoalAC	MCoalAC	Bio-1	MBio-1	OrgBio	MOrgBio
	Q_m	231.15	145.51	207.62	131.52	25.21	18.85	14.49	6.78
	K_L	0.23	0.10	0.13	0.08	0.44	0.34	0.10	0.08
LANG	R^2	0.9854	0.9843	0.9830	0.9761	0.9717	0.9773	0.9486	0.9783
	$1/n$	0.28	0.27	0.31	0.27	0.35	0.33	0.38	0.54
	K_F	63.71	35.13	46.31	30.37	7.36	5.31	2.57	0.69
FREU	R^2	0.9422	0.9533	0.9552	0.9702	0.9737	0.9745	0.9731	0.9914
	K_R	433.25	84.79	192.62	70.87	61.26	40.63	3.82	0.85
	A_R	4.80	1.54	2.89	1.58	5.82	5.64	0.82	0.35
	γ	0.80	0.82	0.77	0.80	0.77	0.76	0.76	0.77
RED-PET	R^2	0.9869	0.9920	0.9867	0.9943	0.9980	0.9956	0.9756	0.9937

Methods of linear regression were used to fit the isotherm data to linear transformed models (LTFM). The plots of the LTFM are presented in appendix A1 and the model parameters presented in Table 4.1 were obtained from the slopes and intercepts of those plots, as explained in 2.10.1.2. These parameters were used to simulate isotherms, and the model that gives the R^2 value closest to unity is regarded as the best to describe the experimental isotherm data. All models correlated well with experimental data and generally, high R^2 values were recorded (0.9422 – 0.9980) as can be seen.

Assessment of the R^2 values indicates that for all sorbents, the Redlich-Peterson model has the highest R^2 value, therefore it has the closest resemblance with the experimental data. Furthermore, except for Bio-1, OrgBio and MOrgBio, the Langmuir model is more capable of describing the

experimental isotherm because its R^2 values are higher than the Freundlich model. Therefore, this indicates that the sorption of phenol on CoAC, MCoAC, CoalAC, MCoalAC and MBio-1 is due to monolayer coverage over a homogenous surface, according to the Langmuir theory. While sorption on Bio-1, OrgBio and MOrgBio likely is due to multilayer coverage over a heterogeneous surface according to the Freundlich theory. It should be noted that this distinction is not significant, since the R^2 values for the two models about a given sorbent are not much different. The Redlich-Peterson model is usually adopted to further distinguish which of the two models (Langmuir or Freundlich) is more appropriate in describing the type of isotherm. If the Redlich-Peterson heterogeneous exponent 'γ' is close to 1, the isotherm is Langmuir type, otherwise it is Freundlich. The value of γ, is not so close to unity and therefore tends to favour the Freundlich type of isotherm which contradicts the outcome of phenol sorption on the ACs and MBio-1 according to the R^2 value. This therefore highlights the need to exercise caution when judgement is drawn based on R^2 value and by extension the limitation of the LTFM methods. It is apparent a more rigorous error analysis involving more error functions is required to further distinguish the suitability of models under consideration.

Table 4.2: Results of optimised error functions for the sorption of phenol @ 22°C on CoAC

Model	CoD	HYBRID	MPSD	ARE	EABS	ERSSQ	ASE*
LANG_L	0.9666	529.14	36.27	19.22	116.75	2134.03	472.58
FR_L	0.9355	346.55	17.03	12.58	157.57	4132.25	777.68
RP_L	0.9865	66.73	7.26	4.96	63.77	655.2	132.99
LANG	0.9700	324.51	22.01	17.19	109.61	1693.59	361.16
FREU	0.9609	272.59	16.55	12.01	100.96	1675.16	346.22
RED-PET	0.9973	35.71	6.98	4.03	44.34	124.6	35.94
DA	0.9996	5.57	3.03	1.26	8.79	18.15	6.13
PDM	0.9996	0.06	3.03	1.53	0.09	0.00	0.79

* ASE = [(1-CoD) + HYBRID + MPSD + ARE + EABS + ERSSQ]/6
Key: LANG_L (LTFM Langmuir), FR_L (LTFM Freundlich), RP_L (LTFM Redlich-Peterson), LANG (Langmuir), FREU (Freundlich), RED-PET (Redlich-Peterson), DA (Dubinin-Ashtakov) and PDM (Polanyi-Dubinin-Manes)

Nonlinear regression method was applied to fit the isotherm data to the models in their original nonlinear form by optimising each of the six error functions mentioned earlier in 3.7.3. For a given model, each error function will generate a unique set of parameters and consequently a unique simulated isotherm. The parameters generated by all the error functions for each model for all the sorbents

are presented in appendix A2. For a given model and sorbent, the error function whose simulated isotherm had the best coefficient of non-determination will have its parameters chosen to represent that model (Kumar *et al.*, 2008b). Furthermore, the values of individual error function were averaged. This average –referred here as the average sum of error (ASE)– was used to compare the conformity of the models to the experimental data. The result for optimised error functions for phenol sorption on CoAC is shown in Table 4.2 as an example.

The ASE is used to evaluate the overall relative error distribution between experimental and simulated isotherm. Therefore, the less the ASE value for a given model, the more is the resemblance between its predicted isotherm and the experimental isotherm. The summary of the ASE for all the sorbents is shown in Table 4.3.

Table 4.3: Summary of ASE for the sorption of phenol @ 22°C on ACs and BCs

Model	CoAC	MCoAC	CoalAC	MCoalAC	Bio-1	MBio-1	OrgBio	MOrgBio
LANG_L	472.58	171.07	300.48	166.68	28.56	18.48	10.64	6.77
FR_L	777.68	178.94	419.28	87.50	15.39	9.37	4.61	4.28
RP_L	132.99	27.81	98.07	15.41	1.74	1.87	4.34	2.52
LANG	361.16	129.72	261.91	133.78	19.40	13.50	7.80	4.80
FREU	346.22	108.62	209.68	56.09	10.27	7.02	4.46	3.96
RED-PET	35.94	16.46	47.47	11.90	1.48	1.62	4.03	1.93
DA	6.13	4.99	21.52	3.99	1.41	0.33	4.41	1.85
PDM	0.79	0.53	1.10	0.42	0.91	0.20	2.38	1.69

Although the LTFM exhibit satisfactory fitting of experimental data, the nonlinear fitting method generally produce better error function values. As a result, the nonlinear models have much lower ASE value than their corresponding LTFM pairs, for all sorbents. Therefore, the nonlinear models are considered henceforth since they are expected to return more accurate model parameters. With particular reference to the 2-parameter models, it should be noted that based on the result of optimised error functions for the nonlinear models, for all sorbents, the Freundlich model has better conformity to experimental data compared to the Langmuir model. This agrees with the conclusion drawn earlier based on the value of γ in the case of the LTFM.

Table 4.4: Summary of MSC for isotherm prediction using optimised model parameters for sorption of phenol @ 22°C on ACs and BCs

Model	CoAC	MCoAC	CoalAC	MCoalAC	Bio-1	MBio-1	OrgBio	MOrgBio
LANG	2.57	2.53	2.84	2.11	2.57	2.47	2.08	3.30
FREU	2.78	2.79	3.06	3.36	3.73	3.69	2.98	4.49
RED-PET	5.22	4.92	4.41	4.87	6.02	5.69	2.76	5.83
DA	7.15	6.16	5.25	6.13	6.50	7.47	2.71	5.76
PDM	7.15	6.16	5.27	6.13	6.50	7.47	2.70	5.76

Compared to the 3-parameter models, the 2-parameter models have higher values of the ASE, which shows that they have higher relative error distribution between their simulated isotherm and the experimental data. This shows the superiority of the 3-parameter models in conforming to experimental data. In particular, the PDM model has the overall best ASE values, suggesting phenol uptake to progress according to the micropore filling mechanism. The result for the test for redundancy of model parameters presented in Table 4.4, shows that that the 3-parameter models actually contain more information about the system (Koeppenkastrop and De Carlo, 1993; Saiers and Hornberger, 1996) and thus have higher MSC values compared to the 2-parameter models. Hence the 3-parameter models can reliably be applied to evaluate the experimental data. It is worth mentioning that, although the two Polanyi related models differ in in terms of their derivations and expressions, they produce very similar parameters.

The summary of the optimised model parameters is presented in Table 4.5, while the parameters obtained using each of the error function for all the sorbents is presented in appendix A2 (Tables A1 to A8). A plot of the optimised simulated isotherms as compared to the experimental curve for CoalAC, MCoalAC, Bio-1 and MBio-1 is shown in Figure 4.3 as example. The remaining plots for the other sorbents are presented in appendix A3. The simulated and experimental isotherms are quite identical. This suggests that their parameters can help in describing the sorption system within the examined range of concentration.
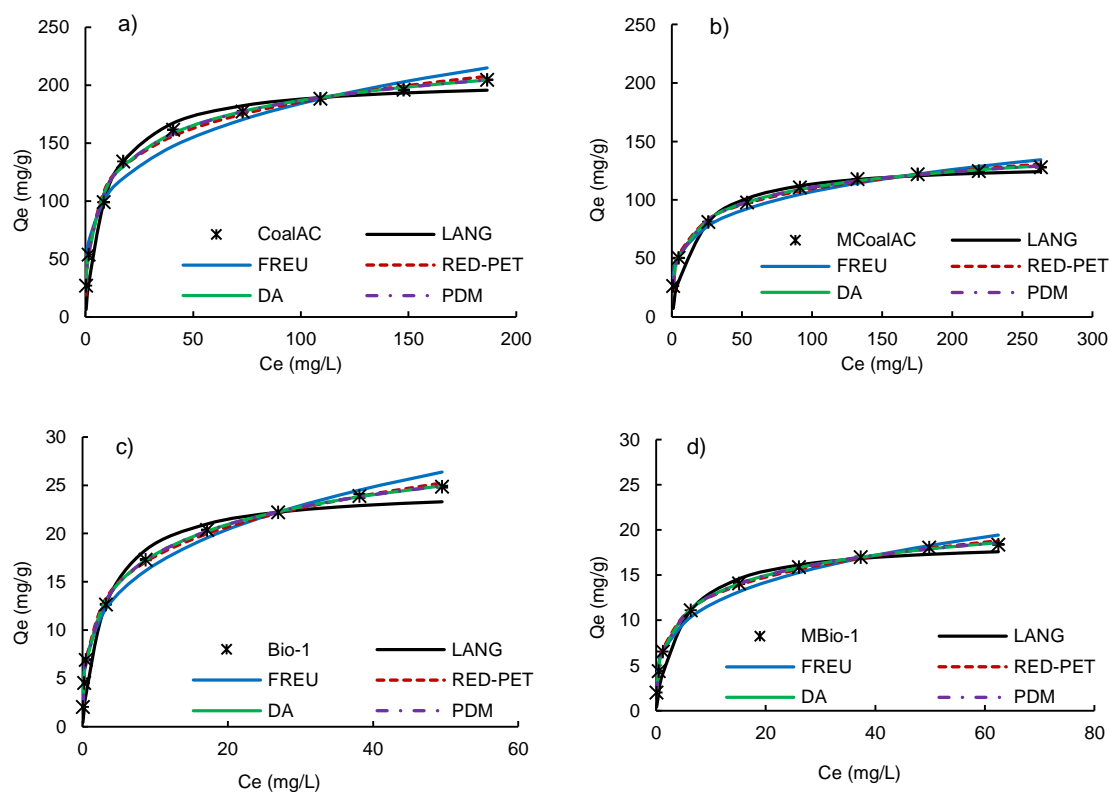
Figure 4.3:   Comparison of simulated and experimental isotherm plot for sorption of phenol @ 22°C on (a) CoalAC, (b) MCoalAC, (c) Bio-1 and (d) MBio-1

Table 4.5:   Optimised isotherm model parameters for sorption of phenol @ 22°C on ACs and BCs

Model	Parameters	CoAC	MCoAC	CoalAC	MCoalAC	Bio-1	MBio-1	OrgBio	MOrgBio
Linear	K_d	1.53E+06	5.98E+05	1.18E+06	6.36E+05	3.84E+04	2.10E+04	1.73E+03	6.42E+02
LANG	Q_m	225.21	144.76	205.35	131.89	24.73	18.83	14.44	7.39
	K_L	0.21	0.10	0.11	0.06	0.33	0.23	0.09	0.06
FREU	$1/n$	0.21	0.22	0.25	0.24	0.28	0.28	0.36	0.47
	K_F	85.03	43.59	58.80	36.19	8.77	6.23	2.76	0.84
RED-PET	K_R	206.06	53.76	86.64	49.71	49.65	24.05	5.69	1.31
	A_R	1.76	0.79	0.98	0.97	4.38	2.83	1.50	0.93
	γ	0.86	0.86	0.83	0.83	0.79	0.80	0.71	0.63
DA	Q_o	272.96	173.32	265.09	171.91	39.78	27.97	44.39	22.47
	E	32.89	30.68	30.52	30.19	32.51	32.13	24.66	23.03
	b	3.42	3.29	3.11	2.78	2.80	2.93	1.81	2.14
PDM	Q_o	272.97	173.34	265.12	171.16	39.74	27.98	41.69	22.49
	a	28.75	31.80	26.82	19.55	16.20	19.06	10.59	17.56
	b	3.42	3.29	3.11	2.79	2.80	2.93	1.88	2.14

4.3.2.3 Phenol Sorption Capacities

According to the capacity parameter of all models presented in Table 4.5, the ACs have higher phenol sorption capacities than the BCs. Similarly, the ACs can be ranked in the order of phenol uptake as MCoalAC < MCoAC < CoalAC < CoAC. However, there is some discrepancy in the ranking of the BCs. According to Langmuir, Freundlich and Redlich-Peterson models, the ranking for the BCs is in the order MOrgBio < OrgBio < MBio-1 < Bio-1, while their order is MOrgBio < MBio-1 < Bio-1 < OrgBio according to the Polanyi based models. Assessment of the MSC values in Table 4.4 indicates that the Polanyi based models are not good in describing the sorption of phenol on OrgBio. Instead, the Freundlich model has highest MSC value and thus can describe its isotherm better. Hence it is more likely that the order for the BCs is as presented by Freundlich.

Table 4.6:   Sorption of phenol @ 22°C on ACs and BCs; Pearson correlation coefficients between model parameters and sorbent properties

Model	Parameters	A_S	V_P	V_{MP}	P_S
Linear	K_d	0.9573	0.8488	0.9731	0.4483
Langmuir	Q_m	0.9834	0.9070	0.9895	0.4512
	K_L	0.0308	0.1637	0.0031	0.3490
Freundlich	$1/n$	0.7726	0.7195	0.7633	0.4405
	K_F	0.9579	0.8418	0.9762	0.4623
Redlich-Peterson	K_R	0.8094	0.6264	0.8483	0.4788
	A_R	0.3158	0.3958	0.2979	0.1782
	γ	0.8029	0.7602	0.7902	0.5079
Dubinin-Ashtakov	Q_o	0.9754	0.8970	0.9829	0.4045
	E	0.6080	0.5584	0.5949	0.6496
	b	0.8242	0.7929	0.8085	0.7720
Polanyi-Dubinin-Manes	Q_o	0.9769	0.8994	0.9841	0.4119
	a	0.8276	0.7997	0.8214	0.6013
	b	0.8280	0.7900	0.8144	0.7522

Additionally, the sorbents capacity influencing properties (A_S, V_P, V_{MP} and P_S) from Table 3.1, were correlated with model capacity parameters (K_d, Q_m, K_F and Q_o) from Table 4.5. The result shown in Table 4.6 reveals that the V_{MP} has the highest correlation (generally, Pearson correlation coefficient $R = 0.9731$ to 0.9895) with model capacity parameters. This suggest that phenol sorption is significantly influenced by V_{MP}. Therefore, it is not unusual that the Polanyi related models –whose derivation were based on the micropore filling

mechanism– are poor in describing the sorption of OrgBio (which is strictly non-microporous).

There still exist some satisfactory correlation (generally, Pearson correlation coefficient $R = 0.9059\ \text{to}\ 0.9711$) as shown in Table 4.7, between the model capacity parameters and the mass normalised sorbents' capacity factors. This therefore is a further indication that the sorption of phenol depends on surface area and pore characteristics. However, there is poor correlation between sorbents capacity influencing properties and the sorption intensity parameters.

Table 4.7:   Sorption of phenol @ 22°C on ACs and BCs; Pearson correlation coefficients between normalised model capacity factors and sorbent properties

Model	Parameters	A_S	V_P	V_{MP}	P_S
Linear	K_d	0.9686	0.9059	0.9711	0.4515
Langmuir	Q_m	0.9312	0.9190	0.9196	0.4330
Freundlich	K_F	0.9424	0.8829	0.9445	0.4567
Dubinin-Ashtakov	Q_o	0.9260	0.9201	0.9132	0.4012
PDM	Q_o	0.9277	0.9221	0.9146	0.4077

Finally, according to Q_m and Q_o, the difference in phenol uptake between the composites and their pristine pairs is in the range of 36.11 to 49.11 % with an average of 36.87 %. This difference is very similar to that due to varied carbon content (ca 36 %) between corresponding pairs. Which is therefore an indication that over the concentration range studied, the presence of iron oxide on the surface of the sorbents does not cause a significant alteration in their phenol partition behaviour.

4.3.2.4   Phenol Sorption Affinity

From Table 4.5, the order of sorbents ranking according to models sorption intensity and heterogeneity factors for Freundlich and Redlich-Peterson models goes as: [n, MOrgBio < OrgBio < MBio-1 = Bio-1 < CoalAC ≈ MCoalAC < MCoAC ≈ CoAC; and γ, MOrgBio < OrgBio < Bio-1 ≈ MBio-1 < MCoalAC = CoalAC < MCoAC = CoAC respectively]. The order of ranking based on the two models is quite similar which in turn differs much from the Langmuir sorption intensity factor whose ranking goes as: [K_L: MOrgBio = MCoalAC < OrgBio < MCoAC < CoalAC < CoAC < MBio-1 < Bio-1]. It has been previously shown in Table 4.3, that the

Freundlich has better conformity to experimental data compared to the Langmuir. Therefore, the Freundlich model is most suitable to describe the sorption preference of phenol with respect to the nature of the sorbent's surfaces. Hence, the sorption of phenol is favourable on the sorbents, since in all instances, the heterogeneity exponent $n > 1$ (Hamdaoui and Naffrechoux, 2007a; Murugesan *et al.*, 2013). The larger the value of $n,$ the more the heterogeneity (Newcombe *et al.*, 1997; Goldberg *et al.*, 2005; Zhang *et al.*, 2007). The values of both n and γ can be grouped into two classes; higher values for the ACs and lower values for the BCs. The ranking of these groups, indicates that the sorption of phenol is more favourable as the heterogeneity of the surfaces increases (Li *et al.*, 2002). It should also be noted that excepting OrgBio and MOrgBio, the intensity and heterogeneity factors for both Freundlich and Redlich-Peterson models for corresponding pairs of sorbents are quite identical. This shows that the phenol sorption affinity for the magnetic composites and the pristine carbon are similar.

From the foregone, it can be concluded that the two ACs have about the same phenol sorption properties. However, since the coconut shell based AC has slightly better sorption capacity and affinity, it is selected to represent the ACs in subsequent experiments. In the case of the BCs, it is obvious that the woodchip based biochar has superior sorption properties and is thus selected to represent the BCs in further work.

4.3.3 EFFECT OF TEMPERATURE ON SORPTION OF PHENOL

Temperature can influence the sorption of a compound from solution for better or for worse, due to its impact on the properties of the sorbate, sorbent surface properties and sorbent-sorbate interactions. Notwithstanding, the outcome of a given sorption system cannot be predicted easily, despite the knowledge of the aforesaid principles, since the influence is not unidirectional in all cases. For instance, increase in temperature can on the one hand, bring about increased mobility of sorbate molecules. This can be advantageous to both sorption systems that have diffusion process as rate determining and those in which the sorbate binds to the surface of the sorbent mainly by chemisorption (endothermic based). While on the other hand, increased solubility at higher temperature can undermine sorption systems in which the removal of sorbate

from solution depends on hydrophobic interactions. Also, the uptake of the sorbate is impaired if sorption progresses mainly as physisorption (exothermic based). Furthermore, it has been reported by Dąbrowski *et al.* (2005); Busca *et al.* (2008) that, in the case of phenol, increase in temperature causes a decrease in the effect of the sorbent's surface-chemical composition on its sorption. Under such a situation, the mechanism of phenol sorption then depends mainly on the porous structure of the sorbent and so sorption kinetics is governed by intraparticle diffusion.
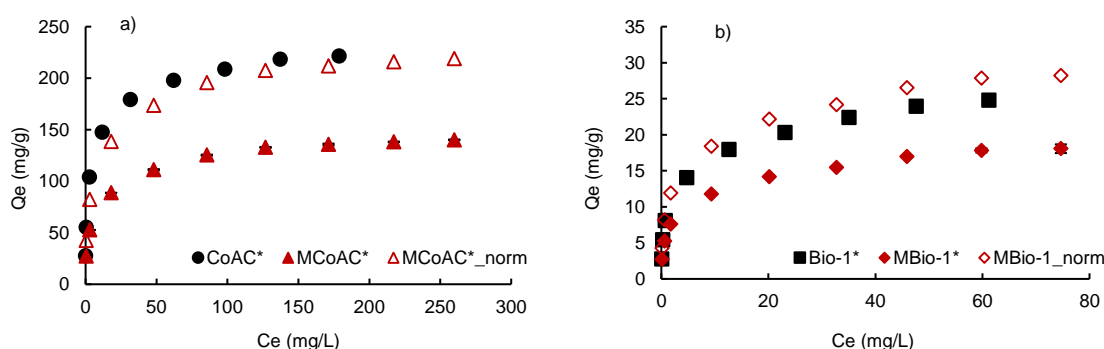
Figure 4.4:   Sorption of phenol @ 10°C on (a) ACs* and (b) BCs*

Most phenol sorption experiments are conducted at moderate temperatures (Banat *et al.*, 2000; Yang *et al.*, 2008; Mohd Din *et al.*, 2009; Kilic *et al.*, 2011), which shows that its uptake is majorly by an exothermic process (physical adsorption). Therefore, within this temperature region it has mostly been reported that adsorption capacities tend to increase with a decrease in temperature (Weber, 1974; Kennedy *et al.*, 2007; Gundogdu *et al.*, 2012; Hua *et al.*, 2012).

Table 4.8:   Summary of ASE for the sorption of phenol @ 10°C on ACs* and BCs*

Model	CoAC*	MCoAC*	Bio-1*	MBio-1*
LANG_L	683.38	238.17	34.37	23.98
FR_L	449.46	124.90	7.79	5.01
RP_L	129.13	44.44	1.75	1.32
LANG	564.76	199.95	24.73	16.74
FREU	215.82	83.41	5.61	4.01
RED-PET	60.46	31.97	1.47	1.19
DA	7.04	10.93	0.30	0.65
PDM	0.61	0.80	0.21	0.38

The isotherm for the sorption of phenol at lowered temperature (10°C) is shown in in Figure 4.4. The isotherms exhibit quite similar features with those obtained at 22°C, i.e. presented in Figure 4.1. In general, there is no significant difference between the two data sets (p-value = 0.697). Hence, quite similar outcomes were obtained when the data was subjected to the same analysis as was done previously and the results are presented in Tables 4.8 to 4.10 and Figure 4.5.

Table 4.9: Optimised isotherm model parameters for sorption of phenol @ 10°C on ACs* and BCs*

Model	Parameters	CoAC*	MCoAC*	Bio-1*	MBio-1*
LANG	Q_m	223.31	143.16	24.65	18.45
	K_L	0.17	0.09	0.28	0.30
FREU	$1/n$	0.19	0.21	0.26	0.24
	K_F	85.65	45.97	8.80	6.69
RED-PET	K_R	540.66	121.14	84.01	50.18
	A_R	5.29	2.03	8.10	6.62
	γ	0.84	0.84	0.78	0.79
DA	Q_o	284.13	182.50	44.19	31.14
	E	32.92	30.64	31.18	31.28
	b	2.75	2.74	2.27	2.29
PDM	Q_o	288.55	182.52	44.03	31.17
	a	14.18	17.88	10.56	10.58
	b	2.70	2.74	2.28	2.28

The nonlinear fitting method generally produce better error function values. As a result, the nonlinear models have much lower ASE value than their corresponding LTFM pairs, for all sorbents (see Table 4.8). Consequently, the nonlinear models are chosen for further discussions. The 3-parameter models have lower ASE values than the 2-parameter model which suggests higher conformity to experimental data. Overall, the PDM model has the best ASE values, once again suggesting phenol sorption according to the micropore filling mechanism as observed at room temperature (22°C). Furthermore, the Freundlich has better conformity to experimental data compared to the Langmuir, suggesting sorption over heterogeneous surface. The optimised isotherm model parameters are summarised in Table 4.9, while the parameters obtained using all the error functions are presented in Appendix A (Tables A9 to A12). Here once again, the Polanyi related models produced very identical parameters.

It can be observed in the Table 4.10, that test for redundancy of model parameters shows that the 3-parameter models have higher MSC values and are thus reliable in describing the experimental isotherm. Also, plots of the optimised simulated isotherms for both the ACs and BCs are overlying the experimental data points as shown in Figure 4.5.

Table 4.10: Summary of MSC for isotherm prediction using optimised model parameters for sorption of phenol @ 10°C on ACs* and BCs*

| MODEL	CoAC*	MCoAC*	Bio-1*	MBio-1*
Langmuir	1.96	2.05	2.16	2.09
Freundlich	3.23	3.18	4.35	4.15
Redlich-Peterson	4.45	4.00	6.20	5.61
Dubinin-Ashtakov	6.70	5.21	7.94	6.37
Polanyi-Dubinin-Manes	6.62	5.21	7.89	6.37
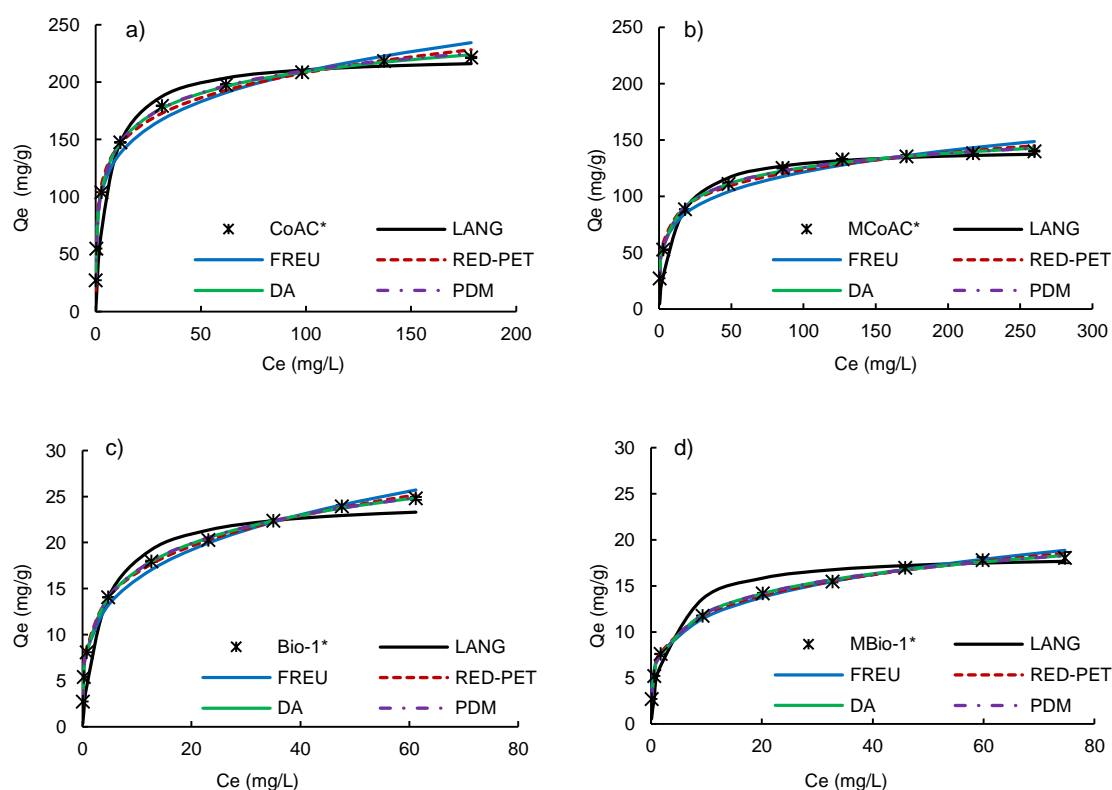
Figure 4.5: Comparison of simulated and experimental isotherm plot for sorption of phenol @ 10°C on (a) CoAC*, (b) MCoAC*, (c) Bio-1* and (d) MBio-1*

While the data for both temperatures are identical, a slight increase in phenol sorption capacity is recorded with decrease in temperature according to the capacity factors of both the Freundlich and the Polanyi theory based models.

However, the decrease is not statistically significant (p-value = 0.697). Probably, the extended equilibrium duration (7 days), as used in this study, may have neutralised the effect of temperature on sorption kinetics over the studied range; [shorter equilibrium periods; 48 hr and less; were used in most studies (Park *et al.*, 2010; Gundogdu *et al.*, 2012; Giraldo and Moreno-Piraján, 2014) where significant increase in sorption was recorded for a decrease in temperature]. Therefore, to have a better understanding of the effect of temperature on phenol sorption for the given sorbents, it is essential that further work should be done over short duration and/or at elevated temperature.

4.3.4 POLANYI CHARACTERISTIC CURVE

From the forgone, the Polanyi theory based models have recorded very high quality data fitting for both temperatures. These models are mainly used to verify whether sorption progresses according to the micropore filling mechanism or not. Essentially, the characteristic curve for the system is used to further test whether the model mechanistically captures this. According to this theory, the correlation curve is temperature invariant for a given system. As such, the curve for the same system at a different temperature will be identical.
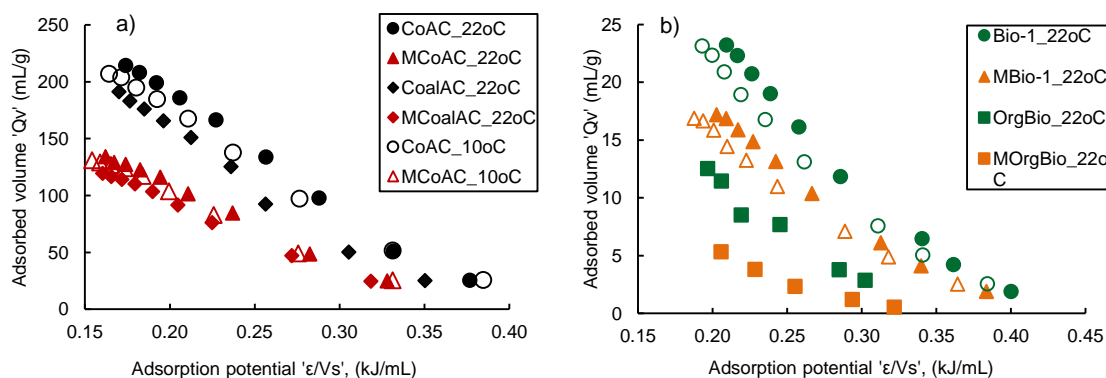
Figure 4.6:   Polanyi characteristic curve for the sorption of phenol @ both 10 and 22°C on; a) ACs and (b) BCs

The characteristic curve for the sorbents at the two temperatures is presented in Figure 4.6. For the ACs, including the coal based AC, two distinct groups of data points representing the somewhat single curve, one each for the magnetic and nonmagnetic types can be observed i.e. Figure 4.6(a). This indicates that the sorption of phenol by micropore filling mechanism is valid on these sorbents. A similar curve for the BCs, including the organic biomass based

biochars is presented in Figure 4.6(b). The seemingly single curve can be observed one each for the magnetic and nonmagnetic type. However, no such single curve was observed for the OrgBio which is strictly non-microporous.

A further test for the validity of the micropore filling mechanism is that a single curve should be obtained for different sorbents when their characteristic curve is normalised with respect to their micropore volume (Long *et al.*, 2008). A single curve was obtained for the ACs after normalisation as can be observed in Figure 4.7(a). This strongly suggests that the Polanyi theory is valid for the sorption of phenol on the ACs. However, from Figure 4.7(b), it can be seen that for the BCs, no such single curve was obtained after normalisation. It can therefore be concluded for the BCs that while the Polanyi theory was satisfied in terms of isotherm fitting, it was only partially satisfied in terms of the characteristic mechanism. This is because of their low microporosity or its complete lack of it.
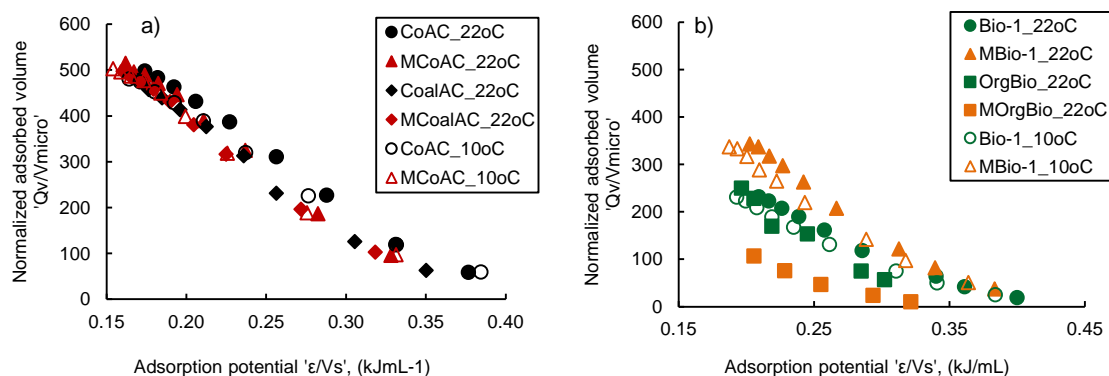
Figure 4.7: Normalised Polanyi correlation curve for the sorption of phenol @ both 10 and 22°C on; (a) ACs and (b) BCs

4.3.5 MECHANISM OF PHENOL SORPTION

It has been established in the forgone section, that the sorption of phenol progresses according to the micropore filling mechanism. This is to say that the main active sites are contained in the micropores of the AC. Although, other active sites located in the macropores and external surface also contribute -to a much lesser degree- to the total sorption of phenol. Generally, phenol sorption on an active site is possible due to the action of electrostatic interactions and van der Waals forces that include the formation of hydrogen bonding, dispersion interactions, aromatic staking and π - π interactions (Busca *et al.*, 2008).

The delocalised π electrons of the basal planes of the microcrystalline structure of the AC can engage the π electrons of the aromatic rings of phenol. This facilitates the binding of phenol to the surface of the AC by the so called "π - π interactions" (Snoeyink and Weber, 1967). In such interaction, the π electron on the basal plane of the AC act as the donor, while that of the aromatic ring of phenol act as the acceptor (Mattson *et al.*, 1969). The π electron rich regions constitute the Lewis base type of sites whose electron density diminishes as the oxygen content of the carbon is increased (Lopez-Ramon *et al.*, 1999). This oxidation brings about the localisation of the π electron (Coughlin and Ezra, 1968) and thus a reduction in phenol uptake, since sorption of phenolic compounds is more favoured on basic carbon surfaces (Dąbrowski *et al.*, 2005) .

Phenol also sorb on active sites by the formation of another donor-acceptor mechanism with surface oxygen groups (Tseng *et al.*, 2003). Particularly the carbonyl oxygen groups which have a larger dipole moment than the carboxylic acid groups can engage phenol in the formation of a strong donor-acceptor complex mechanism. The carbonyl oxygen and other basic surface groups will act as the electron donors and the aromatic ring of phenol acts as the acceptor (Dąbrowski *et al.*, 2005). In contrast, the oxidation of the surface carbonyl groups to carboxylic acid groups reduces the carbon's electron acceptor capacity and this causes a reduction in phenol sorption (Mattson *et al.*, 1969). Also, at low pH, the sorption of phenol is decreased due to the competition of H^+ for sorption to carbonyl sites.

Electrostatic interaction is another mechanism by which phenols sorb to the carbon. This interaction is governed by the influence of pH on both the dissociation potentials of phenol molecules and the surface charge of the carbon. At low pH, i.e. pH < pKa, phenol molecules exist in neutral form. At high pH, they exist as dissociated phenolate anions. In a similar manner, the surface of the AC is positively charged at pH < pH$_{PZC}$ and negatively charged at pH > pH$_{PZC}$. At moderate pH, i.e. pH > pKa and pH < pH$_{PZC}$, there will be electrostatic attraction between the positively charged carbon surface and negatively charged phenolate anion. Therefore, phenol sorption is favoured in this region. At high pH, i.e. if pH > pKa and pH > pH$_{PZC}$, there will be electrostatic repulsion between the negatively charged carbon surface and the phenolate anion. Therefore, phenol sorption is not favoured in this region, because in addition to electrostatic repulsion, the

dissociated form of the phenol molecule is more soluble (Liu and Pinto, 1997; Snoeyink and Summers, 1999; Dąbrowski *et al.*, 2005).
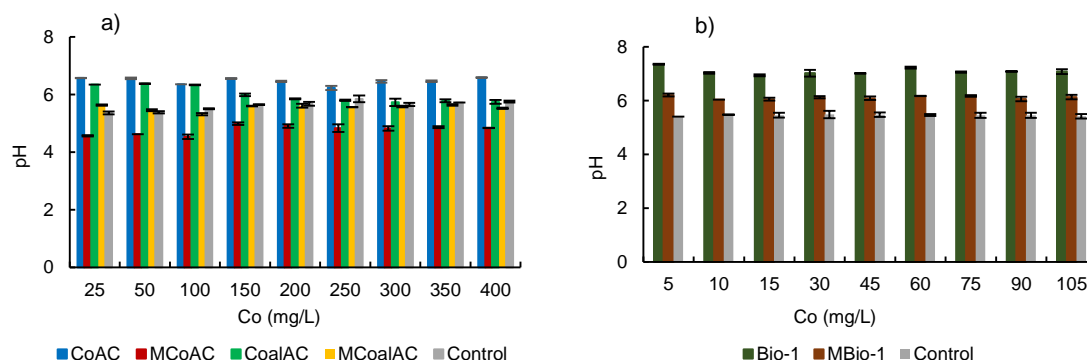
Figure 4.8: Final solution pH for the sorption isotherm of phenol on (a) ACs and (b) BCs

The experiments were conducted at moderate pH (see Figure 4.8), which is below both the pKa of phenol and the pH_{PZC} value for all the sorbents except MCoAC. Therefore, it is generally expected that since the neutral specie is predominant, phenol sorption should have progressed through the action of π - π dispersion interactions, electron donor-acceptor complex and solvent effects (Nevskaia *et al.*, 1999; Fierro *et al.*, 2008; Hameed and Rahman, 2008; Rodrigues *et al.*, 2011).

4.3.6 EFFECT OF SOLUTION PH ON SORPTION

According to the sorption pattern depicted by the AC over the range of pH examined. CoAC and MCoAC behaved in a similar way, the sorption of phenol was low at both extreme ends of the pH range (refer to Figure 4.9(a)). The sorption of phenol has be shown (Mattson *et al.*, 1969) to be governed by the "donor-acceptor complex" mechanism in which the carbonyl surface-oxygen groups acts as electron donor, and the aromatic ring of the solute acts as an acceptor. Thus at low pH, there exist additional/excess protons in the solution which compete with phenol for carbonyl sites resulting in a decrease in adsorption with decrease in solution pH (Snoeyink *et al.*, 1969; Dąbrowski *et al.*, 2005).
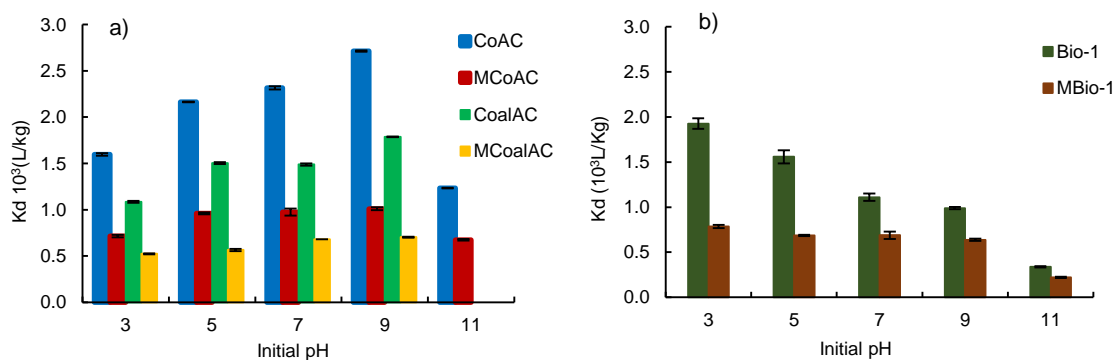
Figure 4.9: Partition coefficient for the effect of pH on sorption of phenol on a) ACs and b) BCs

Additionally, the sorbent becomes more polar and hydrophilic. Therefore, it preferentially engages water molecules to form hydrogen bonds and as a result, water clusters are formed that prevents phenol molecules access to sorption sites. It has been reported (Moreno-Castilla, 2004) that phenol is poorly adsorbed on acidic activated carbons. Increasing the surface acidity of activated carbons resulted in a decrease in the amount of phenol adsorbed from diluted aqueous solutions. Also the π electrons on the basal plane of the sorbent are localised due to increased oxidation. This impairs the sorption of phenol by the interaction of the π electrons. Hence, there is a general decrease in the uptake of phenol with increased acidity of the sorbent.

According to (Yang and Xing, 2010), neutral and dissociated species (cations by protonation) are the dominant species for organic acids and organic bases respectively at pH < pKa, while dissociated species (anion) and neutral species are dominant species for organic acids and organic bases respectively at pH > pKa. Acidic phenol exist in non-dissociated form at pH less than its pKa and it is preferentially adsorbed on carbon sorbents in this molecular form (Moreno-Castilla *et al.*, 1995). That is why there is an increase in phenol uptake as the acidity decreases. Also, the surface becomes increasingly hydrophobic as the pH increases resulting in an increase in phenol uptake (Weber, 1974). This continues until peak sorption is recorded around pH 9. In their work on the sorption of lubricating oil on Spirulina sp. and Scenedesmus abundans with pHPZC of 8.5 and 7.5 respectively, (Mishra and Mukherji, 2012) reported that the uptake of lube oil increased with increase pH to a peak around their respective pHPZC. This has been reported for several compounds.

In the high pH region, i.e. beyond the pKa region, the molecule dissociates and the concentration of the anionic specie continues to increase as the pH is increased further (Srivastava *et al.*, 1987; Aravindhan *et al.*, 2009). Our sorbents have high pH$_{PZC}$ values, all in excess of 9.0 (except for MCoAC). So it is expected that they will have net negative charge within the pH range higher than their pH$_{PZC}$. Therefore, the decrease in phenol uptake at pH above both the pH$_{PZC}$ of the sorbents and pKa of phenol is due to repulsion between the negatively charged sorbent surface and the anionic phenolate and also that between neighbouring anionic species (Dąbrowski *et al.*, 2005). However, the presence of 0.01 M CaCl$_2$ background solution can aid in neutralising this repulsive forces due to increased pairing of calcium ion with the phenolate specie. This trend was observed in the sorption of p-nitrophenol (PNP) on coconut-shell activated carbon in the presence of 1.0 M NaCl solution at pH 10.0 (Snoeyink *et al.*, 1969). Nonetheless, the dissociated specie is more hydrophilic, therefore its removal from the aqueous medium becomes even harder and can be possible only after a relatively higher solute-solvent bond is broken. The coal based ACs also exhibited the same trend to a lesser extent as observed in the coconut shell based ACs.

For the biochars, Figure 4.9(b) shows that there is a general decrease in phenol uptake with increase in pH. Although, the sorption of phenol on MBio-1 appears somewhat resistive to pH changes up to pH 9, the least phenol uptake was recorded at the highest pH. This is due to the increased solubility of the phenolate anion and electrostatic repulsion due to it having similar charge with the sorbent's surface. The high uptake of phenol on Bio-1 recorded at low pH is a bit unexpected, because the sorption of phenol is normally impaired in this region due to the high oxidation of its surface, its increased hydrophilicity and competition by H$^+$ for carbonyl adsorption sites. It is possible that the Bio-1 has special sites which makes it possible to preferentially bond with phenol. This could be due to the formation of ester bonds between the hydroxyl group of phenol and the carboxylic groups on the biochar surface (Salame and Bandosz, 2003).

The adsorption edge plot can show the relative fractions of the phenol sorbed in either neutral or ionised species over the studied pH range. The speciation model can be used to fit the adsorption edge data, the usual

expression for the model is given as (Schwarzenbach *et al.*, 2005; Yang *et al.*, 2008; Werner *et al.*, 2013).

$$K_d = A \frac{1}{1+10^{(\text{pH}-pKa)}} + B \left(1 - \frac{1}{1+10^{(\text{pH}-pKa)}} \right) \qquad - \qquad - \qquad - \qquad (4.1)$$

Where: A and B are the distribution coefficients of the neutral and ionised species of the sorbate respectively.
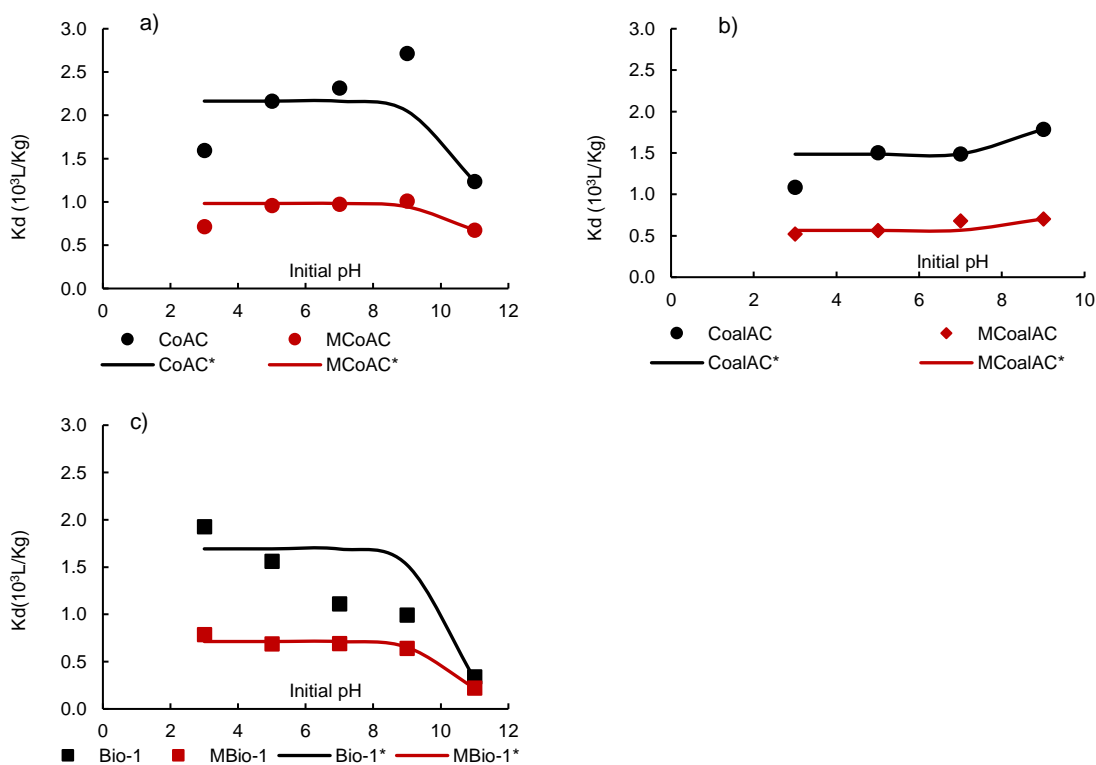
Figure 4.10: Modelling of pH data for sorption of phenol on (a) coconut shell AC, (b) coal AC and (c) biochar. Asterisk (*) represents fitted data

In situations where the model mechanistically captures the adsorption edge of a compound, good fitting is recoded and a point of inflection appears at a pH region near its pKa value. In this study, except for MBio-1 with $R^2 = 0.9658$, the model failed to yield good fitting to the adsorption edge data (generally $R^2 <$ 0.6850) as presented in Figure 4.10.

This model is mostly used to evaluate the sorption involving homoionic or non-functionalised, extremely low variable-charge surface sorbents (Haderlein and Schwarzenbach, 1993; Xiao and Pignatello, 2014). In essence, only the variation in the speciation of the sorbate and not the variation in the charge density of the sorbent is considered. Xiao and Pignatello (2014), reported many

similar cases where the model failed to mechanistically capture the adsorption edge of various compounds and sorbents. They postulated that due to inherent adsorption nonlinearity, it is possible for deviations to occur between the model predicted and observed adsorption edge. They even proposed a new model that considers the nonlinear nature of sorption and requires the isotherm data at different pH values to enable a better prediction of the adsorption edge. According to (Schwarzenbach *et al.*, 2005) the sorption of anionic species may be considered when dealing with hydrophobic acids. Otherwise, in weak acids with B significantly smaller than A, the sorption of neutral species dominates up to a pH of about 2 units above their pKa. Therefore the sorption of the anion may be neglected and consequently, A can be assumed to be constant over the whole pH range considered (Haderlein and Schwarzenbach, 1993) and the adsorption edge model reduces to the expression;

$$K_d = A \frac{1}{1+10^{(\text{pH}-pKa)}}$$ - - - - - - - (4.2)

4.3.7 EVALUATION OF SORPTION KINETICS
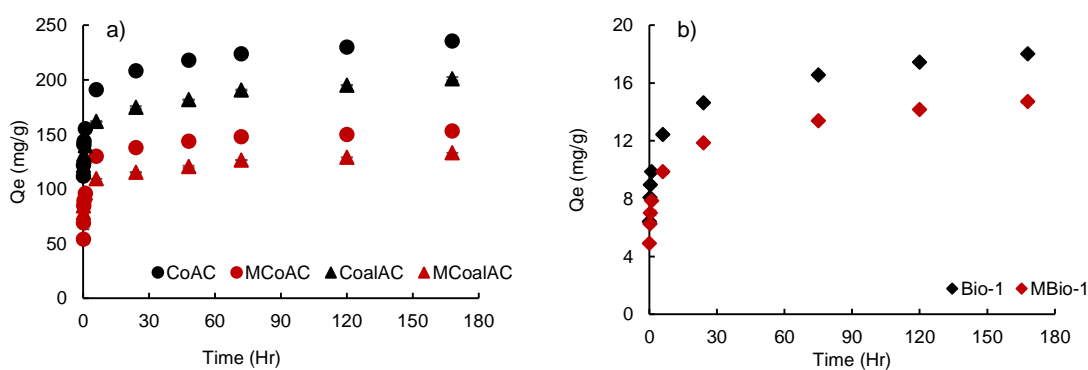
Figure 4.11: Plot of sorption kinetics for phenol on; (a) ACs and (b) BCs

Within 24 and 48 hours, all sorbents have reached at least 87 and 90% of the 7-day equilibrium respectively. In other words, it took another 24 hours just to add about 3% more uptake of phenol. This shows that phenol sorption continues at a very slow rate beyond the first 24 h. Therefore, apparent equilibrium is assumed to be attained within 48 hours and only the data within the first 24 hours is considered for analysis of the rapid adsorption kinetics.

The plot for the sorption kinetics is shown in Figure 4.11, and the curves are generally characterised by steep slopes within the first 6 hours. This zone of very fast kinetics is due to high concentration gradient and abundance of free potential sorption sites. The pores are more or less empty, hence the phenol molecules can access the interior sorption sites with much ease. With time, the pores and sorption sites gets progressively loaded. This in addition to loss in concentration gradient, leads to a reduction in sorption kinetics, consequently, the slope assumes a somewhat horizontal or plateau status which is maintained as the system approaches or attains equilibrium.

4.3.7.1   Attainment to Equilibrium
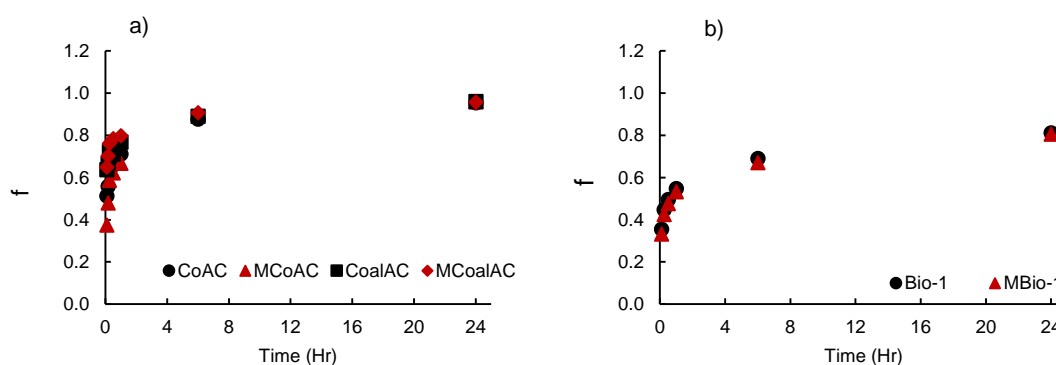
Figure 4.12:   Phenol sorption kinetics fractional uptake on; (a) ACs and (b) BCs

A plot of fractional uptake with time, the "$f - t$ plot", Figure 4.12, gives an insight to how close the system is to attaining an apparent equilibrium. It can be observed that magnetic sorbents have slightly lower f value compared to their corresponding pristine counterparts. In fact, there is no strong evidence to suggest that they are statistically similar (p-value $\leq$ 0.063; α = 0.05, in both MAC and MBC). This suggests that the magnetite impregnation hinders the smooth access of phenol molecules to sorption sites and this results in slower kinetics. Within the first hour, the coal based AC has the highest kinetics with an average of 78% attainment, followed by coconut based ACs with 69% and the slowest is the biochar with 59% attainment. This will be relevant for practical applications; as shorter contact times enable smaller dimensions of contact tanks in continuous flow systems.

4.3.8 MODELLING OF KINETICS DATA

Reaction and diffusion based kinetics models were used to fit the experimental data using linear and nonlinear regression methods.

4.3.8.1 *Linear Sorption Kinetics Models*

The suitability of a given model in describing the experimental data was assessed using the correlation method. Usually, the model that gives the highest R^2 value with respect to the fitted experimental data is chosen as the best model to describe the sorption kinetics of the system under consideration. The model parameters were obtained from the slope and intercept of the plots of linear fitted data in Figures 4.13 – 4.16.
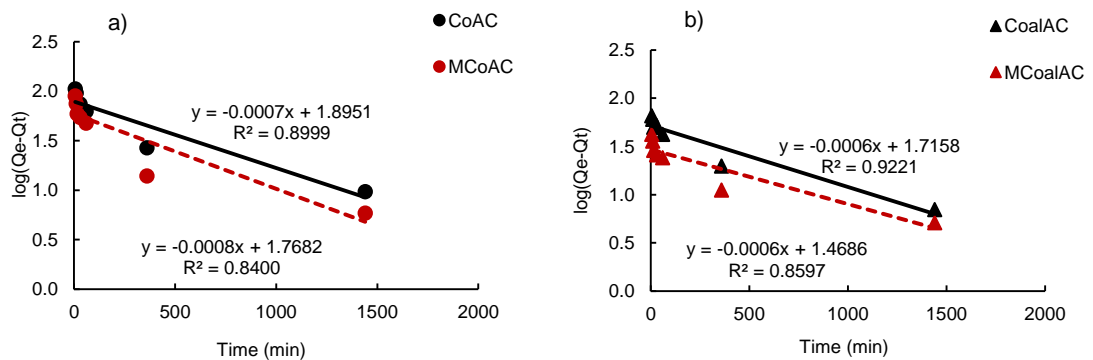
Figure 4.13: Data fitting using pseudo 1st order linear model for sorption kinetics of phenol on (a) Coconut based ACs and, (b) Coal based ACs.
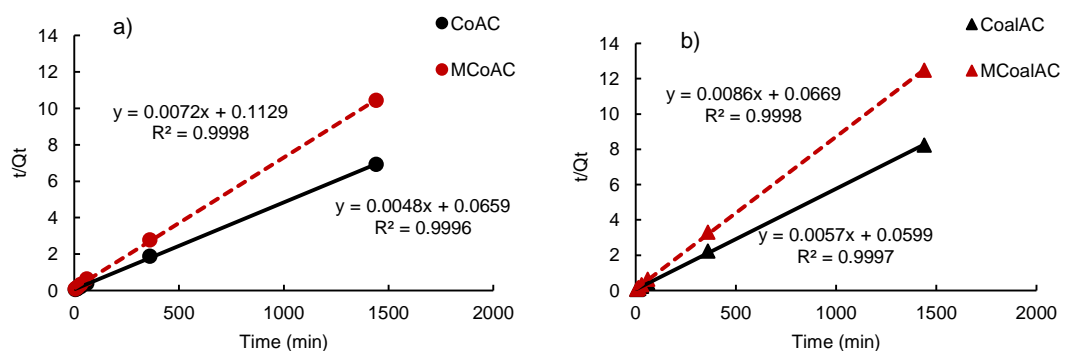
Figure 4.14: Data fitting using pseudo 2nd order linear model for sorption kinetics of phenol on (a) Coconut based ACs and, (b) Coal based ACs
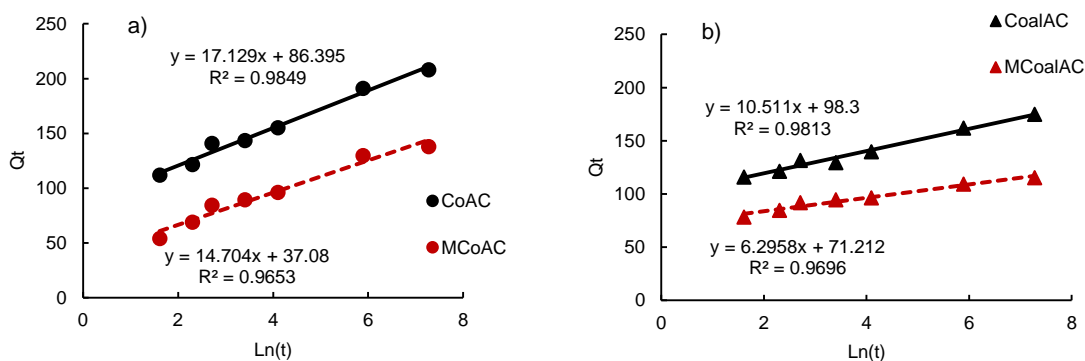
Figure 4.15:   Data fitting using Elovich model for sorption kinetics of phenol on (a) Coconut based ACs and, (b) Coal based ACs.
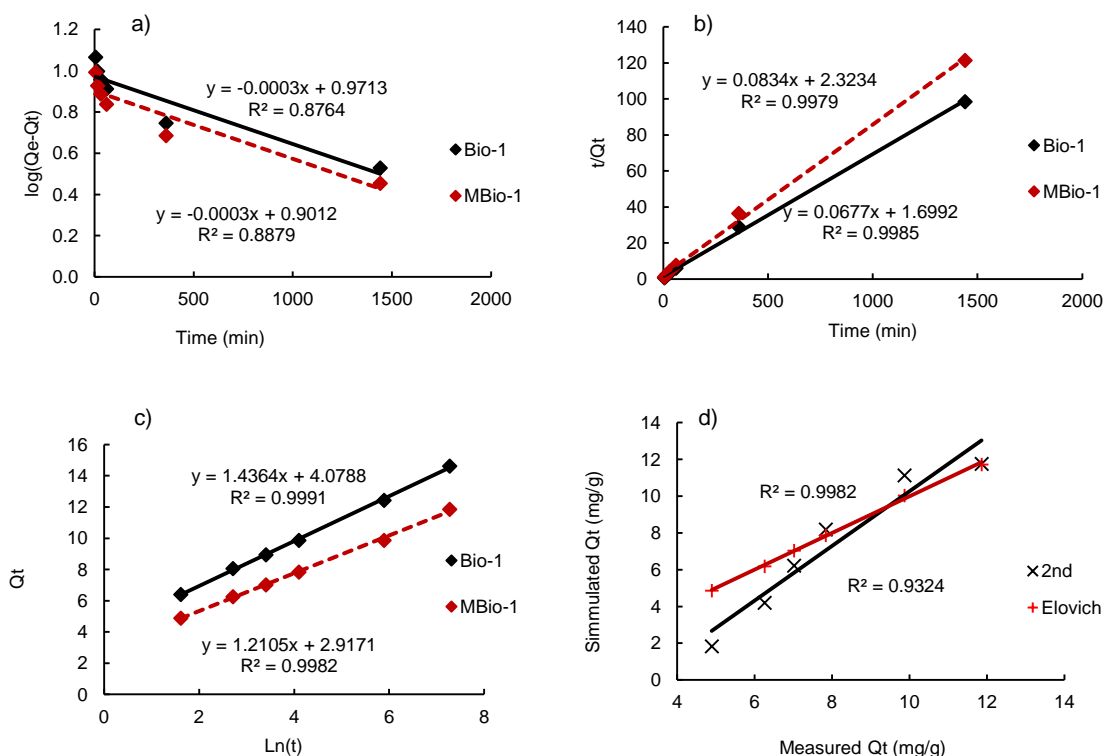
Figure 4.16:   Phenol sorption on biochars: fitting kinetics data using (a) pseudo 1st order, (b) pseudo 2nd order, (c) Elovich and (d) correlation between experimental and simulated data for MBio-1

Model parameters obtained from the linear data fitting are summarised in Table 4.11. It can be observed that the Elovich model has the highest R^2 value for all sorbents, this suggests it has the best compatibility with the experimental kinetics data. It may therefore be inferred that the sorption kinetics of the examined sorbents is governed by the rate of chemisorption of phenol on their heterogeneous surfaces. The pseudo 1st order model has the least R^2 value, and as reported in other similar works (Park *et al.*, 2010; Kilic *et al.*, 2011; Gundogdu *et al.*, 2012), the Q_e predicted by this model is not similar to the experimental Q_e.

Table 4.11: Model parameters for kinetics of phenol sorption on ACs and BCs; (obtained using linear regression).

Model	Parameter	CoAC	MCoAC	CoalAC	MCoalAC	Bio-1	MBio-1
1st	Q_e	78.54	58.64	51.97	29.42	7.95	6.68
	k_1	1.54E-03	1.74E-03	1.47E-03	1.30E-03	1.03E-03	1.08E-03
	R^2	0.8247	0.7710	0.8657	0.7549	0.8379	0.8482
2nd	Q_e	209.30	139.12	175.44	115.71	14.77	11.99
	k_2	3.46E-04	4.58E-04	0.00	0.00	2.70E-03	2.99E-03
	R^2	0.9023	0.9394	0.8228	0.8948	0.9283	0.9324
Elovich	α	2.66E+03	1.83E+02	1.21E+05	5.14E+05	24.57	13.48
	β	0.06	0.07	0.10	0.16	0.70	0.83
	R^2	0.9849	0.9653	0.9813	0.9696	0.9991	0.9982
Intra-P	k_{id}	98.16	49.20	103.79	73.81	5.38	4.07
	z	0.11	0.16	0.07	0.06	0.14	0.15
	R^2	0.9709	0.9223	0.9817	0.9563	0.9907	0.9905
Experimental Q_e		208.08	137.89	174.77	115.36	14.63	11.86

4.3.8.2 *Nonlinear Sorption Kinetics Models*

A nonlinear fitting method was used to simulate the experimental data. The parameters generated by all the error functions for each model for all the sorbents are presented in appendix B1. Compared to the linear fitting method, the kinetic curves obtained were closer in resemblance to the experimental data. The superiority of the Elovich model is obvious. For instance, in Figure 4.17, the kinetics for sorption of phenol on CoAC, the curves obtained from Elovich for both linear and nonlinear fits overlap the experimental data.
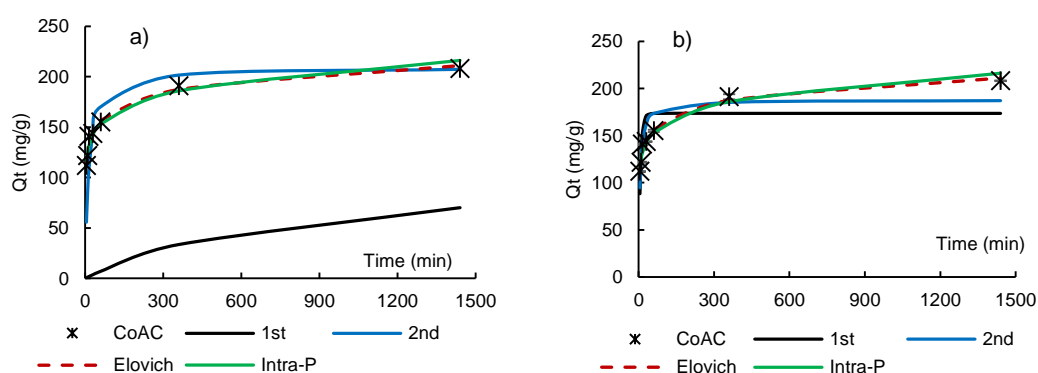
Figure 4.17: Sorption kinetics of phenol on CoAC: Fitting of experimental data using (a) linear models and (b) nonlinear models

The plots for nonlinear fitting method is presented in appendix B2. Consequently, the curves obtained using nonlinear method produced better error

function values (see Table 4.12 and 4.13) compared to what was obtained for the linear method.

Table 4.12:   Results of optimised error functions for the kinetics of phenol sorption on CoAC

Err. Fxn	1st_L	2nd_L	Elovich_L	Intra-P_L	1st	2nd	Elovich	Intra-P
CoD	0.5049	0.7910	0.9849	0.9717	0.7526	0.8561	0.9851	0.9719
HYBRID	1.73E+04	936.00	15.46	29.09	418.07	183.01	15.37	28.67
MPSD	108.88	28.02	3.31	4.46	15.92	10.67	3.27	4.45
ARE	91.29	16.62	2.29	3.35	10.98	7.94	1.83	3.11
EABS	954.28	148.36	23.46	35.15	135.24	82.34	19.72	33.37
ERSSQ	1.32E+05	5644.00	111.47	223.19	3401.55	1443.60	111.47	209.54
ASE	2.50E+04	1128.87	26.00	49.21	663.67	287.95	25.28	46.53

Table 4.13:   Summary of ASE for optimised error functions for the kinetics of phenol sorption on ACs and BCs

Sorbent	1st_L	2nd_L	Elovich_L	Intra-P_L	1st	2nd	Elovich	Intra-P
CoAC	2.50E+04	1128.87	26.00	49.21	663.67	287.95	25.28	46.53
MCoAC	9727.20	259.73	47.31	109.37	332.44	119.63	46.48	94.21
CoalAC	22286.99	1156.32	13.15	13.00	357.27	179.99	13.14	12.71
MCoalAC	11615.06	384.53	9.26	12.63	112.25	43.06	9.08	12.40
Bio-1	3.00E+02	29.67	0.36	1.65	24.89	10.84	0.35	1.47
MBio-1	226.15	25.48	0.46	1.69	24.04	9.66	0.43	1.60

The parameters obtained using the nonlinear methods appear to be more suitable for the evaluation of the sorption kinetics. Table 4.14 presents the summary of optimised model parameters and once again, the Elovich model is best in describing the experimental data. It can be observed that according to the Elovich constant α (the initial chemisorption rate), the sorbents can be ranked in the order; MBio-1 < Bio-1 < MCoAC < CoAC < CoalAC < MCoalAC. This arrangement agrees well with the result obtained for the fractional attainment i.e. Figure 4.12. Hence, it can be inferred that the coal based ACs have faster kinetics compared to the other sorbents. This is likely due to its superiority in pore volume over the other sorbents. Additionally, the data shows that MCoalAC has faster kinetics than CoalAC, (p-value = 0.02; α = 0.05), hence, the presence of the magnetite on its surface enhances its rate of phenol uptake. Therefore, the coal based ACs could be better sorbents in the removal of phenol from aqueous medium.

Table 4.14:   Optimised model parameters for kinetics of phenol sorption on ACs and BCs.

Model	Parameter	CoAC	MCoAC	CoalAC	MCoalAC	Bio-1	MBio-1
1st	Q_e	173.52	117.73	147.40	101.50	11.86	9.87
	k_1	1.42E-01	8.41E-02	2.48E-01	2.44E-01	8.57E-02	6.70E-02
	R^2	0.5678	0.7450	0.3730	0.5329	0.6000	0.6571
2nd	Q_e	187.66	128.59	157.24	107.23	12.90	10.44
	k_2	1.08E-03	8.58E-04	0.00	0.00	9.12E-03	9.74E-03
	R^2	0.8099	0.9065	0.6908	0.8214	0.8111	0.8236
Elovich	α	2.66E+03	183.0724	1.21E+05	5.14E+05	24.57	13.48
	β	0.06	0.07	0.10	0.16	0.70	0.83
	R^2	0.9849	0.9653	0.9813	0.9696	0.9991	0.9982
Intra-P	k_{id}	98.16	49.20	103.99	75.96	5.38	4.07
	z	0.11	0.16	0.07	0.06	0.14	0.15
	R^2	0.9709	0.9223	0.9817	0.9580	0.9907	0.9905
Experimental Q_e		208.08	137.89	174.77	115.36	14.63	11.86

The sorbents can be arranged in order of the Elovich constant β (the desorption constant) as; CoAC < MCoAC < CoalAC < MCoalAC < Bio-1 < MBio-1. This is about the reversed order of their sorption capacity, hence it confirms that the coconut ACs have higher number of sites available (assessed as $1/\beta$) for the chemisorption of phenol (Tseng *et al.*, 2003; Baccar *et al.*, 2012; Guedidi *et al.*, 2013). Generally, a higher β value is an indication that desorption becomes relevant at a much earlier stage due to faster attainment of equilibrium. Therefore, it implies that due to higher β value, the coal based ACs will be exhausted faster than the coconut based ACs. Consequently, in order to benefit from the faster kinetics of the coal based AC, higher dosage has to be used to compensate for the deficit of sorption capacity, particularly compared to the coconut based ACs.

The intraparticle model next to the Elovich model, has good error function values and as such conforms to the experimental data. This indicates that part of the kinetics is controlled also by intraparticle diffusion. The sorbents can be arranged in terms of their k_{id} values as; MBio-1 < Bio-1 < MCoAC < MCoalAC < CoAC < CoalAC. This supports the suggestion that phenol sorption progresses according to the micropore filling mechanism, since it can be seen that the ACs have higher k_{id} values due to their amplified pore structure compared to the BCs.

Also the presence of magnetite could be the reason why the magnetic sorbents have lower k_{id} value compared to their corresponding pair of pristine sorbent.

4.3.9 INFLUENCE OF CaCl₂ ON SORPTION OF PHENOL

The essence of using CaCl₂ as background solution it to maintain constant ionic strength to the system. This is because in real scenario, phenol exist together with dissolved metals, therefore the CaCl₂ solution represents possible metals that could exist in real refinery wastewater. The result for the influence of background ionic solution is shown in Figure 4.18
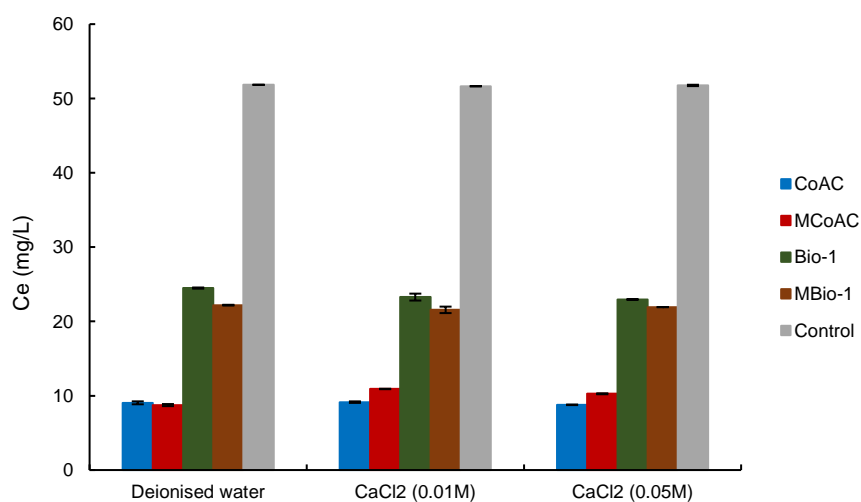
Figure 4.18:   Effect of background ionic solution on sorption of phenol on ACs and BCs

It can be seen that the residual phenol concentration for each sorbent and control remained the same irrespective of the concentration of CaCl₂ background solution. These results show that the presence of CaCl₂ does not affect the sorption of phenol on the sorbents. The residual concentrations of samples with 0.01 and 0.05M CaCl₂ background solution are statistically similar (p-values 0.896 and 0.842 respectively) to those of the deionised water. Therefore the presence of similar salts in refinery wastewater are not expected to exert a significant effect on the sorption of phenol on the sorbents. Similar findings have been reported in literature (Chen *et al.*, 2008; Zhang *et al.*, 2010b)

4.3.10   SORPTION IN SYNTHETIC WASTEWATER
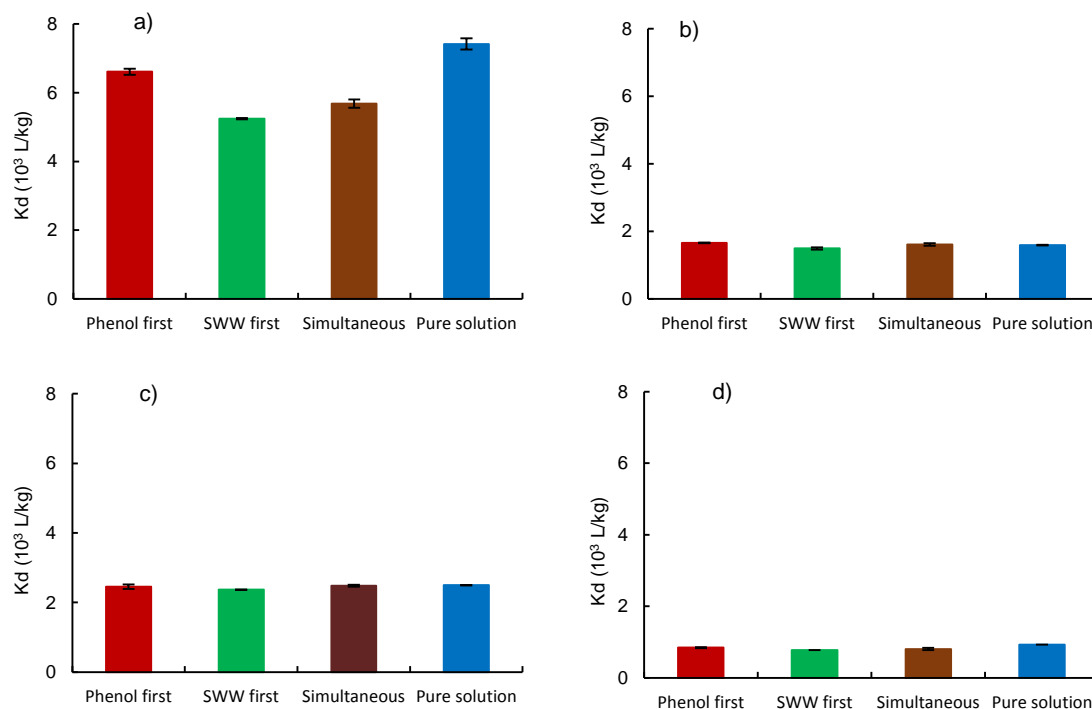
Figure 4.19:   Effect of fouling on the sorption of phenol on (a) CoAC, (b) MCoAC, (c) Bio-1 and (d) MBio-1

The effect of fouling due to competition with compounds in synthetic wastewater (SWW); at 16 mg/L DOC, is shown in Figure 4.19. Among the sorbents, the highest impact, a decrease of 29.29 % was recorded when phenol was contacted to CoAC after the SWW had a 24 hr sorption head start. This means that some of the sites were inaccessible to the phenol molecules after the sorption of the SWW. There is an average general decrease of about 21.19 and 13 % phenol sorption on CoAC, and MBio-1 respectively, irrespective of the order of contact (see Figure 4.19(a & d)).

The decrease observed due to competition from compounds in the SWW in phenol sorption on MCoAC and Bio-1 is generally insignificant (highest 6.4 %) as can be seen in Figure 4.19(b & c). Generally, the decrease in the uptake of phenol on all sorbents due to the presence of competing organics depends on the order of contact between the sorbents, phenol and the SWW. The least impact, an average of 7 % decrease for all sorbents was recorded when phenol was given 24 hr sorption head start. The most impact, an average of 20.55 % for all sorbents was recorded when the SWW was contacted with the sorbents before the addition

of phenol. Finally, when both phenol and SWW were simultaneously contacted with the sorbents, a decrease of 14.97 % was recorded. This suggests that the phenol and the competing compounds share some common sites and not all available sites. This is due to variation in sorption mechanisms as a result of differences in their properties which determines the possible form of interaction that results in the removal of each of species from the solution. The sorption of SWW in the presence of phenol could not be measured due to its complex composition. According to the partition coefficient for sorption of pure SWW on the sorbents, it can be seen in Figure 4.20(a), that the ACs have high affinity for SWW, while it sorbs poorly on the BCs (Figure 4.20(b)).
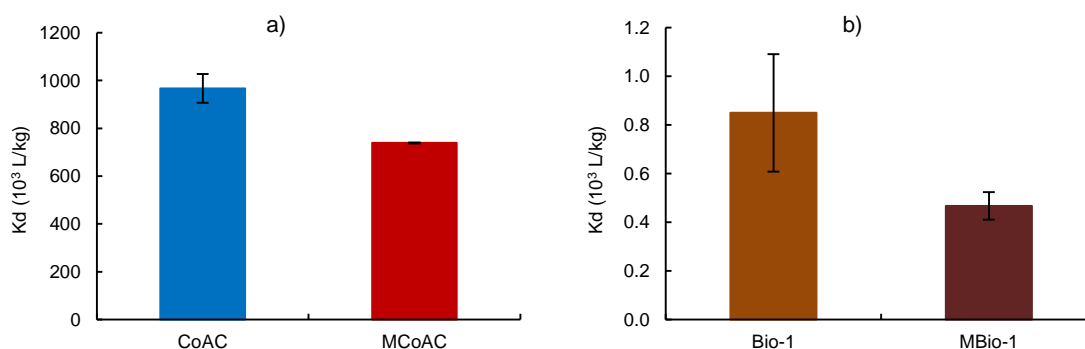
Figure 4.20:   Sorption of pure SWW on a) ACs and b) BCs. [Note; figures have different scales]

4.4   SUMMARY

The sorption of phenol on magnetic activated carbon and biochar has been investigated. In terms of sorption capacities, it was observed that the ACs have about 87 % higher phenol uptake than the BCs. This is due to the ACs having larger surface area (A_S) and micropore volume (V_{MP}) as a result of activation. There is also a difference in phenol uptake capacity between the composites and pristine sorbents of about 36.87 %. This is proportional to their difference in carbon content and accordingly, the composites have lesser A_S and V_{MP}. Therefore, it can be concluded that the sorption capacities of the sorbents are being influenced by their A_S and V_{MP}. Hence, to achieve equal sorption capacities as obtains for the pristine sorbents, higher dosages of the composites must be used. Likewise, higher BCs dosages are required to achieve the same level of phenol removal that is obtained using the ACs. The influence of

temperature was not noticeable. Sorption isotherm data obtained at both 295.15 and 10°C were statistically similar (p-value = 0.697). According to isotherm models, phenol sorption is more favourable over heterogeneous surfaces and it progresses according to the micropore filling mechanism, especially the ACs.

The rate of phenol uptake differs between the ACs and the BCs as well as between composites and pristine sorbents. Judgements derived using the parameters of the Elovich model is in good agreement with deductions obtained from analysis of plots of experimental data. The presence of iron oxide deposits on the surface of the carbon hinders the smooth access of phenol molecules to sorption sites. As a result, slower kinetics were recorded in all composites but MCoalAC, whose kinetics seem to be better (p-value = 0.02) than CoalAC. The reason behind this increase need to be investigated further so as to take advantage of possible sorption enhancement. With faster kinetics and lesser concentration of sorption sites compared to the coconut based AC, the coal based AC is most likely to be exhausted faster. Therefore, higher dosage of the coal ACs are required to compensate for the deficit to make it a better alternative to the coconut AC.

Nonlinear fitting method can be used to optimise model parameters. In majority of cases for both sorption isotherm and kinetics, the nonlinear method generates lower error distribution between experimental and simulated data. The use of nonlinear methods is therefore recommended for the analysis of phenol sorption isotherms at high concentrations. At low concentrations, the linear isotherm model is most appropriate.

The ACs and the BCs behave differently under the influence of pH. For the ACs, phenol uptake is highest at pH within the vicinity of the pKa value and is lower at both ends of the pH scale. Therefore, the sorption is favoured by electrostatic interactions between positively charged surface and negatively charged phenolate anion. At lower pH sorption is hindered due to competition with H^+ and the localisation of sorbent π electrons due to increased oxidation. For all sorbents, sorption of phenol is lowest at high end of the pH due to electrostatic repulsion between negatively charged surface and phenolate carboxylate anion. This could also be due to increased solubility of the dissociated phenol specie. The adsorption edge model could not simulate the influence of pH on phenol

sorption, likely because it was mostly applicable where homoionic or non-functionalised, extremely low variable-charge surface sorbents are involved. In practical applications, pH adjustment to around pH 9 would facilitate phenol removal by these sorbents.

The attenuation of phenol sorption due to competition from synthetic wastewater was observed. Highest reduction in phenol uptake of about 20.55 % on average for all sorbents was recorded when the sorbents were contacted with the SWW for 24 hr before phenol was introduced. Therefore, both phenol and SWW share some common sorption sites and not all available sites. Nevertheless, the results clearly show that activated carbon in pure and magnetised form can be used in the removal of phenol from solutions even in the presence of other, dissimilar DOC

In this chapter competition was appraised using single concentration of target pollutant. The proceeding chapter presents investigations into the effect of competition using real wastewaters and varied concentration of target pollutants. This will provide more insights into effect of competing compounds on the sorption of target pollutants' at different concentration levels. Additionally, it will help in the selection of appropriate models that can be used in describing the sorption of pollutants from such realistic conditions.

CHAPTER 5.   SORPTION OF PHARMACEUTICALS

5.1   INTRODUCTION

This chapter is a consolidation of the findings of the previous chapters. Experiments were conducted using CoAC, MCoAC, Bio-1 and MBio-1, because they have exhibited better sorption characteristics among each category of the sorbents. Two additional variations were tested as follows;

i)   It has been observed from chapter 4, that the magnetic sorbents have lesser sorption capacity due to their lower carbon content compared to their nonmagnetic pairs. Hence the amount of the magnetic sorbents used in this chapter was increased by about 36% (more than what is used for the nonmagnetic pairs) to make up for the deficit in the carbon content. The magnetic sorbents are therefore expected to have similar sorption capacities than their pristine pairs, especially when solid phase concentrations are computed based on the carbon content used.

ii)   In chapter 4, fouling effect was evaluated using 1-point concentration of phenol in the presence of SWW. To have a broader appraisal of fouling effect, 5-point sorption isotherm experiments were conducted for the pharmaceuticals using $CaCl_2$ and real wastewater sample separately as background solutions. This will give an insight of the effect of competitors to the sorption of micropollutants in quasi real scenario.

5.2   EXPERIMENTAL SECTION

5.2.1   DETERMINATION OF SORPTION ISOTHERMS IN $CaCl_2$ SOLUTION

Batch experiment tests were conducted to evaluate the sorption characteristics of sorbents. The materials to be used were autoclaved before the commencement of experiments, to minimise the effect of microbial degradation of pollutants.

Equilibrium experiment was conducted using $CaCl_2$ solution and wastewater treatment plant effluent (WWTPE) separately as background solutions. Stock

solution was prepared using UHQ water (Ultra High Quality, 18.2 MΩ purity) containing 75 % (v/v) of methanol to increase the solubility of the compounds.

5.2.1.1   Determination of Sorption Isotherms

Approximately, 4.0 mg of CoAC or 6.0 mg of MCoAC (ca. 3.8 mg carbon material) were contacted with 90 mL of autoclaved 0.01 M CaCl$_2$ solution in a 250 mL glass bottles. In the same manner, 40.0 and 60.0 mg of Bio-1 and MBio-1 were contacted with 29 mL of autoclaved 0.01 M CaCl$_2$ solution in 40 mL glass vials. The mixture was shaken overnight at 155 rpm on a shaker at room temperature and thereafter, an aliquot (10 and 1 mL for ACs and BCs resp.) of stock ibuprofen or diclofenac solution was added to the CaCl$_2$ conditioned sorbent such as to achieve a predetermined desired initial concentration of 5, 10, 15, 20 and 30 mg/L. It is ensured that the fraction of methanol in each sample at the commencement of the experiment is not more than 2.5% to avoid co-solvent effects (Durán-Álvarez *et al.*, 2012; Murillo-Torres *et al.*, 2012; Guedidi *et al.*, 2013). The samples were set to shake for 24 hours under the conditions mentioned earlier, but this time in total darkness to avoid photodegradation effects. Similar samples with varied initial concentrations containing no sorbent (to serve as control) were run in parallel to determine the possible degradation of the sorbate or its adsorption to the walls of the glass vials. At the end of the shaking sequence, the samples were removed from the shaker and separated by centrifugation at 5000 rpm for 5 mins. The supernatant was carefully transferred with a pipette into a vial for the measurement of residual ibuprofen or diclofenac concentration. Duplicate samples were used throughout the experiment and average values were reported. Equilibrium concentrations were measured using a Waters-UPLC Acquity equipped with TQ-S Mass Spec, with a negative ionization in ESI source, a BEH C18 column, 100x2.1 mm, 1.7um, operated at a flow rate of 0.3 mL/min and temperature 30 °C. Gradient operation mode was used with an injection volume of 5-20 uL and the mobile phases were A (water + 0.025% NH$_3$) and B (acetonitrile+0.025% NH$_3$).

5.2.1.2   Determination of Sorption Kinetics

To evaluate the sorption kinetics, samples having an initial concentration of 10 mg/L were processed as in 5.1.1.1 and the residual concentration was measured at the following time intervals, 15, 30 and 60 min, 3, 6, 12 and 24 hr.

5.2.1.3   Determination of pH Influence on Sorption

To evaluate the influence of pH on the sorption system, 4.0 mg of CoAC or 6.0 mg of MCoAC (ca. 3.8 mg carbon material) were contacted with 90 mL of autoclaved 0.01 M $CaCl_2$ solution in a 250 mL glass bottles. In the same manner, 40.0 and 60.0 mg of Bio-1 and MBio-1 were contacted with 29 mL of autoclaved 0.01 M $CaCl_2$ solution in 40 mL glass vials. The mixture was shaken overnight at 155 rpm on a shaker at room temperature and thereafter, the pH of the $CaCl_2$ conditioned samples were then adjusted to 3, 5, 7, 9 and 11 using aliquot amounts of 0.1 M of HNO_3 or 0.1 M of KOH. The mixture was shaken overnight at 155 rpm on a shaker at room temperature and necessary adjustments were made to maintain target values. All pH measurements were done using a Jenway 3310 pH meter. Thereafter, an aliquot (10 and 1 mL for ACs and BCs resp.) of stock ibuprofen or diclofenac solution was added to the pH preconditioned sorbent such as to achieve a predetermined desired initial concentration of 10 mg/L. It is ensured that the fraction of methanol in each sample at the commencement of the experiment is not more than 2.5% to avoid co-solvent effects. The samples were set to shake for 24 hours under the conditions mentioned earlier. Control samples containing no sorbent and treated in similar manner to determine the possible degradation of the sorbate or its adsorption to the walls of the glass vials. At the end of the shaking sequence, the samples were removed from the shaker and separated by centrifugation at 5000 rpm for 5 mins. The supernatant was carefully transferred with a pipette into a vial and the residual ibuprofen or diclofenac concentration was determined using the UPLC. Duplicate samples were used throughout the experiment and average values were reported.

5.2.2 EQUILIBRIUM IN SPIKED WWTPE:

Samples from the WWTPE described in 3.4.1, were spiked with aliquot amount of stock ibuprofen or diclofenac stock solution such as to achieve a

predetermined desired initial concentration of 5, 10, 15, 20 and 30 mg/L of the pharmaceuticals. The spiked effluent was added to 4.0 mg of CoAC or 6.0 mg of MCoAC (ca. to 4.0 mg carbon material) in a 250 mL glass bottles and the samples were processed as explained in 5.2.1.1.

5.3 RESULT AND DISCUSSION

5.3.1 EVALUATION OF IBUPROFEN SORPTION ISOTHERMS FROM $CaCl_2$ SOLUTION

The sorption isotherm of ibuprofen on magnetic and nonmagnetic activated carbon and biochar is shown in Figure 5.1. Sorption pattern depicts nonlinear isotherms in all samples suggesting that the amount sorbed is related to the interaction of sorbent and sorbate properties in addition to the equilibrium concentration. Isotherm curves are characterised by steep rise at the lower end of the plot with data points within the vicinity of the ordinate axis, suggesting a higher relative sorbate uptake at lower concentrations. This is due to the relative abundance of free limited sorption sites to be occupied by a less number of sorbate molecules (Roop and Meenakshi, 2005; Çeçen and Aktas, 2011). Consequently, more sorbate molecules bind to the surface of the sorbents and are thus removed from the solution.
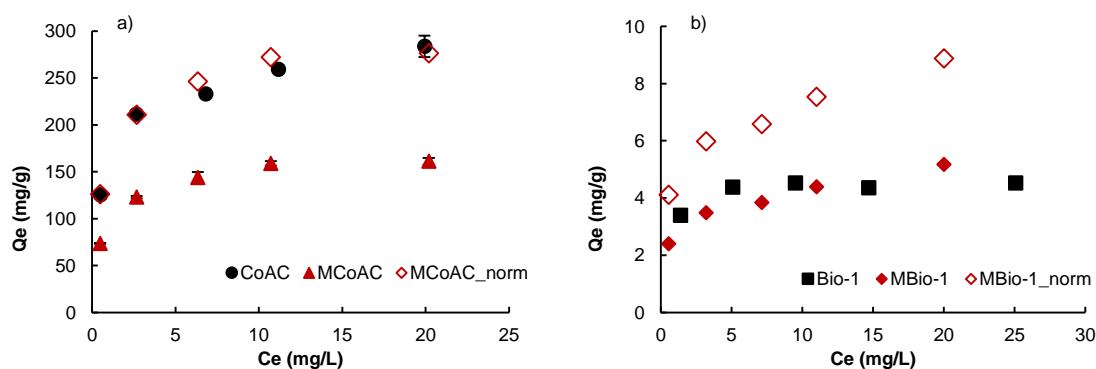
Figure 5.1: Isotherm plot for sorption of ibuprofen on (a) ACs and (b) BCs. [Note; figures have different scales]

The steepness of the plots progressively decreases because the number of the available sorption sites remain constant, hence, increase in the initial sorbate concentration is not met with a corresponding increase in the number of available sorption site (Baccar *et al.*, 2012). As such, only a limited number of free sorbate

molecules will be removed from the solution at equilibrium (Limousin *et al.*, 2007). Therefore, the concentration of residual sorbate molecules increases as the initial concentration increases.

The activated carbons present about 2 order of magnitude of higher uptake of ibuprofen as compared to the biochars due to their superior surface area (A_S) and better developed pores. This clearly shows the benefit of activation. CoAC exhibits highest uptake of ibuprofen and unlike MCoAC, its isotherm does not assume a plateau within the range of concentration studied. In other words, it does not portray a Langmuir type of isotherm where sorption is restricted to monolayer coverage on homogenous surface, sorbate molecules do not interact and sorption sites have equal activation energy (Ho and McKay, 2002). In the case of the biochars, the isotherm of MBio-1 did not assume a plateau within the range studied. This is typical of sorption on heterogeneous surface as postulated by the Freundlich type of isotherm.

The solid phase concentrations were computed with respect to the total mass of sorbents used; 4.0 mg for CoAC and 6.0 mg for MCoAC (ca. 3.8 mg activated carbon content); 40 mg for Bio-1 and 60 mg for MBio-1 (ca. 40 mg biochar content). It has been shown (Jiang *et al.*, 2015) that the uptake of pollutants on magnetic carbon composites decreases as the amount of carbon content decreases. Then in theory, it is expected that the sorption capacity of the pristine sorbent will be similar to that obtained if the sorption on composite is normalised with respect to its carbon content (Han *et al.*, 2015b). When the sorption of ibuprofen on the magnetic sorbents is normalised (MCoAC_norm & MBio-1_norm) with respect to the mass of carbon in the matrices, the isotherms of the CoAC and MCoAC overlap, while the isotherms of the MBio-1 shoots above that of Bio-1. On one hand, it is apparent that CoAC has a larger S$_A$ than MCoAC (975 vs 643 m^2/g) and therefore may be an indication of the reason for a higher sorption capacity. On the other hand, however, the difference in A_S between the BCs is much less in proportion to that between the ACs. Therefore, in addition to the A_S, other parameters –perhaps pore related- are also influencing the ibuprofen sorption capacities of the sorbents.

Of the pore related parameters, only the micropore volume (V_{MP}) and pore volume (V_P) show strong correlation with the A_S (Pearson correlation R = 0.9962 and 0.9528 respectively), and are likely the important factors. The V_P of the ACs are about the same, while MBio-1 has a larger V_P as compared to Bio-1. During the production of the magnetic biochar, the acidity of the initial solution dissolves carbonate deposits in the pores of biochar, thus creating new accessible pore-space. Also, Nguyen *et al.* (2011), observed that the deposition of magnetic particles on the surface of AC resulted in the formation of new pores. This could improve the sorption capacity of such modified sorbents. Also, sorbent pairs will have about the A_S when normalised with respect to the mass of their carbon contents (some magnetic biochar sorbent samples have shown carbon content up to 80% carbon content). It is therefore plausible that the ibuprofen sorption capacities of the BCs are being influenced by their V_P in addition to their A_S and V_{MP}. Furthermore, with relatively small A_S ca. 66 – 96 m^{2}g^{-1} (Sun *et al.*, 1998; Oliveira *et al.*, 2002) compared to that of the sorbents, it can be inferred that the iron oxide in the MCoAC does not contribute to the sorption of ibuprofen, which is similar to the finding of (Han *et al.*, 2015b).

5.3.1.1   *Modelling of Sorption Isotherms Data:*

A.   Ibuprofen sorption: Linear isotherm model

This model is applicable to lower concentration of the isotherm data. Comparing sorption of the sorbents can be done using the partition coefficient (K_d). Figure 5.2 shows two order of magnitude higher ibuprofen uptake for the ACs compared to the BCs due to amplified A_S and pore structure in the case of the ACs. The higher K_d value of the CoAC against the MCoAC (has 38 % less) also suggest that in the ACs sorption is influenced mostly by the A_S. Accordingly, the higher K_d value of MBio-1 (78 % more) against Bio-1 indicates the significance of pore volume in the sorption of ibuprofen on the biochars.
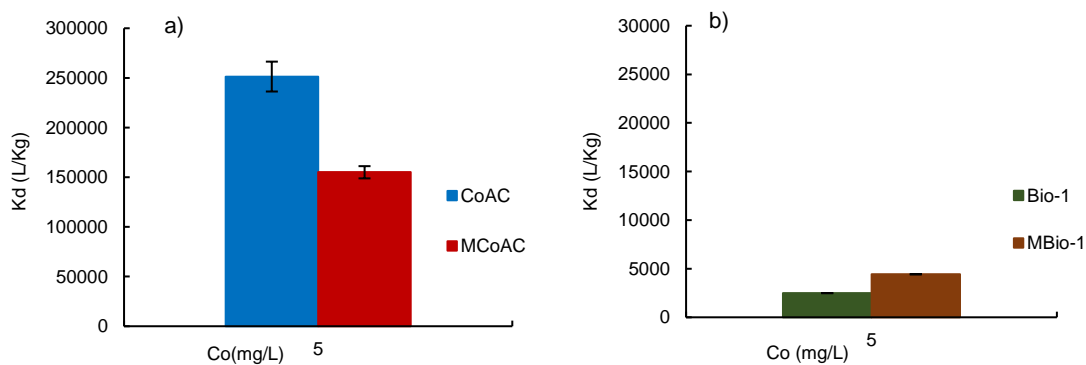
Figure 5.2:   Partitioning coefficient for sorption of ibuprofen on (a) ACs and (b) BCs. [Note; figures have different scales]

B.   Ibuprofen sorption: Nonlinear models

The isotherm data was fitted using both linear and nonlinear regression methods for the nonlinear models. For each sorption system and a given isotherm model, parameters were determined using all six error functions mentioned in 3.7.3, in addition to the methods of least square. Since each method generated unique sets of parameters, the error function that produced the least coefficient of non-determination was chosen as the best in representing that model (Kumar *et al.*, 2008b). In general, both methods fit the data reasonably well, although, for all error functions considered, the nonlinear methods exhibit less error distribution than the LTFM method.

Table 5.1:   Results of optimised error functions for the sorption of ibuprofen on CoAC

Err. Fxn	LANG_L	FR_L	RP_L	LANG	FREU	RED-PET	DA	PDM
CoD	0.9301	0.9622	0.9907	0.9557	0.9639	0.9912	0.9854	0.9854
HYBRID	424.30	99.20	28.84	100.97	95.84	27.58	49.59	0.24
MPSD	17.70	7.02	3.50	6.37	6.99	3.47	4.62	4.62
ARE	9.02	4.11	1.66	3.99	3.62	1.64	2.02	2.34
EABS	74.71	41.85	19.63	62.02	38.48	19.47	25.37	0.16
ERSSQ	1819.20	630.13	136.71	734.45	533.64	125.07	218.05	0.01
ASE*	390.84	130.39	31.73	151.31	113.10	29.54	49.94	1.23

* ASE = [(1-CoD) + HYBRID + MPSD + ARE + EABS + ERSSQ]/6

Key: Err. Fxn (Error function), Lang_L (LTFM Langmuir), FR_L (LTFM Freundlich), RP_L (LTFM Redlich-Peterson), LANG (Langmuir), FREU (Freundlich), RED-PET (Redlich-Peterson), DA (Dubinin-Ashtakov) and PDM (Polanyi-Dubinin-Manes)

The data for the optimised error functions for the sorption of ibuprofen on CoAC is shown in Table 5.1 and the summary of the average sum of errors (ASE) for all the sorbents is shown in Table 5.2. From these Tables, it can be seen that

the ASE for the nonlinear models is less than that for the corresponding LTFMs. This is not unexpected because in their nonlinear forms, the models are in harmony with the assumptions upon which they have originally been derived and so their error structure is unaltered (Porter *et al.*, 1999; Ho, 2004).

Table 5.2:   Summary of ASE for the sorption of ibuprofen on ACs and BCs

Sorbent	LANG_L	FR_L	RP_L	LANG	FREU	RED-PET	DA	PDM
CoAC	390.84	130.39	31.73	151.31	113.10	29.54	49.94	1.23
MCoAC	54.21	94.15	12.01	35.70	80.48	11.69	6.06	0.51
Bio-1	1.54	2.52	1.17	0.97	2.35	1.11	0.60	0.55
MBio-1	11.30	1.23	1.42	81.66	16.95	18.64	1.03	1.91

Nonetheless, the LTFMs serve as a good approximation of the nonlinear models (Boulinguiez *et al.*, 2008; Worch, 2012). As recorded in the work of Allen *et al.* (2004), in some instances, the LTFMs resulted in better data fitting than their corresponding nonlinear models. Type 1 linear Langmuir model (Equation 2.5) is a better approximation of the nonlinear model than the type 2 (Equation 2.6) in all instances; as has been observed by others (Ho, 2004; Kumar and Sivanesan, 2005; Kumar, 2007; Boulinguiez *et al.*, 2008) and is therefore chosen to represent the LTFM Langmuir.

Table 5.3:   Summary of MSC for isotherm prediction using optimised model parameters for sorption of ibuprofen on ACs and BCs

Model	CoAC	MCoAC	Bio-1	MBio-1
LANG	1.3	2.38	1.5	0.15
FREU	2.52	1.93	0.34	3.27
RED-PET	3.57	3.62	1.67	2.86
DA	2.82	4.12	2.62	3.65
PDM	2.82	4.12	2.62	3.64

For all sorbents, the 3-parameter models have the least values of the ASE and therefore exhibit higher degree of data fitting compared to the 2-parameter models. This means that they have better conformity to the experimental data, which is similar to the observation of others (Ho *et al.*, 2002; Allen *et al.*, 2004; Wong *et al.*, 2004). In particular, the Polanyi-Dubinin-Manes model has the least ASE and highest coefficient of determination. Similar observations were previously made by others (Yang *et al.*, 2006a; Xu *et al.*, 2008; Yang and Xing, 2010). Yan *et al.* (2008) proposed that this is because the model does not assume

a homogeneous surface with respect to adsorption energies as is the case in Langmuir.
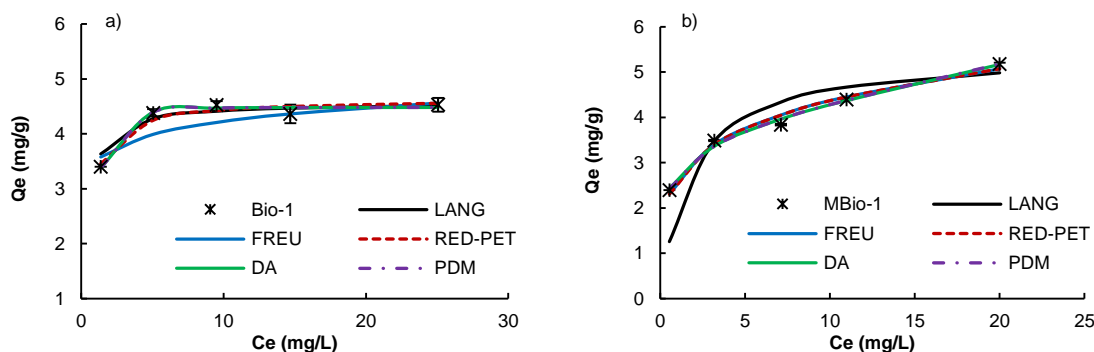
Figure 5.3: Comparison of simulated and experimental isotherm plot for sorption of ibuprofen on (a) Bio-1 and (b) MBio-1

Table 5.4: Optimised model parameters for isotherm of ibuprofen sorption on ACs and BCs

Model	Parameters	CoAC	MCoAC	Bio-1	MBio-1
Linear	K_d*	251.36	155.03	2.49	4.43
LANG	Q_m	294.85	287.96	4.58	5.43
	K_L	0.86	1.22	2.82	0.56
	R^2	0.9690	0.9813	0.9482	0.8859
	ASE	151.31	35.70	0.97	81.66
FREU	$1/n$	0.19	0.19	0.08	0.22
	K_F	162.99	165.53	3.49	2.64
	R^2	0.9663	0.9357	0.7418	0.9836
	ASE	113.10	80.48	2.35	16.95
RED-PET	K_R	784.13	607.70	9.89	7284.62
	A_R	3.86	2.64	2.13	2760.56
	γ	0.89	0.92	1.00	0.78
	R^2	0.9915	0.9921	0.9441	0.9837
	ASE	29.54	11.69	1.11	18.64
DA	Q_o	293.72	167.16	4.48	7.97
	E	20.48	18.43	12.68	32.44
	b	1.75	2.19	5.99	0.63
	R^2	0.9853	0.9961	0.9784	0.9912
	ASE	49.94	6.06	0.60	1.03
PDM	Q_o	293.73	167.16	4.48	7.97
	a	12.80	30.36	76669.05	1.88
	b	1.75	2.19	5.84	0.63
	R^2	0.9853	0.9961	0.9784	0.9912
	ASE	1.23	0.51	0.55	1.91

*$\times 10^3$

This superiority in data fitting by the 3-parameter models could be due to their having more degrees of freedom, perhaps as a result of having redundant fitting parameters. Test for redundancy of model parameters was conducted using the MSC method. The result for the MSC is summarised in Table 5.3 and it shows that the 3-parameter models actually contain higher information about the system (Koeppenkastrop and De Carlo, 1993; Saiers and Hornberger, 1996) and thus have higher MSC values compared to the 2-parameter models.

The result of optimised model parameters is shown in Table 5.4, and a plot of the optimised simulated isotherms are compared to the experimental curve for the BCs is shown in Figure 5.3. It can be seen that except for Freundlich for Bio-1 and Langmuir for MBio-1, the isotherms predicted by these chosen parameters are significantly similar to the experimental isotherms. This suggests that their parameters can help in describing the sorption system within the examined range of concentration.

For the 2-parameter models, assessments of the R^2 and ASE values suggest that the sorption of ibuprofen on MCoAC and Bio-1 is best described by the Langmuir model, while MBio-1 is best described by Freundlich model and CoAC was almost equally described by the two models. The 3-parameter Redlich-Peterson model is useful in distinguishing between the types of isotherm i.e. as being either of Langmuir or Freundlich type (Ho, 2004; Kumar and Sivanesan, 2005). Close observation of the Redlich Peterson homogeneity factor 'γ' shows good correlation with the pattern suggested earlier. In the case of Bio-1, γ is equal to unity and in such situation, the Redlich-Peterson model becomes a special case of the Langmuir model (Ng *et al.*, 2002). In MCoAC, γ is also close to unity, indicating conformity to Langmuir, while in MBio-1 it is low suggesting Freundlich type of sorption (Ho *et al.*, 2005b) and finally, γ is just at the border between Langmuir and Freundlich in the case of CoAC.

5.3.1.2   *Ibuprofen Sorption Capacities*

As has been shown in the linear model, the sorption capacities of the ACs is 2 order magnitude higher than the BCs with respect to the capacity factors of the two and 3-parameter models. This further proves the applicability of the linear model in obtaining an estimate of sorption capacities. In the case of the 2-

parameter models, comparing sorption capacities based on their capacity parameters is not straight forward due to difference in the goodness of fitting. According to Langmuir's Q_m, the capacities of the sorbents are in the order Bio-1 < MBio-1 < MCoAC < CoAC, while according to the Freundlich's K_F, the order is MBio-1 < Bio-1 < CoAC ≈ MCoAC. Nonetheless, in this instance, the sorption capacities can rather be more conveniently compared based on Q_m according to the following two considerations. Firstly, Q_m is quite similar to the highest observed solid phase concentration for all sorbents (see Table 5.4 and Figure 5.1). This is usually the advantage the Langmuir model has over the Freundlich model whose capacity factor has an implicit unit making it difficult to compare directly with the experimental solid phase concentration (Worch, 2012). Secondly, the order depicted by Q_m is the same as compared to the capacity factors Q_o of the 3-parameter Polanyi based models; according to the two models, the order of sorption capacities of the sorbents is Bio-1 < MBio-1 < MCoAC < CoAC. It should be noted that although the two Polanyi related models have different expressions, they produce very identical parameters and in this instance, their Q_o is much similar to that obtained in the Q_m especially for the pristine sorbents.

Table 5.5:   Sorption of ibuprofen on ACs and BCs; Pearson correlation coefficients between model parameters and sorbent properties.

Model	Parameters	A_S	V_P	V_{MP}	P_S
Linear	K_d	0.9965	0.9747	0.9881	0.1983
Langmuir	Q_m	0.9296	0.9733	0.9136	0.0997
	K_L	0.3542	0.5425	0.2868	0.1438
Freundlich	$1/n$	0.2932	0.5209	0.2210	0.3179
	K_F	0.9192	0.9675	0.9030	0.1251
Redlich-Peterson	K_R	0.4932	0.3304	0.5458	0.1501
	A_R	0.5720	0.4197	0.6203	0.1475
	γ	0.0636	0.1108	0.1273	0.0789
Dubinin-Ashtakov	Q_o	0.9982	0.9663	0.9909	0.2452
	E	0.2078	0.0257	0.2705	0.1336
	b	0.2903	0.4964	0.2202	0.2121
Polanyi-Dubinin-Manes	Q_o	0.9982	0.9663	0.9909	0.2453
	a	0.4936	0.7000	0.4266	0.2808
	b	0.2836	0.4894	0.2136	0.2095

Table 5.6: Sorption of ibuprofen on ACs and BCs; Pearson correlation coefficients between normalised model capacity factors and sorbent properties

Model	Parameters	A_S	V_P	V_{MP}	P_S
Linear	K_d	0.9056	0.9643	0.8873	0.1597
Langmuir	Q_m	0.7375	0.8548	0.7139	0.4375
Freundlich	K_F	0.7221	0.8424	0.6984	0.4559
Dubinin-Ashtakov	Q_o	0.9287	0.9768	0.9112	0.1042

The model parameters from Table 5.4, were correlated with sorbent properties from Table 3.1 to evaluate the influence of the latter over the former. The result is presented in Table 5.5, where it can be observed that while there is poor correlation between sorbents properties and the sorption intensity parameters, the correlation with capacity determining parameters i.e. 'A_S', 'V_P' and 'V_{MP}', is fairly strong (generally Pearson correlation coefficient $R = 0.9030 \text{ to } 0.9982$). Yang *et al.* (2006b), also had similar observation and thus suggested mesopore filling to be considered as component of sorption capacity. Furthermore, when the capacity factors are normalised according to the actual carbon content as shown in Table 5.6, V_P showed stronger correlation with K_d and Q_o. This observation is limited due to differences in model parameters and degree of goodness of fitting, yet it agrees well with the previous observation (i.e. in the discussion of Figure 5.1), that the sorption of ibuprofen is influenced by the volume of pores of the sorbents. Therefore, it can be concluded that in the sorption of ibuprofen, the sorbent's sorption capacity is dependent upon these parameters and magnetisation does not detrimentally affect the ibuprofen sorption capacities of the AC and BC studied, especially when assessed with respect to the actual carbon content applied.

5.3.1.3 Ibuprofen Sorption Affinity

Almost identical variation of the heterogeneity factors in Freundlich and Redlich-Peterson models can be observed among the sorbents. The order for γ is MBio-1 < CoAC ≈ MCoAC < Bio-1. In terms of n, MBio-1 < MCoAC ≈ CoAC <Bio-1, suggesting an increasing order of heterogeneity among the sorbents (Li *et al.*, 2002). The Langmuir K_L also compares among the sorbents according to this observed pattern, MBio-1 < CoAC < MCoAC < Bio-1. Considering these

parameters, it can therefore be stated that the sorption of ibuprofen within the studied concentration range is more favourable on heterogeneous surfaced sorbents as can be observed in Figure 5.4.
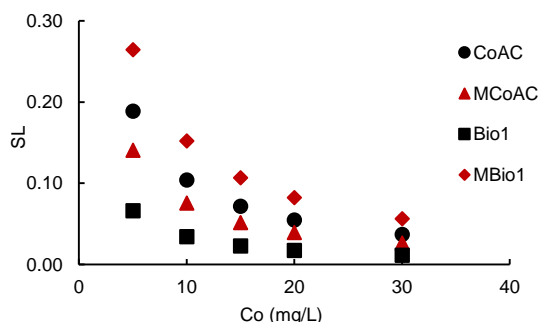
Figure 5.4:   Plot of Langmuir separation factor for sorption of ibuprofen on ACs and BCs

It can be observed that the sorption of ibuprofen is more favourable at higher initial concentration than lower ones. This result is similar to what has been observed in the sorption of dyes on biosorbents (Ho *et al.*, 2005a). The separation factors of the magnetic sorbents are significantly different (p-value <0.02; α = 0.05, in both MAC and MBC) from those recorded for their corresponding pristine pairs. Accordingly, with reference to the pristine sorbents, significant alteration of energetic heterogeneity was not observed due the presence of iron oxide in MCoAC as was observed in the MBio-1. The variation in S_L between corresponding pairs of sorbents is likely to be influenced by the sorbent's capacity determining properties. For instance, for the same dosage of magnetite per gram of pristine sorbent (as used in the production of magnetic sorbent), there is excess surface area and pore system in the pristine AC, to accommodate the iron oxide. This causes marginal variation of S_L on the MAC as compared to limited surface area and pore system of the pristine BC whence the variation was profound on the MBC

5.3.2 EVALUATION OF DICLOFENAC SORPTION ISOTHERMS FROM CaCl₂ SOLUTION.

The isotherm plot for the sorption of diclofenac is shown in Figure 5.5 and all curves shows nonlinear lines. In this instance however, none of the isotherms exhibits a clear plateau feature within the concentration range studied, unlike in

the sorption of ibuprofen. This could mean that the sorption sites are not completely exhausted or perhaps sorption takes the form of multilayer surface coverage, although the steepness of the curves is not prominent either. The ACs outperformed the BCs in the uptake of diclofenac up to by about two order of magnitude. Here also, the isotherms for the CoAC and MCoAC_norm overlap when the uptake of diclofenac on MCoAC is normalised with respect to the actual carbon content. In the case of the BCs however, the isotherm for MBio-1_norm overshoots that for Bio-1. Similar deductions as discussed in the sorption of ibuprofen on these sorbents can be proposed here as well, bearing in mind that, it has been earlier show that the influence of V_{MP} has been superimposed on that of the A_S, (Pearson correlation R = 0.9962). Although the A_S dictates the diclofenac sorption capacities (as can distinctively be seen between the ACs with superior A_S and BCs with lesser A_S), V_{MP} also influences the overall sorption capacities of the BC system, although to a lesser degree when compared to the ibuprofen sorption.
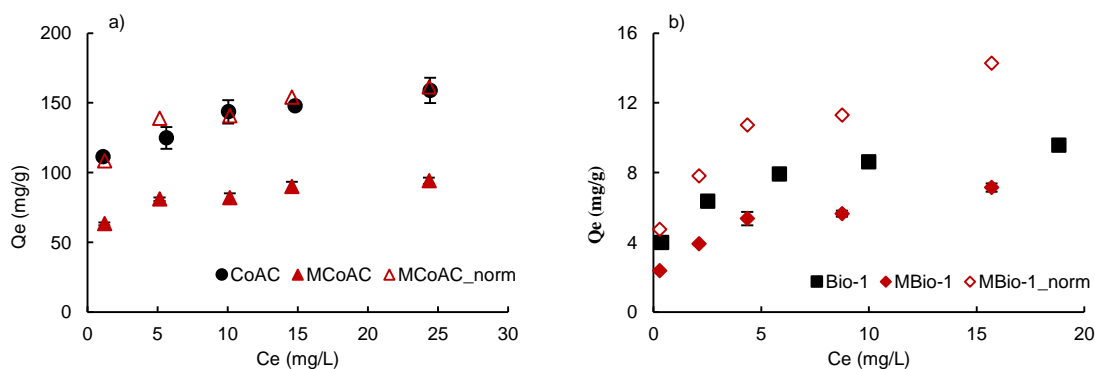
Figure 5.5:   Isotherm plot for sorption of diclofenac on (a) ACs and (b) BCs. [Note; figures have different scales]

5.3.2.1   Modelling of Sorption Isotherm Data

A.   Diclofenac sorption: Linear isotherm model

The K_d for CoAC is 48% more than MCoAC while the K_d for Bio-1 is just about 19% more than that of MBio-1. The composite materials show lesser sorption capacity due to the presence of less carbon material per mass as compared to the pristine carbon. This is in agreement with the findings of Castro *et al.* (2009), where it was shown that decrease in sorption capabilities of composites is due to the presence of magnetic material which causes a reduction

in the total amount of carbon sorbent available for sorption. The ACs present almost two order of magnitude higher diclofenac uptake compared to the BCs.
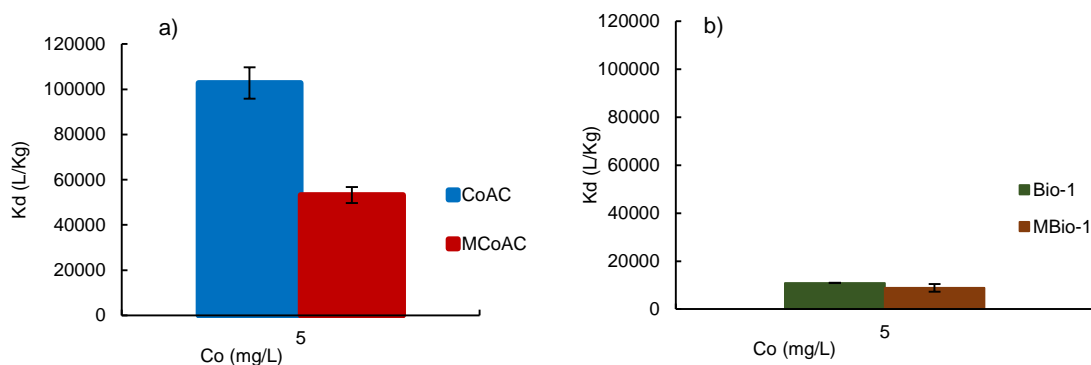
Figure 5.6: Partitioning coefficient for sorption of diclofenac on (a) ACs and (b) BCs

B. Diclofenac sorption: Nonlinear models

Data fits reasonably well to all models using both linear and nonlinear regression methods, except for Langmuir models. As expected, the nonlinear method has superior data fitting ability due to conservation of models' original error structure, which is not strongly so in the case of the LTFM method (Goldberg *et al.*, 2005). Hence, the ASE for the nonlinear models is less than that for the corresponding LTFMs (see Table 5.7).

Table 5.7: Summary of ASE for the sorption of diclofenac on ACs and BCs

Sorbent	LANG_L	FR_L	RP_L	LANG	FREU	RED-PET	DA	PDM
CoAC	298.60	17.72	19.67	81.66	16.95	18.64	13.04	0.88
MCoAC	54.61	7.42	6.68	14.97	7.24	6.35	6.99	0.92
Bio-1	11.21	1.23	0.81	5.39	1.18	0.80	0.53	0.44
MBio-1	13.44	2.28	2.69	8.83	2.24	2.65	2.58	1.91

Table 5.8: Summary of MSC for isotherm prediction using optimised model parameters for sorption of diclofenac on ACs and BCs

Sorbent	CoAC	MCoAC	Bio-1	MBio-1
LANG	-0.71	0.28	0.8	0.74
FREU	2.23	2.48	3.82	2.82
RED-PET	1.82	2.3	4.42	2.48
DA	2.22	2.19	5.1	2.51
PDM	2.22	2.19	5.1	2.5

From Table 5.8, to select a representative model, it can be observed that except for Bio-1, the Freundlich model has the highest MSC value for all the

models tested. In contrast, Langmuir model has the least MSC value in all cases. Accordingly, the Freundlich is the best model (having higher information about the system) that can describe the sorption of diclofenac on CoAC, MCoAC and MBio-1. In the case of Bio-1, the 3-parameter models have higher MSC value than Freundlich; the DA model has the highest value.

Table 5.9:   Optimised model parameters for isotherm of diclofenac sorption on ACs and BCs

Model	Parameters	CoAC	MCoAC	Bio-1	MBio-1
Linear	K_d*	102.71	53.20	10.92	8.83
LANG	Q_m	164.19	97.09	9.76	8.072
	K_L	0.81	0.92	0.74	0.45
	R^2	0.8071	0.9270	0.9600	0.9427
	ASE	81.66	14.97	5.39	8.83
FREU	$1/n$	0.13	0.13	0.22	0.27
	K_F	105.74	63.10	5.20	3.36
	R^2	0.9546	0.9624	0.9903	0.9754
	ASE	16.95	7.24	1.18	2.24
RED-PET	K_R	1.73E+05	505.63	58.19	1584.99
	A_R	1633.20	7.25	10.05	480.17
	γ	0.87	0.91	0.82	0.72
	R^2	0.9545	0.9699	0.9964	0.9754
	ASE	18.64	6.35	0.80	2.65
DA	Q_o	204.82	98.72	10.67	9.81
	E	94.77	33.46	22.36	21.24
	b	0.56	1.29	1.38	0.97
	R^2	0.9684	0.9664	0.9982	0.9754
	ASE	13.04	6.99	0.53	2.58
PDM	Q_o	204.94	98.72	10.67	9.817
	a	2.57	33.47	74.44	21.243
	b	0.56	1.29	1.38	0.964
	R^2	0.9684	0.9664	0.9982	0.9754
	ASE	0.88	0.92	0.44	1.91

*x10^3

As compared to the Langmuir, the Freundlich model offers better values for both R^2 and ASE (see Table 5.9), suggesting better description of the sorption of diclofenac on the ACs and BCs. Therefore according to the Freundlich theory, the interaction between diclofenac and sorbents' surface would result in multilayer diclofenac coverage over an energetically non homogenous surface

(Çeçen and Aktas, 2011; Worch, 2012). The simulated and experimental isotherms are almost identical as shown in Figure 5.7. This suggests that their parameters can help in describing the sorption system within the examined range of concentration.
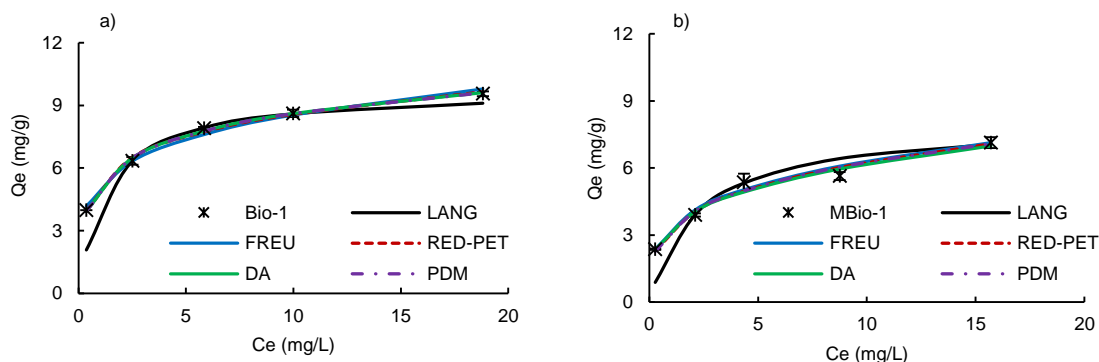
Figure 5.7:   Comparison of simulated and experimental isotherm plot for sorption of diclofenac on (a) Bio-1 and (b) MBio-1

5.3.2.2   *Diclofenac Sorption Affinity*

The Freundlich and the other three 3-parameter models align almost perfectly with the experimental isotherm. The Redlich-Peterson model in such instance is a special case of the Freundlich model. Close assessment of the heterogeneity and intensity parameters in Langmuir, Freundlich, and Redlich-Peterson models in Table 5.9, reveals a very similar order [K_L: MBio-1 < Bio-1 <CoAC < MCoAC; n: MBio-1 < Bio-1 < CoAC ≈ MCoAC; and γ: MBio-1 < Bio-1 < CoAC ≈ MCoAC respectively]. Accordingly, it can be deduced from the Langmuir's S_L plot in Figure 5.8, that the sorption of diclofenac is more favourable over heterogeneous surfaced sorbents.
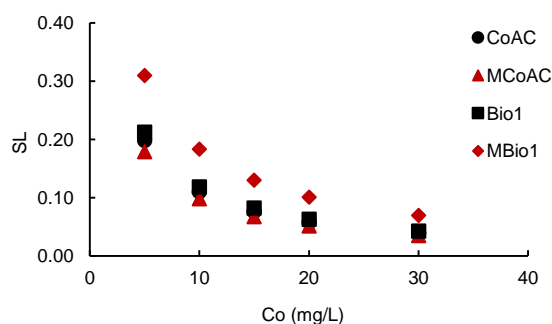
Figure 5.8:   Plot of Langmuir separation factor for sorption of diclofenac ACs and BCs

Here once again, the separation factors of the magnetic sorbents are significantly different (p-value < 0.02; α = 0.05, in both MAC and MBC) from those recorded for their corresponding pristine pairs. The difference can be attributed to the presence of iron oxide in the magnetic pairs and is most visible in the MBio-1 whose S_L curve is distinctly separate from the rest. The sorption on both ACs and BCs is favourable according to Freundlich theory because $n > 1$ in all cases (Mc Kay *et al.*, 1983; Worch, 2012).

5.3.2.3   *Diclofenac Sorption Capacities*

Assessment of the capacity parameters in Table 5.9, shows that the sorption capacity of the ACs is 1 to 2 order of magnitude higher than that of the BCs. According to the capacity parameters of all models, the sorption capacities of the sorbents are in the order; MBio-1 < Bio-1 < MCoAC < CoAC. Xu *et al.* (2008) have shown the contribution of both micropore and mesopore volumes as key components that determine the sorption capacity of sorbents in the sorption of organic compounds. Hence, these capacity determining sorbent properties from Table 3.1, were correlated with model capacity parameters from Table 5.9. The result obtained in Table 5.10, shows that there is a strong correlation (generally, Pearson correlation coefficient $R = 0.9367$ to 0.9990) between these factors.

Table 5.10:   Sorption of diclofenac on ACs and BCs; Pearson correlation coefficients between model parameters and sorbent properties.

Model	Parameters	A_S	V_P	V_{MP}	P_S
Linear	K_d	0.9962	0.9374	0.9938	0.3404
Langmuir	Q_m	0.9990	0.9646	0.9929	0.2427
	K_L	0.6555	0.6064	0.6801	0.1439
Freundlich	$1/n$	0.8913	0.8628	0.8990	0.0177
	K_F	0.9990	0.9657	0.9929	0.2333
Redlich-Peterson	K_R	0.8428	0.7002	0.8517	0.7148
	A_R	0.7177	0.6116	0.7128	0.7138
	γ	0.7431	0.7035	0.7619	0.1156
Dubinin-Ashtakov	Q_o	0.9944	0.9368	0.9910	0.3477
	E	0.9181	0.7980	0.9240	0.6084
	b	0.6368	0.5875	0.6165	0.6036
Polanyi-Dubinin-Manes	Q_o	0.9944	0.9367	0.9910	0.3480
	a	0.6455	0.7419	0.5955	0.1444
	b	0.6346	0.5855	0.6142	0.6036

When normalised with respect to carbon content, sorption of diclofenac within the studied concentration is shown to be mostly dependent upon the pore volume, then by surface area and/or micropore volume as shown in Table 5.11. Therefore, magnetite impregnation does not have a significant detrimental effect on the diclofenac sorption capacities of CoAC and Bio-1, especially when assessed with respect to the actual content of carbon used in the experiment.

Table 5.11: Sorption of diclofenac on ACs and BCs; Pearson correlation coefficients between normalised model capacity factors and sorbent properties

Model	Parameters	A_S	V_P	V_{MP}	P_S
Linear	K_d	0.9537	0.9870	0.9375	0.0311
Langmuir	Q_m	0.9183	0.9714	0.9004	0.1303
Freundlich	K_F	0.9165	0.9678	0.8996	0.1327
Dubinin-Ashtakov	Q_o	0.9670	0.9887	0.9525	0.0169

5.3.3 POLANYI CHARACTERISTIC CURVE

According to the Polanyi theory, a plot of volume of sorbed sorbate 'Q_V' against the adsorption potential 'ε' for a given pair of sorbent and sorbate will yield a characteristic curve that is temperature invariant and is determined by the structure of the sorbent (Yang and Xing, 2010). Another way of expressing the relationship between the amount adsorbed and the adsorption potential is the correlation curve, which is the modified version of the characteristic curve. The correlation curve is a plot of Q_V against adsorption potential density (ε/Vs), such that Polanyi theory mechanistically captures the sorption process if a single curve is obtained for the sorption of a given sorbate on different sorbents.

The Figures 5.9 & 5.10 shows the correlation curves for the sorption of ibuprofen and diclofenac on ACs and BCs. It can be seen that for both pairs of sorbents and a given sorbate, the correlation curves do not collapse to a single curve, to show conformity to Polanyi theory. This has been reported to be usual in sorption systems involving polymeric and activated carbon type of sorbents (Yang *et al.*, 2006b). This separation of correlation curves is usually due to difference in sorbents' pore structure (Long *et al.*, 2008) and the curves can be made to collapse when their respective amount adsorbed is normalised with respect to their micropore volume. Thus, if sorption is according to Polanyi theory,

the normalised correlation curve should be a single curve for a given sorbate on different sorbents.
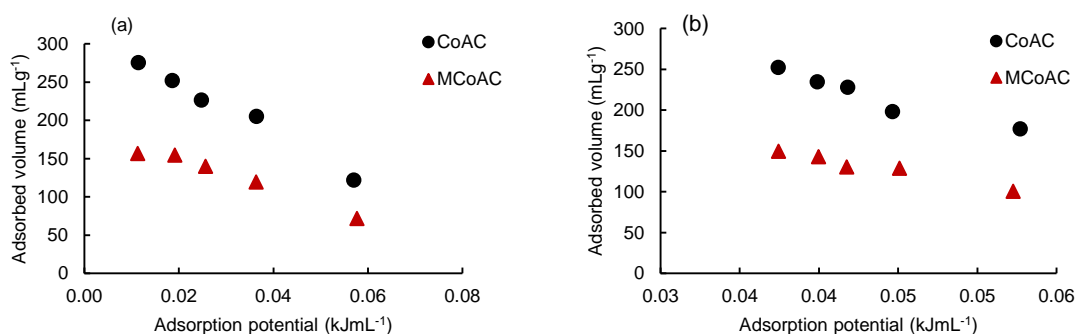
Figure 5.9: Polanyi correlation curve for the sorption of (a) ibuprofen and (b) diclofenac on CoAC and MCoAC
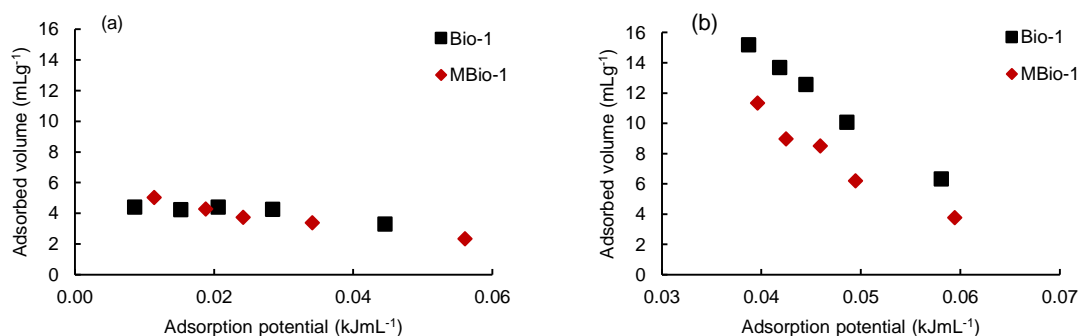
Figure 5.10: Polanyi correlation curve for the sorption of (a) ibuprofen and (b) diclofenac on Bio-1 and MBio-1
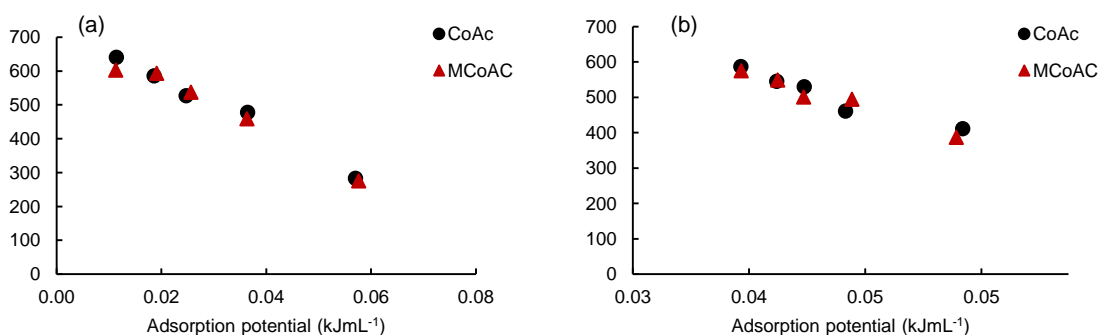
Figure 5.11: Normalised Polanyi correlation curve for the sorption of (a) ibuprofen and (b) diclofenac on CoAC and MCoAC

The ACs correlation curves (Figure 5.11) have collapsed to a single line when normalised with respect to their V_{MP}, while such was not achieved in the case of the BCs (Figure 5.12). Assessment of their respective microporosity shows that, while the ACs are mainly microporous with higher V_{MP}/V_P ratio, the

BCs are not as microporous and thus have a lower V_{MP}/V_P ratio, especially the MBio-1. According to the Polanyi theory, sorption takes place by pore filling mechanism. This is relatively satisfied in the case of the ACs with respect to both the isotherm fitting and characteristic curve. Therefore, van der Waals force and pore-filling play significant roles in the sorption of ibuprofen and diclofenac on these sorbents (Xu *et al.*, 2008).
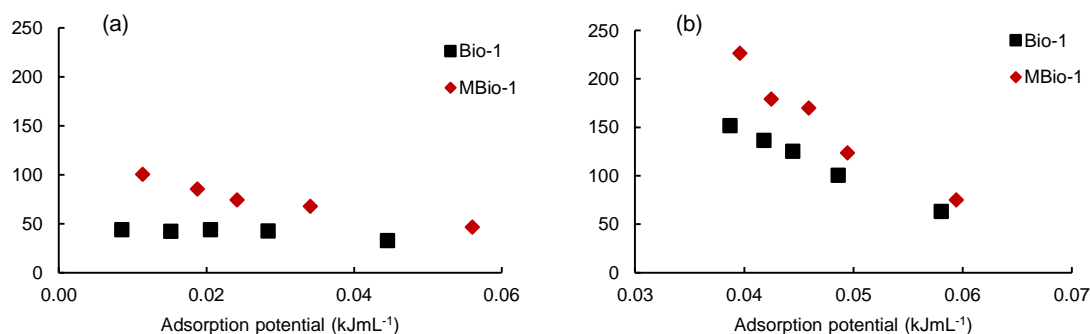
Figure 5.12:   Normalised Polanyi correlation curve for the sorption of (a) ibuprofen and (b) diclofenac on Bio-1 and MBio-1

In the case of the BCs however, the Polanyi theory was satisfied with respect to the isotherm fitting and not the characteristic curve. Dąbrowski (1999), has reported that although sorption in micropores is essentially due to pore filling process which is influenced by their volume, the layer-by-layer sorption mechanism in macropores and mesopores is plausible. This suggest that Polanyi theory may still be applied to sorption due to open surface as has been observed in the sorption of organic sorbent on carbon nanotubes and nanosized particles with poor microporosity (Yang and Xing, 2010). Cross comparison of the sorption capacities of the sorbents for a corresponding sorbate pair also supports the aforementioned nonconformity to the Polanyi theory by the BCs when strictly evaluated based on the correlation curve. For both pharmaceuticals, the sorption capacities of the ACs are by far superior to those of the BCs, essentially due to amplified surface area and better developed pores.

5.3.4   COMPARISON OF SORPTION CAPACITIES

Comparing the uptake of the pharmaceuticals according to Q_m reveals that, ibuprofen sorbs about 1.8 and 3 times more on CoAC and MCoAC respectively

than diclofenac. While in the case of the BCs, the uptake is reversed, whence diclofenac sorbs about 2.13 and 1.49 times more on Bio-1 and MBio-1 respectively than ibuprofen. This is similar to the findings of (Baccar *et al.*, 2012) where according to Q_m, diclofenac was reported to sorb about 5 times more than ibuprofen on mesoporous activated carbon. In a study by Margot *et al.* (2013) covering the treatment of about 70 different pharmaceuticals from wastewater on a pilot scale, diclofenac and ibuprofen were categorised among those with medium affinity for powdered activated carbon. It was further reported that; better removal of ibuprofen was observed over diclofenac due to different characteristics of the PACs applied. Another explanation for the varied uptake is in terms of differences in additional sorbents' surface characteristics such as pH$_{PZC}$, types and concentration of functional groups and affinity for individual sorbate.

Differences of sorbate properties such as; pKa, LogK$_{OW}$, molecular structure and size can cause the preferential uptake of one sorbate on a given sorbent over the other (Rakić *et al.*, 2015). For instance, diclofenac has slightly higher LogK$_{OW}$ value (4.51) than ibuprofen (LogK$_{OW}$ =3.97), so it is less soluble. Therefore, as compared to diclofenac, removal of ibuprofen molecules from solution takes place only after sorption forces are able to overcome relatively higher hydrophilic forces (Li *et al.*, 2002; Çeçen and Aktas, 2011; Worch, 2012). In this study, the concept of hydrophobic dependence of sorption did not hold for the sorption of the two pharmaceuticals on the ACs, whence, ibuprofen sorbs more than diclofenac. This higher affinity for ibuprofen as compared to diclofenac could likely be due to the nature and concentration of the surface groups present.

The surface chemistry of ACs influences the wettability and as a result the sorption of a relatively more hydrophilic compound can be favoured over a less hydrophilic one under favourable conditions (Cho *et al.*, 2011). Spatial interactions could be responsible for this varied uptake of the pharmaceutical. In the BCs system, molecular sieving could hinder the uptake of ibuprofen due to its larger longitudinal size compared to diclofenac. Yet, this mechanism does not explain the higher uptake of larger ibuprofen over diclofenac in the ACs system. It is therefore most likely that the ACs have active sites that could specifically bind more ibuprofen than diclofenac.

The dependence of sorption on pH could be another reason behind the more uptake of ibuprofen on the ACs compared to diclofenac. It can be observed from Figure 5.13(a) that in the ACs, system, the sorption of ibuprofen takes place at low pH i.e. within the vicinity of its pKa value. In this pH range, ibuprofen exists majorly in the neutral form. This was not the case for the BC system. It can be seen from Figure 5.13(b), that, although the pH of the control samples also assumed a steady decline, the treatment samples remained more or less steady. For the diclofenac system, the pH of both the treatment and control samples for the ACs and BCs remained somewhat unchanged. To further understand this varied uptake, the influence of pH on the sorption of both pharmaceuticals was investigated and the result is discussed in 5.3.6.

5.3.5 MECHANISM OF SORPTION

The mechanism of sorption of both sorbates is proposed to be possible due to van der Waals forces that include hydrogen bonding, dispersion forces, aromatic stacking, π - π interactions and electrostatic attractions (Rivera-Utrilla *et al.*, 2013). Molecules of both sorbents consist of aromatic rings which could coordinate with the fused hexagonal carbon rings on the surface of the sorbent, hence propagating their sorption due to aromatic stacking induced by dipole-dipole attractions (Mohan *et al.*, 2011). It can as well be due to π - π electron donor-acceptor interactions, with the polar aromatic rings of the sorbates acting as acceptors and the delocalised electrons at the edges and basal planes of the sorbents acting as donors. Another donor-acceptor interaction could be between the carbonyl and hydroxyl type functional groups on the carbon surface as donors and the aromatic ring of the sorbates acting as acceptors (Guedidi *et al.*, 2013; Kyzas *et al.*, 2013).

Electrostatic interactions can as well be another sorption mechanism by which these pharmaceuticals sorb to the ACs and BCs. The sorbents have high pH$_{PZC}$ values (all in excess of 9 except for MCoAC with a value of 6.3). Experiments were conducted within the pH ranges 4.5 to 6.0 and 6.3 to 6.9 for the ibuprofen and diclofenac systems respectively as shown in Figures 5.13 & 5.14. Both have low pKa values; 4.91 and 4.15 for ibuprofen and diclofenac respectively. Being organic acids, they exist in their neutral undissociated form at

pH < pKa and in form of dissociated carboxylate anion at pH > pKa (Iovino *et al.*, 2015). With reference to sorption of charged species of sorbates, sorption of both pharmaceuticals on the sorbents may be due to coordination between the positively charged sorbent surfaces and the negatively charged carboxylate anion specie of the sorbates (Dubey *et al.*, 2010). In the case of sorption of diclofenac on MCoAC, it can be assumed that the surface is not completely deprotonated so sorption by electrostatic attraction is still possible (Cho *et al.*, 2011).
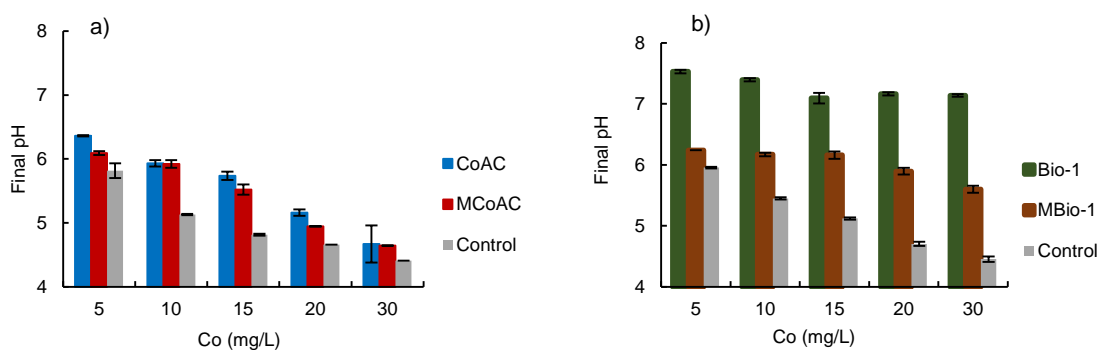
Figure 5.13:   Final solution pH for the sorption isotherm of ibuprofen on (a) ACs and (b) BCs
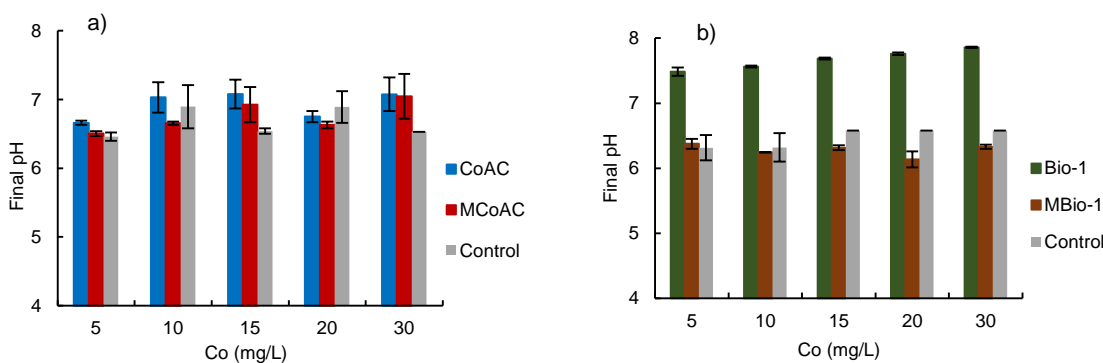
Figure 5.14:   Final solution pH for the sorption isotherm of diclofenac on (a) ACs and (b) BCs

5.3.6 EFFECT OF SOLUTION PH ON SORPTION

The net surface charge of the sorbents, the type and concentration of surface functional groups and speciation of sorbents are influenced by the pH of the solution (Worch, 2012; Iovino *et al.*, 2015). At pH < pH_{PZC}, there will be excess protonation of the sorbent's surface and it will have a net positive charge, while

at high pH > pH$_{PZC}$, the surface will have a net negative charge due to excess deprotonation (i.e. as a result of the ionisation of acid surface groups). In between these two is the pH$_{PZC}$, when the surface will have a neutral or net zero charge (Roop and Meenakshi, 2005). For acidic organic sorbates, they can exist in neutral form as conjugate acids when the pH is less than their dissociation constant (pH < pKa) or in ionised dissociated form as carboxylate ibuprofen anion at pH > pKa (Essandoh *et al.*, 2015). The sorption of ibuprofen and diclofenac on the ACs and BCs is therefore expected to be influenced by the pH of the system.

The sorption of pharmaceuticals and some micropollutants on activated carbons has been shown to be influenced by the system's pH. Salman and Hameed (2010), studied the sorption of 2,4-dichlorophenoxyacetic acid (2,4-D) and carbofuran on granular activated carbon. Sorption of both compounds decrease with an increase in pH, but it is more pronounced in the (2,4-D) than the carbofuran system. Highest sorption for both compounds was recorded at pH 2 and the authors suggested that it was as a result of interactions involving variations in both sorbent surface conditions and sorbate speciation. Nam *et al.* (2014), observed that pH has a significant influence in the sorption of especially hydrophilic micropollutants due to electrostatic interactions between ionised pollutant's species and charged sorbents' surface. Kyzas *et al.* (2013), reported that the sorption of pramipexole dihydrochloride on oxidised and non-oxidised activated carbon was the highest at pH 3, even though the oxidised sorbent has the higher concentration of oxygen based functional groups thus making it more polar and more hydrophilic.

5.3.6.1   Effect of pH on Sorption of Ibuprofen

From Figure 5.15, it can be seen that the sorption of ibuprofen on both ACs and BCs is remarkably affected by the initial pH. In fact, the pH has a negative influence on the system, such that an increase in pH results in a corresponding decrease in the sorption of ibuprofen. It has been reported that the sorption of ibuprofen on activated carbons, biochar and carbon nanotubes is influenced by pH in a similar way (Dubey *et al.*, 2010; Cho *et al.*, 2011; Baccar *et al.*, 2012; Guedidi *et al.*, 2013; Essandoh *et al.*, 2015). As an organic acid, ibuprofen will exist in neutral form and anionic form at pH below and above its pKa value (4.91) respectively. At pH 3, (pH < pKa < pH$_{PZC}$), in theory, it is assumed that the surface

of the sorbents will have a net positive charge and ibuprofen will be in its neutral form and generally, the sorption of neutral species is relatively favoured (Limousin *et al.*, 2007), so this resulted in the highest uptake of ibuprofen. Sorption under this condition is most likely due to van der Waals interaction and/or hydrogen bonding (Baccar *et al.*, 2012). Guedidi *et al.* (2013), also reported higher sorption of ibuprofen at low pH, they attributed this to the influence of dispersive interaction as the dominant mechanism of sorption of neutral form of ibuprofen moieties on activated carbon.
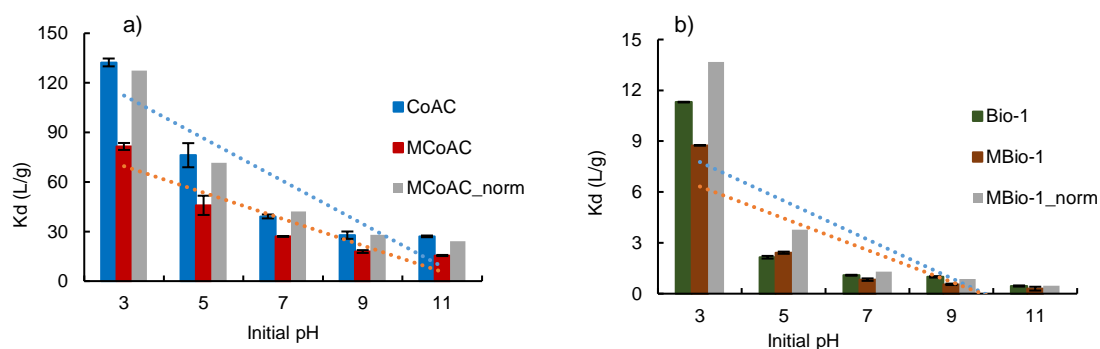
Figure 5.15:   Effect of initial pH on sorption of ibuprofen on (a) ACs and (b) BCs. [Note; figures have different scales]

As the pH is increased beyond pKa, (pKa < pH < pH$_{PZC}$), the concentration of the charged anionic form of ibuprofen gradually increases and sorption due to electrostatic attraction between positively charged surface and negatively charged carboxylate anionic specie of ibuprofen becomes active. Finally, at pH 11, (pH > pH$_{PZC}$ > pKa), both the sorbents' surface and ibuprofen anionic specie have negative charge, resulting in electrostatic repulsion and a decrease in sorption, which is the lowest observed within the pH range studied. Furthermore, charged species have higher polarity and are therefore more soluble, hence as the pH increases, the solubility of ibuprofen increases causing a reduction in sorption capacities due to higher solute-solvent interaction (Snoeyink and Summers, 1999).

It has been shown by Iovino *et al.* (2015), that the pH dependence of ibuprofen sorption is strictly related to its % of ionisation. At pH = 2, it exists almost entirely in non-ionised form (0.4% ionised), at pH = pKa it is about 50% ionised and at pH > 8 it is almost entirely (99.9%) ionised. This explains why the sorption of ibuprofen does not decrease when the pH of the system is lowered due to

oxidation of the surface of the sorbents. It has been reported (Snoeyink and Summers, 1999; Li *et al.*, 2002), that lowering the pH of the system makes the surface of a sorbent more oxidised by increasing the concentration of oxygen related functional groups, such as carboxylic and phenolic hydroxyl groups. This causes the localisation of the π electron of the aromatic rings on the surface of the sorbent and in theory, this should cause a decrease in the sorption of organic compounds due to impaired interaction with the sorbent's π electrons. Sorption of ibuprofen could then probably be due to hydrogen bonding or dispersive interaction, which have been reported to be possible on oxidised surfaces (Li *et al.*, 2002; Guedidi *et al.*, 2013).

Dispersive forces have also been reported to be the main interactions that facilitate the sorption of similar micropollutants (Cabrita *et al.*, 2010). At low pH, the surface of the sorbents is expected to have a net positive charge and sorption of ibuprofen is still possible due to hydrogen bonds between carbon and ibuprofen molecules. Also, ibuprofen can be sorbed by means of donor-acceptor interactions with the surface carbonyl groups or electron rich regions of the sorbents (as electron donors) and aromatic ring of ibuprofen (as electron acceptors) (Iovino *et al.*, 2015; Rakić *et al.*, 2015). Finally, the presence of impregnated iron oxide on the surface of sorption of MCoAC and MBio-1 due to magnetisation did not detrimentally affect the sorption of ibuprofen since the sorption capacities (K_d) of the pristine sorbent and that of normalised composite are statistically similar (p-value = 0.297 and 0.177; α = 0.05, in both MAC and MBC) for all pH values.

It is obvious that over the pH range considered, both neutral and dissociated species of ibuprofen are sorbed on the sorbents. To estimate the ratio of these sorbed species, the data is fitted to the speciation model (Schwarzenbach *et al.*, 2005; Yang *et al.*, 2008; Werner *et al.*, 2013).

$$K_{d,\text{Ibu}} = A \frac{1}{1+10^{(\text{pH}-\text{pKa})}} + B \left(1 - \frac{1}{1+10^{(\text{pH}-\text{pKa})}}\right) \qquad - \qquad - \qquad - \qquad (5.1)$$

The terms A and B are the fitting constants and they represent the partition coefficients of neutral and dissociated species respectively. The data fits very well to the model (see Figure 5.16(a)) and generally for all the sorbents, very high

correlation was recorded, resulting in a straight line passing through the origin as can be observed in Figure 5.16(b).
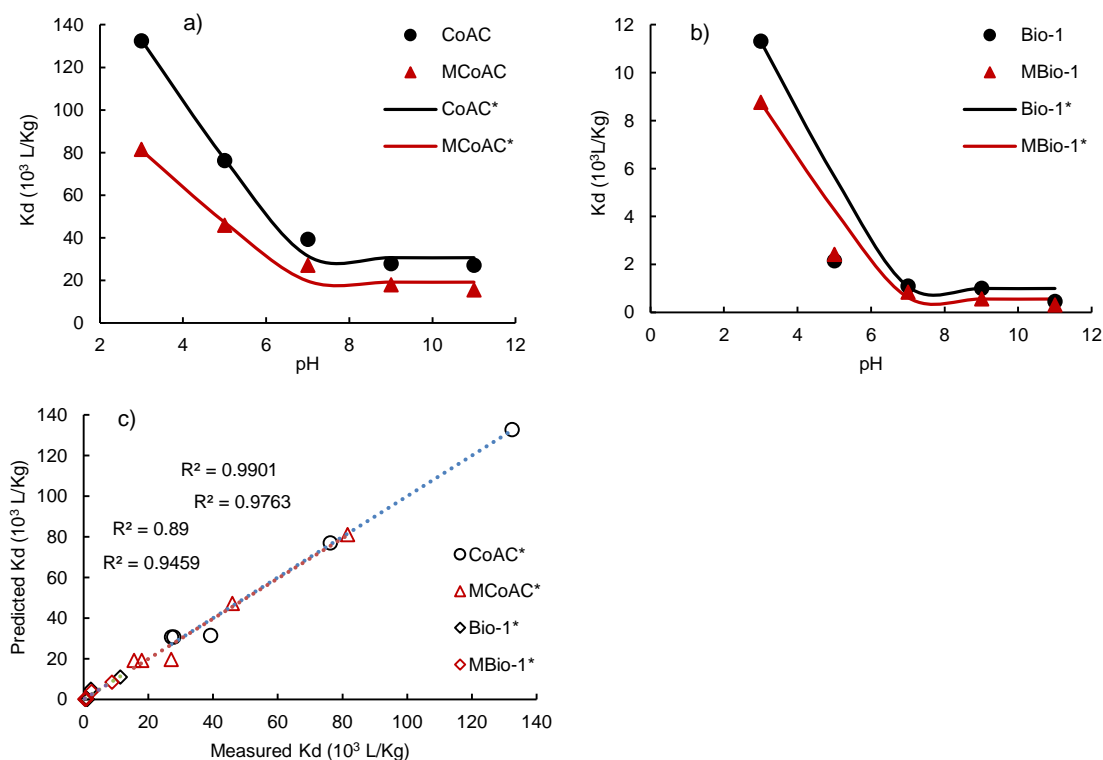
Figure 5.16:   Modelling of pH data for sorption of ibuprofen on (a) CoAC and (b)Bio-1, (c) correlation for pH fitting. Asterisk (*) represents fitted data

The result for the fitting constants is presented in Table 5.12. It can be seen that the neutral specie constitutes the much larger fraction of the sorbed ibuprofen. At pH > pKa > pH$_{PZC}$, sorption impairment due to electrostatic repulsion becomes prominent. Therefore, the sorption of ibuprofen in this condition is likely due to the presence of 0.01 M CaCl background solution that could aid in neutralising the repulsive forces resulting from increased pairing of calcium ion with the anionic specie (Snoeyink *et al.*, 1969).

Table 5.12:   Partition coefficients for neutral and dissociated ibuprofen species

Sorbent	A	B
CoAC*	133.64	29.49
MCoAC*	82.07	18.71
Bio-1*	8.61	0.47
MBio-1*	7.56	0.34

5.3.6.2   Effect of pH on Sorption of Diclofenac
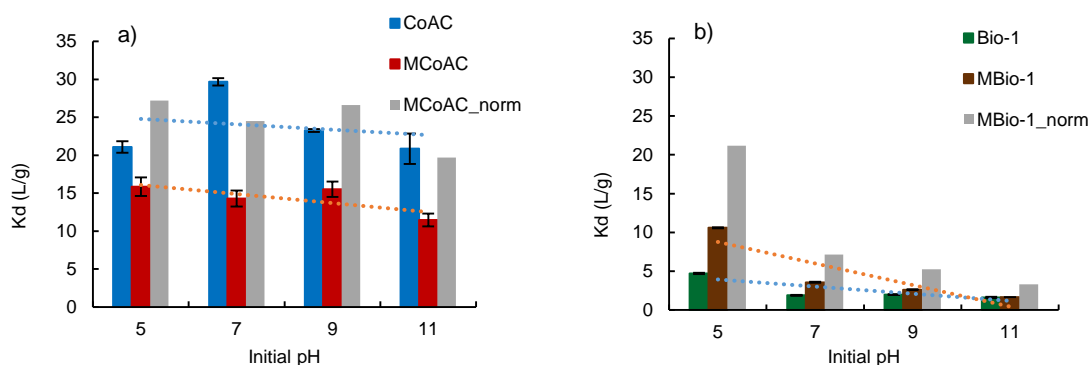
Figure 5.17:   Effect of initial pH on sorption of diclofenac on (a) ACs and (b) BCs

It should be noted that the attempt to lower the pH to 3 for the diclofenac solution resulted in the formation of precipitates that settled out of the solution. This could be the reason why pH below 5 was not considered also by other authors (Bajpai and Bhowmik, 2010; Wei *et al.*, 2013; Nam *et al.*, 2014). Therefore, as can be observed especially in Figure 5.17(a), the pH has less influence over the ACs' sorption system, in this instance, pH range is above the pKa, such that the diclofenac molecules exist majorly in the carboxylate anionic form. Hence, the sorption of diclofenac takes place mainly in its deprotonated species. The uptake of diclofenac increased from pH 5 to reach maximum at pH 7 and then it dropped back to the initial sorption level. Hence over the entire range, a nearly horizontal trend was presented. This could be due to electrostatic attraction between the positively charged surface of the AC and the negatively charged carboxylate form of the dissociated diclofenac molecules. Sorption of diclofenac on polymer and activated carbon has been reported not to be significantly affected by changes in pH (Bajpai and Bhowmik, 2010; Nam *et al.*, 2014) and both related this to the hydrophobic nature of diclofenac molecule. Although (Suriyanon *et al.*, 2013) observed that pH had influence on the sorption of diclofenac on silicate material, they also found that pH does not have much influence the sorption of diclofenac on AC. They related this non pH dependence sorption to the nature and concentration of functional groups present on the AC's surface that causes variations in both electrostatic interaction and other sorption driving forces.
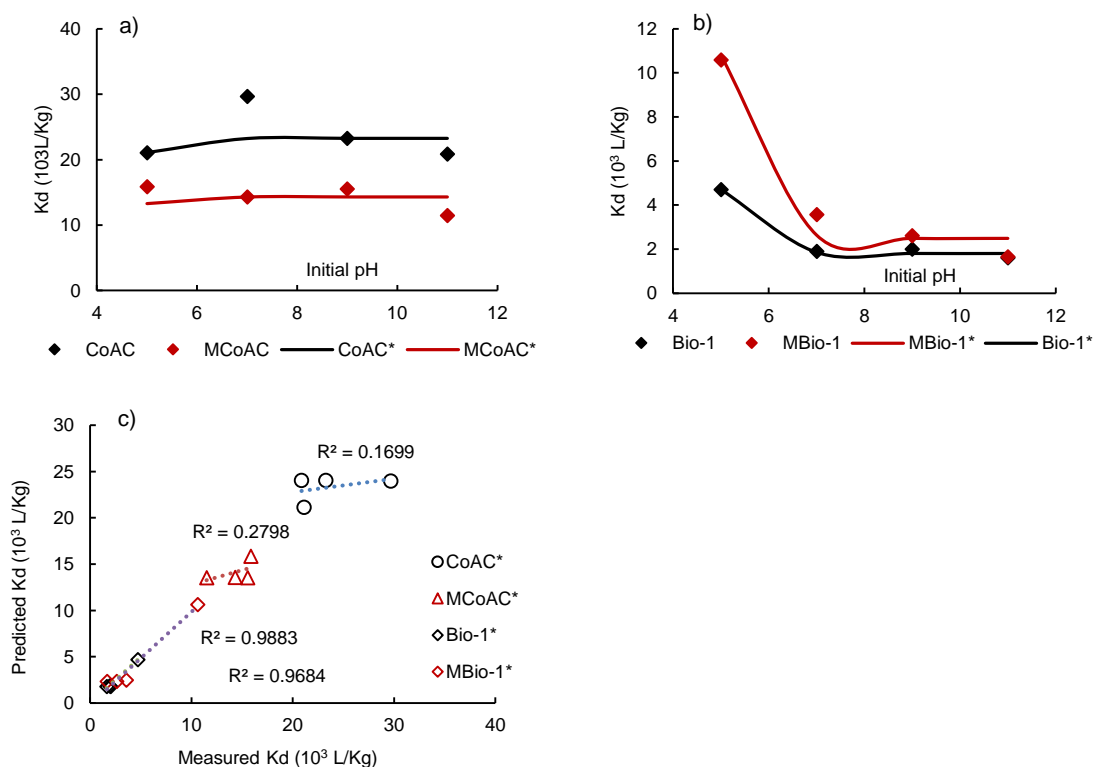
Figure 5.18:   Modelling of pH data for sorption of diclofenac on (a) CoAC and (b)Bio-1, (c) correlation for pH fitting. Asterisk (*) represents fitted data

Diclofenac has a relatively low pKa, hence in the range of pH tested, it exists substantially in ionised form, ca. 48.28% even at pH 4.12 (Baccar *et al.*, 2012). In theory, dissociated species are more soluble and therefore can be removed from solution after the hydrophilic forces are overcome by the sorption forces. For instance, in the case of the BCs', it can be seen from Figure 5.18(b) that pH influences the uptake of diclofenac, especially on MBio-1, sorption decreases as the pH increases. So it is likely, that electrostatic repulsion is more pronounced at high pH due to the presence of diclofenac mainly in carboxylate anionic form which is repelled by the negatively charged surface of the sorbents. This is similar to the finding of Wei *et al.* (2013), they reported that, the sorption of diclofenac on granular carbon nanotubes/alumina hybrid adsorbents was the lowest at high pH due to increased electrostatic repulsion between negatively charged sorbent surface and the anionic diclofenac specie.

The data for the pH for the BCs fitted very well to Equation 5.1, while poor fitting resulted for the ACs data, as can be seen in Figure 5.18. This is a further proof that on the one hand, the sorption of diclofenac on the ACs is less sensitive

to pH variations, while on the other hand its sorption on the BCs is influenced by pH variation. Accordingly, the sorption of the neutral specie is most favoured on the BCs as presented in Table 5.13.

As we have seen, the speciation model fits reasonably well to the adsorption edge curve for the BC, while poor fitting was observed for the AC. The varied success in the fitting of the model is not unusual since it was mostly applied in sorption on homoionic or non-functionalised, extremely low variable-charge surface sorbents (Haderlein and Schwarzenbach, 1993; Xiao and Pignatello, 2014). In essence, only the variation in the speciation of the sorbate and not the variation in the charge density of the sorbent is considered.

Table 5.13:   Partition coefficients for neutral and dissociated diclofenac species

Sorbent	A	B
CoAC*	2.33	46.08
MCoAC*	33.95	13.65
Bio-1*	25.07	1.84
MBio-1*	68.11	2.53

Nevertheless, in their normalised form, the sorption capacities of the composites are quite similar to those of the pristine carbon (p-value = 0.773 and 0.141; α = 0.05, in both MAC and MBC). Therefore, pH will influence the sorption of diclofenac on both the composites and the pristine carbons in quite similar ways.

The results presented herein are in agreement with the findings of previous works which reported that the sorption of various compound on magnetised sorbents is being influenced by the pH of the system. The influence has been shown to be due to the effect of pH on the chemistry of the sorbents' surface, the speciation of the sorbates and electrostatic interactions. For instance, Mohan *et al.* (2014) studied the sorption of fluoride on magnetic biochar and found it to be influenced by the solution pH, such that sorption was highest at low pH and it decreased with increases in pH. They related this variation to the protonation of surface functional groups; from highly protonated surface at low pH which favours the sorption of hydrated fluoride ions to a less protonated surface at higher pH. In another study, Rai *et al.* (2015) reported that the sorption of crystal violet (a cationic dye) on $SnFe_2O_4$@activated carbon magnetic nanocomposite is

favoured at higher pH due to electrostatic attractions between negatively charged magnetic nanocomposite and positively charged cationic dye. The sorption of methyl orange dye was shown (Jiang *et al.*, 2015) to be higher at low pH due to hydrogen bonding with oxygen and hydroxyl groups on the surface of AC/NiFe2O4 composite surface.

5.3.7 IBUPROFEN SORPTION KINETICS
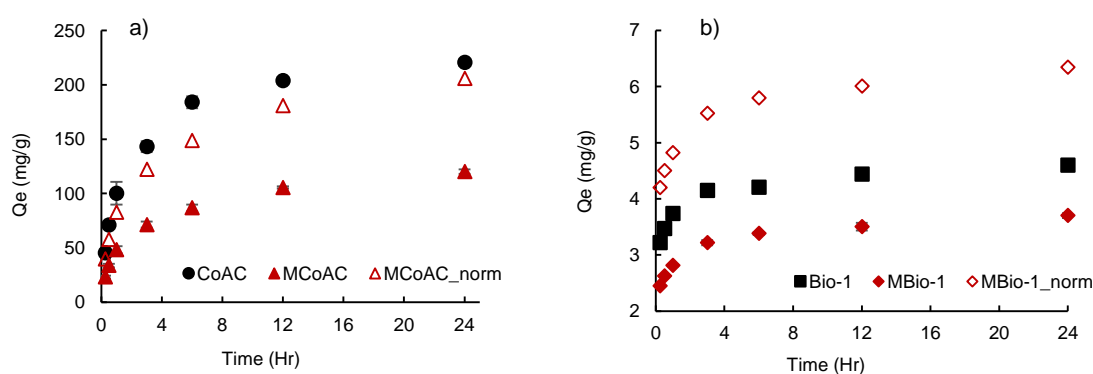
Figure 5.19:   Plot of sorption kinetics for ibuprofen on (a) ACs and (b) BCs. [Note; figures have different scales]

The kinetics for sorption of ibuprofen on magnetic and nonmagnetic activated carbon and biochar is shown in Figure 5.19. Once again, due to the benefits of activation, the ACs display superior uptake of ibuprofen over the BCs for the entire duration of the experiment. Kinetic plots exhibit nonlinear curves characterised by steep slope at the lower end of the plot with data points within the vicinity of the ordinate axis, suggesting a relatively faster uptake of ibuprofen molecules as sorption commences. At this stage, there is abundance of free potential sorption sites and the concentration gradient due to difference in the concentration of ibuprofen molecules in the bulk solution and that on the solid particles is at its highest (Chowdhury *et al.*, 2013).

The formation of sorption bond between the molecules of solutes and the surface of the sorbents occurs very fast (Snoeyink and Summers, 1999; Çeçen and Aktas, 2011). This attachment commences with the most accessible sites around the exterior and shallow pores of the particle, hence sorption commences almost instantaneously (Chowdhury *et al.*, 2011; Wang *et al.*, 2015b). Also, the pores are highly accessible at this stage, hence, sorption is expected to progress at its fastest rate. At each point on the curve, the slope gives the instantaneous

rate of sorption dQ/dt (Yang and Al-Duri, 2005). With time, the sorption sites and pores become progressively occupied by the sorbate molecules such that the sorption driving force gets progressively diminished due to decrease in both free sorption sites and bulk concentration of the sorbate in solution (Chen *et al.*, 2010). At this stage, the slopes of the plots progressively decrease until equilibrium is attained, i.e. when the concentration gradient between the bulk solution and the solid is expected to become zero.

It can be observed that the curves for the magnetic sorbents are distinctively different from those of their corresponding pristine pairs. Also, the slopes of the pristine sorbents at the early stages are steeper than those of their corresponding magnetic pairs, which is perhaps due to a higher concentration of sorption sites per mass of sorbent. Nonetheless, for the magnetic carbon, kinetics is still a bit slower when normalized with respect to the carbon content. This is probably due to the magnetite deposits on the AC surface hindering the immediate adsorption from the aqueous solution, and extending diffusion pathways to the micropores of the AC

5.3.7.1   *Attainment to Equilibrium*
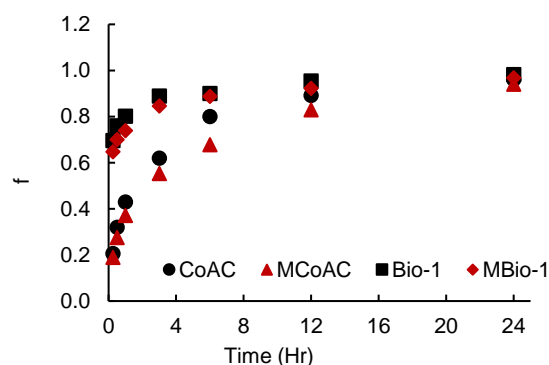
Figure 5.20:   Ibuprofen sorption kinetics fractional uptake

A plot of fractional uptake with time is shown in Figure 5.20, it provides a means of assessing how close the sorption system is towards its equilibrium state (Yang and Al-Duri, 2005). From the $f - t$ plot, it can be observed that the curves for magnetic sorbents lag behind those of the nonmagnetic pairs, which means they have slower kinetics. In fact, there is no strong statistical evidence (generally, p-value ≤ 0.01) to suggest the curves for corresponding pairs of sorbents are similar.

Within the first 1 hr, the BCs have attained at least 74% of equilibrium sorption, while the AC have only attained at most 44%. This indicates therefore, that the BCs have better kinetics than the ACs. Although in reality, the ACs are expected to have higher number of sorption sites than the BCs, as was seen on Figure 5.19; so in essence, the BCs are exhausted much faster for the same ibuprofen concentration. In both cases, the magnetite impregnated sorbent has slightly slower kinetics, which can be explained by the magnetite deposits blocking part of the surface area and pores.

The above proposed kinetic behaviours could further be evaluated using sorption kinetics models.

5.3.7.2   Modelling of Kinetics Data

In the evaluation of ibuprofen sorption kinetics data, both reaction based and mass transfer based models are being used. The most commonly reported among these models are the pseudo first order, pseudo second order and Elovich reaction based kinetics models and the intra-particle diffusion which is a mass transfer based kinetics model (Dubey *et al.*, 2010; Guedidi *et al.*, 2013; Mestre *et al.*, 2014)

A.   Linear sorption kinetics models,

This has been the most widely applied methods in the evaluation of sorption kinetics data. Methods of linear regression is applied to linear forms of both reactions based and diffusion based models. The parameters of the models are obtained from the slope and intercept of a linear fit of experimental data using the kinetics models, an example is shown in Figures 5.21(a) & (b) for the sorption of ibuprofen on magnetic and nonmagnetic activated carbon. Usually, the model that gives the highest R^2 value with respect to the fitted experimental data is chosen as the best to describe the sorption kinetics of the system under consideration. The conformity of models to experimental data was assessed using the correlation method. An example of the correlation plot for the linear fitted systems is shown in Figures 5.22 (a) & (b).
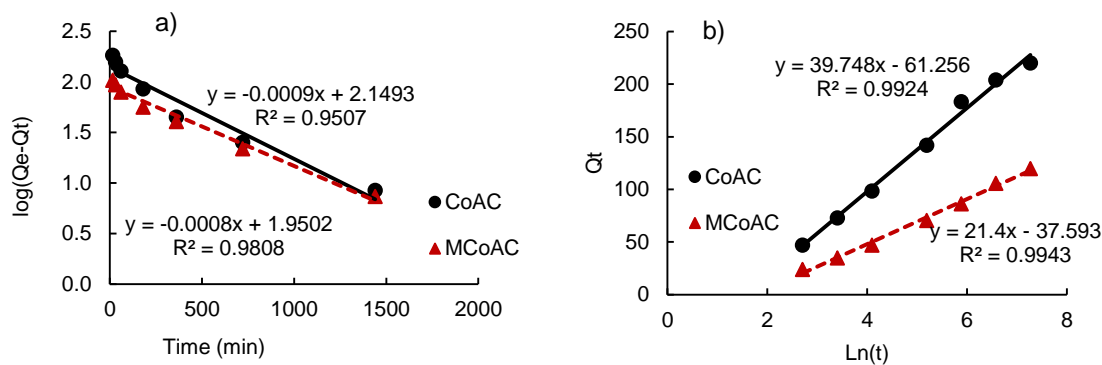
Figure 5.21:   Sorption kinetics of ibuprofen on ACs: (a) linear pseudo 1st order kinetics model plot, (b) linear Elovich kinetics model plot.
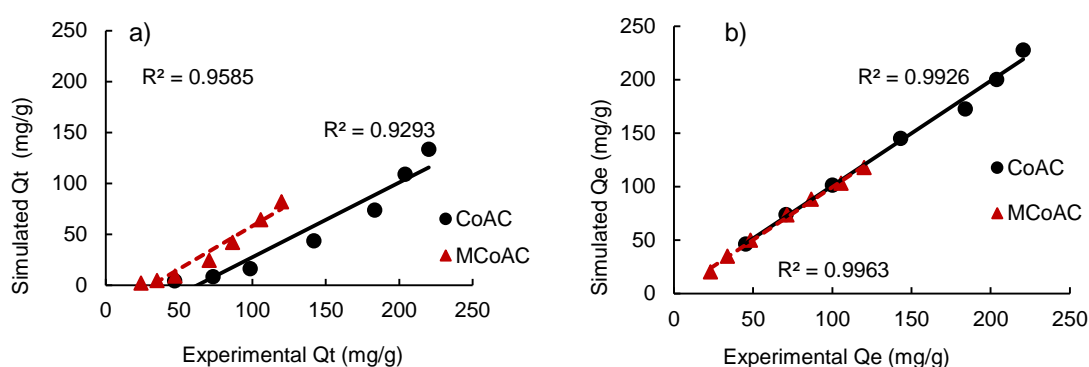
Figure 5.22:   Sorption kinetics of ibuprofen on ACs: correlation between experimental data and data simulated using: (a) linear pseudo 1st order model and (b) linear Elovich kinetics model.

The result for the linear data fitting is summarised in Table 5.14. Of all the models analysed in this study, the pseudo first order model has the least R^2 value and the Q_e predicted by this model is not similar to the experimental Q_e. This is in agreement with reports from literature that shows the sorption kinetics of ibuprofen on carbon sorbents does not follow the pseudo first order model, in most cases (Baccar *et al.*, 2012; Guedidi *et al.*, 2013; Essandoh *et al.*, 2015). Although the pseudo second order model has been shown in these previous works to best represent ibuprofen kinetics data, in this study according to both linear fitting and correlation plots, the Elovich kinetic model describes the experimental kinetic data better than the other three models. This is similar to the findings of (Tseng *et al.*, 2003) This suggests that the sorption kinetics is influenced by the rate of chemisorption of ibuprofen molecules to heterogeneous surfaced sorbents (Baccar *et al.*, 2012; Belaid *et al.*, 2013; Mestre *et al.*, 2014). This is compatible with the results of the sorption isotherm modelling, whence the

Freundlich model was observed to have better fitting with experimental data than what obtains with the Langmuir model.

Table 5.14:   Model parameters for kinetics of sorption of ibuprofen on ACs and BCs; (obtained using linear regression)

Model	Parameter	CoAC	MCoAC	Bio-1	MBio-1
1st	Q_e	140.67	89.00	1.02	1.02
	k_1	2.07E-03	1.78E-03	1.83E-03	1.59E-03
	R^2	0.9293	0.9585	0.8634	0.8802
2nd	Q_e	230.82	126.38	4.59	3.70
	k_2	5.27E-05	7.18E-05	1.31E-02	1.26E-02
	R^2	0.9876	0.9772	0.9352	0.9232
Elovich	α	8.51	3.69	1969.97	162.39
	β	0.03	0.05	3.49	3.68
	R^2	0.9926	0.9963	0.9834	0.9931
Intra-P	k_{id}	22.56	10.49	2.73	1.96
	z	0.34	0.35	0.07	0.09
	R^2	0.9364	0.9758	0.9726	0.9849
Experimental Q_e		229.00	127.50	4.65	3.80

From Table 5.14, it can be seen that the Elovich constant α (the initial chemisorption rate) due to the BCs is higher compared to the ACs, which is in agreement with the observation proposed earlier from the fractional uptake plot, Figure 5.20, that the BCs have faster kinetics. Although in this work, the pseudo order models are not the best in describing the ibuprofen sorption kinetics, the principle behind their derivation supports the sites exhaustion theory, which can be used to explain the kinetics data. According these models, the driving force behind the sorption kinetics is the relative concentration of potential sorption sites with time ($Q_e - Q_t$) as the sorption progresses (Chiou and Li, 2002; Yang and Al-Duri, 2005). From the analysis of isotherm data presented in 5.3.1.2, the ACs have about 2 order of magnitude higher Q_e values, therefore, the BCs have less concentration of potential sorption sites as compared to the ACs, and as a result, the driving force of the BCs gets depleted rapidly for the same concentration of ibuprofen as the sorption commences. This result in a steeper initial f plot or larger Elovich α value. Among sorbent pairs, α values for the nonmagnetic sorbents are larger than those of their corresponding magnetic pairs. This could be due to the presence of more sorption sites as a result of higher carbon content

per mass of sorbent used for the experiment in the nonmagnetic sorbents. This is in agreement with the findings of (Ho and McKay, 2002), that increasing the sorbent dosage usually resulted in an increase in the α value. Furthermore, this conforms to our initial analysis of the sorption kinetics plot, i.e. Figure 5.19, whence the kinetics curves for the pristine sorbents have a steeper slope at the commencement of the sorption process.

The Elovich constant β – the desorption constant - due to the BCs is higher compared to the ACs system. It is hence an evidence that the ACs have higher number of sites (assessed as $1/\beta$) available for sorption of ibuprofen (Tseng *et al.*, 2003; Baccar *et al.*, 2012; Guedidi *et al.*, 2013). This also explains the exhaustion of the BCs, because unlike the ACs, desorption is relevant almost over the entire duration under consideration. From the f data, it was observed that within the first 1 hr, the BCs have attained at least 74% of equilibrium sorption, while the AC have only attained at most 44%. Consequently, the β value for the magnetic sorbents are similar to those of their corresponding pairs of nonmagnetic sorbents.

B.   Nonlinear sorption kinetics models,
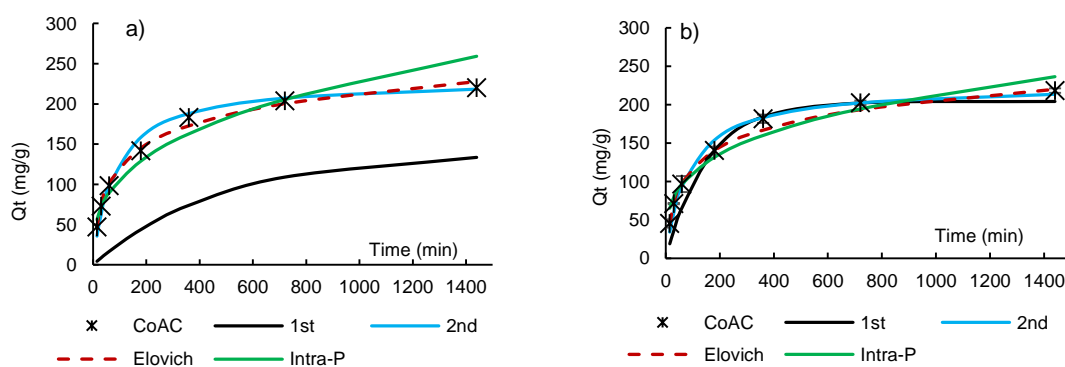
Figure 5.23:   Sorption kinetics of ibuprofen on ACs: Fitting of experimental data using (a) linear models and (b) nonlinear models.

A plot of experimental and fitted kinetics curves is shown in Figure 5.23. The superiority of the nonlinear fitting can be appreciated by comparing the curves due to the pseudo first and second order models. Using the linear fitting, the simulated and experimental curves are not as identical especially for the pseudo first order model. While using the nonlinear fittings, the simulated and

experimental curves are almost identical. As a result, their respective predicted values of the equilibrium 'Q_e' are quite similar with those obtained experimentally.

Comparison between optimised error functions is shown in Table 5.15 for CoAC as an example and the summary of ASE values for all the sorbents is shown in Table 5.16. As expected, the nonlinear models generally have the least values of ASE and are therefore anticipated to produce more accurate model parameters. It is interesting to note that unlike the other models, the same value of ASE was obtained from the Elovich using both linear and nonlinear methods. This is a further validation of its conformity to the experimental data.

Table 5.15:   Results of optimised error functions for the sorption kinetics of ibuprofen on CoAC

Err. Fxn	1st_L	2nd_L	Elovich_L	Intra-P_L	1st	2nd	Elovich	Intra-P
CoD	0.5557	0.9826	0.9924	0.9361	0.9449	0.9837	0.9925	0.9484
HYBRID	7510.33	132.63	22.83	261.65	342.54	89.45	22.79	223.56
MPSD	83.74	13.94	3.68	14.05	16.65	8.72	3.66	13.84
ARE	68.18	8.17	2.73	10.07	11.63	5.90	2.20	9.51
EABS	578.27	49.80	29.91	94.53	113.43	48.11	27.48	78.88
ERSSQ	50820.74	568.34	206.64	2290.57	2050.06	497.25	206.64	1368.07
ASE	9843.62	128.82	44.30	445.15	422.39	108.24	43.80	282.32

As mentioned previously, in 2.11.2.1, the intra-particle model is only an approximation of the real intraparticle diffusion differential equation. It is only reasonably valid at the initial stage of the kinetics and has been reported to have varying outcome of conformity to sorption kinetics data. For instance, while (Guedidi *et al.*, 2013) have reported it not to agree well with experimental kinetics, (Dubey *et al.*, 2010) found it applicable and even suggested that intra-particle diffusion as a major rate determining step in the sorption of ibuprofen on honeycomb shaped AC.

Table 5.16:   Summary of ASE for optimised error functions for the sorption kinetics of ibuprofen on ACs and BCs

Sorbent	1st_L	2nd_L	Elovich_L	Intra-P_L	1st	2nd	Elovich	Intra-P
CoAC	9843.62	128.82	44.30	445.15	422.39	108.24	43.80	282.32
MCoAC	2271.55	95.76	15.53	61.58	199.65	74.49	14.41	38.85
Bio-1	129.05	6.38	0.58	0.76	8.23	1.60	0.57	0.74
MBio-1	102.10	6.93	0.42	0.62	4.21	2.21	0.40	0.60

In this study, the intra-particle diffusion model exhibits good fitting with the experimental data. According to this model, the ACs have higher intra-particle diffusion rate constant than the BCs. Intra-particle diffusion is a pore dependent phenomenon, so it is expected that the ACs will have higher k_{id} due to their amplified pore structure compared to the BCs. The ACs are microporous and the larger portion of sorption takes place in accordance to the pore filling mechanism. This conforms to the earlier observation of the isotherm data when analysed according to the Polanyi's theory of potential adsorption in 5.3.3. It can also be observed that magnetic sorbents have lower values of k_{id} against their corresponding pair of nonmagnetic sorbent, because of lower micropore volume per gross mass of sorbent used in the experiment.

Table 5.17:   Optimised model parameters for kinetics of sorption of ibuprofen on ACs and BCs.

Model	Parameters	CoAC	MCoAC	Bio-1	MBio-1
1st	Q_e	205.90	111.93	4.34	3.49
	k_1	0.01	0.01	0.06	0.05
	R^2	0.9820	0.9521	0.7149	0.7132
	ASE	402.78	199.65	8.23	4.21
2nd	Q_e	227.48	122.34	4.59	3.70
	k_2	0.00	0.00	0.01	0.01
	R^2	0.9879	0.9785	0.9352	0.9232
	ASE	101.19	74.49	1.60	2.21
Elovich	α	8.53	3.65	2535.16	151.16
	β	0.03	0.05	3.54	3.66
	R^2	0.9924	0.9943	0.9834	0.9931
	ASE	43.80	14.41	0.57	0.40
Intra-P	k_{id}	31.28	13.33	2.77	1.98
	z	0.28	0.31	0.07	0.09
	R^2	0.9515	0.9827	0.9729	0.9851
	ASE	289.15	38.85	0.74	0.60
Experimental Qe		229.00	127.50	4.65	3.80

From Table 5.17, it can be seen that the Elovich kinetics model has the best optimised error function values suggesting that chemisorption is rate determining in the sorption of ibuprofen on the ACs and BCs for the given concentration. This confirms earlier proposed sorption mechanism of ibuprofen as being due to hydrogen bonding and dispersive interactions as is the case with similar micropollutants (Cabrita *et al.*, 2010). Also, ibuprofen can be sorbed by means of

donor-acceptor interactions with the surface carbonyl groups of the sorbents (as electron donors) and aromatic ring of ibuprofen (as electron acceptors) (Iovino *et al.*, 2015). Considering the Elovich model, the magnetic composites have slightly larger desorption constant β than their corresponding pristine pair. This indicates that they have lesser sorption sites and as a result slower kinetics due to magnetite impregnation.

5.3.8 DICLOFENAC SORPTION KINETICS.

The plot for kinetics curves for sorption of diclofenac on ACs and BCs is shown in Figure 5.24. It shows sorption kinetics exhibits a nonlinear character, with steep slopes at the initial stage of the system. The steepness gradually decreases with time as the driving force gets diminished due to exhaustion of sorption sites and decrease in bulk concentration (Yang and Al-Duri, 2005).
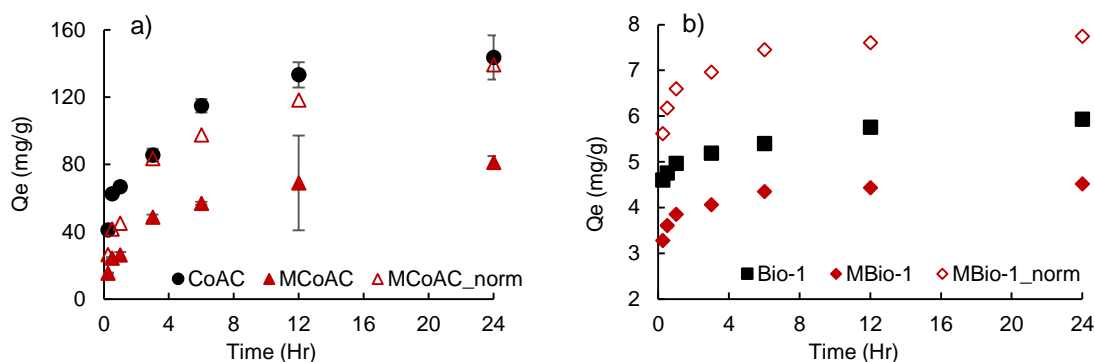
Figure 5.24: Plot of sorption kinetics for diclofenac on (a) ACs and (b) BCs. [Note; figures have different scales]

The curve for the normalised MCoAC is quite similar to that of CoAC while that of normalised MBio-1 overshoots that of Bio-1 due to the influence of pore volume on the sorption capacity of the BCs system as earlier explained. The plot for the BCs assumes a steady near horizontal plateau within the first 4 hours, suggesting attainment of equilibrium.

5.3.8.1 *Attainment to Equilibrium*

The fractional uptake plot, Figure 5.25, shows that while the ACs attained at most 42% equilibrium within the first hour, the BCs have at least 83% equilibrium. This suggests that the BCs system is more rapidly exhausted due to limited potential sorption sites compared to the ACs system. Here also, it can be

seen that the BCs have faster kinetics than the ACs and are more likely to get exhausted earlier due to their limited sorption capacities.
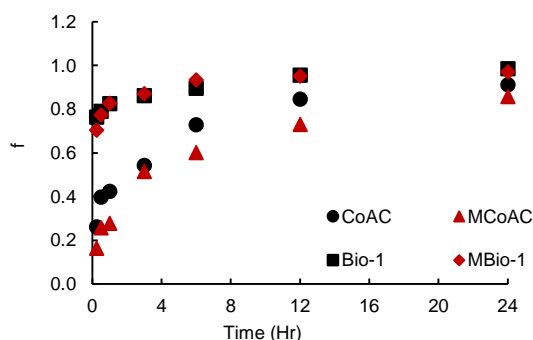
Figure 5.25:   Diclofenac sorption kinetics fractional uptake

Corresponding pairs of magnetic and nonmagnetic sorbents have quite similar kinetics. Unlike in sorption capacity, the difference of pore volume does not influence the sorption kinetics of the BC system. Although it is apparent that they have slower kinetics than the pristine pairs. Mathematical modelling was used to have a quantitative comparison of the kinetics data.

5.3.8.2   Modelling of Kinetics Data

A.   Linear sorption kinetics models
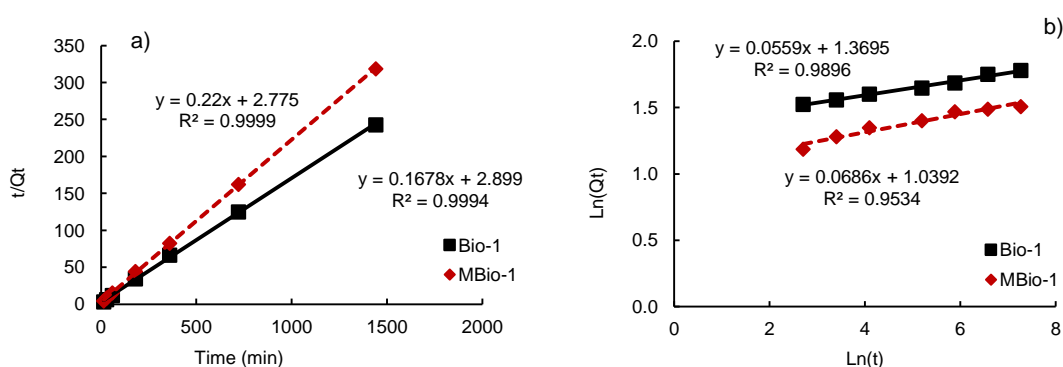
Figure 5.26:   Sorption kinetics of diclofenac on BCs: (a) linear pseudo second order kinetics model plot, (b) linear intra-particle diffusion model plot

An example of the linear fitting method is shown in Figure 5.26. Care should be taken when choosing models based on linear model fit of experimental data. It can be observed, that the pseudo second order linear kinetics model shows better fitting ($R^2 > 0.9994$) with experimental data compared to the linear intra-

particle kinetics model ($R^2 \leq 0.9896$). However, Figure 5.27 reveals that the kinetics data simulated by the intra-particle kinetics model is closer in resemblance ($R^2 > 0.9531$) to the experimental data compared to that obtained using the pseudo second order kinetics model ($R^2 \leq 0.9444$).
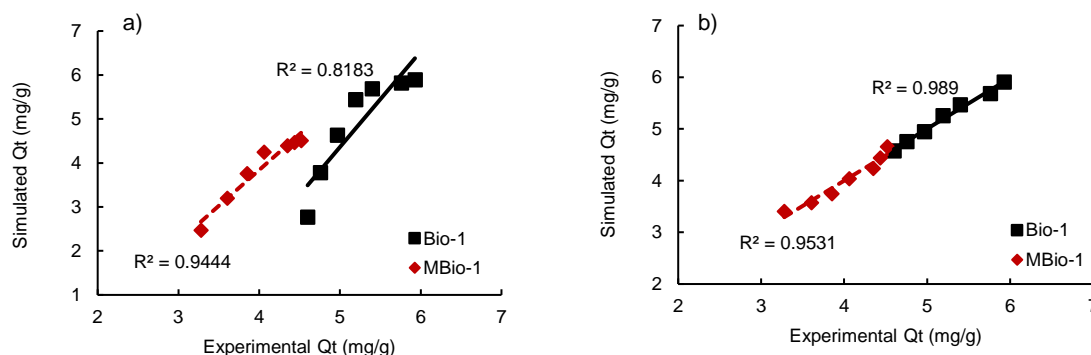
Figure 5.27: Sorption kinetics of diclofenac on BCs: correlation between experimental data and data simulated using: (a) linear pseudo second order kinetics model and (b) linear intra-particle kinetics model.

The summary of parameters obtained from the linear method is shown in Table 5.18.

Table 5.18: Model parameters for kinetics of diclofenac sorption on ACs and BCs; (obtained using linear regression).

Model	Parameters	CoAC	MCoAC	Bio-1	MBio-1
1st	Q_e	93.91	58.36	1.25	0.89
	k_1	1.46E-03	7.23E-04	1.86E-03	1.48E-03
	R^2	0.9310	0.9068	0.9671	0.7965
2nd	Q_e	149.60	97.46	5.96	4.54
	k_2	8.56E-05	5.68E-05	9.71E-03	1.74E-02
	R^2	0.9359	0.9710	0.8183	0.9444
Elovich	α	8.88E+00	2.15E+00	1.12E+05	5.30E+03
	β	0.04	0.07	3.42	3.71
	R^2	0.9753	0.9860	0.9837	0.9677
Intra-P	k_{id}	22.44	7.04	3.93	2.83
	z	0.27	0.34	0.06	0.07
	R^2	0.9696	0.9700	0.9890	0.9531
Experimental Q_e		157.70	94.72	6.03	4.66

B. Nonlinear sorption kinetics models

The kinetics data was subjected to thorough error analysis and the summary of the ASE results is shown in Table 5.19. In general, the nonlinear models had

better values of optimised error functions and thus presented the least ASE value. Overall, the Elovich and intra-particle models had the least error distribution with respect to the experimental data and are therefore the ones that are most likely to give the best description of the kinetics of the system.

Table 5.19:   Summary of ASE for optimised error functions for the sorption kinetics of diclofenac on ACs and BCs

Sorbent	1st_L	2nd_L	Elovich_L	Intra-P_L	1st	2nd	Elovich	Intra-P
CoAC	5676.34	273.91	53.91	68.91	448.46	206.06	53.45	62.10
MCoAC	1286.77	60.97	24.91	36.75	108.42	54.97	23.22	27.48
Bio-1	167.20	10.00	0.45	0.36	3.32	2.11	0.43	0.35
MBio-1	135.15	4.43	0.78	0.96	2.90	1.31	0.77	0.93

Accordingly, the rate of sorption of diclofenac on both the ACs and BCs is controlled by chemisorption and diffusion kinetics. It has also been reported in previous studies, that the sorption of diclofenac is controlled by chemisorption and diffusion processes (Antunes *et al.*, 2012; Suriyanon *et al.*, 2013). Generally, the pseudo second order sorption mechanism is the dominant followed by the Elovich (Baccar *et al.*, 2012).

Table 5.20:   Optimised model parameters for kinetics of diclofenac sorption on ACs and BCs.

Model	Parameters	CoAC	MCoAC	Bio-1	MBio-1
1st	Q_e	143.75	86.27	5.79	4.37
	k_1	5.03E-03	3.89E-03	5.49E-02	5.81E-02
	R^2	0.9451	0.9451	0.5495	0.7257
	ASE	448.46	108.42	3.32	2.90
2nd	Q_e	160.50	91.59	6.05	4.67
	k_2	5.87E-05	5.95E-05	7.50E-03	1.01E-02
	R^2	0.9510	0.9718	0.8282	0.9460
	ASE	206.06	54.97	2.11	1.31
Elovich	α	9.34E+00	2.08E+00	1.75E+05	7.06E+03
	β	0.04	0.07	3.52	3.81
	R^2	0.9822	0.9860	0.9867	0.9671
	ASE	53.45	23.22	0.43	0.77
Intra-P	k_{id}	28.23	9.39	3.96	2.96
	z	0.22	0.30	0.05	0.06
	R^2	0.9647	0.9788	0.9874	0.9523
	ASE	62.10	27.48	0.35	0.93
Experimental Q_e		157.70	94.72	6.03	4.66

The summary of optimised model parameters is shown in Table 5.20. The nonlinear pseudo first and second order models were able to predict 'Q_e' values that are quite similar to those obtained experimentally and the estimate is significantly better than that obtained by the linear pseudo first order model (see Table 5.18). Figure 5.28 shows the fitted kinetic curves obtained using linear and nonlinear methods. It can be observed that the curves simulated using the nonlinear method have the closest resemblance with the experimental data. This agrees well with the earlier comparison based on the results of error analysis and thus, the optimisation is indeed capable of producing more accurate model parameters.
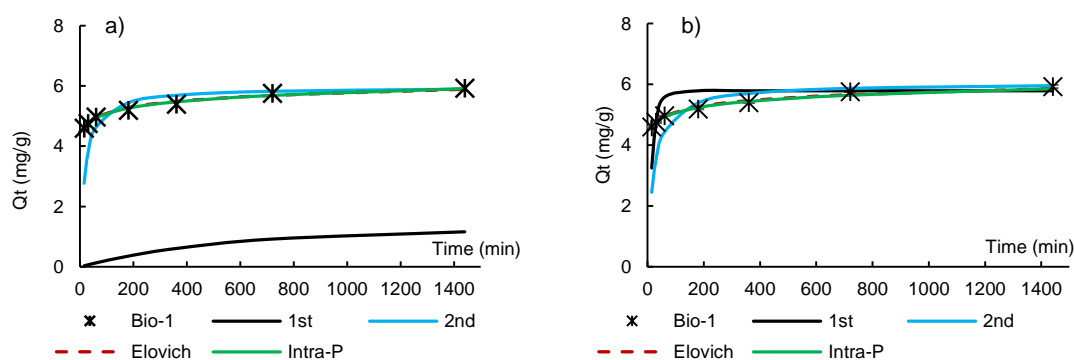
Figure 5.28:   Sorption kinetics of diclofenac on Bio-1: Fitting of experimental data using (a) linear models and (b) nonlinear models.

To describe the sorption kinetics based on the Elovich model, from Table 5.20, it can be observed that α values for the BCs are much higher than those for the ACs. This correlates well with the f plot and it suggests faster uptake of diclofenac by the BCs at the onset of the sorption compared to the ACs. This leads to the quick exhaustion of the BCs compared to the ACs because the former have less concentration of potential sorption sites over the latter. Therefore, the BCs have a larger value of the Elovich β, since desorption becomes relevant at a much earlier stage of the sorption due to faster attainment of equilibrium. Among corresponding pairs of sorbents, the α values of the magnetic sorbents are lower than those of the nonmagnetic sorbents due to lower carbon dosage as used in the experiment. This is in agreement with the findings of (Ho and McKay, 2002), that increasing the sorbent dosage usually resulted in an increase in the α value.

Comparison of kinetics properties of the ibuprofen and diclofenac systems was done using Tables 5.17 and 5.20. The sorption kinetics of ibuprofen and diclofenac on the magnetic and nonmagnetic sorbents follows the same pattern as observed in their respective sorption capacities. For instance, according to Q_e, ibuprofen sorbs better on the ACs as compared to diclofenac, while the BC system sorbs diclofenac better than ibuprofen. In the same vein, Elovich α values are larger for the BC-diclofenac system compared to the BC–ibuprofen system and accordingly, the former system has better kinetics. This can also be deduced from the intra-particle kinetics model, whence the k_{id}. for the BC–ibuprofen system is lower than that for the diclofenac system. In the case of the ACs, the ibuprofen system presents better kinetics over the diclofenac system, according to both Elovich α and intra-particle k_{id}. The reversed kinetics of the ibuprofen and diclofenac with respect to the ACs and BCs systems is likely the outcome of all possible forms of interaction as a result of varied sorbates' and sorbents' properties as reported by (Rakić *et al.*, 2015).

5.3.9   EVALUATION OF SORPTION ISOTHERMS FROM SPIKED WWTPE
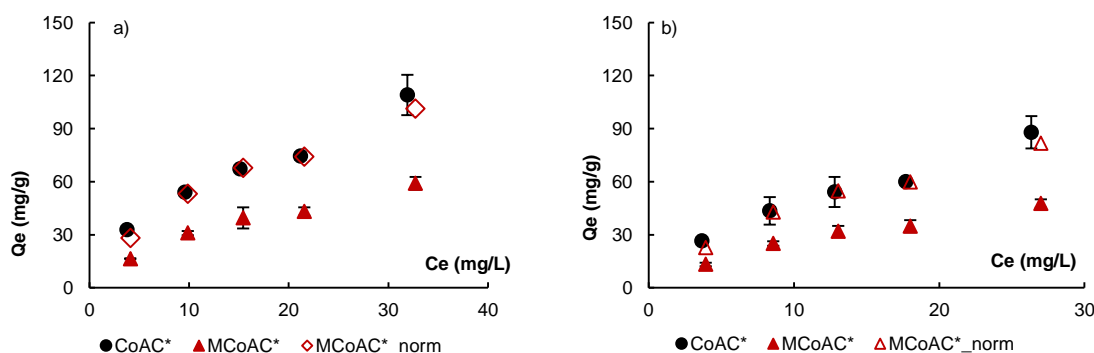
Figure 5.29:   Isotherm plot for sorption of (a) ibuprofen and (b) diclofenac on CoAC* and MCoAC* (in spiked WWTPE)

The isotherm for the sorption of ibuprofen and diclofenac spiked in WWTPE on CoAC and MCoAC is shown in Figure 5.29. Compared to Figures 5.1 and 5.5 for the sorption of ibuprofen and diclofenac in CaCl₂ solution, the isotherm curves here appear somewhat more linear and much less steep. This change of the isotherm of primary solute from significantly nonlinear to somewhat linear due to competition has also been observed in the sorption of organic compounds on

carbon nanotubes (Yang and Xing, 2010). The measured solid phase concentrations are much less than what obtains from the sorption of the pharmaceuticals in $CaCl_2$ solutions. The sorption capacities are compared using models capacity parameters later in 5.3.9.2.

Isotherms of MCoAC_norm are quite similar to those of CoAC for both ibuprofen and diclofenac; p-value = 0.174 and α = 0.05. Once again this confirms that the difference in sorption capacities among the AC pairs is basically due to unequal masses of carbon material between the two.

5.3.9.1   *Attenuation of Sorption Capacities*

The WWTPE is characterised by 11 mg/L, dissolved organic compounds. Such an amount is high enough to significantly compete with the target pharmaceuticals for available sorption site, thereby attenuating the sorption capacities of the sorbents (Weber, 1974). Figure 5.30 shows the relative attenuation of sorption capacities for CoAC and MCoAC. Quite similar curves for each pharmaceutical can be observed.
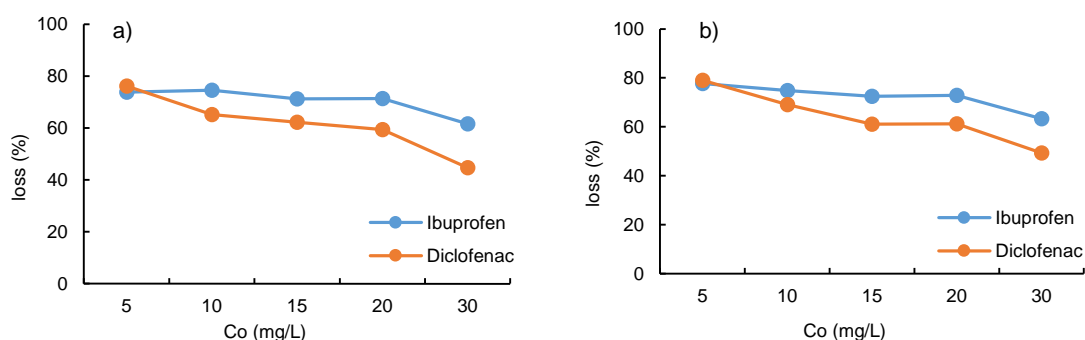
Figure 5.30:   Attenuation (ΔQe) of sorption of ibuprofen and diclofenac on (a) CoAC* and (b) MCoAC* (in spiked WWTPE).

Where: $$\Delta Qe_i = 100 \frac{(Qe_i - Qe_i^*)}{Qe_i}$$ -   -   -   --   (5.2)

Q_e and Q_e^* are the solid phase concentration from $CaCl_2$ solution and WWTPE respectively.

Pore blockage mechanism could be another way by which such dissolved organic matter (DOM) could reduce the uptake of target pollutants. Through spatial interference, larger molecules from the DOM could seal the pores of the ACs thus denying access to target pollutants (Chowdhury *et al.*, 2013), resulting

in a loss of potential sorption capacity (Pelekani and Snoeyink, 1999). Substantial decrease in sorption performance due to the presence of competing DOM has also been observed in the treatment of various organic pollutants from aqueous medium (Shih *et al.,* 2003; Jasper *et al.,* 2010; Nam *et al.,* 2014).
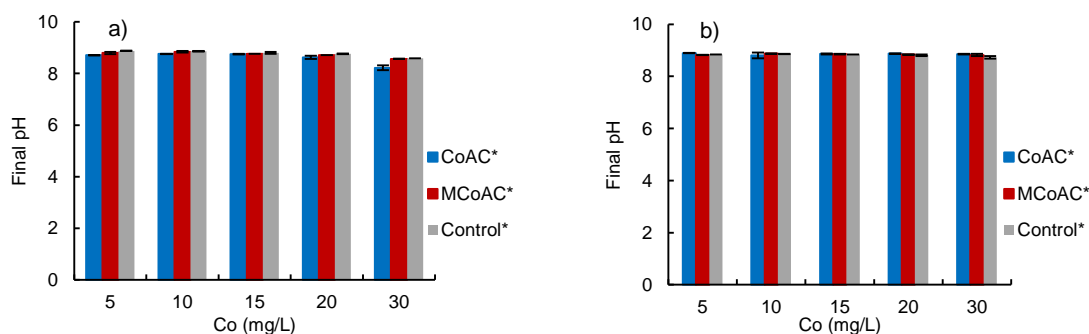
Figure 5.31:   Final solution pH for the sorption isotherm of (a) ibuprofen and (b) diclofenac on CoAC* and MCoAC* (in spiked WWTPE)

The reduction in sorption capacity may also be as a result of solution pH. This has earlier been shown (refer to 5.3.6.1) to have a negative influence on the uptake of these pharmaceuticals on CoAC and MCoAC. The pH of the system is within the alkaline region (about pH 9; see Figure 5.31) and the sorption of such pharmaceutical compounds under similar condition has been shown to be unfavourable (Dubey *et al.,* 2010; Cho *et al.,* 2011; Baccar *et al.,* 2012; Guedidi *et al.,* 2013; Wei *et al.,* 2013; Essandoh *et al.,* 2015). Furthermore, the decrease could be as a result of direct competition for existing sorption sites. This could be possible if the background DOM has the same specific sorption mechanism as does the target pharmaceuticals (Newcombe *et al.,* 1997). This will result in the decimation of the concentration of available sites that could otherwise be occupied by the target compounds.

On the one hand, sorption of ibuprofen on both sorbents is slightly more than that of diclofenac as was observed in their sorption from $CaCl_2$ solution. On the other hand, the sorption of ibuprofen, is more adversely affected in the WWTPE. For instance, let us assume that the attenuation rate is uniform over the studied range of concentration in the data from Figure 5.30. It can then be deduced that, ibuprofen sorption suffers higher attenuation than diclofenac by about 19 and 15% on both CoAC and MCoAC respectively. The reason could primarily be due the higher sensitivity of ibuprofen sorption to changes in pH,

especially in the alkaline region. It has earlier been shown (refer to 5.3.6.2), that the sorption of diclofenac is less influenced by the pH of the medium, which is similar to the findings of (Bajpai and Bhowmik, 2010; Suriyanon *et al.*, 2013; Nam *et al.*, 2014).

Also in terms of spatial interference, the competing DOM could sorb on the walls of pores, thereby constricting the pores without necessarily blocking them (Pelekani and Snoeyink, 2001). Under such conditions, size exclusion effect becomes activated and only molecules small enough to pass through such narrowed pores could have access to vacant sorption sites in the interior of the sorbent (Newcombe *et al.*, 1997). Therefore, it is likely that molecular sieve effect will further impair the uptake of ibuprofen molecule due to its relatively larger longitudinal dimension compared to diclofenac.

5.3.9.2   *Modelling of Isotherm Data*

A.   Linear Isotherm Model

According to the linear model, there is about 92 and 96 % less uptake of diclofenac and ibuprofen respectively than what was recorded for their sorption from CaCl$_2$ solution. Also, ibuprofen sorbs about 1.2 more than diclofenac on both CoAC and MCoAC. This is about 1.49 less than the difference in sorption between the two compounds from CaCl$_2$ solution. The linear model has captured the higher decrease in the sorption of ibuprofen from the spiked WWTPE than is recorded for diclofenac.
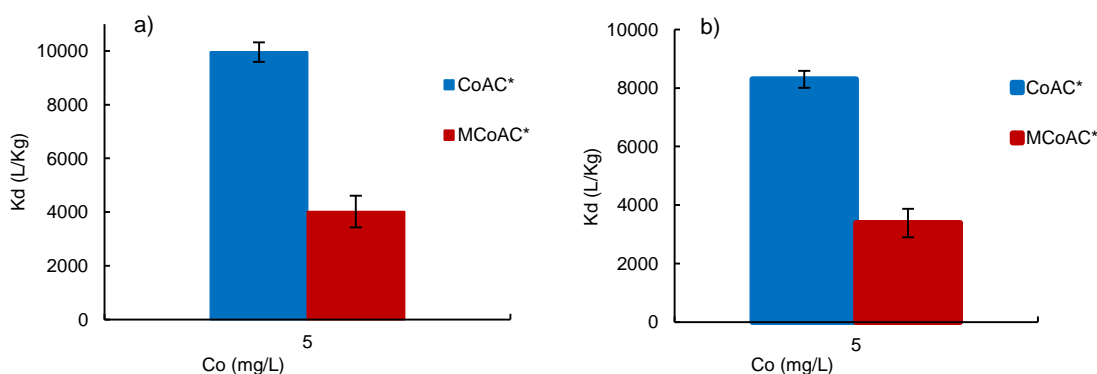
Figure 5.32:   Partitioning coefficient for sorption of (a) ibuprofen and (b) diclofenac on CoAC* and MCoAC* (in spiked WWTPE)

B. Nonlinear Isotherm Models

The nonlinear models were fitted to the experimental data using both linear and nonlinear regression methods. The error functions were optimised and the result of the ASE is summarised in Table 5.21.

Table 5.21: Summary of ASE for the sorption of ibuprofen and diclofenac on CoAC* and MCoAC* (in spiked WWTPE)

Sorbate	Sorbent	LANG_L	FR_L	RP_L	LANG	FREU	RED-PET	DA	PDM
Ibuprofen	CoAC*	67.62	29.86	33.55	64.50	27.19	30.91	15.92	1.89
	MCoAC*	10.64	8.50	11.36	10.19	8.01	8.22	9.03	1.87
Diclofenac	CoAC*	39.29	18.92	24.31	37.14	17.63	20.53	13.07	1.96
	MCoAC*	6.99	7.94	8.28	6.69	7.26	6.83	7.38	1.91

Table 5.22: Optimised model parameters for sorption isotherm of ibuprofen and diclofenac on CoAC* and MCoAC* (in spiked WWTPE)

Model	Parameters	Ibuprofen		Diclofenac	
		CoAC*	MCoAC*	CoAC*	MCoAC*
Linear	K_d **	9.96	4.02	7.26	3.38
LANG	Q_m	198.84	97.12	173.87	84.84
	K_L	0.035	0.044	0.036	0.045
	R^2	0.9490	0.9774	0.9564	0.9801
FREU	$1/n$	0.60	0.56	0.63	0.60
	K_F	13.30	8.48	10.76	6.52
	R^2	0.9715	0.9848	0.9743	0.9830
RED-PET	K_R	354.27	12.80	3407.58	7.20
	A_R	25.95	0.96	315.68	0.45
	γ	0.41	0.54	0.37	0.59
	R^2	0.9713	0.9852	0.9743	0.9844
DA	Q_o	264.36	73.62	340.58	63.35
	E	9.36	9.79	5.86	9.26
	b	0.45	1.05	0.41	1.13
	R^2	0.9875	0.9845	0.9861	0.9835
PDM	Q_o	264.63	73.64	278.61	62.79
	a	4.15	23.33	7.30	97.20
	b	0.46	1.05	0.46	1.16
	R^2	0.9874	0.9846	0.9859	0.9838

**x10^3

The ASE values of the linear models are quite similar to those of the nonlinear models. However, the nonlinear fitting method has lower error distribution between experimental and simulated isotherms. Consequently, they

have lower ASE value than what obtains for the LTFM method and thus are more appropriate to describe the data. In the overall, the 3-parameter PDM model has the least ASE values. While in the sorption of ibuprofen, the Freundlich model has the lesser ASE value among the 2-parameter model. The ASE values for the 2-parameter models are lower than what was recorded in the sorption of the pharmaceuticals from $CaCl_2$ solutions.

Table 5.23: Summary of MSC for isotherm prediction using optimised model parameters for sorption of ibuprofen and diclofenac on CoAC* and MCoAC* (in spiked WWTPE)

Sorbate	Sorbent	LANG	FREU	RED-PET	DA	PDM
Ibuprofen	CoAC*	1.80	2.67	2.26	2.65	2.92
	MCoAC*	2.87	3.14	3.01	2.84	2.80
Diclofenac	CoAC*	2.03	2.79	2.39	2.52	2.56
	MCoAC*	3.05	3.22	2.96	2.90	2.49

The result of the optimised model parameters is summarised in Table 5.22 and in terms of MSC values, the Freundlich model has the highest values in all except in the sorption of ibuprofen on CoAC* where the PDM has a higher value (as recorded in Table 5.23). The decision to have a particular model to describe the sorption of the two pharmaceuticals is not straight forward. The simulated and experimental isotherms are quite similar and hence, their curves are overlapping especially for the sorption on MCoAC* as can be seen in Figure 5.33. However, the Freundlich model seem to have better fitting than the Langmuir as suggested by the low γ values recorded in the Redlich-Peterson model (Ho *et al.*, 2005b).
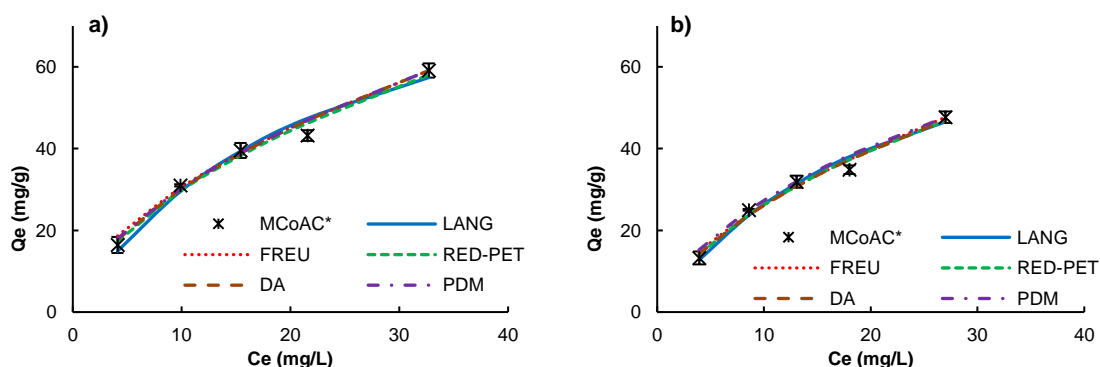
Figure 5.33: Comparison of simulated and experimental isotherm plot for sorption of (a) ibuprofen and (b) diclofenac on MCoAC* (in spiked WWTPE)

5.3.9.3   Sorption Capacities

Assessment of the sorption capacity parameters shows that, ibuprofen sorbs at least about 1.14 more than diclofenac, according to K_d, Q_m and K_F values. This is less than the difference recorded for their sorption in $CaCl_2$ solution. As explained earlier, the sorption of ibuprofen is more sensitive to changes in solution chemistry than that of diclofenac. Although the Polanyi based models have as usual exhibited very good fitting, they do not appear to represent the pattern of the isotherm plot observed in Figure 5.33. For instance, the assessment of the Q_o in Table 5.22 shows that diclofenac sorbs more than ibuprofen on CoAC (significantly more according to the DA model). Furthermore, the sorption of diclofenac on CoAC from WWTPE is estimated by this model to be much more than that from $CaCl_2$ solution. The overestimation of the sorption capacity by these models is due to the fact that the solubility of compounds is considered in their computations. It is obvious that the solubility of these compounds in the WWTPE is different from that in $CaCl_2$ solution. It is not surprising therefore that in this instance, the Freundlich model has higher MSC value than the Polanyi models as recorded in Table 5.23. Hence, the solubility of the pharmaceuticals in the medium they are to be removed from should be evaluated first before these models can be used, otherwise, conclusions drawn from their results could be misleading.

5.3.9.4   Sorption Affinity

The sorption affinity constants for all the models are lower than what was observed in the sorption of the pharmaceuticals from $CaCl_2$ solutions. This is due to effect of competition or the existence of unfavourable solution chemistry due to higher pH. Consequently, the plot of S_L Figure 5.34 shows elevated curves compared to those recorded for the sorption from $CaCl_2$ solution.
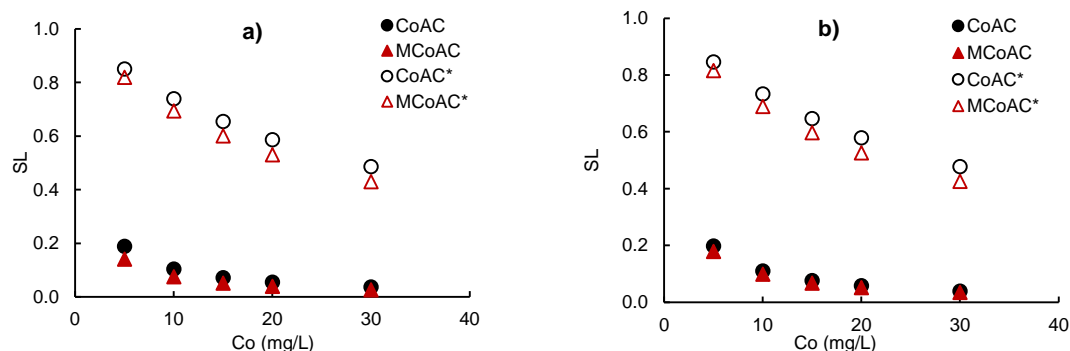
Figure 5.34:   Plot of Langmuir separation factor. Sorption of (a) ibuprofen and (b) diclofenac on CoAC and MCoAC in CaCl₂ solution and in spiked WWTPE.

This indicates that the sorption of both pharmaceuticals from CaCl$_2$ solution is more favourable than from the spiked WWTPE (Ofomaja and Ho, 2007; He *et al.*, 2010), suggesting that their molecules are held rather loosely by sorption bonds. They may even be attached to the adsorbed DOM and not directly to the surface of the sorbents which usually result in isotherm linearity (Yang and Xing, 2010). Or they may have to attach to sorption sites with lesser affinity, because the strong affinity sites have been occupied by competing DOM. Also the higher the curves, the closer the sorption get to becoming of the linear form; because, when $S_L = 1$ the sorption becomes linear. This condition is also satisfied when conclusion is drawn considering the Freundlich 'n' (Worch, 2012).
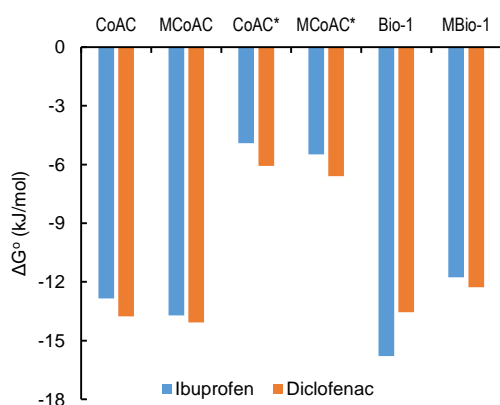
Figure 5.35:   Change in Gibbs free energy for the sorption of ibuprofen and diclofenac on ACs and BCs from CaCl₂ solution and spiked WWTPE.(*asterisked)

Both ibuprofen and diclofenac are weakly charged organic sorbates and thus the Langmuir equilibrium constant 'K_L' in 'L/mol' can be used as the

thermodynamic equilibrium constant 'K_{eq}' to estimate the change in free Gibbs energy (Liu, 2009). The result presented in Figure 5.35 shows that the sorption of both pharmaceuticals is spontaneous. Higher values of negative ΔG^o is an indication of a more favourable sorption (Dubey *et al.*, 2010). Accordingly, the sorption of ibuprofen and diclofenac is more favourable in CaCl₂ solutions than in the presence of competitors. It can also be observed that the BCs exhibit about the same ΔG^o as the ACs for both sorbates; the ibuprofen/Bio-1 system has the highest. Probably the biochar has specific sorption sites that have higher affinity for ibuprofen more than the other sorbents.

5.4   SUMMARY

Results from sorption equilibrium experiments for CaCl₂ solutions and spiked wastewater treatment plant effluent were analysed to ascertain how magnetisation has affected the sorption properties of the sorbents. Six error functions were used to fit experimental result to isotherm and kinetics models. In some instances, use of linear models fitted the data reasonably well. However, in general, analysis of data by nonlinear methods resulted in better data fit and as such returned more accurate model parameters. Likewise, 3-parameter models especially the Polanyi based, have the best approximation of the isotherm data. This suggests that the pore filling mechanism is valid for the sorption of both pharmaceuticals on the magnetic and nonmagnetic sorbents, especially the ACs. The BCs are not as microporous as the ACs, hence a single characteristic curve could not be obtained for them.

The difference in sorption capacities between the magnetic and nonmagnetic ACs and BCs was found to be due to the lesser content (ca 36%) of carbon material in the composites. The magnitude of the uptake of both pharmaceuticals recorded among corresponding pairs of magnetic and nonmagnetic ACs and BCs was almost the same when the data was normalised with respect to the approximate content of carbon material. So in practice, more magnetic composite is required to achieve the same level of pharmaceutical removal from the treatment medium as obtained using the pristine material. The MBC however has better uptake of ibuprofen than the BC due to higher pore volume. In general, the sorption capacities of the sorbents are strongly influenced

by the surface area and especially the pore volume in the case of MBC. The models' capacity parameters show strong correlation (generally, Pearson correlation coefficient $R > 0.9990$) with the sorbents' capacity influencing properties especially pore volume when normalised according to the carbon content used in each experiment. This suggest that enhanced removal of ibuprofen could be achieved if the system is optimised by focusing on the sorbents' pore structure.

The relative removal of both pharmaceuticals differs between the AC and BC system. Diclofenac sorbs more than ibuprofen on the BCs, while the reverse is the case on the ACs. In this instance, hydrophobic interactions alone could not explain why the relatively more hydrophobic diclofenac sorbs less than ibuprofen. Differences in sorbate, sorbent and solution properties can influence a sorption system for better or for worse. For example, ibuprofen sorption on the ACs and BCs is sensitive to pH variation whereas, the diclofenac AC system is much less so. Sorption of both is proposed to be due to interaction of van der Waals, dispersive and electrostatic forces between sorbent surface and their molecules as well as solute-solvent interactions. This is the reason why their sorption at lower pH is relatively higher than it is at higher pH, due to the influence of pH on both surface charge and the speciation of the molecule. In the presence of competing DOM, the isotherms of both pharmaceuticals became significantly diminished and somewhat linear. This is quite different from the nonlinear form recorded for their sorption from $CaCl_2$ solutions. Compared to diclofenac, ibuprofen is more sensitive to competing DOM. The ibuprofen sorption capacity of the ACs for $CaCl_2$ solution was attenuated in the WWTPE by up to 19% more than what was recorded for diclofenac. This was proposed to be due to the higher sensitivity of ibuprofen to solution pH and its higher vulnerability to molecular sieving effects compered to diclofenac. Nonetheless, their sorption intensity was affected to an almost equal degree, such that their sorption was substantially less favourable and almost linear according to isotherm model intensity parameters. This suggest weaker bonding to the surface of the sorbents. It is evident then, that the sorbent, sorbate and solution properties could be manipulated to achieve specific sorption outcomes. Furthermore, due to changes in the solubility of the pharmaceuticals in the WWTPE, the sorption capacities of the sorbents were overestimated the Polanyi based models.

The data for the rate of utilisation of sorption capacities shows once again the superiority of the ACs over the BCs. Due to limitation of sorption sites, the BCs are exhausted much faster than the ACs. Of the kinetic models tested, the reaction based Elovich model had the best fitting to experimental data. The diffusion based fractional power intra-particle model also exhibited very good fitting. The outcome of mathematical modelling is in good agreement with deductions obtained from the observation of the plots of the experimental data. For instance, according to both model results and data plots, the BCs have faster kinetics than the AC. The Elovich model parameters showed that the ACs have higher concentration of sorption sites, while the BCs have higher initial sorption rate. Unlike the sorption capacity, there was no indication of the influence of the pore volume on the kinetics of ibuprofen on the MBC. The intra-particle model showed that the ACs have higher diffusion constant as compared to the BCs. This correlates with the difference in microporosity between the two systems and a proof of the propagation of sorption according to the pore filling mechanism in the AC system. Once again, the sorption of the two pharmaceuticals is varied among the ACs and BCs in a similar way as observed in their respective sorption capacities. In the overall, the magnetised sorbents behaved in very similar manner with their corresponding pristine pair under all tested conditions. Therefore, the presence of magnetic iron oxide in the composites did not cause a detrimental change in their sorption properties. In all sense, the results obtained have proven that under right conditions, magnetic activated carbon and biochar can be used in the removal of ibuprofen and diclofenac from the environment, especially when used in adequate quantities.

In this and the previous chapters, the sorption of organic compounds from aqueous and real wastewaters have been investigated. However, both compounds share common sorption mechanisms and as such responds in a similar way to variations in the sorption system properties. Heavy metals have other sorption mechanisms that are different from those of organic compounds. Therefore, to they are likely to respond in different ways to what was observed for the organic compounds. The next chapter presents investigations into the sorption of heavy metals on magnetic and nonmagnetic sorbents and the nature of competition that exists among metals in pure solutions and in the presence of background organic compounds

CHAPTER 6.   SORPTION OF HEAVY METALS

6.1   INTRODUCTION

This chapter investigates the sorption characteristics of heavy metals in single and equimolar mixed solutions onto magnetic and nonmagnetic activated carbons (ACs) and biochars (BCs). Sorption capacities were determined through isotherm experiments. Effect of pH variation and competition from other compounds were assessed to understand the influence of solution chemistry on the uptake of metals on the sorbents.

A part of the work in this chapter on the evaluation of sorption isotherms has been published as a paper in the following peer reviewed academic journal;

Magnetite impregnation effects on the sorbent properties of activated carbons and biochars

CrossMark

Zhantao Han [a,b,c], Badruddeen Sani [a], Wojciech Mrozik [a,d], Martin Obst [e], Barbara Beckingham [e,f], Hrissi K. Karapanagioti [g], David Werner [a,*]

[a] School of Civil Engineering and Geosciences, Newcastle University, Newcastle upon Tyne NE1 7RU, England, United Kingdom
[b] Institute of Hydrogeology and Environmental Geology, Chinese Academy of Geological Sciences, Shijiazhuang 050061, China
[c] Hebei Key Laboratory of Groundwater Remediation, Shijiazhuang 050061, China
[d] Department of Inorganic Chemistry, Medical University of Gdańsk, 80-210 Gdańsk, Poland
[e] Department of Geosciences, Center for Applied Geoscience, University of Tübingen, 72074 Tübingen, Germany
[f] Department of Geology and Environmental Geosciences, College of Charleston, Charleston, SC 29401, USA
[g] Department of Chemistry, University of Patras, 26504 Patras, Greece

ARTICLE INFO

ABSTRACT

This paper discusses the sorbent properties of magnetic activated carbons and biochars produced by wet impregnation with iron oxides. The sorbents had magnetic susceptibilities consistent with theoretical predictions for carbon-magnetite composites. The high

6.2   EXPERIMENTAL SECTION

6.2.1   DETERMINATION OF SORPTION ISOTHERMS:

In this experiment, mixed metal salts solution was tested on all sorbents including magnetite, while single metal salt solutions were tested only on OrgBio, MOrgBio and magnetite. Mixed (or single) metal salts stock solution having the same molar concentrations of each metal was prepared from $Pb(NO_3)_2$, $CuCl_2 \cdot 2H_2O$, and $ZnCl_2$.

The sorption isotherm were determined according to the method used by (Han *et al.*, 2015b). Briefly, 50 mg of the sorbent was weighed into 50 mL polyethylene plastic vials with screw caps, obtained from VWR (Lutterworth, UK). The sorbents were contacted with 39 mL of deionised water with the vials closed using the screw cap. The sample was then placed on a platform shaker (STUART SCIENTIFIC STR6) set to shake at 70 rpm overnight at 22 °C. Afterwards, 1 mL of appropriate mixed (or single) metal salts stock solution was added such as to have 40 mL of the desired initial concentration of 0.01, 0.04, 0.08, 0.16 or 0.30 mM. The vials were immediately closed again and returned to shake for 7 days on the shaker using the previous settings. After shaking, the samples were filtered using a 0.45 mm PTFE membrane syringe filter and the filtrate was analysed for residual individual metal concentration using a Varian Vista MPX axial ICP-OES with CCD, operated according to standard methods for examination of water and wastewater. Metals were detected at several wavelengths and the readings averaged for each: Cu^{2+} (213.598, 324.745 and 327.395 nm); Pb^{2+} (182.143, 217.000 and 220.353 nm); and Zn^{2+} (202.548, 206.200 and 213.857 nm). Control samples containing only metal(s) solution without sorbent were processed in a similar manner. All samples are in duplicate and average values were reported. The amount of metal species adsorbed per unit weight of adsorbent was computed using the difference between concentrations measured in batches with sorbents and batches without sorbents, using a mass balance approach.

6.2.2 DETERMINATION OF pH INFLUENCE ON SORPTION OF METALS

In this experiment mixed metal salts solution was tested on CoAC, MCoAC, OrgBio and MOrgBio, while single metal salt solutions were tested only on OrgBio and MOrgBio.

To evaluate the influence of pH on the sorption of heavy metals, 50 mg of the sorbent was weighed into 50 mL polyethylene plastic vials with screw cap, obtained from VWR (Lutterworth, UK). The sorbents were contacted with 39 mL of deionised water with the vials closed using the screw cap and were then placed on a platform shaker (STUART SCIENTIFIC STR6) set to shake at 70 rpm overnight at 22 ^{o}C. The pH of the conditioned samples was then adjusted to 3, 5, 7 and 9 using aliquot of 0.01 M of HNO_3 or KOH. The pH was monitored over 72 hours and necessary adjustments were made to maintain target values. Thereafter, 1 mL of appropriate mixed (or single) metal salts stock solution was then added to the preconditioned sorbents to have a predetermined volume of 40 mL and initial concentration of 0.16 mM. The vials were immediately closed again and returned to shake for 7 days on the shaker using the previous settings. Control samples containing only metal(s) solution without sorbent were processed in a similar manner. All samples were then handled as explained in 6.2.1.

6.2.3 DETERMINATION OF EFFECT OF FOULING ON SORPTION

In this experiment mixed metal salts solution was tested on CoAC, MCoAC, OrgBio and MOrgBio, while single metal salt solutions were tested only on OrgBio and MOrgBio.

In order to evaluate the effect of fouling on the sorption of heavy metals, synthetic wastewater (SWW) prepared according to the OECD test guidelines 209 protocols (OECD, 2010) as described in 3.4.2, was introduced into the sorption system. As a factor of safety, all materials for the experiment were autoclaved. The experiment was planned in such a way as to allow for the appraisal of how the sorption of heavy metals is impacted by the order in which the heavy metal(s) at 0.16 mM (in single or mixed salt solution) and the SWW at 16 mg/L (measured as DOC) were contacted with the sorbents at 1.25 mg/mL. The following order of contact was adopted;

6.2.3.1   Heavy metal(s) Sorbed before SWW Addition

In this order, the metal(s) was given a 24-hour head start for adsorption before the SWW was introduced. The sorbents (50 mg) were contacted with 39 mL of deionised water in a 50 mL polyethylene plastic vials with screw cap, supplied by VWR (Lutterworth, UK). The set up was allowed to shake overnight on a platform shaker (STUART SCIENTIFIC STR6) set to shake at 70 rpm overnight at 22 °C. Thereafter, 1 mL of appropriate metal(s) salt stock solution was then added to the preconditioned sorbents to have a predetermined initial metal(s) concentration of 0.16 mM. The samples were returned to shake for 24 hours and then 1 mL of appropriate SWW stock solution was added such as to have a concentration of 16 mg/L. The vials were shaken for a further 6 days using the same shaker settings, after which they were filtered using a 25 mm syringe filter with a 0.45 µm PTFE membrane supplied by VWR International (Lutterworth, UK). Control samples containing only metal(s) solution without sorbent were processed in a similar manner. All samples were then handled as explained in 6.2.1.

6.2.3.2   Synthetic Wastewater Sorbed Before Metals(s) Addition

In this order, SWW was given a 24-hour head start for adsorption before the metal(s) was introduced. The same procedure as in 6.2.3.1 was adopted, it should be noted that 7 days shaking was maintained after the metal(s) was added.

6.2.3.3   Simultaneous Contact of Metal(s) and SWW

In this order, both the metal(s) and SWW were added at the same time. The same procedure as in 6.2.3.1 was adopted, with slight modification. Sorbents were conditioned with 38 mL of deionised water overnight before the addition of 1 mL each of the metal(s) and SWW stock solutions. The rest is the same as in 6.2.3.1.

6.3   RESULT AND DISCUSSION

6.3.1   EVALUATION OF SORPTION ISOTHERMS FOR SORPTION OF Cu^{2+} IN THE PRESENCE OF Pb^{2+} AND Zn^{2+} IN AN EQUIMOLAR MIXED SOLUTION.

The sorption isotherm for Cu^{2+} in the presence of Pb^{2+} and Zn^{2+} on ACs, BCs and magnetite in an equimolar mixed metal salts solution is presented in Figure 6.1. Different patterns of isotherms can be seen, with most data points overlaying the ordinate axis, especially CoAC, Bio-1 and MOrgBio. These sorbents exhibit high affinity for Cu^{2+} at lower concentrations. Almost all sorbents appear to reach saturation from about an initial concentration of 0.08 mM and as a result the isotherms assumes a plateau due to exhaustion of sorption sites. Compared to their sorption capacities for organic compounds, very low uptake of Cu^{2+} is recorded on all sorbents. This shows that they have limited metal sorption capacities.
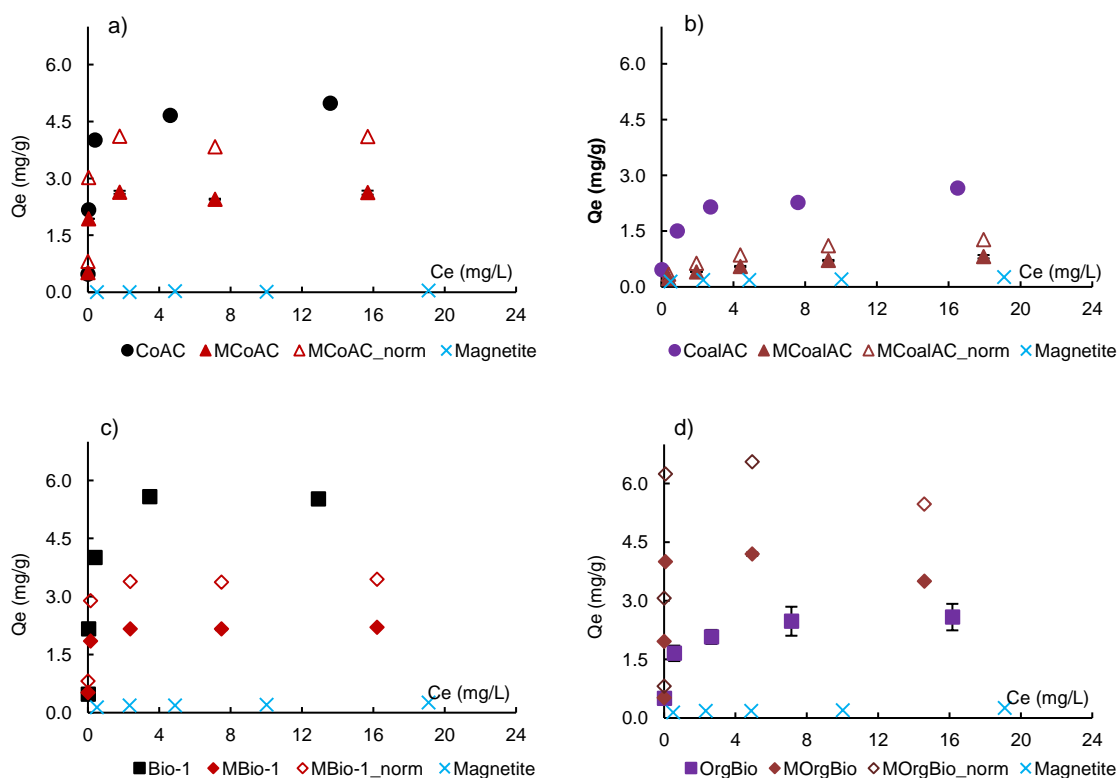
Figure 6.1:   Sorption of Cu^{2+} in the presence of Pb^{2+} and Zn^{2+} on; (a) CoAC & MCoAC, (b) CoalAC & MCoalAC, (c) Bio-1 & MBio-1 and (d) OrgBio & MOrgBio

Additionally, the activated carbons in spite of their amplified surface areas and pore system have similar or in some instances even lower Cu^{2+} sorption than the biochars. Therefore, the availability of surface area (A_S) is not the main factor that govern the sorption of Cu^{2+} (Pyrzyńska and Bystrzejewski, 2010). This clearly shows that the sorption of the metal on the basal plane of the sorbent's microcrystallite contributes little to its overall uptake. Rather, more Cu^{2+} uptake occurs through binding with specific active sorption sites (Leyva Ramos *et al.*, 2002) along the edges and points of dislocations of the carbon planes (Coughlin and Ezra, 1968; Mattson *et al.*, 1969; Li *et al.*, 2002; Dąbrowski *et al.*, 2005; Roop and Meenakshi, 2005). This could then be the reason why magnetite has the least uptake of the metal since it lacks these types of specific active sorption sites. Another interesting observation is that, while all the other magnetised sorbents have lower Cu^{2+} uptake than their corresponding pristine pairs, MOrgBio has higher uptake than OrgBio. This means that the process of magnetisation might have caused the production of more active sites that could bind to even more Cu^{2+} for this sorbent. The evidence is that MOrgBio contains magnetite which does not contribute to the Cu^{2+} uptake, yet despite having about 36 % lesser carbon content, it performs better than OrgBio. As for the other magnetic carbon composites, even their mass normalised isotherms are still lower than the isotherms of their corresponding pristine pair, indicating that magnetite impregnation inhibited metal uptake.

6.3.1.1   *Modelling of Sorption Isotherms Data:*

A.   Linear Isotherm Model
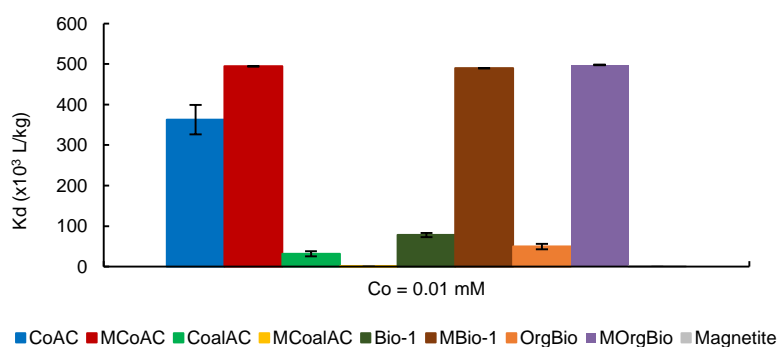
Figure 6.2:   Partitioning coefficient for sorption of Cu^{2+} in the presence of Pb^{2+} and Zn^{2+} on ACs, BCs and magnetite

As can be seen in Figure 6.2, the linear model shows that magnetisation has impacted the sorbents' Cu^{2+} uptake differently. While the uptake of Cu^{2+} on CoalAC was reduced by 98.18 % (i.e. difference between sorption of Cu^{2+} on CoalAC and MCoalAC), there is an increase of about 37.90 % uptake on CoAC due to magnetisation. By the same judgement, there is a remarkable increase of 527.97 and 904.89 % uptake on Bio-1 and OrgBio respectively following magnetization. Furthermore, the MBCs have the same level of Cu^{2+} uptake than MCoAC (the best of the ACs). This clearly show that magnetisation is beneficial to the removal of Cu^{2+} at low concentration solutions by some of the magnetic sorbents. It is obvious that magnetisation did not enhance the uptake through the magnetic attraction of the metal since magnetite has the least uptake. Rather the process of magnetisation is likely to have produced additional edges and points of dislocation on the surface of the biochars. Puziy *et al.* (2002), have reported the existence of carboxylic and phenolic monoprotic sorption sites that are formed due to chemical activation of carbon. They found that the sorption of Cu^{2+} is through the formation of complexes with these sites. It is likely then that such sites were formed on the magnetic-carbon composites during the process of magnetisation when the sorbents were subjected to very high acidic conditions. Hence the performance of the magnetic-carbon composites was enhanced at low concentration. Another observation is that a decrease in pH_{PZC} for the sorbents was recorded especially MCoAC and MOrgBio. This could make it possible for sorption of to progress due to electrostatic interaction when the pH is above the pH_{PZC} of these sorbents.

B. Nonlinear Isotherm Models

Table 6.1: Summary of ASE for the sorption of Cu^{2+} in the presence of Pb^{2+} and Zn^{2+} on ACs, BCs and magnetite.

SORBENT	CoAC	MCoAC	CoalAC	MCoalAC	Bio-1	MBio-1	OrgBio	MOrgBio	Magnetite
LANG_L	19.53	2.40	14.06	5.96	4.53	14.61	13.99	28.72	8.96
FR_L	20.64	13.99	4.22	1.47	28.15	9.18	4.84	36.47	2.27
RP_L	3.16	1.54	2.17	0.92	4.95	0.72	0.91	38.39	2.58
LANG	7.72	2.35	8.68	4.59	3.82	1.99	7.51	12.40	3.37
FREU	16.15	11.64	3.75	1.35	22.15	8.02	4.48	28.60	2.17
RED-PET	2.97	1.52	2.11	0.90	3.61	0.67	0.87	18.29	2.50

Methods of linear and nonlinear data fitting were applied in the evaluation of the experimental results. In general, the nonlinear regression method

generated more accurate parameters and the isotherm simulated hence produced lower residuals about the experimental isotherm. Consequently, better error function values were obtained as can be seen in Table 6.1.

The optimised parameters for the isotherm model are summarised in Table 6.2. Except in the case of MOrgBio, the Redlich-Peterson model generally has the best ASE values. Of the two 2-parameter models, the Langmuir model has better fitting than the Freundlich models for most of the sorbents. This is also confirmed by the Redlich-Peterson model exponent 'γ', which in most instances is closer to 1.

Table 6.2:   Optimised isotherm model parameters for sorption of Cu^{2+} in the presence of Pb^{2+} and Zn^{2+} on ACs, BCs and magnetite.

Model	Parameter	CoAC	MCoAC	CoalAC	MCoalAC	Bio-1	MBio-1	OrgBio	MOrgBio	Magnetite
LANG	Q_m	4.75	2.51	2.68	0.89	5.48	2.11	2.62	3.95	0.27
	K_L	27.49	178.17	1.49	0.48	13.57	291.08	2.82	369.84	0.69
	R^2	0.9874	0.9775	0.9804	0.9689	0.9746	0.9724	0.9801	0.9139	0.7458
FREU	$1/n$	0.150	0.102	0.192	0.348	0.159	0.148	0.151	0.088	0.180
	K_F	3.70	2.13	1.55	0.31	3.68	1.74	1.79	3.31	0.15
	R^2	0.8893	0.7798	0.9679	0.9872	0.8839	0.7812	0.9699	0.5753	0.8873
RED-PET	K_R	198.98	528.41	56.23	2.34	113.98	729.65	89.53	1460.11	1557.04
	A_R	45.40	216.25	33.00	6.20	23.03	357.59	47.99	369.83	10590.12
	γ	0.951	0.974	0.839	0.719	0.943	0.968	0.874	1.000	0.820
	R^2	0.9979	0.9873	0.9841	0.9951	0.9885	0.9968	0.9951	0.9139	0.8872

Examples of optimised simulated isotherms in which the Langmuir model has closer resemblance to the experimental curve are presented in Figure 6.3. Hence, the sorption is likely to be due to homogenous surface interaction that could result in the formation of monolayer coverage. Both linear and nonlinear models have shown that magnetisation resulted in the enhancement of the Cu^{2+} sorption potentials of OrgBio at both low and high concentrations. This agrees with the pattern exhibited by the isotherm plots in Figure 6.1. In the case of CoAC and Bio-1, magnetisation increased Cu^{2+} sorption at low aqueous concentrations (see Figure 6.2), but not high concentrations.
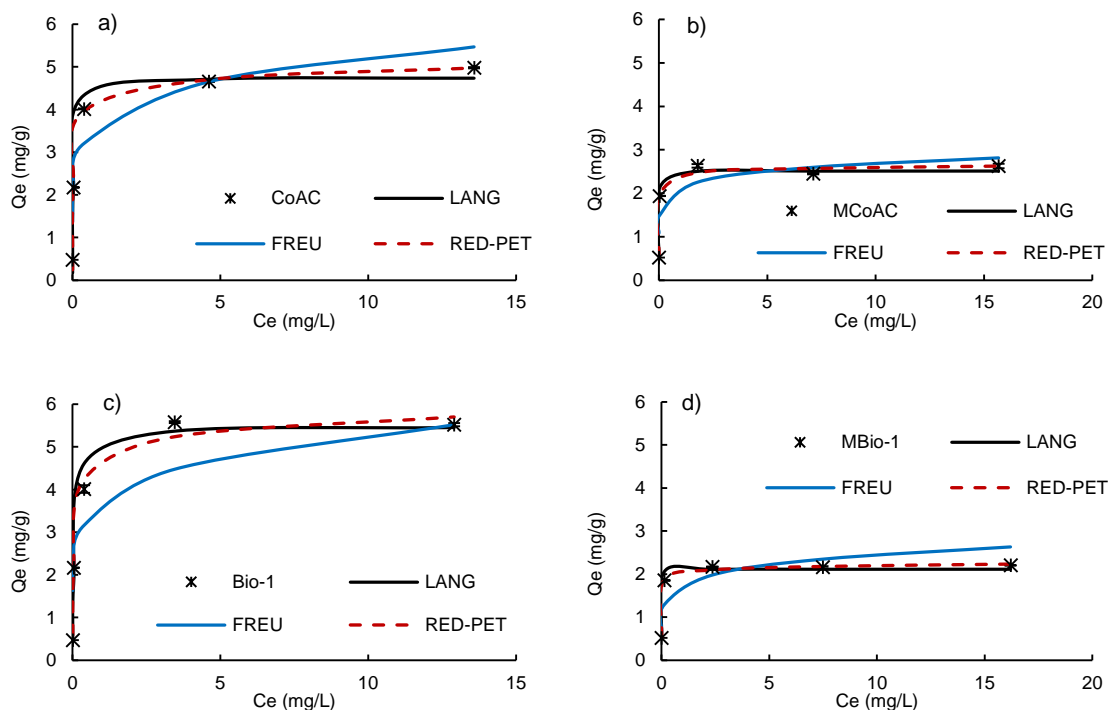
Figure 6.3:   Comparison of simulated and experimental isotherm plot for sorption of Cu^{2+} in the presence of Pb^{2+} and Zn^{2+} on; (a) CoAC, (b) MCoAC, (c) Bio-1 and (d) MBio-1

6.3.1.2   Sorption Capacities

According to the Langmuir's capacity factor shown in Table 6.2, with a value of 5.48 mg/g, Bio-1 has the highest Cu^{2+} uptake. Unfortunately, however, unlike what was observed in the linear model, the sorption capacity of its magnetised form was decreased. Interestingly, MOrgBio still had better performance over OrgBio according to the isotherm models, showing the benefits of magnetisation in this instance also. The sorbents can be arranged according to the Langmuir model's capacity parameter in the following order; magnetite < MCoalAC < MBio-1 < MCoAC < OrgBio < CoalAC < MOrgBio < CoAC < Bio-1. While the order according to the Freundlich model's capacity parameter is as follows; magnetite < MCoalAC < CoalAC < MBio-1 < OrgBio < MCoAC < MOrgBio < Bio-1 < CoAC. According to both models, magnetite has negligible capacity, while the sorption capacities of the three best sorbents; MOrgBio, Bio-1 and CoAC are not far apart.

Unlike what was observed in the case of organic compounds (as discussed in 4.3.2.3, 5.3.1.2 and 5.3.2.3), it can be observed from Tables 6.3 and 6.4 that correlation between the capacity influencing sorbent properties (from Table 3.1) and the models' capacity parameters (from Table 6.2) is generally poor

(generally, Pearson correlation coefficient $R \leq 0.3685$). This clearly indicates that neither the surface area nor the pore volumes are the main properties that influences the sorption of Cu^{2+} on these sorbents.

Table 6.3: Sorption of Cu^{2+} in the presence of Pb^{2+} and Zn^{2+} on ACs and BCs; Pearson correlation coefficients between model parameters and sorbent properties.

Model	Parameters	A_S	V_P	V_{MP}	P_S
Linear	K_d	0.1837	0.1588	0.1916	0.2513
Langmuir	Q_m	0.0668	0.2726	0.0048	0.2121
	K_L	0.4557	0.3165	0.4923	0.1355
Freundlich	$1/n$	0.3330	0.4590	0.2798	0.1416
	K_F	0.1208	0.3132	0.0518	0.2050
Redlich-Peterson	K_R	0.4658	0.3546	0.4877	0.0973
	A_R	0.4614	0.3297	0.4976	0.0840
	γ	0.3191	0.4187	0.2800	0.0941

Table 6.4: Sorption of Cu^{2+} in the presence of Pb^{2+} and Zn^{2+} on ACs and BCs; Pearson correlation coefficients between normalised model capacity factors and sorbent properties.

Model	Parameters	A_S	V_P	V_{MP}	P_S
Linear	K_d	0.2763	0.2017	0.2978	0.2087
Langmuir	Q_m	0.2641	0.3602	0.2209	0.2625
Freundlich	K_F	0.2900	0.3685	0.2521	0.2158

6.3.1.3   Sorption Affinity

According to the models' sorption intensity and heterogeneity factors, the sorbents can be ranked as follows; [K_L: MCoalAC < magnetite < CoalAC < OrgBio < Bio-1 < CoAC < MCoAC < MBio-1 < MOrgBio], [n: MCoalAC < CoalAC < magnetite < Bio-1 < OrgBio < CoAC < MBio-1 < MCoAC < MOrgBio] and [γ: MCoalAC < magnetite < CoalAC < OrgBio < Bio-1 < CoAC < MBio-1 < MCoAC < MOrgBio]. This patter resembles what was obtained from ranking according to capacity parameters. Therefore from the forgone observation, and the deduction that most isotherms happens to be of the Langmuir type, it can stated that sorption of Cu^{2+} is favoured as the binding intensity and surface homogeneity increases (Chen *et al.*, 2011b). According to all models, MOrgBio is the best sorbent that can be used to remove Cu^{2+} in the presence of Pb^{2+} and Zn^{2+} in an equimolar solution.

6.3.2 EVALUATION OF SORPTION ISOTHERMS FOR SORPTION OF Pb²⁺ IN THE PRESENCE OF Cu²⁺ AND Zn²⁺ IN AN EQUIMOLAR MIXED SOLUTION.

The sorption isotherm for Pb^{2+} in the presence of Cu^{2+} and Zn^{2+} on ACs, BCs and magnetite in an equimolar mixed metal salts solution is presented in Figure 6.4. With the exception of the coal based AC, all sorbents exhibit high affinity of Pb^{2+} within the lower concentration region. Compared to their sorption of Cu^{2+}, the sorbents did not show the same pattern of exhaustion. The isotherms of the BCs are quite comparable to those of the ACs, or even better especially when compared to the coal based AC.
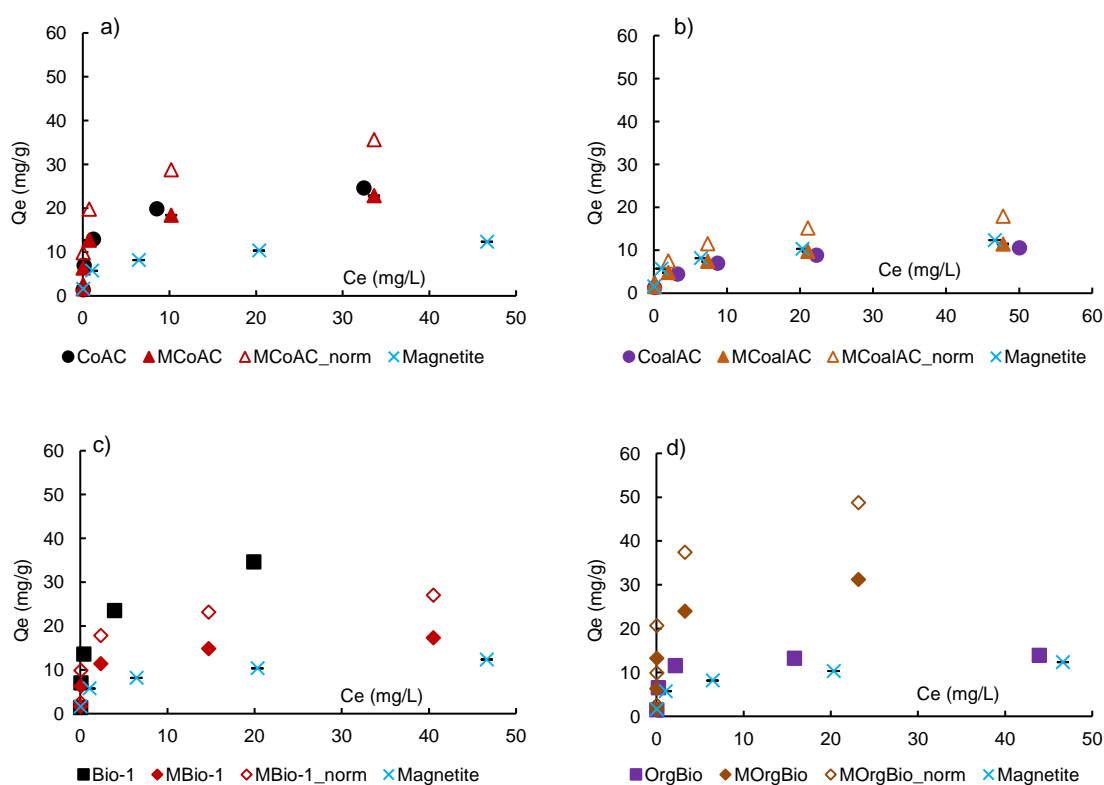
Figure 6.4: Sorption of Pb^{2+} in the presence of Cu^{2+} and Zn^{2+} on; (a) CoAC & MCoAC, (b) CoalAC & MCoalAC, (c) Bio-1 & MBio-1 and (d) OrgBio & MOrgBio

Thus, as in the case of the Cu^{2+} sorption, the sorbents' Pb^{2+} sorption capacities are not mainly dependent upon the availability of A_S. This suggests also that their uptake of Pb^{2+} is due to its binding with specific sorption sites, through the formation surface complexation with carboxyl and hydroxyl functional groups and coulombic interactions (Lu *et al.*, 2012). It can be observed that this time around, the magnetic iron oxide has shown some affinity for the metal, and

as a result, the composites MCoaAC and MCoalAC have about the same level of Pb^{2+} uptake with their pristine pairs, while MOrgBio again has better uptake than OrgBio. This observation confirms the suggestion that the process of magnetisation has altered the metal sorption property of the OrgBio for the better.

6.3.2.1   *Modelling of Sorption Isotherms Data*

A   Linear Isotherm Model
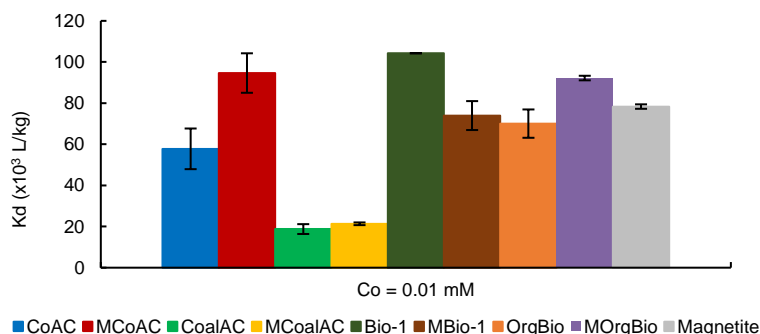
Figure 6.5:   Partitioning coefficient for sorption of Pb^{2+} in the presence of Cu^{2+} and Zn^{2+} on ACs, BCs and magnetite

It can be observed in Figure 6.5, that the BCs have higher uptake than the ACs, indicating once again that the total surface area is not the most important sorbent parameter that governs the sorption of Pb^{2+}. This is in agreement with the findings of Cao *et al.* (2009). According to the linear model, magnetisation has enhanced the uptake of Pb^{2+} on CoalAC by 13.68 %, OrgBio by 31.63 % and CoAC by a remarkable 63.76 %. Excepting Bio-1, where a decrease of 29.06 % was recorded, it can be inferred that magnetisation is beneficial to the removal of Pb^{2+} at low concentrations. On the average, the MBCs have about 30.20 % more uptake of Pb^{2+} than does the MACs. Unlike in the sorption of Cu^{2+}, the pure magnetite has demonstrated satisfactory removal of Pb^{2+} according to the linear model.

B   Nonlinear Isotherm Models

Method of nonlinear regression generally produced optimised error functions and as such model parameters obtained are more reliable than those obtained using methods of least square. The result for the average errors for the

isotherms obtained from model simulation using linear and nonlinear fitting is presented in Table 6.5.

Table 6.5: Summary of ASE for the sorption of Pb^{2+} in the presence of Cu^{2+} and Zn^{2+} on ACs, BCs and magnetite.

Sorbent	CoAC	MCoAC	CoalAC	MCoalAC	Bio-1	MBio-1	OrgBio	MOrgBio	Magnetite
LANG_L	32.65	58.03	20.01	19.81	56.50	54.88	14.34	110.66	28.09
FR_L	57.66	49.70	2.95	3.22	74.03	34.38	42.82	117.00	5.01
RP_L	26.49	61.30	3.20	1.50	71.79	42.82	0.39	148.88	0.44
LANG	17.76	33.40	15.26	16.31	35.52	20.73	2.79	66.36	19.54
FREU	34.13	38.19	2.77	2.81	38.78	27.77	31.54	89.68	4.04
RED-PET	7.66	27.12	3.10	1.47	15.34	19.48	0.34	87.30	0.43

Table 6.6: Optimised isotherm model parameters for sorption of Pb^{2+} in the presence of Cu^{2+} and Zn^{2+} on ACs, BCs and magnetite.

| Model	Parameter	CoAC	MCoAC	CoalAC	MCoalAC	Bio-1	MBio-1	OrgBio	MOrgBio	Magnetite
	Q_m	25.48	23.23	11.50	11.91	35.45	14.85	13.47	28.06	12.57
	K_L	0.85	1.62	0.18	0.35	1.38	9.60	4.57	14.47	0.50
LANG	R^2	0.9680	0.9445	0.9924	0.9704	0.9467	0.8994	0.9937	0.9110	0.9556
	$1/n$	0.234	0.284	0.296	0.313	0.250	0.262	0.162	0.209	0.210
	K_F	10.90	9.93	3.41	3.68	16.41	7.60	8.47	16.83	5.52
FREU	R^2	0.9666	0.9248	0.9882	0.9869	0.9856	0.9207	0.8714	0.8932	0.9949
	K_R	113.57	3104.72	60.07	55.72	565.12	3278.75	79.34	538.52	204.69
	A_R	7.96	306.88	16.43	12.39	31.76	426.01	6.60	23.73	35.74
	γ	0.841	0.723	0.724	0.753	0.776	0.742	0.961	0.904	0.801
RED-PET	R^2	0.9975	0.9292	0.9900	0.9970	0.9965	0.9237	1.0000	0.9342	0.9996
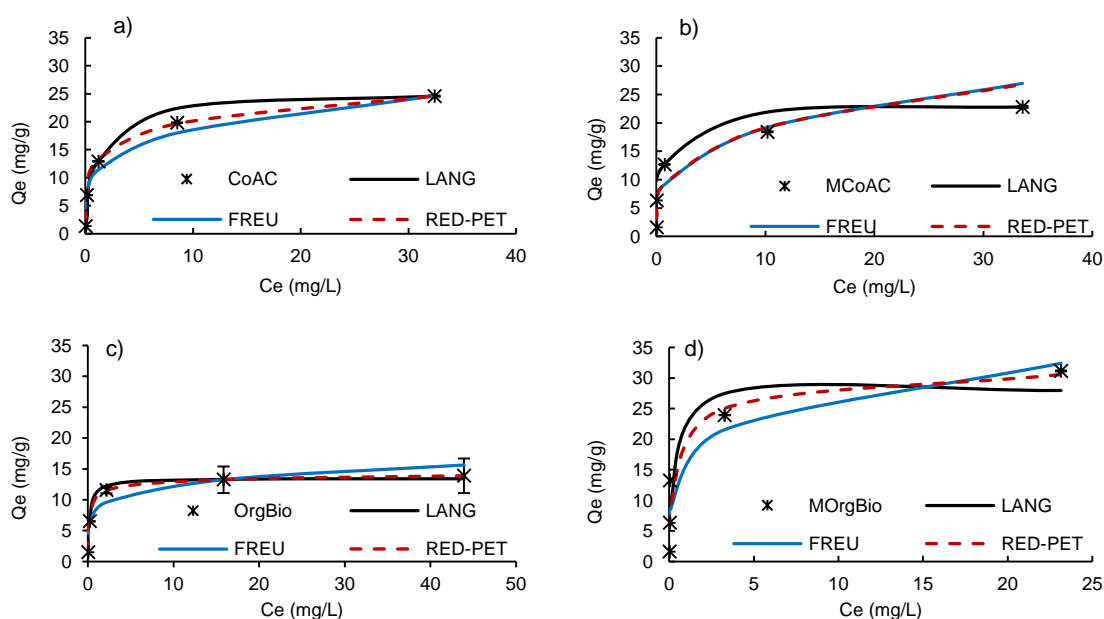
Figure 6.6: Comparison of simulated and experimental isotherm plot for sorption of Pb^{2+} in the presence of Cu^{2+} and Zn^{2+} on; (a) CoAC, (b) MCoAC, (c) OrgBio and (d) MOrgBio

Except for CoalAC, the Redlich-Peterson model produces the best ASE values for all the sorbents. In a like manner, the Langmuir model appears to have closer resemblance to the experimental isotherms compared to the Freundlich model. Similar findings have also been reported in literature (Liu and Zhang, 2009; Chen *et al.*, 2011b). The summary of optimised model parameters is shown in Table 6.6, and the isotherms obtained from them for CoAC MCoAC, OrgBio and MOrgBio are shown in Figure 6.6 as examples.

6.3.2.2   *Sorption Capacities*

The sorption capacities of the sorbents over the range of the isotherm data can be arranged according to the models' capacity parameters in the order; [Q_m; CoalAC < MCoalAC < magnetite < OrgBio < MBio-1 < MCoAC < CoAC < MOrgBio < Bio-1], [K_F; CoalAC < MCoalAC < magnetite < MBio-1 < OrgBio < MCoAC < CoAC < Bio-1< MOrgBio]. The orders are similar and they affirm the superiority of the Pb^{2+} sorption capacity of MOrgBio over OrgBio, which once again clearly shows the benefit of magnetisation. With a value of Langmuir's Q_m of 28.06 mg/g, MOrgBio has the second highest sorption capacity, next to Bio-1 which has a value of 35.45 mg/g. Despite competition from Cu^{2+} and Zn^{2+}, the sorption capacities recoded for the sorbents in this study are similar or even higher than those reported in previous works (Liu and Zhang, 2009; Lu *et al.*, 2012). Since Pb^{2+} has a higher density than Cu^{2+}, it is more accurate to compare their uptake on the various sorbents according to the molar solid phase concentration. The metals' uptake on the sorbents according to Langmuir Q_m (in mmoles/kg) was computed on molar bases and the result is presented in Table 6.7. It can be observed that Pb^{2+} is sorbed more than Cu^{2+} on all the sorbents by about 31.76 to 1352 %.

Table 6.7:   Summarised molar based sorption capacities according to Langmuir Qm (mmoles/kg).

Metal	CoAC	MCoAC	CoalAC	MCoalAC	Bio-1	MBio-1	OrgBio	MOrgBio	Magnetite
Cu^{2+}	74.71	39.53	42.11	14.02	86.31	33.24	41.30	62.13	4.18
Pb^{2+}	122.96	112.11	55.49	57.46	171.11	71.67	65.00	135.41	60.66

Once again it can be observed from Tables 6.8 and 6.9, that there is poor correlation (generally, Pearson correlation coefficient $R \leq 0.6934$) between models' capacity parameters (from Table 6.6) and the sorbents' surface area,

pore volumes and sizes (from Table 3.1). This means that unlike in the sorption of organic compounds, activation is not beneficial in the sorption of these metals.

Table 6.8: Sorption of Pb^{2+} in the presence of Cu^{2+} and Zn^{2+} on ACs and BCs; Pearson correlation coefficients between model parameters and sorbent properties.

Model	Parameters	A_S	V_P	V_{MP}	P_S
Linear	K_d	0.6261	0.6934	0.5867	0.1385
Langmuir	Q_m	0.1932	0.2980	0.1484	0.3100
	K_L	0.6991	0.5943	0.7190	0.1540
Freundlich	$1/n$	0.6490	0.8190	0.5739	0.7168
	K_F	0.4963	0.5824	0.4499	0.0494
Redlich-Peterson	K_R	0.1600	0.0688	0.1961	0.1515
	A_R	0.1403	0.0415	0.1834	0.1499
	γ	0.5627	0.6928	0.4982	0.7066

Table 6.9: Sorption of Pb^{2+} in the presence of Cu^{2+} and Zn^{2+} on ACs and BCs; Pearson correlation coefficients between normalised model capacity factors and sorbent properties.

Model	Parameters	A_S	V_P	V_{MP}	P_S
Linear	K_d	0.5764	0.5358	0.5728	0.0274
Langmuir	Q_m	0.3108	0.2781	0.3055	0.3136
Freundlich	K_F	0.5353	0.5092	0.5230	0.0903

6.3.2.3 Sorption Affinity

With reference to Table 6.6, the sorbents can be ranked according to the models' sorption intensity and sorbents' surface heterogeneity parameters as follows; [K_L: CoalAC < MCoalAC < magnetite < CoAC < Bio-1 < MCoAC < OrgBio < MBio-1 < MOrgBio], [n: MCoalAC < CoalAC < MCoAC < MBio-1 < Bio-1 < CoAC < magnetite < MOrgBio < OrgBio] and [γ: MCoAC < CoalAC < MBio-1 < MCoalAC < Bio-1 < magnetite < CoAC < MOrgBio < OrgBio]. It is obvious that these orders differ substantially. However, it can be observed that while the coal based ACs mostly ranked lower, MOrgBio is almost always positioned at the upper end of the scale. This pattern is similar to what was obtained when the sorbents' were ranked according to the models' capacity parameters in 6.3.2.2. Already it has been shown that the isotherms are mostly of the Langmuir type. Therefore, it can be deduced that the sorption of Pb^{2+} is favoured as the binding intensity and surface homogeneity increases. This clearly implies that MOrgBio

is the preferable sorbent that can be used to remove Pb^{2+} in the presence of Cu^{2+} and Zn^{2+} in an equimolar solution.

6.3.3 SORPTION OF Zn^{2+} IN THE PRESENCE OF Pb^{2+} AND Cu^{2+} IN AN EQUIMOLAR MIXED SOLUTION.

The results presented here are for the linear model only, because the Zn^{2+} was outcompeted by the other two metals at higher concentration and as such, its isotherms were undefined. A similar trend was also reported by (Han *et al.*, 2013b), where in an equimolar binary solution, the sorption of Cu^{2+} was found to be greater than that of Zn^{2+} biochars and activated carbons. Chen *et al.* (2011b), also observed this trend of competition in the sorption of Zn^{2+} from a binary solution containing Cu^{2+}. They found that while the presence of Zn^{2+} at higher concentration did not have much impact on the sorption of Cu^{2+}, the sorption of Zn^{2+} was dramatically reduced in the presence of higher Cu^{2+} concentration. However, at low concentration they observed that the sorption of either metals was minimally affected by the presence of the other metal.

6.3.3.1 Linear Isotherm Model
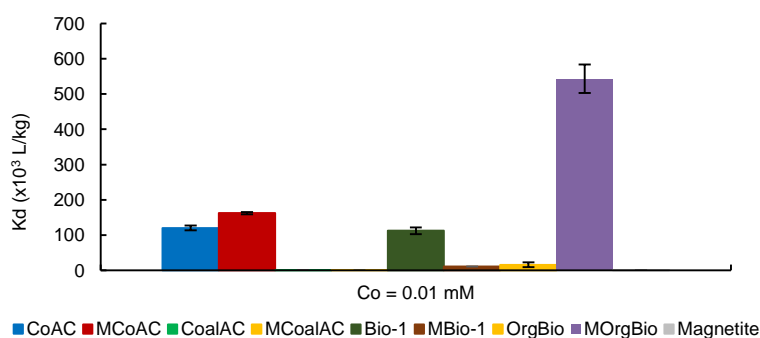
Figure 6.7: Partitioning coefficient for sorption of Zn^{2+} in the presence of Cu^{2+} and Pb^{2+} on ACs, BCs and magnetite

From Figure 6.7, it can be observed that Zn^{2+} sorbs satisfactorily on CoAC, MCoAC and Bio-1. Interestingly, while magnetisation caused about 90 % decrease in Zn^{2+} sorption on Bio-1, MOrgBio displayed an outstanding uptake of Zn^{2+}, about 3378 % more than OrgBio. This enhancement is not due to the imbedded magnetite, since it can be clearly seen that the pure magnetite has

poor affinity of Zn^{2+}. It can be deduced then that magnetisation is beneficial to some but not all of the sorbents.

The fact that these metals can be simultaneously sorbed at low concentration indicates that they either have affinity to different sites or there is an excess of the sorption sites which minimises the impact of competition (Chen *et al.*, 2011b).

6.3.4 MECHANISM OF SORPTION

The fact that the performance of the BCs is similar or even better that the ACs in the uptake of these metals, implies that neither surface area nor pore volumes are significant in determining their sorption capacities. This agrees with the findings of (Cao *et al.*, 2009; Pyrzyńska and Bystrzejewski, 2010; Tong *et al.*, 2011). This is unlike what has been observed in the sorption of organic compounds, where the sorption capacities are mainly dependent upon the surface area and pore volumes. Furthermore, the sorbents' basal plane and the pore walls that constitute a substantial fraction of the total A_S have affinity for organic compounds (Worch, 2012). Sorption of organic compounds in these surfaces are mainly due to the interaction of van der Waals forces (Snoeyink and Weber, 1967; Roop and Meenakshi, 2005; Çeçen and Aktas, 2011). In contrast therefore, the metals appear not to have affinity for these sites. Instead, they are then most likely to bind to specific active sorption sites on the edges, points of fractures and dislocations of the microcrystallite planes and pore walls of the sorbents (Leyva Ramos *et al.*, 2002). Surface area will only be of advantage if it is associated with high concentration of the specific sorption sites.

The metals can react with surface functional groups such as –COOH and –OH that exists on the specific sites through electron sharing and electrostatic attraction to form surface complexes (Tong *et al.*, 2011; Paradelo and Barral, 2012). Therefore, metals with higher electronegativity are preferentially sorbed over others with lesser such potentials (Faur-Brasquet *et al.*, 2002). The solubility of the metal salt also plays a significant role in the uptake of the dissolved metal specie from solution. In this regard, the sorption of metals with higher solubility is disfavoured over those with lower values. The force of attraction between active sites on the sorbent and metal specie increases with increasing electronegativity

and ionic radius (Wiwid Pranata *et al.*, 2014). For these reasons, the sorption of Cu^{2+} and Pb^{2+} with higher electronegative potential and lower solubilities was favoured over that of Zn^{2+} at higher concentrations in equimolar solutions. Pagnanelli *et al.* (2003), reported that metal uptake is related to its first hydrolysis constant. Consequently, heavy metal species with higher first hydrolysis constant are always more sorbed than those with lower ones. They went further to suggest that the metal acidic property has more influence on its sorption than the specific functional groups present on the sorbent surface. In their own words, "metal speciation predominates on adsorbent characteristics".

Another mechanism by which these metals can sorb is by precipitation (Inyang *et al.*, 2012; Lu *et al.*, 2012; Xu *et al.*, 2013) when they interact with negatively charged ions such as phosphates and carbonates that are usually associated especially with biochars. Of these metals, Pb^{2+} has been reported (Cao *et al.*, 2009; Xu *et al.*, 2013) to have high affinity for these ions and it is not surprising therefore it recorded the highest uptake among the metals in this study. The sorption can also be due to ion exchange through substitution of cations on the sorbents by the metals in solution. Therefore, at low pH the metal specie will compete with H^+ for sorption on the ion exchangeable sites, which causes a decrease in metal ion removal (Kadirvelu *et al.*, 2001). According to this mechanism, ions in solution with higher valence or charge can easily substitute those with lower charge on the sorbents. Furthermore, for ions with the same charge, those with a higher atomic number and smaller radius of hydrated ion are preferentially sorbed (Pehlivan and Altun, 2006). Thus, Pb^{2+} will be preferentially sorbed over the other two metals and as a result, the following order was observed $Pb^{2+} > Cu^{2+} > Zn^{2+}$. This order has also been reported for the removal of these metals using various sorbents (Pagnanelli *et al.*, 2003; Perić *et al.*, 2004; Zhang, 2011; Paradelo and Barral, 2012).
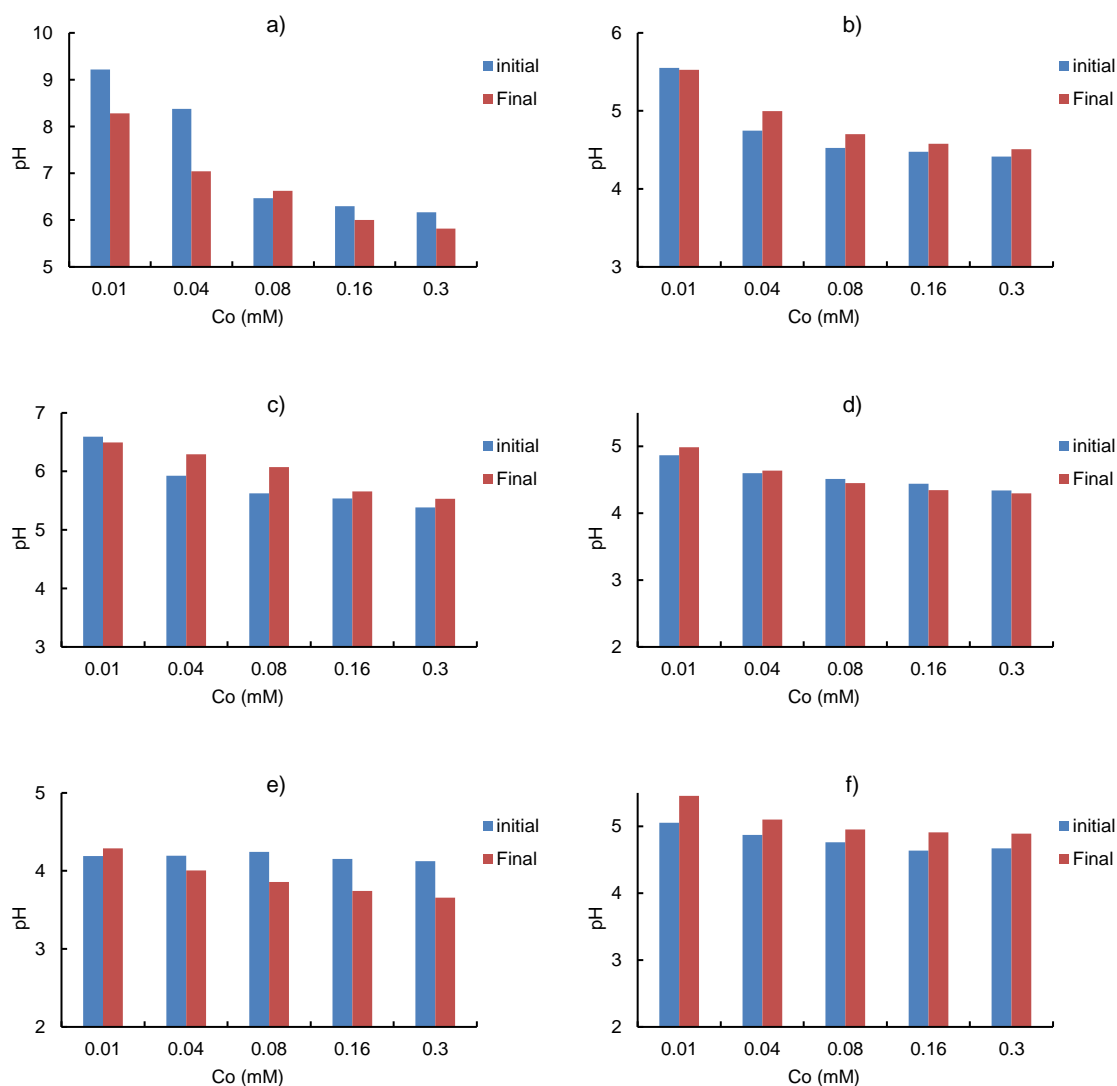
Figure 6.8: Solution pH for the sorption of Pb^{2+}, Cu^{2+} and Zn^{2+} in mixed equimolar solution. (a) CoAC, (b) MCoAC, (c) OrgBio, (d) MOrgBio, (e) Magnetite and (f) Control

Columbic interactions also play a role in the sorption of the metals. It can be observed from Figure 6.8, that the experiments were conducted within the pH 4 – 9, most of the observed values are well below the pH_{PZC} of the sorbents, hence the surface of the sorbents will have a net positive charge. In this range, free metal specie (Me^{2+}) is dominant (Faur-Brasquet et al., 2002; Liu and Zhang, 2009). Consequently, the sorption of these metals by coulombic interactions might not be possible since there will be mutual repulsion instead of attraction between the both positively charged surface and metal ions. This is even more pronounced as the pH decreases due to an increase in initial concentration. This could be the reason for the poor sorption of the metals on most of the sorbents at high concentration leading to their saturation. Such a decrease in sorption due

to decrease in pH for increased initial concentration was also reported by (Paradelo and Barral, 2012). The result for the influence of pH on the sorption of the metals is presented in 6.3.6.

6.3.5 EVALUATION OF SORPTION ISOTHERMS FOR SORPTION OF SINGLE METAL SOLUTION

The isotherms for the sorption of Cu^{2+}, Pb^{2+} and Zn^{2+} on OrgBio, MOrgBio and magnetite are shown in Figure 6.9. With the exception of the sorption of Pb^{2+}, the isotherms of MOrgBio are comparable or higher than those of OrgBio. This further supports earlier observations that the magnetisation process has modified the surface properties of OrgBio for the better. The sorption of Pb^{2+} on magnetite and MOrgBio remained similar to what was recorded in its sorption from equimolar solution. There is however a slight improvement in the sorption of Cu^{2+} on the biochars and magnetite, indicating that its sorption was inhibited by the presence of Pb^{2+}. It can thus be inferred that in combined solution, the metals compete for the same sorption sites. Therefore, Pb^{2+} was the dominant sorbed specie both in single and combined solution since it is more easily removed from solution because of its higher density and lower solubility.

6.3.5.1 Modelling of Sorption Isotherms Data
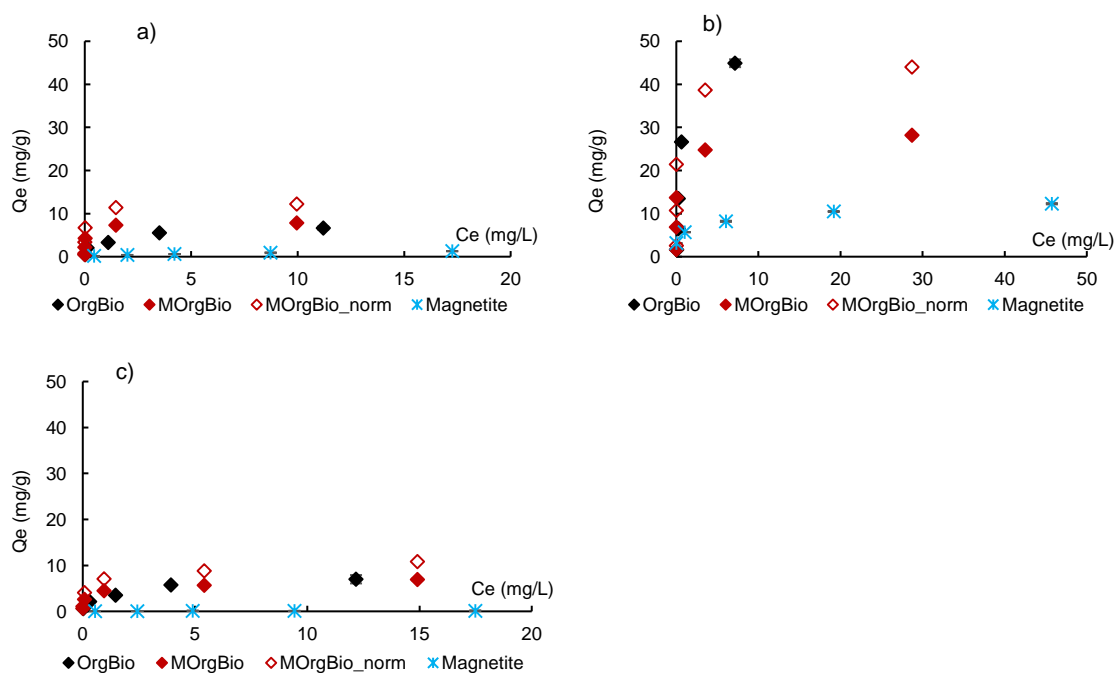
Figure 6.9: Sorption of (a) Cu^{2+} (b) Pb^{2+} and (c) Zn^{2+} on OrgBio, MOrgBio & magnetite from single metal salt solution.

A. Linear Isotherm Model

The result of the linear model for the three metals as presented in Figure 6.10 was able to clearly show that at low concentration, the sorption capacity of MOrgBio is remarkably higher than that of OrgBio by about 381.41, 91.22 and 1105.17 % for Cu^{2+}, Pb^{2+} and Zn^{2+} respectively. Interestingly, it can be observed that magnetite has no affinity for Cu^{2+} and Zn^{2+} at such low concentrations, yet, its Pb^{2+} sorption is outstanding. Therefore, the enhanced uptake of these metals recorded on MOrgBio could not have been due to the presence of the magnetite impregnation on its surface. Neither did the presence of magnetite on MOrgBio contribute to its sorption of Pb^{2+} from single solution. This is because an insignificant decrease of about 5.20 % was recorded for MOrgBio, compared to what was recorded it its sorption from mixed solution, even though an outstanding increase of 187.15 % was recorded for magnetite uptake of Pb^{2+}, (against its sorption in mixed solution).
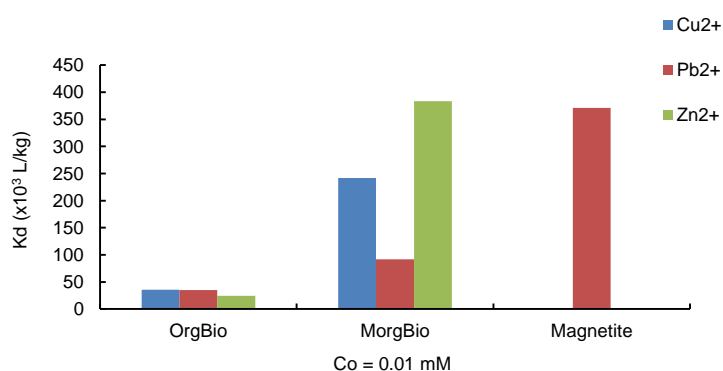
Figure 6.10:   Partitioning coefficient for Sorption of Cu^{2+}, Pb^{2+}, and Zn^{2+} on OrgBio, MOrgBio & magnetite from single metal salt solution.

B. Nonlinear Isotherm Models

The optimised model parameters are presented in Table 6.10, and the isotherms obtained from these parameters are shown in Figure 6.11 for Pb^{2+} sorption on OrgBio and MOrgBio as examples.

The Redlich-Peterson had the best fitting to the isotherm data. On the average, the Langmuir had better fitting compared to the Freundlich model. The sorption capacities for the sorbents are compared in Figure 6.12 and it can be observed that according to both models, Pb^{2+} was sorbed the highest on all sorbents, while Cu^{2+} and Zn^{2+} have about equal uptake on OrgBio and MOrgBio.

The magnetite did not exhibit affinity for Cu^{2+} and Zn^{2+} similar to what was observed at low concentration.

Table 6.10: Optimised isotherm model parameters for sorption of phenol @ 295.15 K on ACs and BCs.

Model	Parameter	Cu			Pb			Zn		
		OrgBio	MOrgBio	Magnetite	OrgBio	MOrgBio	Magnetite	OrgBio	MOrgBio	Magnetite
	Q_m	7.46	7.62	1.97	49.55	28.36	12.36	7.79	6.62	0.09
	K_L	0.73	70.79	0.11	1.35	3.44	0.55	0.72	2.25	0.48
LANG	R^2	0.9697	0.9820	0.9966	0.9654	0.8382	0.9423	0.9808	0.9475	0.9244
	$1/n$	0.292	0.162	0.536	0.359	0.169	0.200	0.327	0.188	0.288
	K_F	3.42	5.85	0.28	22.15	16.94	5.72	3.09	4.18	0.03
FREU	R^2	0.9726	0.8421	0.9988	0.8989	0.7940	0.9935	0.9739	0.9852	0.8976
	K_R	75.76	539.54	0.85	67.71	5.33E+06	1.35E+06	18.67	635.32	0.05
	A_R	19.74	70.78	2.20	1.35	3.11E+05	2.21E+05	4.47	145.10	0.93
	γ	0.761	1.000	0.549	1.000	0.833	0.821	0.770	0.832	0.894
RED-PET	R^2	0.9825	0.9820	0.9998	0.9653	0.7943	0.9894	0.9846	0.9969	0.9308
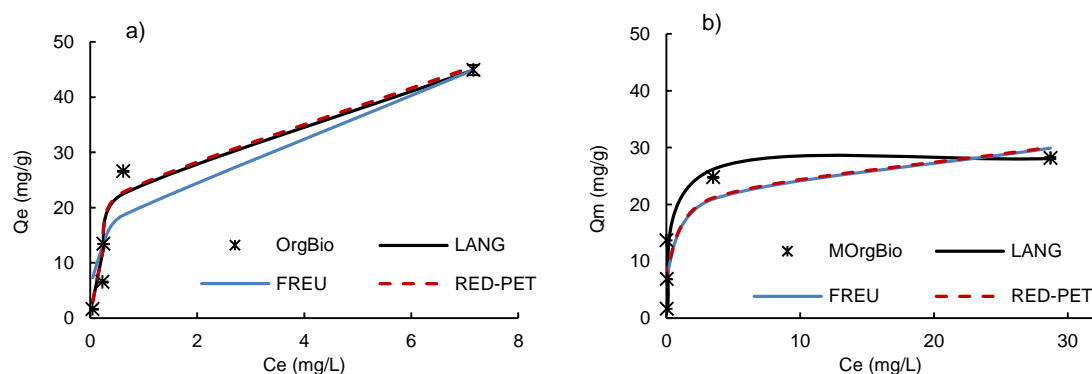
Figure 6.11: Comparison of simulated and experimental isotherm plot for sorption of Pb^{2+} from single solution on; (a) OrgBio and (b) MOrgBio

6.3.5.2 Sorption Capacities

Comparison of the sorbents' capacities for the sorption of the metals from mixed and single solutions revealed the impact of competition. In the absence of competition, sorption of Cu^{2+} increased by about 3, 2 and 7 fold on OrgBio, MOrgBio and magnetite respectively.
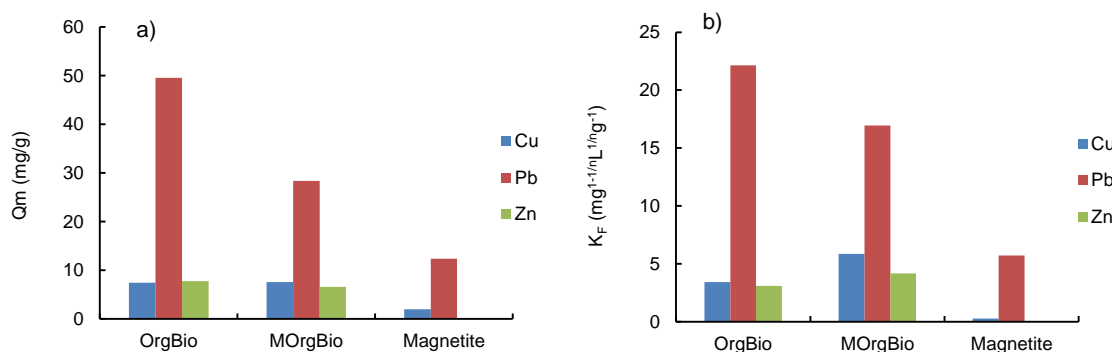
Figure 6.12:   Sorption capacities of OrgBio, MOrgBio and magnetite for sorption of metals from single solution according to (a) Langmuir constant, (b) Freundlich constant.

The sorption of Pb^{2+} increased by about 3.7 fold on OrgBio, while it remained the same on MOrgBio and magnetite. Zn^{2+} was outcompeted by the other two metals at high concentration and as such its isotherm was undefined hence not presented. However, its sorption capacities on OrgBio and MOrgBio in the absence of competition compare favourably to those of Cu^{2+}. This shows that the metals have very similar sorption mechanisms, thus compete with each other for the available specific sorption sites on the sorbents, with Pb^{2+} being the most and Zn^{2+} the least competitive metal cation.

6.3.6   EFFECT OF SOLUTION pH ON SORPTION OF HEAVY METALS

The solution pH has an effect on both sorbent and metal properties. It determines the charge on the surface of the sorbent as well as the nature of active sites on it. It also determines whether the metal exist in either free or hydrolysed form in the solution. Therefore, the sorption of metals can be influenced for better or for worse depending on the prevailing nature of interaction that exist between the metal and the surface of the sorbent at a given pH level (Leyva Ramos *et al.*, 2002; Amuda *et al.*, 2007). The variation of pH affects the sorbent and metals sorption influencing properties in the following ways;

6.3.6.1 Metal Speciation with pH
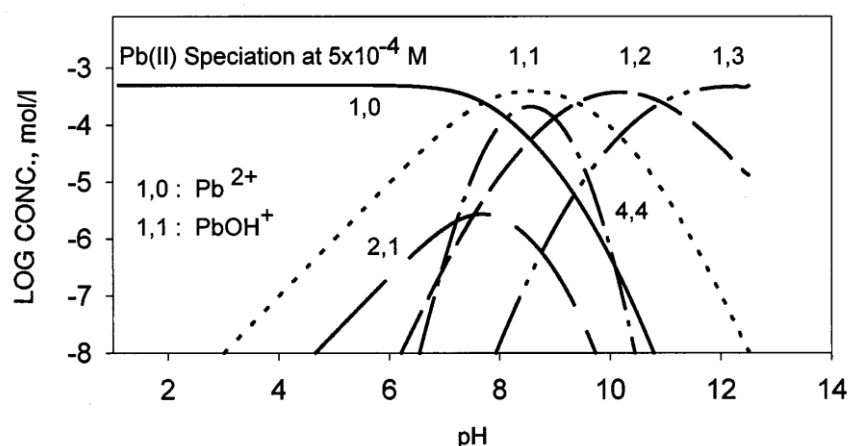
Figure 6.13:   Speciation of Pb^{2+} with pH. 1,2: $Pb(OH)_2$; 1,3: $Pb(OH)_3^{1-}$; 4,4: $Pb_4(OH)_4^{4+}$; 2,1: Pb_2OH^{3+} (Huang and Fuerstenau, 2001)

Metals in solution can exist as free or hydrolysed species depending on the pH level. At lower pH, the free specie is the dominant and the concentration of the hydrolysed specie increases to a peak as the pH increases. Further increase in pH result in the domination of uncharged or negatively charged species due to hydrolysis reaction, as demonstrated in the speciation diagram in Figure 6.13. In general, the hydrolysed metal specie are preferentially sorbed over free ones. Therefore, sorption increases at as the pH increases due to the formation of less charged and less soluble hydrolysed species which can easily be attached to the surface as a result of decrease of electrostatic repulsion (Faur-Brasquet *et al.*, 2002).

Thus metals removal at higher pH could be due to both sorption and metal hydroxide precipitation (Huang and Fuerstenau, 2001; Lu *et al.*, 2012). Also at low pH the solution is rich in H^+ which compete with the cations for active sorption sites (Pellera *et al.*, 2012). As pH increases, solubility of metals decreases, at very high pH, metals precipitate and removal is due to both sorption and precipitation (Schiewer and Volesky, 1995). However, from the speciation diagram, it can be inferred that, within the acidic to neutral pH range, the removal of Me^{2+} specie is majorly by sorption.

6.3.6.2 Surface Charge

At pH below the pH_{PZC} of the sorbent the surface is positively charged and this is unfavourable for the sorption of cations due to repulsion between

the positive charged surface and the cation. As the pH increases, the surface charge becomes negative at pH above the pH$_{PZC}$ for the sorbent. This can happen due to deprotonation of hydroxyl and carboxylic groups (Pagnanelli *et al.*, 2003; Lu *et al.*, 2012). This favours the sorption of metals as a result of enhanced electrostatic coordination between the negatively charged surface and the cations (Kula *et al.*, 2008; Liu and Zhang, 2009).

6.3.6.3 Surface Functional Groups

Metal cations are denied coordination with the oxygen-containing surface functional groups at lower pH by the presence of linked H$^+$ to the groups. This enhances electrostatic repulsion between the protonated amine and hydroxyl groups with the cationic adsorbates (Norouzian and Lakouraj, 2015). For similar reasons, metal removal by ion exchange mechanism is impaired at lower pH due to competition between H$^+$ and metal ions for sorption to the ion exchangeable sites (Kadirvelu *et al.*, 2001). As the pH increases, the deprotonation of the functional groups gradually takes place and thereby making it possible for them to coordinate with the cations. Thus making the metals removal more favourable (Kula *et al.*, 2008; Liu and Zhang, 2009).
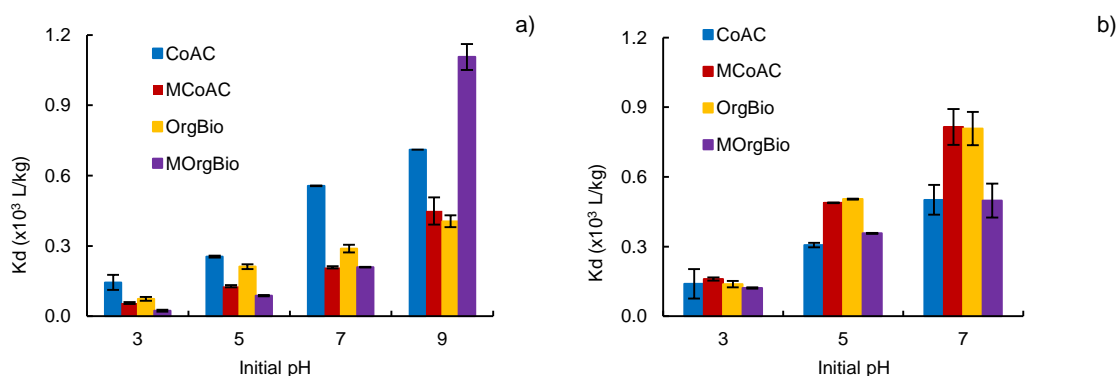
Figure 6.14: The effect of pH on sorption of metals on ACs and BCs form mixed equimolar (0.16 mM) solution (a) Cu^{2+} sorption in presence of Pb^{2+} and Zn^{2+}, (b) Pb^{2+} sorption in presence of Cu^{2+} and Zn^{2+}
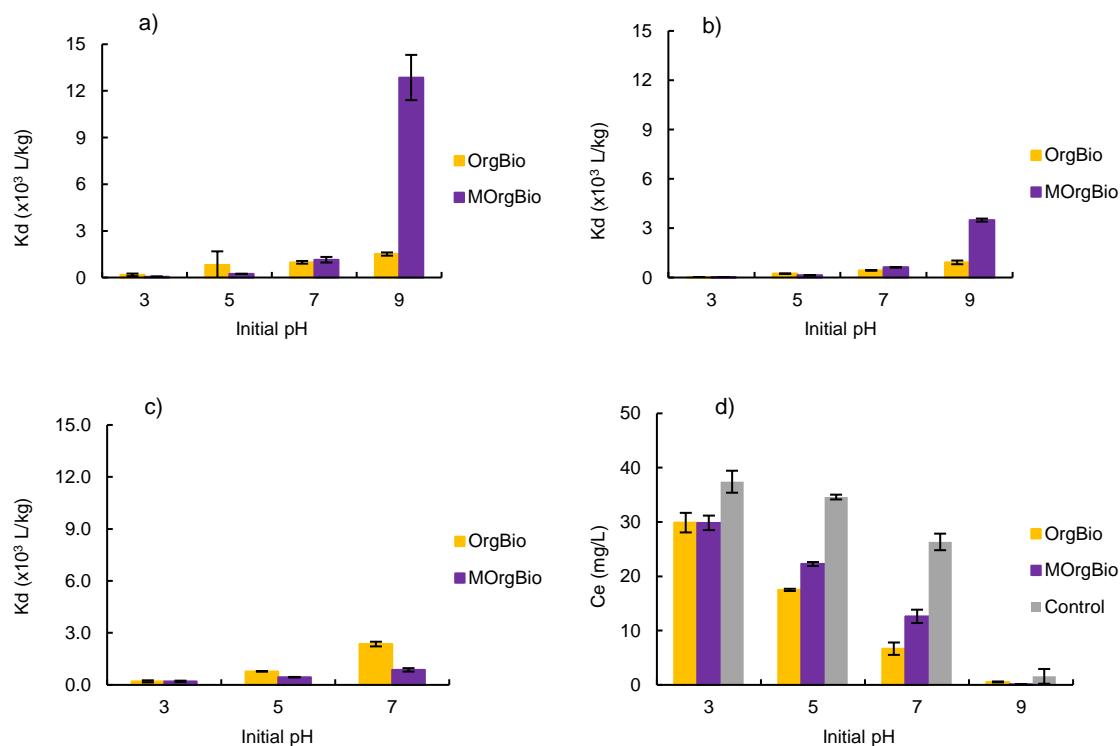
Figure 6.15:   Effect of pH on sorption of metals on OrgBio & MOrgBio from single equimolar (0.16 mM) solution (a) Cu^{2+}, (b) Zn^{2+}, (c) Pb^{2+} and (d) equilibrium concentration for Pb^{2+} sorption.

From Figures 6.14 and 6.15, it can be observed that as the solution pH is increased, there is a general increase in the sorption of the metals on the sorbents from both equimolar mixed and single solution. The residual concentrations of the control samples in the Cu^{2+} and Zn^{2+} remained at the same level throughout the experiment. This suggests that there is no loss of concentration due to the metals precipitating out of the solution in the absence of a sorbent material (Chen *et al.*, 2011b). The Pb^{2+} system however showed substantial decrease for the measurements in the controls from pH 5 and above, such that at pH 9 very little Pb^{2+} was detected (see Figure 6.15 (d)). It is likely then that the metal might have precipitated out of the solution which caused some loss of concentration.

6.3.7   SORPTION IN SYNTHETIC WASTEWATER (16 mg/L DOC)

6.3.7.1   *Mixed Equimolar Solution*

It can be observed from Figure 6.16(a), that there is a general increase in the sorption of Cu^{2+} on CoAC and MCoAC under multiple competition. For

instance, when Cu^{2+} sorption was given 24 hr head start, highest increase of 29.16 % and 62.64 % was recorded for CoAC and MCoAC respectively. The increase recorded is likely due to chelation of Cu^{2+} to organic compounds (Hochuli *et al.*, 1987; Iwata *et al.*, 1991) in SWW introduced into the system. This could be the reason why a general decrease was observed in the equilibrium concentration of Cu^{2+} in the control samples of both pure and SWW fouled solution as presented in Figure 6.16(b). On the other hand, the sorption of Cu^{2+} on OrgBio was decreased (up to 30.50 %) and remarkably so (up to 85.68 %) for MOrgBio, following the simultaneous contact of sorbents with metals and SWW. This implies that even though some of the Cu^{2+} might be removed by other means, the sorption of the biochars was significantly attenuated by the competition of SWW.
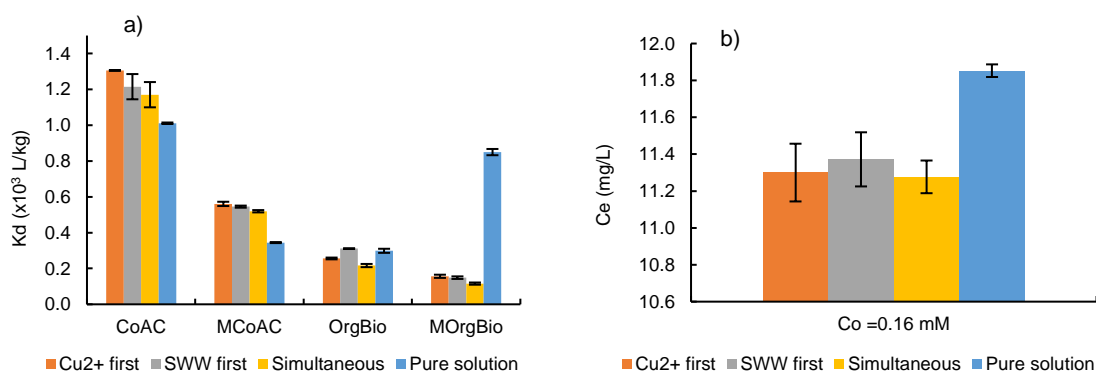
Figure 6.16: Effect of fouling on the sorption of Cu^{2+} on ACs and BCs form mixed equimolar (0.16 mM) solution (a) Cu^{2+} sorption in presence of Pb^{2+} and Zn^{2+}, (b) residual Cu^{2+} concentration in control samples.

It should be noted that the experiment was conducted using high initial concentration (0.16 mM) of metal salt, i.e. a level that has resulted in the near exhaustion of the sorbents' capacities as discussed in 6.3.1. The ACs have exhibited higher sorption of SWW (measured in terms of DOC) compared to the BCs see Figure 6.17(a). It can then be suggested that, surface area might be important in the sorption of Cu^{2+}, in the presence of additional competing organic compounds, at higher concentrations. The sorption of the organic compounds to the general sorption sites on the basal planes and walls of their pores will reduce the pressure on the specific sites where the metal can still occupy with lesser competition. In the case of the BCs, the organic compounds from the SWW will in the absence of sufficient general sorption sites, competed with the Cu^{2+} for

specific sorption sites which resulted in the attenuation of their metal sorption capacity. In addition, the ACs are then more likely to possess ligands from the sorbed organic compounds on their surface which can facilitate the removal of more Cu^{2+} through chelation with the ligands (Juang *et al.*, 1999; Lu *et al.*, 2012). Le Cloirec and Faur-Brasquet (2008), also reported an increase in Cu^{2+} sorption on activated carbon cloth preloaded with benzoic acid. They attributed this increase to the formation of ligand between benzonate ions ($C_6H_5COO^-$) with Cu^{2+}.
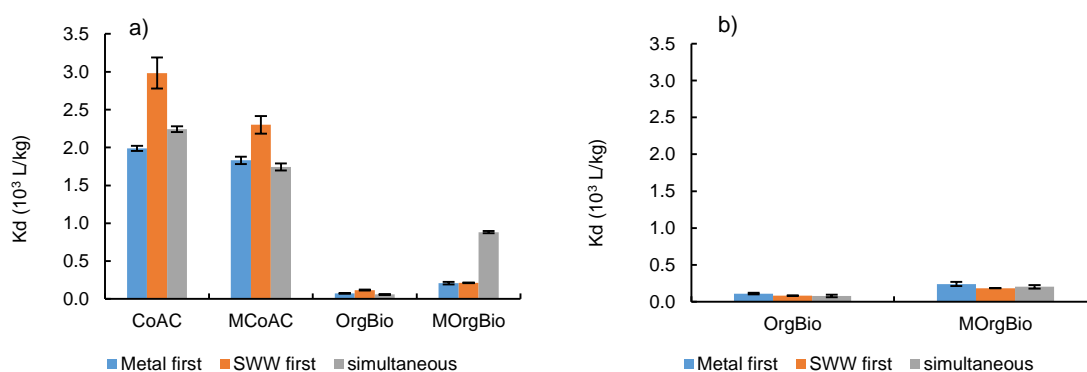
Figure 6.17:   Sorption of SWW (as DOC) on ACs and BCs in presence of (a) mixed equimolar (0.16 mM) solution and (b) Pb^{2+} in single solution (0.16 mM).

For the sorption of Pb^{2+}, in most cases a decrease in sorption capacity was recorded as can be seen in Figure 6.18(a). For the ACs, the highest decrease of about 44.16 % was recorded on CoAC, when the metals and SWW were contacted simultaneously. For the BCs, while a general increase was recorded for OrgBio (up to 143.42 %), a general decrease (up to 92.11 %) was recorded for MOrgBio. Also, from Figure 6.18(b) it can be observed that the equilibrium concentration for control samples of both pure and SWW fouled solution are about the same when the SWW was added first. This means that removal of Pb^{2+} by means of chelation was low and as such, the competing compounds only occupied the sorption sites without necessarily aiding in the removal of Pb^{2+} via chelation. On the other hand, there is a decrease in the equilibrium concentration when metals solution was added first and when both solutions were added simultaneously. This suggests that the sorption of Pb^{2+} on CoAC and MOrgBio is adversely affected by the presence of SWW.
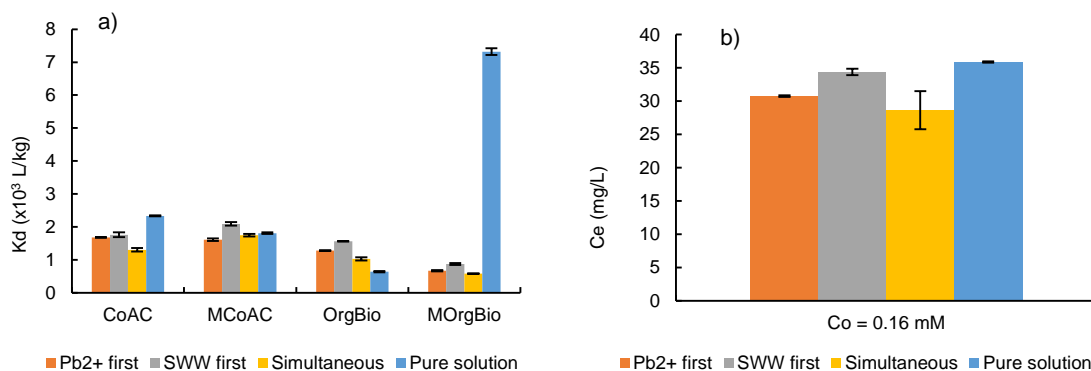
Figure 6.18: Effect of fouling on the sorption of metals on ACs and BCs form mixed equimolar (0.16 mM) solution (a) Pb^{2+} sorption in presence of Pb^{2+} and Zn^{2+}, (b) residual Pb^{2+} concentration in control samples

6.3.7.2 Single Equimolar Solution
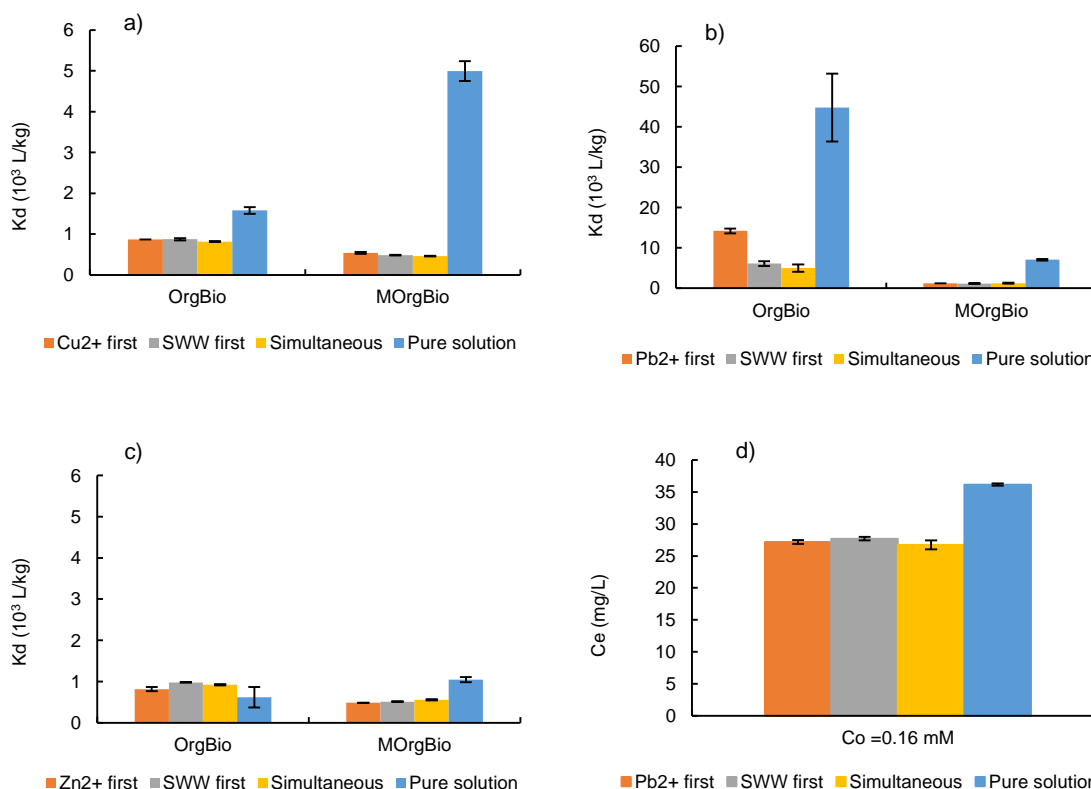
Figure 6.19: Effect of fouling on the sorption of metals on OrgBio & MOrgBio form single equimolar (0.16 mM) solution (a) Cu^{2+}, (b) Pb^{2+} and (c) Zn^{2+} and (d) residual Pb^{2+} concentration in control samples

Similar sorption pattern was observed for the single metals. As presented in Figure 6.19, there is a general decrease (for instance, up to 90.72, 83.34 and 53.55 % for Cu^{2+}, Pb^{2+} and Zn^{2+} on MOrgBio) in the sorption of single metals on the BCs in the presence of SWW. In the case of Pb^{2+} sorption (refer to Figure

6.19(b)), metal chelation is likely to contribute to its removal, since the equilibrium concentration of fouled control samples are lower than that of pure control sample as presented in Figure 6.19 (d). However, this was not sufficient to record an increase in Pb^{2+} removal, instead, a decrease was recorded. The reduction in the performance of MOrgBio is due to competition by compounds in SWW to specific sorption sites, since it was shown to have higher SWW sorption compared to OrgBio (see Figure 6.17(b)). Consequently, OrgBio had more sites available for specific sorption of all the metals and therefore had better performance than MOrgBio.

6.4   SUMMARY

The aim of this chapter is to investigate the behaviour of magnetic carbon composites in the sorption of bivalent metal cations. The results suggest that sorption capacities are influenced by factors that includes the initial concentration of the metal, presence and type of competing compounds, the sorbents' affinity for the metal and the pH of the solution.

Generally, the sorption capacity was found not to be influenced by the sorbents' surface areas or pore volumes. Therefore, activation is not in all cases advantageous, because the biochars have the same or even better sorption of the metals than the activated carbons. The process of magnetisation has been found to be beneficial to the organic biomass biochar. The result clearly showed that the process of magnetisation has the tendency of enhancing the biochar's sorption capacity, even though, the presence of impregnated magnetic iron oxide on the sorbents did not -in most instances- contribute to the uptake of the metals.

At low concentrations, almost all the metals can be sorbed. At higher concentrations, the sorbents appear to be exhausted due to limitation of specific sorption sites. Pb^{2+} is less sensitive to competition from Cu^{2+} and Zn^{2+}, its sorption potential on MOrgBio was maintained irrespective of the presence of the two metals. Generally, the metal's affinity for the sorbets is in the order $Zn^{2+} < Cu^{2+} < Pb^{2+}$. Accordingly, it was deduced that the metals sorption capacity increases with increasing electronegativity, effective ionic radius and decrease in solubility. For this reason, Zn^{2+} was outcompeted by the other two metals at high concentration.

The presence of competitors from the addition of synthetic wastewater enhanced the removal of Cu^{2+} from mixed equimolar metal solution on the activated carbons by up to 62.64 %. The result indicated the possibility of Cu^{2+} removal by other means such as chelation with ligands due to the sorption of SWW on the sorbents. This is attributed to the benefit of sufficient surface area which made the simultaneous sorption of Cu^{2+} and SWW possible. On the other hand, it attenuated the sorption capacities of the biochars by at least 30.50 %. It can be deduced that competing compounds from the SWW occupied the already limited specific sorption sites on the biochars at the expense Cu^{2+}, and they did not facilitate its removal by other means. This attenuation was also observed in the sorption of Pb^{2+} from mixed equimolar metal solution, especially on CoAC and MOrgBio by up to 44.16 and 92.11 % respectively. Similarly, the sorption of all the metals from their single equimolar solution on the biochars, especially MOrgBio, was decreased by up to 90 % due to competition from SWW.

Sorption of the metals from both mixed and single equimolar solution was positively influenced by the solution pH. The result clearly shows that the sorption of the metals is most favourable at higher pH, but not high enough to cause the precipitation of the metals from the solution. In this regard, both magnetite carbon composites and the pristine sorbents exhibited similar response to pH changes.

Finally, the result has shown that the magnetic sorbents can be used to achieve the same level of metal removal in appropriate circumstances. The sorbents can be selected carefully according to the conditions of the wastewater. In situations where there is high concentration of organic compounds, activated carbons are most suitable. The vast surface area of the activated carbons will be available for the removal of a wide range of organic compounds and heavy metals. However, if the wastewater is characterised such that heavy metals exist against a background of low organic compounds, the cost of activation can be save by using biochars, since the advantage of large surface area is not necessarily required in the removal of heavy metals. In both instances, the adsorption can be aided by adjusting the pH of the wastewater to values close to the pH_{PZC} of the sorbents, where optimum sorption is normally possible. Generally, since adsorption is applied as a polishing stage in wastewater treatment, it is expected that the organic content must have been reduced by preceding secondary treatment processes and so the sorbents will be effective in

the removal of both the heavy metals and micropollutnts. In the case higher concentration of DOM, the dosage of the sorbents should be increased to provide enough sorption capacity for both target and competing compounds.

CHAPTER 7.   CONCLUSION

7.1 SUMMARY

Magnetic activated carbons and biochars were successfully produced and used in the treatment of the target pollutants from aqueous solutions, synthetic and real wastewaters. Sorption experimental data was effectively simulated using rigorous mathematical modelling. It is strongly believed that the modelling results are highly representative of the experimental data. The results clearly indicated that the sorption of organic compounds depends on the carbon content in the magnetic carbon composites. In general, the performances of the magnetic sorbents compares favourably (in some instances performs even better) with those of their corresponding pristine pairs, in terms of sorption isotherms, kinetics and response to solution chemistry and temperature. Mostly, appreciable sorption of phenol, diclofenac, ibuprofen and bivalent metal cations were recorded, in levels that compare well with what has been reported in literature.

The results from isotherm and kinetic studies obtained from aqueous solutions and SWW represent near ideal scenario. It evaluates the possible interactions that can exist between sorbents and sorbates, i.e. when target compounds do not face severe competition from secondary compounds. This serves as a proof of concept on the feasibility of using magnetised sorbents in the treatment of refinery wastewaters. Notwithstanding however, since each refinery has unique configuration and wastewater characteristics, the results presented herein will only approximate performance of the sorbents under similar conditions provided during the experiments. In real wastewaters, there will be a decrease in both sorption capacity and rate of its utilisation due to the effect of competition. This is significant if the wastewaters under consideration have higher concentrations of secondary compounds. Thus, for this technology to be used effectively in the treatment of refinery wastewater, the preceding treatment stages should be capable of providing effluents with characteristics that would facilitate the transfer of target compounds from solution to the surface of the sorbents. It is essential thus that adsorption by magnetic sorbents be applied as a polishing stage when other compounds that could cause a significant infringement in the sorption of target pollutants have been removed by preceding

treatment processes. This is particularly true if normal dosages of these sorbents are to be used or practicable retention times are to be applied as feasible economic situations can permit. This will ensure the success of carbon adsorption in attending to exigencies of producing a final effluent that conforms to environmental requirements as recommended by regulatory agencies.

The decrease in both surface area and micropore volume of the sorbents due to the process of magnetisation has been shown to be largely as a result of lower carbon contents (ca. 36% less) in the magnetic carbon composites. On the other hand however, an increase in both the surface area and micropore volume of the OrgBio was recorded following the magnetisation process. It has been speculated that the highly acidic condition to which the biochar was subjected to during the magnetisation process has led to dissolution of the carbonate deposits in the pores thereby creating additional pore spaces. This suggests that the magnetisation process can be manipulated such as to increase the surface areas and pore characteristics of the sorbents and ultimately enhance their sorption of target compounds.

In the case of the sorption of bivalent heavy metals, magnetisation appears to be beneficial, because enhanced metal uptake was recorded on some of the sorbents after magnetisation. Since the sorption of metals is due to specific interactions, the pure magnetite did not exhibit good sorption properties. Therefore, the enhancement is more likely to be due to the production of additional active sites on the surface of the sorbent during the process of magnetisation and not due to the presence of magnetite in the composites.

The concentration of certain pollutants encountered in effluents of some refinery units can be very high as has been presented in table 1.1. Also, in some instances, pollutants including phenol and heavy metals can be detected in high concentrations even effluents of secondary treatment units as has been reported in section 2.1. Notwithstanding, the concentrations of organic pollutants used in this study are much higher than those encountered in refinery wastewaters. Particularly, it is expected that the levels of dissolved compounds will be reduced drastically almost close to trace concentration after undergoing biological treatment process, s. Therefore, the results obtained in this study are more appropriate in comparing the behaviour of the magnetic and nonmagnetic

sorbents at high concentration. Hence, nonlinear models are applicable in this concentration range. At low concentrations, the isotherm data is best explained using the linear model, especially, when the impact of competition from other compounds in refinery wastewaters is considered. However, it is still likely that the relative behaviour between corresponding magnetic and nonmagnetic pairs of sorbents used in this study will hold even at low concentrations. For instance the data can be used to assess the relative sorption capacities of corresponding pairs of magnetic and nonmagnetic sorbents for the sorbates investigated.

The influence of competing compounds on the sorption of the target compounds depends on the pollutants under consideration. For organics, even at such high initial concentrations used, there is a general decrease in their sorption due to the presence of competitors. This indicates that they share similar sorption mechanisms with the competing compounds or they are deprived binding to sorption sites due to size exclusions or conditions of solution chemistry that retains them in solution. In real wastewaters, Mailler *et al.* (2016) have reported that the sorption of micropollutants are impacted negatively by DOC competition. Another study has shown that both pore blocking and hydrophobic competition from NOM can impair the sorption of a number of pharmaceuticals (de Ridder *et al.*, 2011). The results of this study therefore can be extended to lower concentrations, and it can thus be concluded that for the organic pollutants to be effectively removed, higher dosages of the carbon sorbents (especially the magnetic composites) need to be applied. In the case of magnetic sorbents, this could lead to higher energy consumption in sorbent separation if induced magnetic separators are used. Therefore to reduce the power consumption, permanent magnets could be used to separate the magnetised sorbents from wastewaters.

For heavy metals, the presence of competing compounds did not impair the uptake of all metals. Although competition takes place among metal species, the sorption of Cu^{2+} on activated carbon seems to be enhanced in the presence of SWW, likely due to its chelation with organic compounds. Therefore, the removal of such metal from refinery wastewaters could be due to both sorption to AC and chelation to organic matter. This will then reduce the load on the AC thereby leaving more sorption sites for the removal of other compounds. The magnetised ACs have much lower sorption of Cu^{2+} compared to their pristine pairs, to achieve

similar sorption level, more amounts need to be used. The sorption of the metals on biochars are generally affected by the presence of competing organic compounds. Their sorption from synthetic wastewater is lower than that from pure solution. Therefore, their removal from refinery wastewater will also be impacted by the DOM present and less removal will be recorded. However, the uptake of these metals on the magnetised and non-magnetised pairs are still comparable. Here also the linear model is more appropriate to use in fitting the isotherm data since the metals exist in low concentrations.

It should be noted that the autoclaving of WWTPE before the introduction of the pharmaceuticals and of course the commencement of sorption process would cause the oxidisation of the organic and metal compounds. This will cause some dissolved species to precipitate and in general have an influence on their sorption characteristics. The experiments were conducted without pH adjustments and the sorbents are expected to have net positive charges. Under such conditions, the sorption of oxidised organics and metals in the autoclaved WWTPE will be impaired due to electrostatic repulsions. This obviously is a deviation from what will be experienced in real refinery effluents, where these compounds exists in non-oxidised form. Therefore, the pharmaceuticals, and by extension similar micropollutants, will be faced with even more competition in such real scenarios.

7.2 FUTURE WORK

The essence of the magnetisation is to facilitate the separation of the sorbents from the treatment matrix. It is vital to establish how resilient the magnetic sorbents are in terms of retaining their magnetic properties, while being subjected to operational procedures necessary during any treatment process. A separate unpublished study presented in appendix C was conducted to have an insight into the versatility of the MBC in the amendment of agricultural soils at laboratory scale. Substantial amount of MBC was retrieved from the soil in the range 72.38 to 98 % of the original mass added to the soil @ 1.2 % (w/w). Although the result is inconclusive -as the biochar was observed to have commingled with other soil materials. Yet it compares favourably with the findings of (Han *et al.*, 2015a), where about 77 % of the added MAC was successfully recovered following laboratory scale amendment of contaminated sediment. In

general, the results suggest that the magnetic sorbents are resilient to operational procedures that are adopted to mix them in and separate them from the soil and sediment matrices. Another study by (Hasan, 2014) also showed that the magnetic sorbents can be reused over several cycles to remove phenol and heavy metals from aqueous solutions and can withstand repeated regeneration using appropriate solvents. These are encouraging results which shows that in the long run, the use of magnetised sorbents will be an economically viable means that can be applied to in the successful treatments of wastewaters and contaminated soils and sediments.

The mechanism of competition should be investigated further, using different levels of sorbate concentrations and wastewaters. This will enable a further understanding of impact of competition by size exclusion, solution chemistry and relative concentrations of target and competing compounds. This will also make it possible to determine whether the removal of target pollutants is by sorption to the surface of the sorbents or by their binding to the DOM present in wastewaters before the sorption. The influence of the nature and concentration of competing DOM on sorption kinetics and isotherms, should be investigated further in compliance to what is normally experienced in practical sense. To obtain comparable background solution chemistry, the WWTPE samples can be sterilised by appropriate membrane filtration procedures.

In this study, the extended duration used in the appraisal of the effect of temperature on the sorption of organic pollutants is not applicable in real wastewater treatment plants. Due to the prolonged period adopted, no significant difference was observed over the temperatures considered. There is the need to further investigate the influence of more levels of temperature over shorter durations. This will enable the assessment of the dominant type of sorption i.e. either due to chemisorption of physisorption of target compounds on the surface of the sorbents.

There is the need for additional investigations to be conducted to further characterise the surface chemistry of the magnetised sorbents in comparison to their pristine pairs. This will help in the evaluation of the presence and concentration of various types of surface functional groups that can influence sorption characteristics of the sorbents with respect to target pollutants.

There is the need to further investigate influence of varied sorbents' surface and solution chemistries on the sorption kinetics. This will shed further lights on the dominant kinetics mechanism as being either due to mass transfer or reaction mechanisms. Also dynamic mass transfer models should be used to evaluate the kinetics data, since they are more representative of the inherent nature of adsorption kinetics that could exist especially over extended durations.

The magnetic sorbents can be synthesised using several methods as outlined previously, with each resulting to a material with different properties. For instance, magnetisation has been found to enhance the metal sorption capacity of biochar. Additional studies should be conducted to optimise the magnetic sorbents' sorption potentials for additional compounds. There is the need to further standardise the procedure so that custom made materials can be produced that can be applied to serve specific purposes. In the case of organic pollutants, the procedure should be optimised such as to have magnetised sorbents with improved surface areas and pore structures. In the case of heavy metals, the procedure should be tailored towards enhancing the concentration and activity of specific sorption sites.

There is need to conduct further tests to specifically assess the potential environmental risk associated with the use magnetic sorbents for the purpose of pollution and control. Through this, best practice guidelines can be developed to ensure the safe and sustainable usage of these sorbents.

REFERENCES

Agegnehu, G., Bass, A.M., Nelson, P.N., Muirhead, B., Wright, G. and Bird, M.I. (2015) 'Biochar and biochar-compost as soil amendments: Effects on peanut yield, soil properties and greenhouse gas emissions in tropical North Queensland, Australia', *Agriculture, Ecosystems & Environment*, 213, pp. 72-85.

Aghav, R.M., Kumar, S. and Mukherjee, S.N. (2011) 'Artificial neural network modeling in competitive adsorption of phenol and resorcinol from water environment using some carbonaceous adsorbents', *Journal of Hazardous Materials*, 2011(67-77).

Ahmaruzzaman, M. and Sharma, D.K. (2005) 'Adsorption of phenols from wastewater', *Journal of Colloid and Interface Science*, 287(1), pp. 14-24.

Ahrer, W., Scherwenk, E. and Buchberger, W. (2001) 'Determination of drug residues in water by the combination of liquid chromatography or capillary electrophoresis with electrospray mass spectrometry', *Journal of Chromatography A*, 910(1), pp. 69-78.

Al-Degs, Y.S., Khraisheh, M.A.M., Allen, S.J. and Ahmad, M.N. (2009) 'Adsorption characteristics of reactive dyes in columns of activated carbon', *Journal of Hazardous Materials*, 165(2009), pp. 944-949.

Al-Zarooni, M. and Elshorbagy, W. (2006) 'Characterization and assessment of Al Ruwais refinery wastewater', *Journal of Hazardous Materials*, A136(2006), pp. 398-405.

Allen, S.J., McKay, G. and Porter, J.F. (2004) 'Adsorption isotherm models for basic dye adsorption by peat in single and binary component systems', *Journal of Colloid and Interface Science*, 280(2), pp. 322-333.

Altmann, J., Zietzschmann, F., Geiling, E.-L., Ruhl, A.S., Sperlich, A. and Jekel, M. (2015) 'Impacts of coagulation on the adsorption of organic micropollutants onto powdered activated carbon in treated domestic wastewater', *Chemosphere*, 125(0), pp. 198-204.

Amuda, O.S., Giwa, A.A. and Bello, I.A. (2007) 'Removal of heavy metal from industrial wastewater using modified activated coconut shell carbon', *Biochemical Engineering Journal*, 36(2), pp. 174-181.

Antunes, M., Esteves, V.I., Guégan, R., Crespo, J.S., Fernandes, A.N. and Giovanela, M. (2012) 'Removal of diclofenac sodium from aqueous solution by Isabel grape bagasse', *Chemical Engineering Journal*, 192, pp. 114-121.

Aravindhan, R., Rao, J.R. and Nair, B.U. (2009) 'Application of a chemically modified green macro alga as a biosorbent for phenol removal', *Journal of Environmental Management*, 90(5), pp. 1877-1883.

Armenante, P.M. (2009a) *Adsorption*. CHE 685 Industrial Waste Control: Physical and Chemical Treatment lecture notes, New Jersey Institute of Technology.

Atkinson, C.J., Fitzgerald, J.D. and Hipps, N.A. (2010) 'Potential mechanisms for achieving agricultural benefits from biochar application to temperate soils: a review', *Plant and Soil*, 337(1), pp. 1-18.

Audry, S., Schäfer, J., Blanc, G. and Jouanneau, J.-M. (2004) 'Fifty-year sedimentary record of heavy metal pollution (Cd, Zn, Cu, Pb) in the Lot River reservoirs (France)', *Environmental Pollution*, 132(3), pp. 413-426.

Azizian, S. (2004) 'Kinetic models of sorption: a theoretical analysis', *Journal of colloid and Interface Science*, 276(1), pp. 47-52.

Baccar, R., Sarrà, M., Bouzid, J., Feki, M. and Blánquez, P. (2012) 'Removal of pharmaceutical compounds by activated carbon prepared from agricultural by-product', *Chemical Engineering Journal*, 211–212(0), pp. 310-317.

Bajpai, S.K. and Bhowmik, M. (2010) 'Adsorption of diclofenac sodium from aqueous solution using polyaniline as a potential sorbent. I. Kinetic studies', *Journal of Applied Polymer Science*, 117(6), pp. 3615-3622.

Banat, F.A., Al-Bashir, B., Al-Asheh, S. and Hayajneh, O. (2000) 'Adsorption of phenol by bentonite', *Environmental Pollution*, 107(3), pp. 391-398.

Barber, J.T., Sharma, H.A., Ensley, H.E., Polito, M.A. and Thomas, D.A. (1995) 'Detoxification of phenol by the aquatic angiosperm, Lemna gibba', *Chemosphere*, 31(6), pp. 3567-3574.

Belaid, K.D., Kacha, S., Kameche, M. and Derriche, Z. (2013) 'Adsorption kinetics of some textile dyes onto granular activated carbon', *Journal of Environmental Chemical Engineering*, 1(3), pp. 496-503.

Belhateche, D.H. (1995) 'Choose appropriate wastewater treatment technologies', *Chemical Engineering Progress*, pp. Medium: X; Size: pp. 32-51.

Bitton, G., Pancorbo, O. and Gifford, G.E. (1976) 'Factors affecting the adsorption of polio virus to magnetite in water and wastewater', *Water Research*, 10(11), pp. 973-980.

Blair, B.D., Crago, J.P., Hedman, C.J. and Klaper, R.D. (2013) 'Pharmaceuticals and personal care products found in the Great Lakes above concentrations of environmental concern', *Chemosphere*, 93(9), pp. 2116-2123.

Bolto, B.A. (1990) 'Magnetic particle technology for wastewater treatment', *Waste Management*, 10(1), pp. 11-21.

Booker, N.A., Keir, D., Priestley, A.J., Ritchie, C.B., Sudarmana, D.L. and Woods, M.A. (1991) 'Sewage clarification with magnetite particles', *Water Science and Technology*, 23(7-9), pp. 1703-1712.

Boparai, H.K., Joseph, M. and O'Carroll, D.M. (2011) 'Kinetics and thermodynamics of cadmium ion removal by adsorption onto nano zerovalent iron particles', *Journal of Hazardous Materials*, 186(1), pp. 458-465.

Boulinguiez, B., Le Cloirec, P. and Wolbert, D. (2008) 'Revisiting the Determination of Langmuir Parameters · Application to Tetrahydrothiophene Adsorption onto Activated Carbon', *Langmuir*, 24(13), pp. 6420-6424.

Boxall, A.B.A. (2004) 'The environmental side effects of medication', *EMBO reports*, 5(12), pp. 1110-1116.

Brown, M.R., Camézuli, S., Davenport, R.J., Petelenz-Kurdziel, E., Øvreås, L. and Curtis, T.P. (2015) 'Flow cytometric quantification of viruses in activated sludge', *Water Research*, 68, pp. 414-422.

Bull, P.C., Thomas, G.R., Rommens, J.M., Forbes, J.R. and Cox, D.W. (1993) 'The Wilson disease gene is a putative copper transporting P-type ATPase similar to the Menkes gene', *Nat Genet*, 5(4), pp. 327-337.

Bundy, C.A., Wu, D., Jong, M.-C., Edwards, S.R., Ahammad, Z.S. and Graham, D.W. (2017) 'Enhanced denitrification in Downflow Hanging Sponge reactors for decentralised domestic wastewater treatment', *Bioresource Technology*, 226, pp. 1-8.

Burwell, R.L.J. (1976) 'Manual of Symbols and Terminology for Physicochemical Quantities and Units-Appendix II', *Pure and Applied Chemistry*, 46, pp. 71-90.

Busca, G., Berardinelli, S., Resini, C. and Arrighi, L. (2008) 'Technologies for the removal of phenol from fluid streams: A short review of recent developments', *Journal of Hazardous Materials*, 160(2–3), pp. 265-288.

Bush, K.E. (1980) 'Refinery Wastewater Treatment and Reuse', in Vincent Cavaseno (ed.) *Industrial Wastewater and Solid Waste Engineering*. New York: McGraw-Hill Publications Co.

Cabrita, I., Ruiz, B., Mestre, A.S., Fonseca, I.M., Carvalho, A.P. and Ania, C.O. (2010) 'Removal of an analgesic using activated carbons prepared from urban and industrial residues', *Chemical Engineering Journal*, 163(3), pp. 249-255.

Calvet, R. (1989) 'Adsorption of organic chemicals in soils', *Environmental Health Perspectives*, 83, pp. 145-177.

Cameron Carbon Incorporated (2006) *Activated Carbon Manufacture Structure and Properties*. Available at: http://www.cameroncarbon.com/documents/carbon_structure.pdf (Accessed: 24-10-2012).

Cantrell, K.J., Serne, R.J. and Last, G.V. (2002) *Applicability of the linear sorption isotherm model to represent contaminant transport processes in site-wide performance assessments* (PNNL-14576). Pacific Northwest National Laboratory: U.S. Department of Energy.

Cao, X., Ma, L., Gao, B. and Harris, W. (2009) 'Dairy-Manure Derived Biochar Effectively Sorbs Lead and Atrazine', *Environmental Science & Technology*, 43(9), pp. 3285-3291.

Carlos, L., Mártire, D.O., Einschlag, F.S.G. and González, M.C. (2013) 'Applications of magnetite nanoparticles for heavy metal removal from wastewater', in Einschlag, F.S.G. and Carlos, L. (eds.) *Wastewater Treatment Technologies and Recent Analytical Developments*. Croatia: INTECH Open Access Publisher.

Carrott, P.J.M., Carrott, M.M.L.R., Nabais, J.M.V. and Ramalho, J.P.P. (1997) 'Influence of surface ionization on the adsorption of aqueous zinc species by activated carbons', *Carbon*, 35(3), pp. 403-410.

Castro, C.S., Guerreiro, M.C., Gonçalves, M., Oliveira, L.C.A. and Anastácio, A.S. (2009) 'Activated carbon/iron oxide composites for the removal of atrazine from aqueous medium', *Journal of Hazardous Materials*, 164(2–3), pp. 609-614.

Çeçen, F. and Aktas, Ö. (2011) *Activated carbon for water and wastewater treatment: Integration of adsorption and biological treatment*. John Wiley & Sons.

Celis, R., Hermosin, M.C. and Cornejo, J. (2000) 'Heavy metal adsorption by functionalized clays', *Environmental Science & Technology*, 34(21), pp. 4593-4599.

Chan, K.Y., Van Zwieten, L., Meszaros, I., Downie, A. and Joseph, S. (2007) 'Agronomic values of greenwaste biochar as a soil amendment', *Soil Research*, 45(8), pp. 629-634.

Chen, B., Chen, Z. and Lv, S. (2011a) 'A novel magnetic biochar efficiently sorbs organic pollutants and phosphate', *Bioresource technology*, 102(2), pp. 716-723.

Chen, D.Z., Zhang, J.X. and Chen, J.M. (2010) 'Adsorption of methyl tert-butyl ether using granular activated carbon: equilibrium and kinetic analysis', *Int. J. Environ. Sci. Tech.*, 7(2), pp. 235-242.

Chen, J., Chen, W. and Zhu, D. (2008) 'Adsorption of Nonionic Aromatic Compounds to Single-Walled Carbon Nanotubes: Effects of Aqueous Solution Chemistry', *Environmental Science & Technology*, 42(19), pp. 7225-7230.

Chen, S., Yue, Q., Gao, B., Li, Q., Xu, X. and Fu, K. (2012) 'Adsorption of hexavalent chromium from aqueous solution by modified corn stalk: A fixed-bed column study', *Bioresource Technology*, 113(2012), pp. 114-120.

Chen, X., Chen, G., Chen, L., Chen, Y., Lehmann, J., McBride, M.B. and Hay, A.G. (2011b) 'Adsorption of copper and zinc by biochars produced from pyrolysis of hardwood and corn straw in aqueous solution', *Bioresource Technology*, 102(19), pp. 8877-8884.

Cheremisinoff, P.N. (2002) *Handbook of Water and Wastewater Treatment Technologies*. Woburn, Massachusetts, United States of America: Butterworth-Heinemann.

Chiou, M.-S. and Li, H.-Y. (2002) 'Equilibrium and kinetic modeling of adsorption of reactive dye on cross-linked chitosan beads', *Journal of Hazardous Materials*, 93(2), pp. 233-248.

Cho, H.-H., Huang, H. and Schwab, K. (2011) 'Effects of Solution Chemistry on the Adsorption of Ibuprofen and Triclosan onto Carbon Nanotubes', *Langmuir*, 27(21), pp. 12960-12967.

Cho, Y.-M., Werner, D., Choi, Y. and Luthy, R.G. (2012) 'Long-term monitoring and modeling of the mass transfer of polychlorinated biphenyls in sediment following pilot-scale in-situ amendment with activated carbon', *Journal of contaminant hydrology*, 129, pp. 25-37.

Chowdhury, S., Mishra, R., Saha, P. and Kushwaha, P. (2011) 'Adsorption thermodynamics, kinetics and isosteric heat of adsorption of malachite green onto chemically modified rice husk', *Desalination*, 265(1–3), pp. 159-168.

Chowdhury, Z.K., Summers, R.S., Westerhoff, G.P., Leto, B.J., Nowack, K.O., Corwin, C.J. and Passantino, L.B. (2013) *Activated carbon: solutions for improving water quality*. American Water Works Association.

Chuah, T.G., Jumasiah, A., Azni, I., Katayon, S. and Thomas, C.S.Y. (2005) 'Rice Husk as a Potentially Low-cost Biosorbent for Heavy Metal and Dye Removal: an overview', *Desalination*, 175, pp. 305-316.

Cleuvers, M. (2004) 'Mixture toxicity of the anti-inflammatory drugs diclofenac, ibuprofen, naproxen, and acetylsalicylic acid', *Ecotoxicology and Environmental Safety*, 59(3), pp. 309-315.

Coelho, A., Castro, A.V., Dezotti, M. and Sant'Anna Jr, G.L. (2006) 'Treatment of petroleum refinery sourwater by advanced oxidation processes', *Journal of Hazardous Materials*, 137(1), pp. 178-184.

Côté, P., Buisson, H., Pound, C. and Arakaki, G. (1997) 'Workshop on Membranes in Drinking Water Production Technical Innovations and Health AspectsImmersed membrane activated sludge for the reuse of municipal wastewater', *Desalination*, 113(2), pp. 189-196.

Coughlin, R.W. and Ezra, F.S. (1968) 'Role of surface acidity in the adsorption of organic pollutants on the surface of carbon', *Environmental Science & Technology*, 2(4), pp. 291-297.

Crini, G. and Badot, P.-M. (2008) 'Application of chitosan, a natural aminopolysaccharide, for dye removal from aqueous solutions by adsorption processes using batch studies: A review of recent literature', *Progress in Polymer Science*, 33(4), pp. 399-447.

Crittenden, J.C., Hand, D.W., Arora, H. and Lykins, B.W. (1987) 'Design Considerations for GAC Treatment of Organic Chemicals', *Journal (American Water Works Association)*, 79(1), pp. 74-82.

Cronje, K.J., Chetty, K., Carsky, M., Sahu, J.N. and Meikap, B.C. (2011) 'Optimization of chromium(VI) sorption potential using developed activated carbon from sugarcane bagasse with chemical activation by zinc chloride', *Desalination*, 275(2011), pp. 276-284.

Dąbrowski, A. (1999) 'Adsorption - its development and application for practical purposes', in Dąbrowski, A. (ed.) *Studies in Surface Science and Catalysis*. Elsevier, pp. 3-68.

Dąbrowski, A. (2001) 'Adsorption—from theory to practice', *Advances in colloid and interface science*, 93(1), pp. 135-224.

Dabrowski, A. and Curie, S. (1999) *Adsorption and its applications in industry and environmental protection*. elsevier Amsterdam.

Dąbrowski, A., Podkościelny, P., Hubicki, Z. and Barczak, M. (2005) 'Adsorption of phenolic compounds by activated carbon—a critical review', *Chemosphere*, 58(8), pp. 1049-1070.

Damaskin, B.B., Petrii, O.A. and Batrakov, V.V. (1971) 'Adsorption of organic compounds on electrodes'.

Daughton, C.G. and Ternes, T.A. (1999) 'Pharmaceuticals and personal care products in the environment: agents of subtle change?', *Environmental health perspectives*, 107(Suppl 6), p. 907.

Davis, C.W. and Di Toro, D.M. (2015) 'Modeling Nonlinear Adsorption to Carbon with a Single Chemical Parameter: A Lognormal Langmuir Isotherm', *Environmental Science & Technology*, 49(13), pp. 7810-7817.

de Ridder, D.J., Verliefde, A.R.D., Heijman, S.G.J., Verberk, J.Q.J.C., Rietveld, L.C., van der Aa, L.T.J., Amy, G.L. and van Dijk, J.C. (2011) 'Influence of natural organic matter on equilibrium adsorption of neutral and charged pharmaceuticals onto activated carbon', *Water Science and Technology*, 63(3), pp. 416-423.

Dearing, J. (1999) *Environmental Magnetic Susceptibility - Using the Bartington MS2 System*.

Diya'uddeen, B.H., Daud, W.M.A.W. and Abdul Aziz, A.R. (2011) 'Treatment technologies for petroleum refinery effluents: A review', *Process Safety and Environmental Protection*, 89(2), pp. 95-105.

Dubey, S.P., Dwivedi, A.D., Sillanpää, M. and Gopal, K. (2010) 'Artemisia vulgaris-derived mesoporous honeycomb-shaped activated carbon for ibuprofen adsorption', *Chemical Engineering Journal*, 165(2), pp. 537-544.

Dubinin, M.M. and Astakhov, V.A. (1971) 'Development of the concepts of volume filling of micropores in the adsorption of gases and vapors by microporous adsorbents', *Bulletin of the Academy of Sciences of the USSR, Division of chemical science*, 20(1), pp. 3-7.

Durán-Álvarez, J.C., Prado-Pano, B. and Jiménez-Cisneros, B. (2012) 'Sorption and desorption of carbamazepine, naproxen and triclosan in a soil irrigated with raw wastewater: Estimation of the sorption parameters

by considering the initial mass of the compounds in the soil', *Chemosphere*, 88(1), pp. 84-90.

Ebie, K., Li, F., Azuma, Y., Yuasa, A. and Hagishita, T. (2001) 'Pore distribution effect of activated carbon in adsorbing organic micropollutants from natural water', *Water Research*, 35(1), pp. 167-179.

Eichbaum, K., Brinkmann, M., Buchinger, S., Reifferscheid, G., Hecker, M., Giesy, J.P., Engwall, M., van Bavel, B. and Hollert, H. (2014) 'In vitro bioassays for detecting dioxin-like activity — Application potentials and limits of detection, a review', *Science of The Total Environment*, 487(0), pp. 37-48.

El-Naas, M.H., Al-Zuhair, S. and Abu Alhaija, M. (2010) 'Removal of phenol from petroleum refinery wastewater through adsorption on date-pit activated carbon', *Chemical Engineering Journal*, 162(3).

Ellis, J.B. (2006) 'Pharmaceutical and personal care products (PPCPs) in urban receiving waters', *Environmental Pollution*, 144(1), pp. 184-189.

Elskens, M., Pussemier, L., Dumortier, P., Van Langenhove, K., Scholl, G., Goeyens, L. and Focant, J.F. (2013) 'Dioxin levels in fertilizers from Belgium: Determination and evaluation of the potential impact on soil contamination', *Science of The Total Environment*, 454–455(0), pp. 366-372.

EPA (1979) *Activated Carbon Treatment of Industrial Wastewaters : Selected Technical Papers* [Online]. Available at: https://nepis.epa.gov/Exe/ZyPURL.cgi?Dockey=91018DOV.txt (Accessed: 30/12/2016).

EPA (2002) *FEDERAL WATER POLLUTION CONTROL ACT*. [Online]. Available at: http://www.epw.senate.gov/water.pdf (Accessed: 18/08/2016).

EPA (2013) *40 CFR Part 419: PETROLEUM REFINING POINT SOURCE CATEGORY*. [Online]. Available at: https://www.gpo.gov/fdsys/pkg/CFR-2013-title40-vol30/xml/CFR-2013-title40-vol30-part419.xml (Accessed: 23/08/2016).

EPA (2014) *40 CFR Part 423, Appendix A, Priority Pollutant List*. [Online]. Available at: https://www.epa.gov/eg/toxic-and-priority-pollutants-under-clean-water-act#toxic (Accessed: 17/08/2016).

EPA (2015) *40 CFR Part 439: PHARMACEUTICAL MANUFACTURING POINT SOURCE CATEGORY*. [Online]. Available at: https://www.gpo.gov/fdsys/pkg/CFR-2015-title40-vol30/xml/CFR-2015-title40-vol30-part439.xml (Accessed: 23/08/2016).

Escwa, U.N. (2010) 'Waste-Water Treatment Technologies–A General Review'. UN ESCWA. http://www. escwa. un. org/information/publications/edit/upload/sdpd-03-6. pdf accessed.

Essandoh, M., Kunwar, B., Pittman Jr, C.U., Mohan, D. and Mlsna, T. (2015) 'Sorptive removal of salicylic acid and ibuprofen from aqueous solutions using pine wood fast pyrolysis biochar', *Chemical Engineering Journal*, 265, pp. 219-227.

European Commission (2000) *Directive 2000/60/EC of the European Parliament and of the Council of 23 October 2000 establishing a framework for Community action in the field of water policy*.

European Commission (2001) *Directive 2000/60/EC Priority Substances*. [Online]. Available at: http://ec.europa.eu/environment/water/water-dangersub/lib_pri_substances.htm#Dcsn2455_docs (Accessed: 17/08/2016).

Everett, D.H. (1972) 'Manual of symbols and terminology for physicochemical quantities and units, appendix II: Definitions, terminology and symbols in colloid and surface chemistry', *Pure and Applied Chemistry*, 31(4), pp. 577-638.

Fairbairn, D.J., Karpuzcu, M.E., Arnold, W.A., Barber, B.L., Kaufenberg, E.F., Koskinen, W.C., Novak, P.J., Rice, P.J. and Swackhamer, D.L. (2015) 'Sediment–water distribution of contaminants of emerging concern in a mixed use watershed', *Science of The Total Environment*, 505(0), pp. 896-904.

Fan, F.-L., Qin, Z., Bai, J., Rong, W.-D., Fan, F.-Y., Tian, W., Wu, X.-L., Wang, Y. and Zhao, L. (2012) 'Rapid removal of uranium from aqueous solutions using magnetic Fe3O4@SiO2 composite particles', *Journal of Environmental Radioactivity*, 106, pp. 40-46.

Fang, H.H.P. and Chan, O.-C. (1997) 'Toxicity of phenol towards anaerobic biogranules', *Water Research*, 31(9), pp. 2229-2242.

Farré, M.l., Ferrer, I., Ginebreda, A., Figueras, M., Olivella, L., Tirapu, L., Vilanova, M. and Barceló, D. (2001) 'Determination of drugs in surface water and wastewater samples by liquid chromatography–mass spectrometry: methods and preliminary results including toxicity studies with Vibrio fischeri', *Journal of Chromatography A*, 938(1–2), pp. 187-197.

Faur-Brasquet, C., Reddad, Z., Kadirvelu, K. and Le Cloirec, P. (2002) 'Modeling the adsorption of metal ions (Cu2+, Ni2+, Pb2+) onto ACCs using surface complexation models', *Applied Surface Science*, 196(1–4), pp. 356-365.

Federation, W.E. (2008) *Industrial Wastewater Management, Treatment, and Disposal, 3e MOP FD-3*. McGraw-Hill Education.

Ferrari, B.t., Paxéus, N., Giudice, R.L., Pollio, A. and Garric, J. (2003) 'Ecotoxicological impact of pharmaceuticals found in treated wastewaters: study of carbamazepine, clofibric acid, and diclofenac', *Ecotoxicology and Environmental Safety*, 55(3), pp. 359-370.

Fierro, V., Torné-Fernández, V., Montané, D. and Celzard, A. (2008) 'Adsorption of phenol onto activated carbons having different textural and surface properties', *Microporous and Mesoporous Materials*, 111(1–3), pp. 276-284.

Figueiredo, J.L., Mahata, N., Pereira, M.F.R., Sanchez, M.M.J., Montero, J. and Salvador, F. (2011) 'Adsorption of phenol on supercritically activated

carbon fibres: Effect of texture and surface chemistry', *Journal of Colloid and Interface Science*, 357(2011), pp. 210-214.

Foo, K.Y. and Hameed, B.H. (2010) 'Insights into the modeling of adsorption isotherm systems', *Chemical Engineering Journal*, 156(1), pp. 2-10.

Foo, K.Y. and Hameed, B.H. (2012) 'Coconut husk derived activated carbon via microwave induced activation: effects of activation agents, preparation parameters and adsorption performance', *Chemical Engineering Journal*, 184, pp. 57-65.

Freundlich, H.M.F. (1906) 'Over the adsorption in solution', *J. Phys. Chem*, 57(385), p. e470.

Gamage McEvoy, J. and Zhang, Z. (2014) 'Synthesis and characterization of magnetically separable Ag/AgCl–magnetic activated carbon composites for visible light induced photocatalytic detoxification and disinfection', *Applied Catalysis B: Environmental*, 160–161, pp. 267-278.

García-Mateos, F.J., Ruiz-Rosas, R., Marqués, M.D., Cotoruelo, L.M., Rodríguez-Mirasol, J. and Cordero, T. (2015) 'Removal of paracetamol on biomass-derived activated carbon: Modeling the fixed bed breakthrough curves using batch adsorption experiments', *Chemical Engineering Journal*, 279(0), pp. 18-30.

Gergova, K., Petrov, N. and Eser, S. (1994) 'Adsorption properties and microstructure of activated carbons produced from agricultural by-products by steam pyrolysis', *Carbon*, 32(4), pp. 693-702.

Ghosh, U., Luthy, R.G., Cornelissen, G., Werner, D. and Menzie, C.A. (2011) 'In-situ sorbent amendments: a new direction in contaminated sediment management', *Environmental Science & Technology*, 45(4), pp. 1163-1168.

Giles, C.H., Smith, D. and Huitson, A. (1974) 'A general treatment and classification of the solute adsorption isotherm. I. Theoretical', *Journal of Colloid and Interface Science*, 47(3), pp. 755-765.

Giraldo, L. and Moreno-Piraján, J.C. (2014) 'Study of adsorption of phenol on activated carbons obtained from eggshells', *Journal of Analytical and Applied Pyrolysis*, 106(0), pp. 41-47.

Girginova, P.I., Daniel-da-Silva, A.L., Lopes, C.B., Figueira, P., Otero, M., Amaral, V.S., Pereira, E. and Trindade, T. (2010) 'Silica coated magnetite particles for magnetic removal of Hg 2+ from water', *Journal of colloid and interface science*, 345(2), pp. 234-240.

Goldberg, S., Tabatabai, M.A., Sparks, D.L., Al-Amoodi, L. and Dick, W.A. (2005) 'Equations and models describing adsorption processes in soils', *Chemical processes in soils*, pp. 489-517.

Góral, M., Shaw, D.G., Mączyński, A. and Wiśniewska-Gocłowska, B. (2011) 'IUPAC-NIST Solubility Data Series. 91. Phenols with Water. Part 2. C8 to C15 Alkane Phenols with Water', *Journal of Physical and Chemical Reference Data*, 40(3), p. 033103.

Gray, N.F. (2004) *Biology of Wastewater Treatment*. Imperial College Press.

Guedidi, H., Reinert, L., Lévêque, J.-M., Soneda, Y., Bellakhal, N. and Duclaux, L. (2013) 'The effects of the surface oxidation of activated carbon, the solution pH and the temperature on adsorption of ibuprofen', *Carbon*, 54(0), pp. 432-443.

Gundogdu, A., Duran, C., Senturk, H.B., Soylak, M., Ozdes, D., Serencam, H. and Imamoglu, M. (2012) 'Adsorption of Phenol from Aqueous Solution on a Low-Cost Activated Carbon Produced from Tea Industry Waste: Equilibrium, Kinetic, and Thermodynamic Study', *Journal of Chemical & Engineering Data*, 57(2012), pp. 2733-2743.

Gupta, V.K., Nayak, A., Agarwal, S. and Tyagi, I. (2014) 'Potential of activated carbon from waste rubber tire for the adsorption of phenolics: Effect of pre-treatment conditions', *Journal of colloid and interface science*, 417, pp. 420-430.

Haderlein, S.B. and Schwarzenbach, R.P. (1993) 'Adsorption of substituted nitrobenzenes and nitrophenols to mineral surfaces', *Environmental Science & Technology*, 27(2), pp. 316-326.

Hale, J.H., Myers, L.H. and Short Jr., T.E. (1979) 'Pilot Plant Activated Carbon Treatment of Petroleum Refinery Wastewater', *EPA-600/2-79-177: Activated Carbon Treatment of Industrial Wastewater-Selected technical papers*, pp. 111-133.

Hall, K.R., Eagleton, L.C., Acrivos, A. and Vermeulen, T. (1966) 'Pore- and Solid-Diffusion Kinetics in Fixed-Bed Adsorption under Constant-Pattern Conditions', *Industrial & Engineering Chemistry Fundamentals*, 5(2), pp. 212-223.

Hallare, A.V., Köhler, H.R. and Triebskorn, R. (2004) 'Developmental toxicity and stress protein responses in zebrafish embryos after exposure to diclofenac and its solvent, DMSO', *Chemosphere*, 56(7), pp. 659-666.

Hamdaoui, O. and Naffrechoux, E. (2007a) 'Modeling of adsorption isotherms of phenol and chlorophenols onto granular activated carbon: Part I. Two-parameter models and equations allowing determination of thermodynamic parameters', *Journal of Hazardous materials*, 147(1), pp. 381-394.

Hamdaoui, O. and Naffrechoux, E. (2007b) 'Modeling of adsorption isotherms of phenol and chlorophenols onto granular activated carbon: Part II. Models with more than two parameters', *Journal of Hazardous Materials*, 147(1–2), pp. 401-411.

Hameed, B.H. and Rahman, A.A. (2008) 'Removal of phenol from aqueous solutions by adsorption onto activated carbon prepared from biomass material', *Journal of Hazardous Materials*, 160(2–3), pp. 576-581.

Han, R., Zhang, J., Han, P., Wang, Y., Zhao, Z. and Tang, M. (2009) 'Study of equilibrium, kinetic and thermodynamic parameters about methylene blue adsorption onto natural zeolite', *Chemical Engineering Journal*, 145(3), pp. 496-504.

Han, S., Choi, K., Kim, J., Ji, K., Kim, S., Ahn, B., Yun, J., Choi, K., Khim, J.S., Zhang, X. and Giesy, J.P. (2010) 'Endocrine disruption and consequences of chronic exposure to ibuprofen in Japanese medaka (Oryzias latipes) and freshwater cladocerans Daphnia magna and Moina macrocopa', *Aquatic Toxicology*, 98(3), pp. 256-264.

Han, S., Zhao, F., Sun, J., Wang, B., Wei, R. and Yan, S. (2013a) 'Removal of p-nitrophenol from aqueous solution by magnetically modified activated carbon', *Journal of Magnetism and Magnetic Materials*, 341(0), pp. 133-137.

Han, Y., Boateng, A.A., Qi, P.X., Lima, I.M. and Chang, J. (2013b) 'Heavy metal and phenol adsorptive properties of biochars from pyrolyzed switchgrass and woody biomass in correlation with surface properties', *Journal of Environmental Management*, 118(0), pp. 196-204.

Han, Z., Sani, B., Akkanen, J., Abel, S., Nybom, I., Karapanagioti, H.K. and Werner, D. (2015a) 'A critical evaluation of magnetic activated carbon's potential for the remediation of sediment impacted by polycyclic aromatic hydrocarbons', *Journal of Hazardous Materials*, 286(0), pp. 41-47.

Han, Z., Sani, B., Mrozik, W., Obst, M., Beckingham, B., Karapanagioti, H.K. and Werner, D. (2015b) 'Magnetite impregnation effects on the sorbent properties of activated carbons and biochars', *Water Research*, 70(0), pp. 394-403.

Harris, P.J.F., Liu, Z. and Suenaga, K. (2008) 'Imaging the atomic structure of activated carbon', *Journal of physics: Condensed matter*, 20(36), p. 362201.

Hasan, M.B. (2014) *Wastewater treatment with magnetic activated carbon*. MSc Dissertation thesis. Newcastle Univeristy.

He, J., Hong, S., Zhang, L., Gan, F. and Ho, Y.-S. (2010) 'Equilibrium and thermodynamic parameters of adsorption of methylene blue onto rectorite', *Fresenius Environmental Bulletin*, 19(11), pp. 2651-2656.

Heibati, B., Rodriguez-Couto, S., Al-Ghouti, M.A., Asif, M., Tyagi, I., Agarwal, S. and Gupta, V.K. (2015) 'Kinetics and thermodynamics of enhanced adsorption of the dye AR 18 using activated carbons prepared from walnut and poplar woods', *Journal of Molecular Liquids*, 208(0), pp. 99-105.

Henrigton, E.F. (1974) 'Recommended reference materials for the realization of physicochemical properties (recommendation approved 1974)', *Pure Appl. Chem*, 40, pp. 391-450.

Hernando, M.D., Mezcua, M., Fernández-Alba, A.R. and Barceló, D. (2006) 'Environmental risk assessment of pharmaceutical residues in wastewater effluents, surface waters and sediments', *Talanta*, 69(2), pp. 334-342.

Ho, Y.-S. (2003) 'Removal of copper ions from aqueous solution by tree fern', *Water Research*, 37(10), pp. 2323-2330.

Ho, Y.-S. (2004) 'Selection of optimum sorption isotherm', *Carbon*, 42(10), pp. 2115-2116.

Ho, Y.-S. (2006) 'Review of second-order models for adsorption systems', *Journal of Hazardous Materials*, 136(3), pp. 681-689.

Ho, Y.-S., Chiang, T.-H. and Hsueh, Y.-M. (2005a) 'Removal of basic dye from aqueous solution using tree fern as a biosorbent', *Process Biochemistry*, 40(1), pp. 119-124.

Ho, Y.-S., Chiu, W.-T. and Wang, C.-C. (2005b) 'Regression analysis for the sorption isotherms of basic dyes on sugarcane dust', *Bioresource technology*, 96(11), pp. 1285-1291.

Ho, Y.S. and McKay, G. (1998) 'A Comparison of Chemisorption Kinetic Models Applied to Pollutant Removal on Various Sorbents', *Process Safety and Environmental Protection*, 76(4), pp. 332-340.

Ho, Y.S. and McKay, G. (1999) 'Pseudo-second order model for sorption processes', *Process Biochemistry*, 34(5), pp. 451-465.

Ho, Y.S. and McKay, G. (2002) 'Application of kinetic models to the sorption of copper (II) on to peat', *Adsorption Science & Technology*, 20(8), pp. 797-815.

Ho, Y.S., Ng, J.C.Y. and McKay, G. (2000) 'Kinetics of pollutant sorption by biosorbents: Review', *Separation and Purification Methods*, 29(2), pp. 189-232.

Ho, Y.S., Porter, J.F. and McKay, G. (2002) 'Equilibrium isotherm studies for the sorption of divalent metal ions onto peat: copper, nickel and lead single component systems', *Water, Air, and Soil Pollution*, 141(1-4), pp. 1-33.

Hochuli, E., Döbeli, H. and Schacher, A. (1987) 'New metal chelate adsorbent selective for proteins and peptides containing neighbouring histidine residues', *Journal of Chromatography A*, 411, pp. 177-184.

Hsieh, C.-T. and Teng, H. (2000) 'Influence of mesopore volume and adsorbate size on adsorption capacities of activated carbons in aqueous solutions', *Carbon*, 38(6), pp. 863-869.

Hu, J., Chen, G. and Lo, I.M.C. (2005) 'Removal and recovery of Cr(VI) from wastewater by maghemite nanoparticles', *Water Research*, 39(18), pp. 4528-4536.

Hu, J. and Shipley, H. (2013) 'Regeneration of spent TiO2 nanoparticles for Pb (II), Cu (II), and Zn (II) removal', *Environmental Science and Pollution Research*, 20(8), pp. 5125-5137.

Hua, C., Zhang, R., Li, L. and Zheng, X. (2012) 'Adsorption of phenol from aqueous solutions using activated carbon prepared from crofton weed', *Desalination and Water Treatment*, 37(1-3), pp. 230-237.

Huang, P. and Fuerstenau, D.W. (2001) 'The effect of the adsorption of lead and cadmium ions on the interfacial behavior of quartz and talc', *Colloids*

and Surfaces A: Physicochemical and Engineering Aspects, 177(2–3), pp. 147-156.

Hung, Y.-T., Wang, L.K. and Shammas, N.K. (2012) *Handbook of environment and waste management: air and water pollution control*. World Scientific.

Indu, N.C., Jayachandran, K. and Shashidhar, S. (2008) 'Biodegredation of Phenol', *African Journal of Biotechnology*, 7(25), pp. 4951-4985.

Inyang, M., Gao, B., Yao, Y., Xue, Y., Zimmerman, A.R., Pullammanappallil, P. and Cao, X. (2012) 'Removal of heavy metals from aqueous solution by biochars derived from anaerobically digested biomass', *Bioresource Technology*, 110(0), pp. 50-56.

Iovino, P., Canzano, S., Capasso, S., Erto, A. and Musmarra, D. (2015) 'A modeling analysis for the assessment of ibuprofen adsorption mechanism onto activated carbons', *Chemical Engineering Journal*, 277, pp. 360-367.

IPIECA (2010) *Petroleum Refining Water/Wastewater Use and Management*. London. [Online]. Available at: http://www.ipieca.org/resources/good-practice/petroleum-refining-water-wastewater-use-and-management/ (Accessed: 28/12/2016).

Islas-Flores, H., Gómez-Oliván, L.M., Galar-Martínez, M., García-Medina, S., Neri-Cruz, N. and Dublán-García, O. (2014) 'Effect of ibuprofen exposure on blood, gill, liver, and brain on common carp (Cyprinus carpio) using oxidative stress biomarkers', *Environmental Science and Pollution Research*, 21(7), pp. 5157-5166.

Iwata, H., Saito, K., Furusaki, S., Sugo, T. and Okamoto, J. (1991) 'Adsorption Characteristics of an Immobilized Metal Affinity Membrane', *Biotechnology Progress*, 7(5), pp. 412-418.

Jain, A.K., Gupta, V.K., Bhatnagar, A. and Suhas (2003) 'Utilization of industrial waste products as adsorbents for the removal of dyes', *Journal of Hazardous Materials*, 101(1), pp. 31-42.

Järup, L. (2003) 'Hazards of heavy metal contamination', *British Medical Bulletin*, 68(1), pp. 167-182.

Järup, L., Hellström, L., Alfvén, T., Carlsson, M.D., Grubb, A., Persson, B., Pettersson, C., Spång, G., Schütz, A. and Elinder, C.-G. (2000) 'Low level exposure to cadmium and early kidney damage: the OSCAR study', *Occupational and Environmental Medicine*, 57(10), pp. 668-672.

Jasper, A., Salih, H.H., Sorial, G.A., Sinha, R., Krishnan, R. and Patterson, C.L. (2010) 'Impact of nanoparticles and natural organic matter on the removal of organic pollutants by activated carbon adsorption', *Environmental Engineering Science*, 27(1), pp. 85-93.

Jiang, T., Liang, Y.-d., He, Y.-j. and Wang, Q. (2015) 'Activated carbon/NiFe2O4 magnetic composite: A magnetic adsorbent for the adsorption of

methyl orange', *Journal of Environmental Chemical Engineering*, 3(3), pp. 1740-1751.

Jing, X.-R., Wang, Y.-Y., Liu, W.-J., Wang, Y.-K. and Jiang, H. (2014) 'Enhanced adsorption performance of tetracycline in aqueous solutions by methanol-modified biochar', *Chemical Engineering Journal*, 248(0), pp. 168-174.

Jolliffe, H.G. and Gerogiorgis, D.I. (2015) *Proceedings of the Joint 12th International Conference on Process Systems Engineering and 25th European Symposium on Computer-Aided Process Engineering (PSE 2015-ESCAPE 25), Elsevier, Amsterdam*.

Jones, D.L., Rousk, J., Edwards-Jones, G., DeLuca, T.H. and Murphy, D.V. (2012) 'Biochar-mediated changes in soil quality and plant growth in a three year field trial', *Soil Biology and Biochemistry*, 45, pp. 113-124.

JRC (2006) *European Union Risk Assessment Report: Phenol*. Germany: Bundesanstalt für Arbeitsschutz und Arbeitsmedizin (BAuA) [Online]. Available at: https://echa.europa.eu/documents/10162/1ca68f98-878f-4ef6-914a-9f21e9ad2234 (Accessed: 17/08/2016).

JRC (2010) *European Union Risk Assessment Report: Zinc Metal*. The Netherlands. [Online]. Available at: https://echa.europa.eu/documents/10162/459c413e-164b-4f69-9506-ed2ca97d35f9 (Accessed: 17/08/2016).

Juang, R.-S., Wu, F.-C. and Tseng, R.-L. (1999) 'Adsorption removal of copper(II) using chitosan from simulated rinse solutions containing chelating agents', *Water Research*, 33(10), pp. 2403-2409.

Jung, C., Boateng, L.K., Flora, J.R.V., Oh, J., Braswell, M.C., Son, A. and Yoon, Y. (2015) 'Competitive adsorption of selected non-steroidal anti-inflammatory drugs on activated biochars: Experimental and molecular modeling study', *Chemical Engineering Journal*, 264(0), pp. 1-9.

Jusoh, A., L, S.S., Ali, N. and Noor, M.J.M.M. (2007) 'A simulation study of the removal efficiency of granular activated carbon on cadmium and lead', *Desalination*, 206(2007), pp. 9-16.

Kadirvelu, K., Thamaraiselvi, K. and Namasivayam, C. (2001) 'Removal of heavy metals from industrial wastewaters by adsorption onto activated carbon prepared from an agricultural solid waste', *Bioresource Technology*, 76(1), pp. 63-65.

Kapoor, A. and Yang, R.T. (1989) 'Correlation of equilibrium adsorption data of condensible vapours on porous adsorbents', *Gas Separation & Purification*, 3(4), pp. 187-192.

Kelessidis, A. and Stasinakis, A.S. (2012) 'Comparative study of the methods used for treatment and final disposal of sewage sludge in European countries', *Waste management*, 32(6), pp. 1186-1195.

Kennedy, L.J., Vijaya, J.J., Kayalvizhi, K. and Sekaran, G. (2007) 'Adsorption of Phenol from Aqueous Solutions Using Mesoporous Carbon Prepared

by Two-stage Process', *Chemical Engineering Journal*, 132(2007), pp. 279-287.

Khambhaty, Y., Mody, K., Basha, S. and Jha, B. (2009) 'Kinetics, equilibrium and thermodynamic studies on biosorption of hexavalent chromium by dead fungal biomass of marine Aspergillus niger', *Chemical Engineering Journal*, 145(3), pp. 489-495.

Khan, A.A. and Singh, R.P. (1987) 'Adsorption thermodynamics of carbofuran on Sn (IV) arsenosilicate in H+, Na+ and Ca2+ forms', *Colloids and Surfaces*, 24(1), pp. 33-42.

Kilic, M., Apaydin-Varol, E. and Putun, A.E. (2011) 'Adsorptive removal of phenol from aqueous solutions on activated carbon prepared from tobacco residues: Equilibrium, kinetics and thermodynamics', *Journal of Hazardous Materials*, 189(2011), pp. 397-403.

Kim, B.R., Snoeyink, V.L. and Saunders, F.M. (1976) 'Adsorption of organic compounds by synthetic resins', *Journal (Water Pollution Control Federation)*, pp. 120-133.

Kim, S.H., Shon, H.K. and Ngo, H.H. (2010) 'Adsorption characteristics of antibiotics trimethoprim on powdered and granular activated carbon', *Journal of Industrial and Engineering Chemistry*, 16(3), pp. 344-349.

Kinney, C.A., Furlong, E.T., Werner, S.L. and Cahill, J.D. (2006) 'Presence and distribution of wastewater-derived pharmaceuticals in soil irrigated with reclaimed water', *Environmental Toxicology and Chemistry*, 25(2), pp. 317-326.

Kinniburgh, D.G. (1986) 'General purpose adsorption isotherms', *Environmental Science & Technology*, 20(9), pp. 895-904.

Koeppenkastrop, D. and De Carlo, E.H. (1993) 'Uptake of rare earth elements from solution by metal oxides', *Environmental Science & Technology*, 27(9), pp. 1796-1802.

Kula, I., Uğurlu, M., Karaoğlu, H. and Çelik, A. (2008) 'Adsorption of Cd(II) ions from aqueous solutions using activated carbon prepared from olive stone by ZnCl2 activation', *Bioresource Technology*, 99(3), pp. 492-501.

Kumar, A., Prasad, B. and Mishra, I.M. (2008a) 'Adsorptive removal of acrylonitrile by commercial grade activated carbon: Kinetics, equilibrium and thermodynamics', *Journal of Hazardous Materials*, 152(2008), pp. 589-600.

Kumar, K.V. (2007) 'Optimum sorption isotherm by linear and non-linear methods for malachite green onto lemon peel', *Dyes and Pigments*, 74(3), pp. 595-597.

Kumar, K.V. and Porkodi, K. (2006) 'Relation between some two- and three-parameter isotherm models for the sorption of methylene blue onto lemon peel', *Journal of Hazardous Materials*, 138(3), pp. 633-635.

Kumar, K.V., Porkodi, K. and Rocha, F. (2008b) 'Comparison of various error functions in predicting the optimum isotherm by linear and non-linear

regression analysis for the sorption of basic red 9 by activated carbon', *Journal of hazardous materials*, 150(1), pp. 158-165.

Kumar, K.V. and Sivanesan, S. (2005) 'Comparison of linear and non-linear method in estimating the sorption isotherm parameters for safranin onto activated carbon', *Journal of hazardous materials*, 123(1), pp. 288-292.

Kundu, S., Lee, M.-H., Lee, S.H. and Kang, S.-W. (2013) 'In Situ Homeotropic Alignment of Nematic Liquid Crystals Based on Photoisomerization of Azo-Dye, Physical Adsorption of Aggregates, and Consequent Topographical Modification', *Advanced Materials*, 25(24), pp. 3365-3370.

Kundzewicz, Z.W. (2007) 'Global freshwater resources for sustainable development', *Ecohydrology & Hydrobiology*, 7(2), pp. 125-134.

Kyzas, G.Z., Lazaridis, N.K. and Deliyanni, E.A. (2013) 'Oxidation time effect of activated carbons for drug adsorption', *Chemical Engineering Journal*, 234(0), pp. 491-499.

Lagergren, S. (1898) 'About the theory of so-called adsorption of soluble substances'.

Lahcen, N. and Jean-Luc, D. (2011) 'Water in Fuel Production: oil production and refining', *Panorama 2011*. Paris. IFP Energies Nouvelles 92852 Rueil-Malmaison Cedex - France. Available at: http://www.ifpenergiesnouvelles.com/Research-themes/Eco-efficient-processes/Fuels-production/(language)/eng-GB (Accessed: 17th September, 2014).

Langmuir, I. (1918) 'The adsorption of gases on plane surfaces of glass, mica and platinum', *Journal of the American Chemical society*, 40(9), pp. 1361-1403.

Lanphear, B.P., Hornung, R., Khoury, J., Yolton, K., Baghurst, P., Bellinger, D.C., Canfield, R.L., Dietrich, K.N., Bornschein, R., Greene, T., Rothenberg, S.J., Needleman, H.L., Schnaas, L., Wasserman, G., Graziano, J. and Roberts, R. (2005) 'Low-Level Environmental Lead Exposure and Children's Intellectual Function: An International Pooled Analysis', *Environmental Health Perspectives*, 113(7), pp. 894-899.

Lataye, D.H., Mishra, I.M. and Mall, I.D. (2006) 'Removal of pyridine from aqueous solution by adsorption on bagasse fly ash', *Industrial & engineering chemistry research*, 45(11), pp. 3934-3943.

Lazar, P., Karlický, F.e., Jurečka, P., Kocman, M.s., Otyepková, E., Šafářová, K.r. and Otyepka, M. (2013) 'Adsorption of small organic molecules on graphene', *Journal of the American Chemical Society*, 135(16), pp. 6372-6377.

Le Cloirec, P. and Faur-Brasquet, C. (2008) 'Chapter Twentyfour - Adsorption of Inorganic Species from Aqueous Solutions', in *Adsorption by Carbons*. Amsterdam: Elsevier, pp. 631-651.

Lee, Y., Kwon, D.-G., Kim, G. and Kwon, Y.-K. (2016) 'Ab initio Study of Aspirin Adsorption on Single-walled Carbon and Carbon Nitride Nanotubes', *arXiv preprint arXiv:1604.05515*.

Lehmann, J. and Joseph, S. (2009) *Biochar for Environmental Management: Science and Technology*. Earthscan.

Lekkerkerker-Teunissen, K., Benotti, M.J., Snyder, S.A. and van Dijk, H.C. (2012) 'Transformation of atrazine, carbamazepine, diclofenac and sulfamethoxazole by low and medium pressure UV and UV/H2O2 treatment', *Separation and Purification Technology*, 96, pp. 33-43.

Leyva Ramos, R., Bernal Jacome, L.A., Mendoza Barron, J., Fuentes Rubio, L. and Guerrero Coronado, R.M. (2002) 'Adsorption of zinc(II) from an aqueous solution onto activated carbon', *Journal of Hazardous Materials*, 90(1), pp. 27-38.

Li, H., Zhang, D., Han, X. and Xing, B. (2014) 'Adsorption of antibiotic ciprofloxacin on carbon nanotubes: pH dependence and thermodynamics', *Chemosphere*, 95, pp. 150-155.

Li, J., Jiang, L., Liu, X. and Lv, J. (2013) 'Adsorption and aerobic biodegradation of four selected endocrine disrupting chemicals in soil–water system', *International Biodeterioration & Biodegradation*, 76(0), pp. 3-7.

Li, L., Quinlivan, P.A. and Knappe, D.R.U. (2002) 'Effects of activated carbon surface chemistry and pore structure on the adsorption of organic contaminants from aqueous solution', *Carbon*, 40(12), pp. 2085-2100.

Li, Q., Snoeyink, V.L., Mariñas, B.J. and Campos, C. (2003) 'Pore blockage effect of NOM on atrazine adsorption kinetics of PAC: the roles of PAC pore size distribution and NOM molecular weight', *Water Research*, 37(20), pp. 4863-4872.

Lijuan, Z., Dan, M., Guiyun, M., Manman, Z. and H, R. (2011) 'Adsorption of Neutral Red from Solution by Bio-Chars Produced from Pyrolysis of Wheat Straw', *Advanced Materials Research*, 322(2011), pp. 72-76.

Limousin, G., Gaudet, J.P., Charlet, L., Szenknect, S., Barthès, V. and Krimissa, M. (2007) 'Sorption isotherms: A review on physical bases, modeling and measurement', *Applied Geochemistry*, 22(2), pp. 249-275.

Lindqvist, N., Tuhkanen, T. and Kronberg, L. (2005) 'Occurrence of acidic pharmaceuticals in raw and treated sewages and in receiving waters', *Water Research*, 39(11), pp. 2219-2228.

Liu, X. and Pinto, N.G. (1997) 'Ideal adsorbed phase model for adsorption of phenolic compounds on activated carbon', *Carbon*, 35(9), pp. 1387-1397.

Liu, Y. (2009) 'Is the Free Energy Change of Adsorption Correctly Calculated?', *Journal of Chemical & Engineering Data*, 54(7), pp. 1981-1985.

Liu, Z. and Zhang, F.-S. (2009) 'Removal of lead from water using biochars prepared from hydrothermal liquefaction of biomass', *Journal of Hazardous Materials*, 167(1–3), pp. 933-939.

Long, C., Li, A., Wu, H., Liu, F. and Zhang, Q. (2008) 'Polanyi-based models for the adsorption of naphthalene from aqueous solutions onto nonpolar polymeric adsorbents', *Journal of Colloid and Interface Science*, 319(1), pp. 12-18.

Lopez-Ramon, M.V., Stoeckli, F., Moreno-Castilla, C. and Carrasco-Marin, F. (1999) 'On the characterization of acidic and basic surface sites on carbons by various techniques', *Carbon*, 37(8), pp. 1215-1221.

Lorenc-Grabowska, E. and Rutkowski, P. (2014) 'High Adsorption Capacity Carbons from Biomass and Synthetic Polymers for the Removal of Organic Compounds from Water', *Water, Air, & Soil Pollution*, 225(8), pp. 1-10.

Lu, H., Zhang, W., Yang, Y., Huang, X., Wang, S. and Qiu, R. (2012) 'Relative distribution of Pb^{2+} sorption mechanisms by sludge-derived biochar', *Water Research*, 46(3), pp. 854-862.

Lukman, S., Essa, M.H., Mu'azu, N.D., Bukhari, A. and Basheer, C. (2013) 'Adsorption and desorption of heavy metals onto natural clay material: influence of initial pH', *Journal of Environmental Science and Technology*, 6(1), p. 1.

Luo, Y., Guo, W., Ngo, H.H., Nghiem, L.D., Hai, F.I., Zhang, J., Liang, S. and Wang, X.C. (2014) 'A review on the occurrence of micropollutants in the aquatic environment and their fate and removal during wastewater treatment', *Science of The Total Environment*, 473–474(0), pp. 619-641.

Maher, E.S., Amal, H.M. and Mohamed, R. (2012) 'Peanut Biochar as a Stable Adsorbent for Removing NH4-N from Wastewater: A Preliminary Study', *Advances in Environmental Biology*, 6(7), pp. 2170-2176.

Mailler, R., Gasperi, J., Coquet, Y., Derome, C., Buleté, A., Vulliet, E., Bressy, A., Varrault, G., Chebbo, G. and Rocher, V. (2016) 'Removal of emerging micropollutants from wastewater by activated carbon adsorption: Experimental study of different activated carbons and factors influencing the adsorption of micropollutants in wastewater', *Journal of Environmental Chemical Engineering*, 4(1), pp. 1102-1109.

Mailler, R., Gasperi, J., Coquet, Y., Deshayes, S., Zedek, S., Cren-Olivé, C., Cartiser, N., Eudes, V., Bressy, A., Caupos, E., Moilleron, R., Chebbo, G. and Rocher, V. (2015) 'Study of a large scale powdered activated carbon pilot: Removals of a wide range of emerging and priority micropollutants from wastewater treatment plant effluents', *Water Research*, 72(0), pp. 315-330.

Makra, L. and Brimblecombe, P. (2004) 'Selections from the history of environmental pollution, with special attention to air pollution. Part 1', *International journal of environment and pollution*, 22(6), pp. 641-656.

Mandu, I., Bin, G., Ying, Y., Yingwe, X., Andrew, R.Z., Pratap, P. and Xinde, C. (2012) 'Removal of heavy metals from aqueous solution by biochars derived from anaerobically digested biomass', *Bioresource Technology*, 110(2012), pp. 50-56.

Manes, M. and Hofer, L.J.E. (1969) 'Application of the Polanyi adsorption potential theory to adsorption from solution on activated carbon', *The Journal of Physical Chemistry*, 73(3), pp. 584-590.

Margot, J., Kienle, C., Magnet, A., Weil, M., Rossi, L., de Alencastro, L.F., Abegglen, C., Thonney, D., Chèvre, N., Schärer, M. and Barry, D.A. (2013) 'Treatment of micropollutants in municipal wastewater: Ozone or powdered activated carbon?', *Science of The Total Environment*, 461–462(0), pp. 480-498.

Marquardt, D.W. (1963) 'An Algorithm for Least-Squares Estimation of Nonlinear Parameters', *Journal of the Society for Industrial and Applied Mathematics*, 11(2), pp. 431-441.

Marrot, B., Barrios-Martinez, A., Moulin, P. and Roche, N. (2006) 'Biodegredation of High Phenol Concentration by Activated Sludge in an Immersed Membrane Bioreactor', *Biochemical Engineering Journal*, 30, pp. 174-183.

Mattson, J.A., Mark Jr, H.B., Malbin, M.D., Weber Jr, W.J. and Crittenden, J.C. (1969) 'Surface chemistry of active carbon: Specific adsorption of phenols', *Journal of Colloid and Interface Science*, 31(1), pp. 116-130.

Mc Kay, G., Blair, H.S. and Gardner, J. (1983) 'Rate studies for the adsorption of dyestuffs onto chitin', *Journal of Colloid and înterface Science*, 95(1), pp. 108-119.

Mestre, A.S., Pires, J., Nogueira, J.M.F., Parra, J.B., Carvalho, A.P. and Ania, C.O. (2009) 'Waste-derived activated carbons for removal of ibuprofen from solution: Role of surface chemistry and pore structure', *Bioresource Technology*, 100(5), pp. 1720-1726.

Mestre, A.S., Pires, R.A., Aroso, I., Fernandes, E.M., Pinto, M.L., Reis, R.L., Andrade, M.A., Pires, J., Silva, S.P. and Carvalho, A.P. (2014) 'Activated carbons prepared from industrial pre-treated cork: Sustainable adsorbents for pharmaceutical compounds removal', *Chemical Engineering Journal*, 253(0), pp. 408-417.

Metcalf & Eddy Inc, George, T., Franklin, L.B. and David, H.S. (2003) *Wastewater Engineering: Treatment and Reuse*. 4th edn. New York USA: McGraw-Hill Companies Inc.

Metcalf, E., Eddy, H.P. and Tchobanoglous, G. (1991) 'Wastewater engineering: treatment, disposal and reuse', *McGraw-Hill, New York*.

Mikhailovsky, V.L. and Radovenchik, V.M. (1996) 'Water and Wastewater Treatment Using Ferrites', in *Chemical Water and Wastewater Treatment IV*. Springer, pp. 49-60.

Milonjić, S.K. (2007) 'A consideration of the correct calculation of thermodynamic parameters of adsorption', *Journal of the Serbian chemical society*, 72(12), pp. 1363-1367.

Mishra, P.K. and Mukherji, S. (2012) 'Biosorption of diesel and lubricating oil on algal biomass', *3 Biotech*, 2(4), pp. 301-310.

Mohammed, A.S., Kapri, A. and Goel, R. (2011) 'Heavy Metal Pollution: Source, Impact, and Remedies', in Khan, S.M., Zaidi, A., Goel, R. and Musarrat, J. (eds.) *Biomanagement of Metal-Contaminated Soils*. Dordrecht: Springer Netherlands, pp. 1-28.

Mohan, D., Kumar, S. and Srivastava, A. (2014) 'Fluoride removal from ground water using magnetic and nonmagnetic corn stover biochars', *Ecological Engineering*, 73, pp. 798-808.

Mohan, D., Sarswat, A., Singh, V.K., Alexandre-Franco, M. and Pittman Jr., C.U. (2011) 'Development of magnetic activated carbon from almond shells for trinitrophenol removal from water', *Chemical Engineering Journal*, 172(2011), pp. 1111-1125.

Mohan, D. and Singh, K.P. (2005) 'Competitive Adsorption of Several Organics and Heavy Metals on Activated Carbon in Water', in *Water Encyclopedia*. John Wiley & Sons, Inc.

Mohd Din, A.T., Hameed, B.H. and Ahmad, A.L. (2009) 'Batch adsorption of phenol onto physiochemical-activated coconut shell', *Journal of Hazardous Materials*, 161(2–3), pp. 1522-1529.

Moore, B.C., Wang, Y., Cannon, F.S., Metz, D.H. and Westrick, J. (2010) 'Relationships between adsorption mechanisms and pore structure for adsorption of natural organic matter by virgin and reactivated granular activated carbons during water treatment', *Environmental Engineering Science*, 27(2), pp. 187-198.

Moreno-Castilla, C. (2004) 'Adsorption of organic molecules from aqueous solutions on carbon materials', *Carbon*, 42(1), pp. 83-94.

Moreno-Castilla, C. (2008) 'Chapter Twentyfive - Adsorption of Organic Solutes from Dilute Aqueous Solutions', in *Adsorption by Carbons*. Amsterdam: Elsevier, pp. 653-678.

Moreno-Castilla, C., Rivera-Utrilla, J., López-Ramón, M.V. and carrasco-Marín, F. (1995) 'Adsorption of some substituted phenols on activated carbons from a bituminous coal', *Carbon*, 33(6), pp. 845-851.

Muga, H.E. and Mihelcic, J.R. (2008) 'Sustainability of wastewater treatment technologies', *Journal of Environmental Management*, 88(3), pp. 437-447.

Muhtab, A., Sang, S.L., Xiaomin, D., Dinesh, M., Jwa-Kyung, S. and Jae, E.Y. (2012) 'Effects of pyrolysis temperature on soybean stover- and peanut shell-derived biochar properties and TCE adsorption in water', *Bioresource Technology*, 118(2012), pp. 536-544.

Murillo-Torres, R., Durán-Álvarez, J.C., Prado, B. and Jiménez-Cisneros, B.E. (2012) 'Sorption and mobility of two micropollutants in three agricultural soils: A comparative analysis of their behavior in batch and column experiments', *Geoderma*, 189–190(0), pp. 462-468.

Murugesan, A., Vidhyadevi, T., Kirupha, S.D., Ravikumar, L. and Sivanesan, S. (2013) 'Removal of chromium (VI) from aqueous solution using chemically modified corncorb‐activated carbon: Equilibrium and

kinetic studies', *Environmental Progress & Sustainable Energy*, 32(3), pp. 673-680.

Nabzar, L. (2011) *Panorama 2011: Water in fuel production Oil production and refining* France. [Online]. Available at: http://www.iaea.org/inis/collection/NCLCollectionStore/_Public/42/05 0/42050183.pdf?r=1 (Accessed: 18/08/2016).

Nakada, N., Tanishima, T., Shinohara, H., Kiri, K. and Takada, H. (2006) 'Pharmaceutical chemicals and endocrine disrupters in municipal wastewater in Tokyo and their removal during activated sludge treatment', *Water Research*, 40(17), pp. 3297-3303.

Nam, S.-W., Choi, D.-J., Kim, S.-K., Her, N. and Zoh, K.-D. (2014) 'Adsorption characteristics of selected hydrophilic and hydrophobic micropollutants in water using activated carbon', *Journal of Hazardous Materials*, 270(0), pp. 144-152.

Narayanan, V. (2008) 'Synthesis of mesoporous silica microsphere from dual surfactant', *Materials Research*, 11(4), pp. 443-446.

Neal, C., Jarvie, H.P., Whitton, B.A. and Gemmell, J. (2000) 'The water quality of the River Wear, north-east England', *Science of The Total Environment*, 251–252, pp. 153-172.

Nekouei, F., Nekouei, S., Tyagi, I. and Gupta, V.K. (2015) 'Kinetic, thermodynamic and isotherm studies for acid blue 129 removal from liquids using copper oxide nanoparticle-modified activated carbon as a novel adsorbent', *Journal of Molecular Liquids*, 201(0), pp. 124-133.

Nevskaia, D.M., Santianes, A., Muñoz, V. and Guerrero-Ruíz, A. (1999) 'Interaction of aqueous solutions of phenol with commercial activated carbons: an adsorption and kinetic study', *Carbon*, 37(7), pp. 1065-1074.

Newcombe, G. (2008) 'Chapter Twentysix - Adsorption from Aqueous Solutions: Water Purification', in *Adsorption by Carbons*. Amsterdam: Elsevier, pp. 679-709.

Newcombe, G., Drikas, M. and Hayes, R. (1997) 'Influence of characterised natural organic material on activated carbon adsorption: II. Effect on pore volume distribution and adsorption of 2-methylisoborneol', *Water Research*, 31(5), pp. 1065-1073.

Ng, J.C.Y., Cheung, W.H. and McKay, G. (2002) 'Equilibrium studies of the sorption of Cu (II) ions onto chitosan', *Journal of Colloid and Interface Science*, 255(1), pp. 64-74.

Nguyen, T.D., Phan, N.H., Do, M.H. and Ngo, K.T. (2011) 'Magnetic Fe2MO4 (M:Fe, Mn) activated carbons: Fabrication, characterization and heterogeneous Fenton oxidation of methyl orange', *Journal of Hazardous Materials*, 185(2–3), pp. 653-661.

Norit Americas Inc. (2012) *What is Activated Carbon?* Available at: http://www.norit.com/carbon-academy/introduction/ (Accessed: 27 October 2012).

Norouzian, R.-S. and Lakouraj, M.M. (2015) 'Preparation and heavy metal ion adsorption behavior of novel supermagnetic nanocomposite based on thiacalix[4]arene and polyaniline: Conductivity, isotherm and kinetic study', *Synthetic Metals*, 203(0), pp. 135-148.

Nriagu, J.O. (1988) 'A silent epidemic of environmental metal poisoning?', *Environmental Pollution*, 50(1–2), pp. 139-161.

Nriagu, J.O. (1996) 'A History of Global Metal Pollution', *Science*, 272(5259), pp. 223-223.

Nurthumbrian Water (2009) *Upgrade is Far from a Waste*. Available at: https://www.nwl.co.uk/media-centre/611_1407.aspx (Accessed: 26/08/2016).

Ochoa-Herrera, V., León, G., Banihani, Q., Field, J.A. and Sierra-Alvarez, R. (2011) 'Toxicity of copper(II) ions to microorganisms in biological wastewater treatment systems', *Science of The Total Environment*, 412–413, pp. 380-385.

OECD (2010) *Test No. 209: Activated Sludge, Respiration Inhibition Test (Carbon and Ammonium Oxidation)*. OECD Publishing.

Ofomaja, A.E. and Ho, Y.-S. (2007) 'Equilibrium sorption of anionic dye from aqueous solution by palm kernel fibre as sorbent', *Dyes and Pigments*, 74(1), pp. 60-66.

Oliveira, L.C.A., Rios, R.V.R.A., Fabris, J.D., Garg, V., Sapag, K. and Lago, R.M. (2002) 'Activated carbon / iron oxide magnetic composites for the adsorption of contaminants in water', *Carbon*, 40(12), pp. 2177-2183.

Onwumere, B.G. and Oladimeji, A.A. (1990) 'Accumulation of Metals and Histopathology in Oreochromis niloticus Exposed to Treated NNPC Kaduna (Nigeria) Petroleum Refinery Effluent', *Ecotoxicology and Environmental Safety*, 19(2), pp. 123-134.

Otokunefor, T.V. and Obiukwu, C. (2005) 'Impact of Refinery Effluent on the Physicochemical Properties of a Water Body in the Niger Delta', *Applied Ecology and Environmental Research*, 3(1), pp. 67-72.

Özacar, M. and Şengil, İ.A. (2003) 'Adsorption of reactive dyes on calcined alunite from aqueous solutions', *Journal of Hazardous Materials*, 98(1–3), pp. 211-224.

Özkaya, B. (2006) 'Adsorption and desorption of phenol on activated carbon and a comparison of isotherm models', *Journal of Hazardous Materials*, 129(1–3), pp. 158-163.

Pagnanelli, F., Esposito, A., Toro, L. and Vegliò, F. (2003) 'Metal speciation and pH effect on Pb, Cu, Zn and Cd biosorption onto Sphaerotilus natans: Langmuir-type empirical model', *Water Research*, 37(3), pp. 627-633.

Paradelo, R. and Barral, M.T. (2012) 'Evaluation of the potential capacity as biosorbents of two MSW composts with different Cu, Pb and Zn concentrations', *Bioresource Technology*, 104(0), pp. 810-813.

Park, J.-S., Brown, M.T. and Han, T. (2012) 'Phenol toxicity to the aquatic macrophyte Lemna paucicostata', *Aquatic Toxicology*, 106–107, pp. 182-188.

Park, K.-H., Balathanigaimani, M.S., Shim, W.-G., Lee, J.-W. and Moon, H. (2010) 'Adsorption characteristics of phenol on novel corn grain-based activated carbons', *Microporous and Mesoporous Materials*, 127(1–2), pp. 1-8.

Pehlivan, E. and Altun, T. (2006) 'The study of various parameters affecting the ion exchange of Cu2+, Zn2+, Ni2+, Cd2+, and Pb2+ from aqueous solution on Dowex 50W synthetic resin', *Journal of Hazardous Materials*, 134(1–3), pp. 149-156.

Pelekani, C. and Snoeyink, V.L. (1999) 'Competitive adsorption in natural water: role of activated carbon pore size', *Water Research*, 33(5), pp. 1209-1219.

Pelekani, C. and Snoeyink, V.L. (2000) 'Competitive adsorption between atrazine and methylene blue on activated carbon: the importance of pore size distribution', *Carbon*, 38(10), pp. 1423-1436.

Pelekani, C. and Snoeyink, V.L. (2001) 'A kinetic and equilibrium study of competitive adsorption between atrazine and Congo red dye on activated carbon: the importance of pore size distribution', *Carbon*, 39(1), pp. 25-37.

Pellera, F.-M., Giannis, A., Kalderis, D., Anastasiadou, K., Stegmann, R., Wang, J.-Y. and Gidarakos, E. (2012) 'Adsorption of Cu(II) ions from aqueous solutions on biochars prepared from agricultural by-products', *Journal of Environmental Management*, 96(1), pp. 35-42.

Perić, J., Trgo, M. and Vukojević Medvidović, N. (2004) 'Removal of zinc, copper and lead by natural zeolite—a comparison of adsorption isotherms', *Water Research*, 38(7), pp. 1893-1899.

Petropoulos, E., Dolfing, J., Davenport, R.J., Bowen, E.J. and Curtis, T.P. (2016) 'Developing cold-adapted biomass for the anaerobic treatment of domestic wastewater at low temperatures (4, 8 and 15° C) with inocula from cold environments', *Water Research*.

Pholchan, P., Jones, M., Donnelly, T. and Sallis, P.J. (2008) 'Fate of Estrogens during the Biological Treatment of Synthetic Wastewater in a Nitrite-Accumulating Sequencing Batch Reactor', *Environmental Science & Technology*, 42(16), pp. 6141-6147.

Piero, M.A. (2009b) *Adsorption with granular activated carbon (GAC)*. CHE 685 Industrial Waste Control: Physical and Chemical Treatment lecture notes, New Jersey Institute of Technology.

Plum, L.M., Rink, L. and Haase, H. (2010) 'The Essential Toxin: Impact of Zinc on Human Health', *International Journal of Environmental Research and Public Health*, 7(4), p. 1342.

Porter, J.F., McKay, G. and Choy, K.H. (1999) 'The prediction of sorption from a binary mixture of acidic dyes using single-and mixed-isotherm variants

of the ideal adsorbed solute theory', *Chemical Engineering Science*, 54(24), pp. 5863-5885.

Potgieter, J.H. (1991) 'Adsorption of Methylene Blue on Activated Carbon', *Journal of Chemical Education*, 68, pp. 349-350.

Puziy, A.M., Poddubnaya, O.I., Martínez-Alonso, A., Suárez-García, F. and Tascón, J.M.D. (2002) 'Synthetic carbons activated with phosphoric acid: I. Surface chemistry and ion binding properties', *Carbon*, 40(9), pp. 1493-1505.

Pyrzyńska, K. and Bystrzejewski, M. (2010) 'Comparative study of heavy metal ions sorption onto activated carbon, carbon nanotubes, and carbon-encapsulated magnetic nanoparticles', *Colloids and Surfaces A: Physicochemical and Engineering Aspects*, 362(1–3), pp. 102-109.

Qiu, H., Lv, L., Pan, B.-c., Zhang, Q.-j., Zhang, W.-m. and Zhang, Q.-x. (2009) 'Critical review in adsorption kinetic models', *Journal of Zhejiang University Science A*, 10(5), pp. 716-724.

Rai, P., Gautam, R.K., Banerjee, S., Rawat, V. and Chattopadhyaya, M.C. (2015) 'Synthesis and characterization of a novel SnFe 2 O 4@ activated carbon magnetic nanocomposite and its effectiveness in the removal of crystal violet from aqueous solution', *Journal of Environmental Chemical Engineering*, 3(4), pp. 2281-2291.

Rakić, V., Rac, V., Krmar, M., Otman, O. and Auroux, A. (2015) 'The adsorption of pharmaceutically active compounds from aqueous solutions onto activated carbons', *Journal of Hazardous Materials*, 282(0), pp. 141-149.

Ramalho, R. (2012) *Introduction to Wastewater Treatment Processes*. Elsevier Science.

Ranade, V.V. and Bhandari, V.M. (2014) *Industrial wastewater treatment, recycling and reuse*. Butterworth-Heinemann.

Ratnayaka, D.D., Brandt, M.J. and Johnson, M. (2009) *Twort's Water Supply*. 6 edn. Butterworth-Heinemann.

Redlich, O. and Peterson, D.L. (1959) 'A Useful Adsorption Isotherm', *The Journal of Physical Chemistry*, 63(6), pp. 1024-1024.

Rivera-Utrilla, J., Sánchez-Polo, M., Ferro-García, M.Á., Prados-Joya, G. and Ocampo-Pérez, R. (2013) 'Pharmaceuticals as emerging contaminants and their removal from water. A review', *Chemosphere*, 93(7), pp. 1268-1287.

Rodrigues, L.A., da Silva, M.L.C.P., Alvarez-Mendes, M.O., Coutinho, A.d.R. and Thim, G.P. (2011) 'Phenol removal from aqueous solution by activated carbon produced from avocado kernel seeds', *Chemical Engineering Journal*, 174(1), pp. 49-57.

Roop, C.B. and Meenakshi, G. (2005) *Activated Carbon Adsorption*. CRC Press Taylor & Francis Group, Boca Raton, FL 33487-2742, Florida, United States.

Roostaei, N. and Tezel, F.H. (2004) 'Removal of phenol from aqueous solutions by adsorption', *Journal of Environmental Management*, 70(2), pp. 157-164.

Šafařík, I., Nymburská, K. and Šafaříková, M. (1997) 'Adsorption of Water‐Soluble Organic Dyes on Magnetic Charcoal', *Journal of Chemical Technology and Biotechnology*, 69(1), pp. 1-4.

Saiers, J.E. and Hornberger, G.M. (1996) 'Migration of 137Cs through quartz sand: experimental results and modeling approaches', *Journal of Contaminant Hydrology*, 22(3–4), pp. 255-270.

Salame, I.I. and Bandosz, T.J. (2003) 'Role of surface chemistry in adsorption of phenol on activated carbons', *Journal of colloid and interface science*, 264(2), pp. 307-312.

Salman, J.M. and Hameed, B.H. (2010) 'Adsorption of 2,4-dichlorophenoxyacetic acid and carbofuran pesticides onto granular activated carbon', *Desalination*, 256(1–3), pp. 129-135.

Salvestrini, S., Leone, V., Iovino, P., Canzano, S. and Capasso, S. (2014) 'Considerations about the correct evaluation of sorption thermodynamic parameters from equilibrium isotherms', *The Journal of Chemical Thermodynamics*, 68, pp. 310-316.

Sander, M. and Pignatello, J.J. (2005) 'Characterization of Charcoal Adsorption Sites for Aromatic Compounds: Insights Drawn from Single-Solute and Bi-Solute Competitive Experiments', *Environmental Science & Technology*, 39(6), pp. 1606-1615.

Sandrin, T.R. and Maier, R.M. (2003) 'Impact of Metals on the Biodegradation of Organic Pollutants', *Environmental Health Perspectives*, 111(8), pp. 1093-1101.

Sawalha, M.F., Peralta-Videa, J.R., Romero-González, J. and Gardea-Torresdey, J.L. (2006) 'Biosorption of Cd(II), Cr(III), and Cr(VI) by saltbush (Atriplex canescens) biomass: Thermodynamic and isotherm studies', *Journal of Colloid and Interface Science*, 300(1), pp. 100-104.

Schiewer, S. and Volesky, B. (1995) 'Modeling of the Proton-Metal Ion Exchange in Biosorption', *Environmental Science & Technology*, 29(12), pp. 3049-3058.

Schneider, R.M., Cavalin, C.F., Barros, M.A.S.D. and G, T.C.R. (2007) 'Adsorption of chromium ions in activated carbon', *Chemical Engineering Journal*, 132(2007), pp. 355-362.

Schwaiger, J., Ferling, H., Mallow, U., Wintermayr, H. and Negele, R.D. (2004) 'Toxic effects of the non-steroidal anti-inflammatory drug diclofenac: Part I: histopathological alterations and bioaccumulation in rainbow trout', *Aquatic Toxicology*, 68(2), pp. 141-150.

Schwarzenbach, R.P., Gschwend, P.M. and Imboden, D.M. (2005) *Environmental organic chemistry*. John Wiley & Sons.

Scully, C., Collins, G. and O'Flaherty, V. (2006) 'Anaerobic biological treatment of phenol at 9.5–15 °C in an expanded granular sludge bed (EGSB)-based bioreactor', *Water Research*, 40(20), pp. 3737-3744.

Secondes, M.F.N., Naddeo, V., Belgiorno, V. and Ballesteros Jr, F. (2014) 'Removal of emerging contaminants by simultaneous application of membrane ultrafiltration, activated carbon adsorption, and ultrasound irradiation', *Journal of Hazardous Materials*, 264(0), pp. 342-349.

SERI and WU Vienna database: Visualising Global Material Flows (2014). Available at: http://www.materialflows.net/data/datadownload/ (Accessed: 25th January, 2015).

Shi, T., Jia, S., Chen, Y., Wen, Y., Du, C., Guo, H. and Wang, Z. (2009) 'Adsorption of Pb(II), Cr(III), Cu(II), Cd(II) and Ni(II) onto a vanadium mine tailing from aqueous solution', *Journal of Hazardous Materials*, 169(1–3), pp. 838-846.

Shih, T.C., Wangpaichitr, M. and Suffet, M. (2003) 'Evaluation of granular activated carbon technology for the removal of methyl tertiary butyl ether (MTBE) from drinking water', *Water research*, 37(2), pp. 375-385.

Sips, R. (1948) 'On the Structure of a Catalyst Surface', *The Journal of Chemical Physics*, 16(5), pp. 490-495.

Sips, R. (1950) 'On the Structure of a Catalyst Surface. II', *The Journal of Chemical Physics*, 18(8), pp. 1024-1026.

Snoeyink, V.L. and Summers, R.S. (1999) 'Adsorption of Organic Compounds', in Raymond, D.L. (ed.) *Water Quality and Treatment: A Handbook of Community Water Supplies*. Fifth edn. United States of America: McGraw-Hill Inc.

Snoeyink, V.L. and Weber, W.J. (1967) 'The surface chemistry of active carbon; a discussion of structure and surface functional groups', *Environmental Science & Technology*, 1(3), pp. 228-234.

Snoeyink, V.L., Weber, W.J. and Mark, H.B. (1969) 'Sorption of phenol and nitrophenol by active carbon', *Environmental Science & Technology*, 3(10), pp. 918-926.

Song, X., Zhang, Y., Yan, C., Jiang, W. and Chang, C. (2012) 'The Langmuir Monolayer Adsorption Model of Organic Matter into Effective Pores in Activated Carbon', *Journal of Colloid and Interface Science*, 389(2013), pp. 213-219.

Sonune, A. and Ghate, R. (2004) 'Developments in wastewater treatment methods', *Desalination*, 167, pp. 55-63.

Šostar-Turk, S., Petrinić, I. and Simonič, M. (2005) 'Laundry wastewater treatment using coagulation and membrane filtration', *Resources, Conservation and Recycling*, 44(2), pp. 185-196.

Sotelo, J.L., Ovejero, G., Rodríguez, A., Álvarez, S. and García, J. (2013) 'Analysis and modeling of fixed bed column operations on flumequine

removal onto activated carbon: pH influence and desorption studies', *Chemical Engineering Journal*, 228(0), pp. 102-113.

Speight, J.G. (2005) *Lange's handbook of chemistry*. McGraw-Hill New York.

Spokas, K.A., Koskinen, W.C., Baker, J.M. and Reicosky, D.C. (2009) 'Impacts of woodchip biochar additions on greenhouse gas production and sorption/degradation of two herbicides in a Minnesota soil', *Chemosphere*, 77(4), pp. 574-581.

Spokas, K.A. and Reicosky, D.C. (2009) 'Impacts of sixteen different biochars on soil greenhouse gas production', *Ann. Environ. Sci*, 3(1), p. 4.

Srivastava, N.K. and Majumder, C.B. (2008) 'Novel biofiltration methods for the treatment of heavy metals from industrial wastewater', *Journal of hazardous materials*, 151(1), pp. 1-8.

Srivastava, S.K., Pant, N. and Pal, N. (1987) 'Studies on THe Efficiency of a Local Fertiliser Waste as a Low Cost Adsorbate', *Water Research*, 21(11), pp. 1389-1394.

Stover, R.C., Sommers, L.E. and Silviera, D.J. (1976) 'Evaluation of metals in wastewater sludge', *Journal (Water Pollution Control Federation)*, pp. 2165-2175.

Stumpf, M., Ternes, T.A., Wilken, R.-D., Silvana Vianna, R. and Baumann, W. (1999) 'Polar drug residues in sewage and natural waters in the state of Rio de Janeiro, Brazil', *Science of The Total Environment*, 225(1–2), pp. 135-141.

Sun, L., Chen, D., Wan, S. and Yu, Z. (2015) 'Performance, kinetics, and equilibrium of methylene blue adsorption on biochar derived from eucalyptus saw dust modified with citric, tartaric, and acetic acids', *Bioresource Technology*, 198, pp. 300-308.

Sun, Z.-X., Su, F.-W., Forsling, W. and Samskog, P.-O. (1998) 'Surface Characteristics of Magnetite in Aqueous Suspension', *Journal of Colloid and Interface Science*, 197(1), pp. 151-159.

Sundstrom, D.W. and Klei, H.E. (1979) *Wastewater treatment*. Prentice Hall.

Suriyanon, N., Punyapalakul, P. and Ngamcharussrivichai, C. (2013) 'Mechanistic study of diclofenac and carbamazepine adsorption on functionalized silica-based porous materials', *Chemical Engineering Journal*, 214, pp. 208-218.

Tchounwou, P.B., Yedjou, C.G., Patlolla, A.K. and Sutton, D.J. (2012) 'Heavy metal toxicity and the environment', in *Molecular, clinical and environmental toxicology*. Springer, pp. 133-164.

Thomas, G.R., Forbes, J.R., Roberts, E.A., Walshe, J.M. and Cox, D.W. (1995) 'The Wilson disease gene: spectrum of mutations and their consequences', *Nat Genet*, 9(2), pp. 210-217.

Tišler, T. and Zagorc-Končan, J. (1997) 'Comparative assessment of toxicity of phenol, formaldehyde, and industrial wastewater to aquatic organisms', *Water, Air, and Soil Pollution*, 97(3), pp. 315-322.

Tong, X.-j., Li, J.-y., Yuan, J.-h. and Xu, R.-k. (2011) 'Adsorption of Cu(II) by biochars generated from three crop straws', *Chemical Engineering Journal*, 172(2–3), pp. 828-834.

Tonucci, M.C., Gurgel, L.V.A. and Aquino, S.F.d. (2015) 'Activated carbons from agricultural byproducts (pine tree and coconut shell), coal, and carbon nanotubes as adsorbents for removal of sulfamethoxazole from spiked aqueous solutions: Kinetic and thermodynamic studies', *Industrial Crops and Products*, 74(0), pp. 111-121.

Tosun, İ. (2012) 'Ammonium Removal from Aqueous Solutions by Clinoptilolite: Determination of Isotherm and Thermodynamic Parameters and Comparison of Kinetics by the Double Exponential Model and Conventional Kinetic Models', *International Journal of Environmental Research and Public Health*, 9(3), p. 970.

Tschapek, M., Tcheichvili, L. and Wasowski, C. (1974) 'The point of zero charge (pzc) of kaolinite and SiO 2+ Al 2 O 3 mixtures', *Clay Miner*, 10, pp. 219-229.

Tseng, R.-L., Wu, F.-C. and Juang, R.-S. (2003) 'Liquid-phase adsorption of dyes and phenols using pinewood-based activated carbons', *Carbon*, 41(3), pp. 487-495.

van Velsen, A.F.M., van der Vos, G., Boersma, R. and de Reuver, J.L. (1991) 'High Gradient Magnetic Separation Technique for Wastewater Treatment', *Water Science and Technology*, 24(10), pp. 195-203.

Verlicchi, P., Al Aukidy, M. and Zambello, E. (2012) 'Occurrence of pharmaceutical compounds in urban wastewater: Removal, mass load and environmental risk after a secondary treatment—A review', *Science of The Total Environment*, 429, pp. 123-155.

Walker, G.M. and Weatherley, L.R. (2001) 'Adsorption of dyes from aqueous solution — the effect of adsorbent pore size distribution and dye aggregation', *Chemical Engineering Journal*, 83(3), pp. 201-206.

Walker, P.L. (1962) 'Carbon—an old but new material', *American Scientist*, 50(2), pp. 259-293.

Wang, S.-y., Tang, Y.-k., Chen, C., Wu, J.-t., Huang, Z., Mo, Y.-y., Zhang, K.-x. and Chen, J.-b. (2015a) 'Regeneration of magnetic biochar derived from eucalyptus leaf residue for lead (II) removal', *Bioresource technology*, 186, pp. 360-364.

Wang, S.-Y., Tsai, M.-H., Lo, S.-F. and Tsai, M.-J. (2008) 'Effects of manufacturing conditions on the adsorption capacity of heavy metal ions by Makino bamboo charcoal', *Bioresource Technology*, 99(15), pp. 7027-7033.

Wang, S., Gao, B., Li, Y., Mosa, A., Zimmerman, A.R., Ma, L.Q., Harris, W.G. and Migliaccio, K.W. (2015b) 'Manganese oxide-modified biochars: Preparation, characterization, and sorption of arsenate and lead', *Bioresource Technology*, 181(0), pp. 13-17.

Wang, T.-T., Cheng, J., Liu, X.-J., Jiang, W., Zhang, C.-L. and Yu, X.-Y. (2012) 'Effect of biochar amendment on the bioavailability of pesticide chlorantraniliprole in soil to earthworm', *Ecotoxicology and Environmental Safety*, 83(0), pp. 96-101.

Weber, W.J. (1974) 'Adsorption Process', *Pure and Applied Chemistry*, 37(3), pp. 375-392.

Weber, W.J. and Morris, J.C. (1963) 'Kinetics of adsorption on carbon from solution', *Journal of the Sanitary Engineering Division*, 89(2), pp. 31-60.

Wei, H., Deng, S., Huang, Q., Nie, Y., Wang, B., Huang, J. and Yu, G. (2013) 'Regenerable granular carbon nanotubes/alumina hybrid adsorbents for diclofenac sodium and carbamazepine removal from aqueous solution', *Water Research*, 47(12), pp. 4139-4147.

Werner, D., Garratt, J.A. and Pigott, G. (2013) 'Sorption of 2,4-D and other phenoxy herbicides to soil, organic matter, and minerals', *Journal of Soils and Sediments*, 13(1), pp. 129-139.

Wiwid Pranata, P., Azlan, K., Siti Najiah Mohd, Y., Che Fauziah, I., Azmi, M., Norhayati, H. and Illyas Md, I. (2014) 'Biosorption of Cu(II), Pb(II) and Zn(II) Ions from Aqueous Solutions Using Selected Waste Materials: Adsorption and Characterisation Studies', *Journal of Encapsulation and Adsorption Sciences*, Vol.04No.01, p. 11.

Wong, Y.C., Szeto, Y.S., Cheung, W.H. and McKay, G. (2004) 'Adsorption of acid dyes on chitosan—equilibrium isotherm analyses', *Process Biochemistry*, 39(6), pp. 695-704.

Worch, E. (2012) *Adsorption technology in water treatment: Fundamentals, processes, and modeling*. Walter de Gruyter.

WORLD BANK GROUP (1998) 'Pollution Prevention and Abatement Handbook '. The International Bank for Reconstruction and Development/THE WORLD BANK 1818 H Street, N.W. Washington, D.C. 20433, U.S.A.

Wu, F.-C., Liu, B.-L., Wu, K.-T. and Tseng, R.-L. (2010) 'A new linear form analysis of Redlich–Peterson isotherm equation for the adsorptions of dyes', *Chemical Engineering Journal*, 162(1), pp. 21-27.

Wu, F.-C., Tseng, R.-L. and Juang, R.-S. (2001) 'Kinetic modeling of liquid-phase adsorption of reactive dyes and metal ions on chitosan', *Water Research*, 35(3), pp. 613-618.

Wu, W., Yang, K., Chen, W., Wang, W., Zhang, J., Lin, D. and Xing, B. (2016) 'Correlation and prediction of adsorption capacity and affinity of aromatic compounds on carbon nanotubes', *Water Research*, 88, pp. 492-501.

Xia, G. and Ball, W.P. (1999) 'Adsorption-Partitioning Uptake of Nine Low-Polarity Organic Chemicals on a Natural Sorbent', *Environmental Science & Technology*, 33(2), pp. 262-269.

Xiao, F. and Pignatello, J.J. (2014) 'Effect of Adsorption Nonlinearity on the pH–Adsorption Profile of Ionizable Organic Compounds', *Langmuir*, 30(8), pp. 1994-2001.

Xu, T., Lou, L., Luo, L., Cao, R., Duan, D. and Chen, Y. (2012) 'Effect of bamboo biochar on pentachlorophenol leachability and bioavailability in agricultural soil', *Science of The Total Environment*, 414, pp. 727-731.

Xu, X., Cao, X., Zhao, L., Wang, H., Yu, H. and Gao, B. (2013) 'Removal of Cu, Zn, and Cd from aqueous solutions by the dairy manure-derived biochar', *Environmental Science and Pollution Research*, 20(1), pp. 358-368.

Xu, Z., Zhang, W., Pan, B., Hong, C., Lv, L., Zhang, Q., Pan, B. and Zhang, Q. (2008) 'Application of the Polanyi potential theory to phthalates adsorption from aqueous solution with hyper-cross-linked polymer resins', *Journal of Colloid and Interface Science*, 319(2), pp. 392-397.

Yalkowsky, S.H. and Dannenfelser, R.M. (1992) 'Aquasol database of aqueous solubility', *College of Pharmacy, University of Arizona, Tucson, AZ.*

Yan, X.M., Shi, B.Y., Lu, J.J., Feng, C.H., Wang, D.S. and Tang, H.X. (2008) 'Adsorption and desorption of atrazine on carbon nanotubes', *Journal of Colloid and Interface Science*, 321(1), pp. 30-38.

Yang, K., Wang, X., Zhu, L. and Xing, B. (2006a) 'Competitive Sorption of Pyrene, Phenanthrene, and Naphthalene on Multiwalled Carbon Nanotubes', *Environmental Science & Technology*, 40(18), pp. 5804-5810.

Yang, K., Wu, W., Jing, Q. and Zhu, L. (2008) 'Aqueous adsorption of aniline, phenol, and their substitutes by multi-walled carbon nanotubes', *Environmental science & technology*, 42(21), pp. 7931-7936.

Yang, K. and Xing, B. (2010) 'Adsorption of organic compounds by carbon nanomaterials in aqueous phase: Polanyi theory and its application', *Chemical reviews*, 110(10), pp. 5989-6008.

Yang, K., Zhu, L. and Xing, B. (2006b) 'Adsorption of Polycyclic Aromatic Hydrocarbons by Carbon Nanomaterials', *Environmental Science & Technology*, 40(6), pp. 1855-1861.

Yang, X. and Al-Duri, B. (2005) 'Kinetic modeling of liquid-phase adsorption of reactive dyes on activated carbon', *Journal of Colloid and Interface Science*, 287(1), pp. 25-34.

Yang, Y. and Sheng, G. (2003) 'Pesticide Adsorptivity of Aged Particulate Matter Arising from Crop Residue Burns', *Journal of Agricultural and Food Chemistry*, 51(17), pp. 5047-5051.

You, Y., Zhao, H. and Vance, G.F. (2002) 'Surfactant-enhanced adsorption of organic compounds by layered double hydroxides', *Colloids and Surfaces A: Physicochemical and Engineering Aspects*, 205(3), pp. 161-172.

Yu, B., Zhang, Y., Shukla, A., Shukla, S.S. and Dorris, K.L. (2000) 'The removal of heavy metal from aqueous solutions by sawdust adsorption —

removal of copper', *Journal of Hazardous Materials*, 80(1–3), pp. 33-42.

Yu, X.-Y., Ying, G.-G. and Kookana, R.S. (2009) 'Reduced plant uptake of pesticides with biochar additions to soil', *Chemosphere*, 76(5), pp. 665-671.

Yu, Z., Peldszus, S. and Huck, P.M. (2008) 'Adsorption characteristics of selected pharmaceuticals and an endocrine disrupting compound—Naproxen, carbamazepine and nonylphenol—on activated carbon', *Water Research*, 42(12), pp. 2873-2882.

Yuh-Shan, H. (2004) 'Citation review of Lagergren kinetic rate equation on adsorption reactions', *Scientometrics*, 59(1), pp. 171-177.

Zhang, G., Qu, J., Liu, H., Cooper, A.T. and Wu, R. (2007) 'CuFe2O4/activated carbon composite: A novel magnetic adsorbent for the removal of acid orange II and catalytic regeneration', *Chemosphere*, 68(6), pp. 1058-1066.

Zhang, H., Lin, K., Wang, H. and Gan, J. (2010a) 'Effect of Pinus radiata derived biochars on soil sorption and desorption of phenanthrene', *Environmental Pollution*, 158(9), pp. 2821-2825.

Zhang, M. (2011) 'Adsorption study of Pb(II), Cu(II) and Zn(II) from simulated acid mine drainage using dairy manure compost', *Chemical Engineering Journal*, 172(1), pp. 361-368.

Zhang, M., Gao, B., Varnoosfaderani, S., Hebard, A., Yao, Y. and Inyang, M. (2013) 'Preparation and characterization of a novel magnetic biochar for arsenic removal', *Bioresource Technology*, 130(0), pp. 457-462.

Zhang, S., Shao, T., Bekaroglu, S.S.K. and Karanfil, T. (2010b) 'Adsorption of synthetic organic chemicals by carbon nanotubes: Effects of background solution chemistry', *Water Research*, 44(6), pp. 2067-2074.

Zhuang, L.W., Zhang, W.H., Lu, H.L., Yang, Y.X. and Qiu, R.L. (2011) *3rd International CEMEPE & SECOTOX Conference*. Skiathos, 19-24 June.

Zuccato, E., Calamari, D., Natangelo, M. and Fanelli, R. (2000) 'Presence of therapeutic drugs in the environment', *The Lancet*, 355(9217), pp. 1789-1790.

APPENDICES

APPENDIX A: PHENOL SORPTION; RESULTS OF ISOTHERM MODELS FITTING

A1 FITTING OF ISOTHERM DATA USING LINEAR TRANSFORMED MODELS (LTFM)
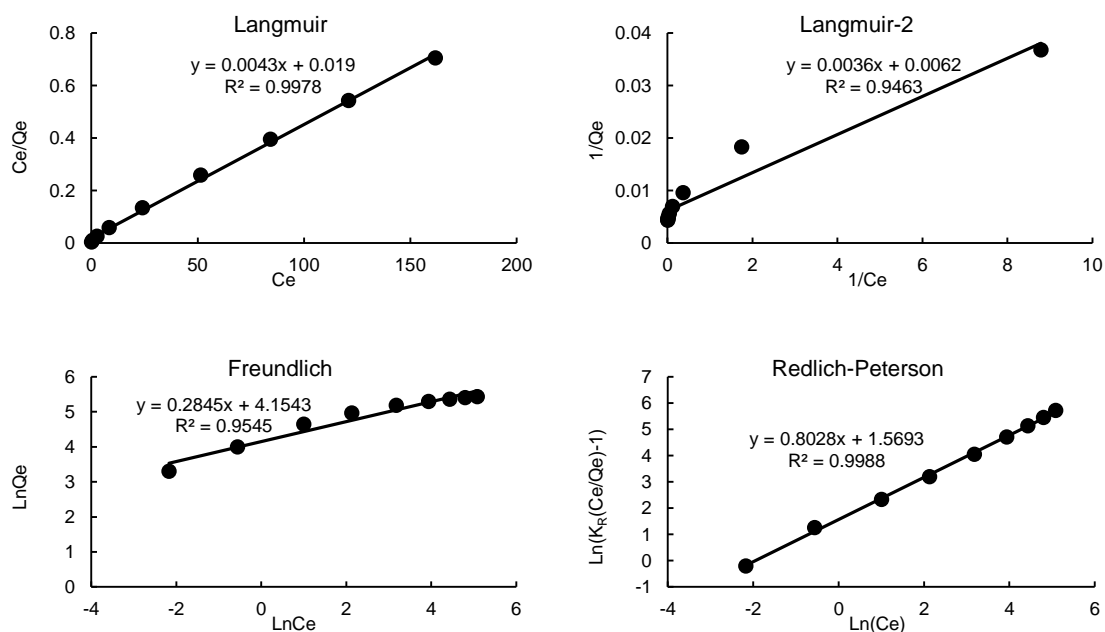
Figure A1: Sorption of phenol on CoAC @ 22°C
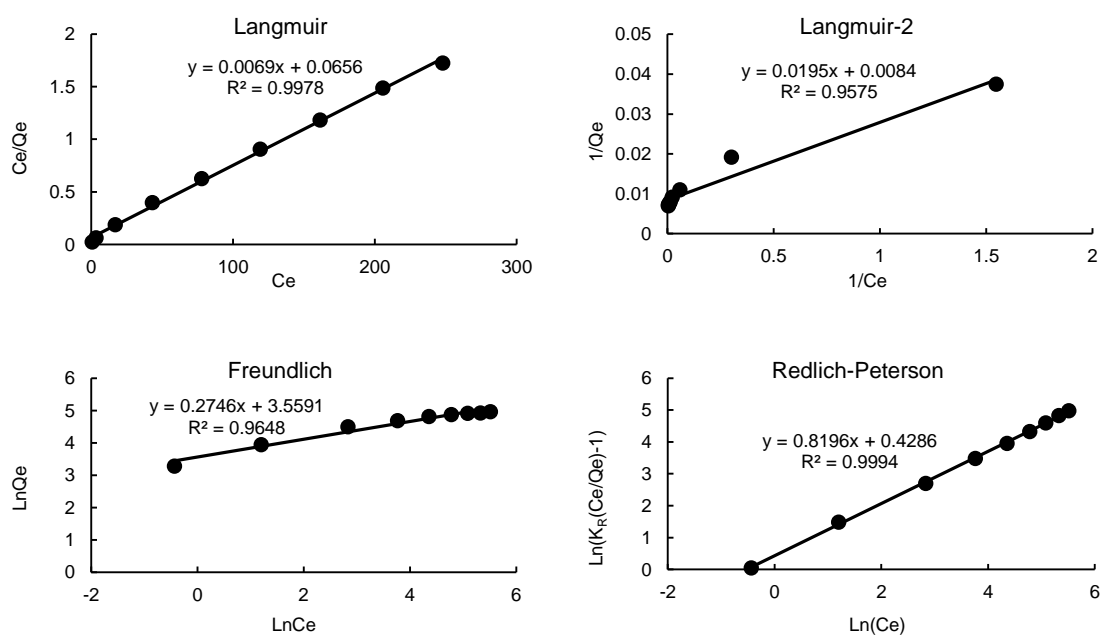
Figure A2: Sorption of phenol on MCoAC @ 22°C
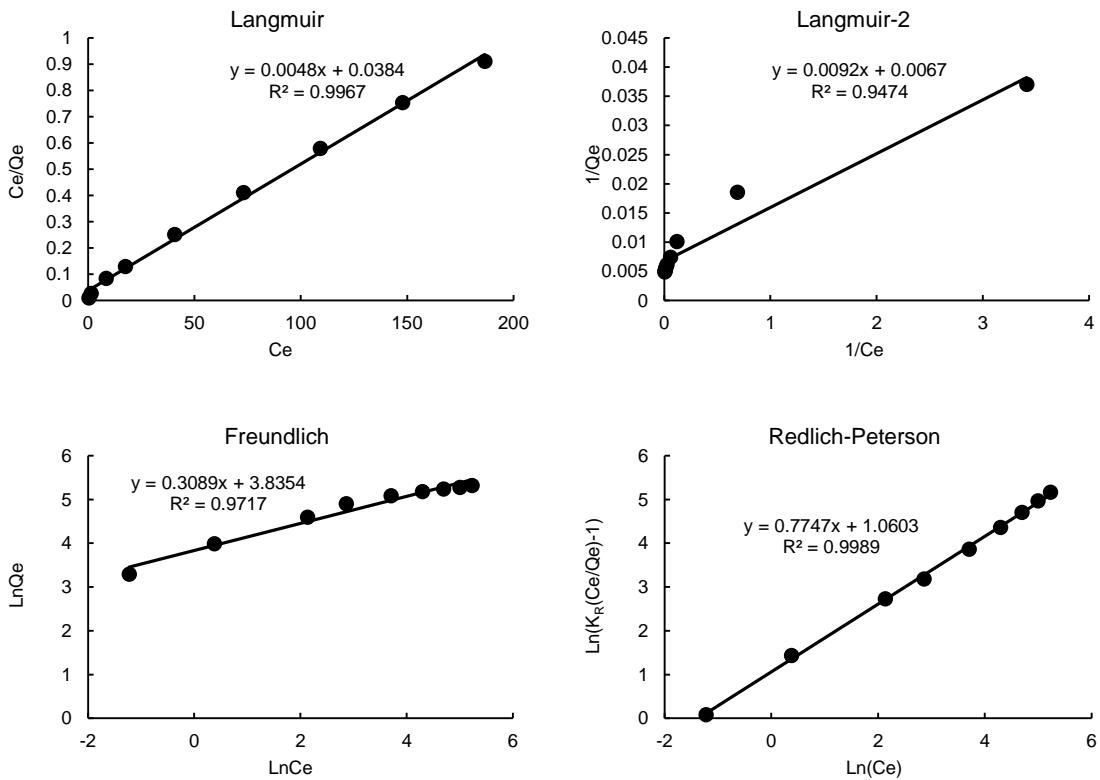
Figure A3:   Sorption of phenol on CoalAC @ 22ºC
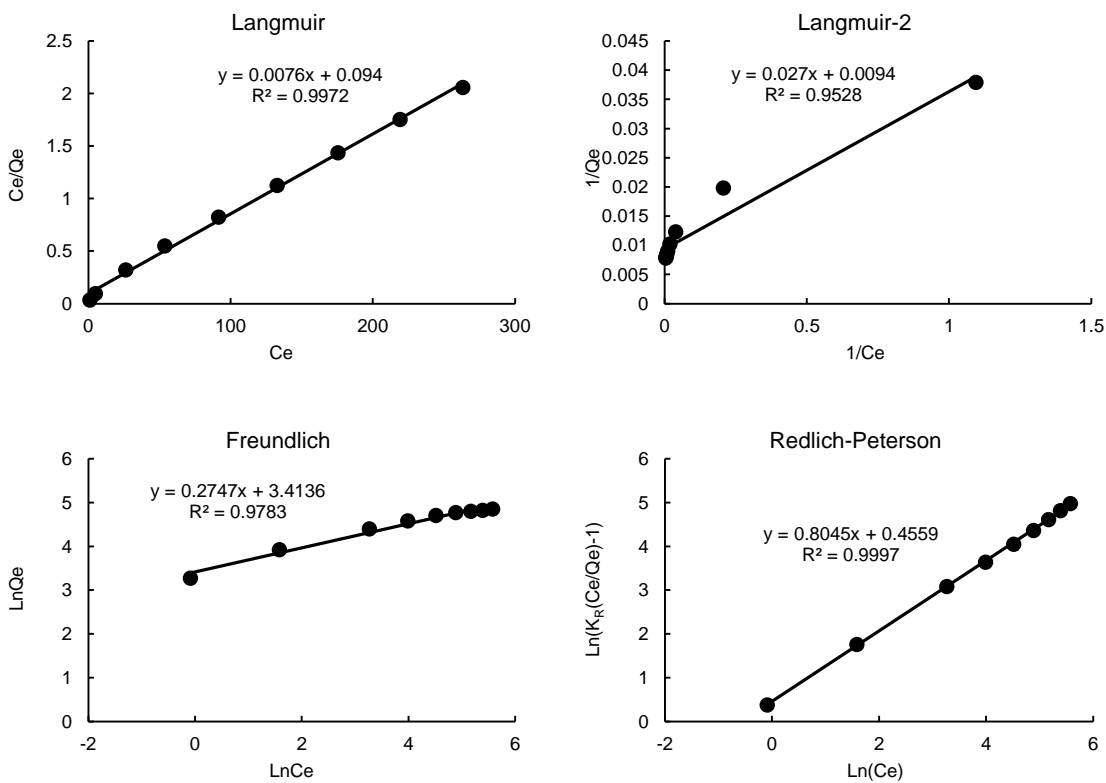
Figure A4:   Sorption of phenol on MCoalAC @ 22ºC
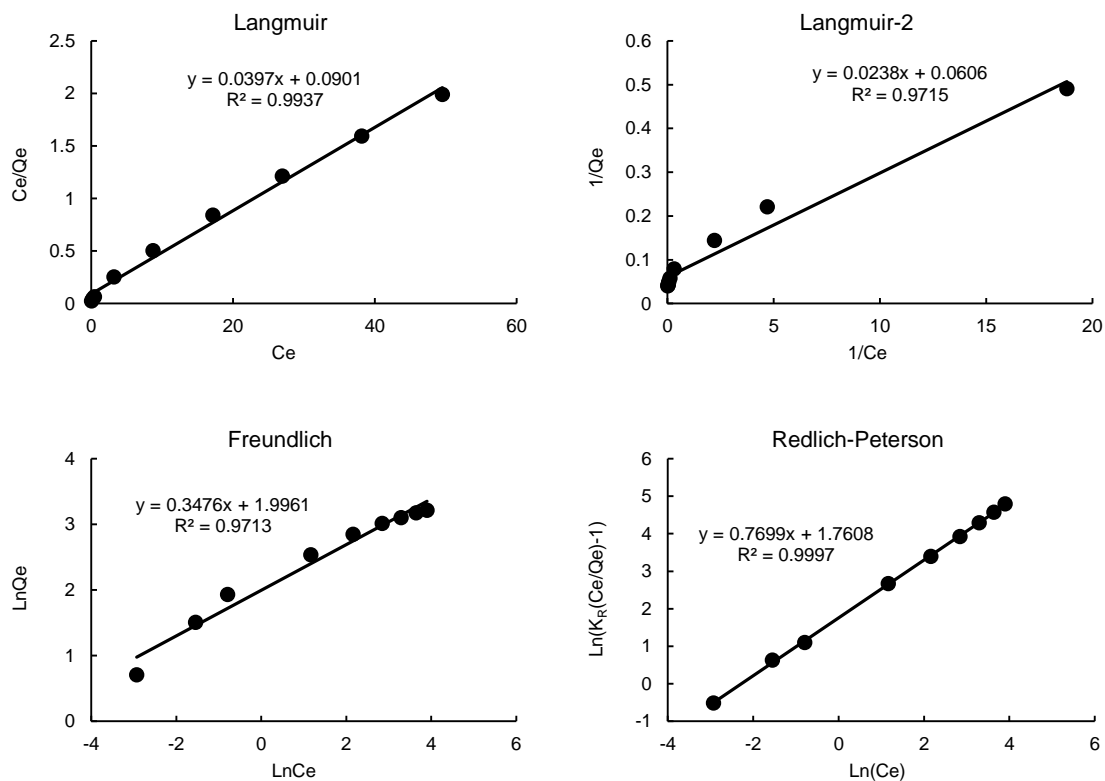
Figure A5: Sorption of phenol on Bio-1 @ 22ºC
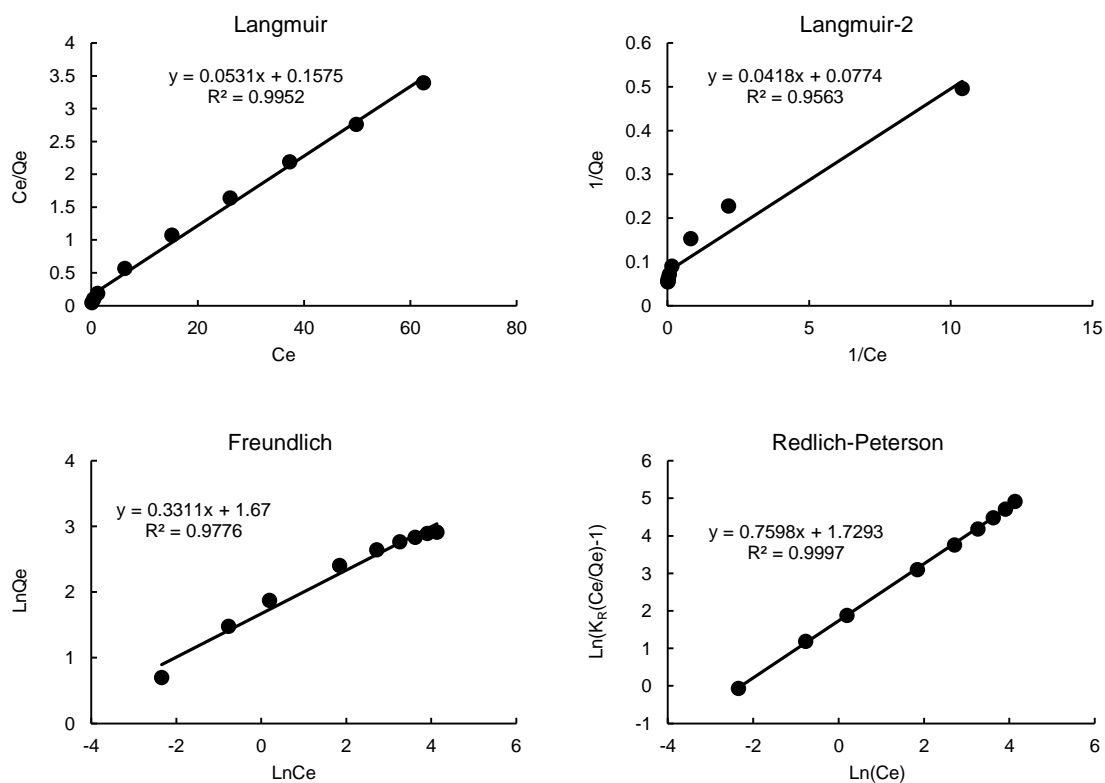
Figure A6: Sorption of phenol on MBio-1 @ 22ºC
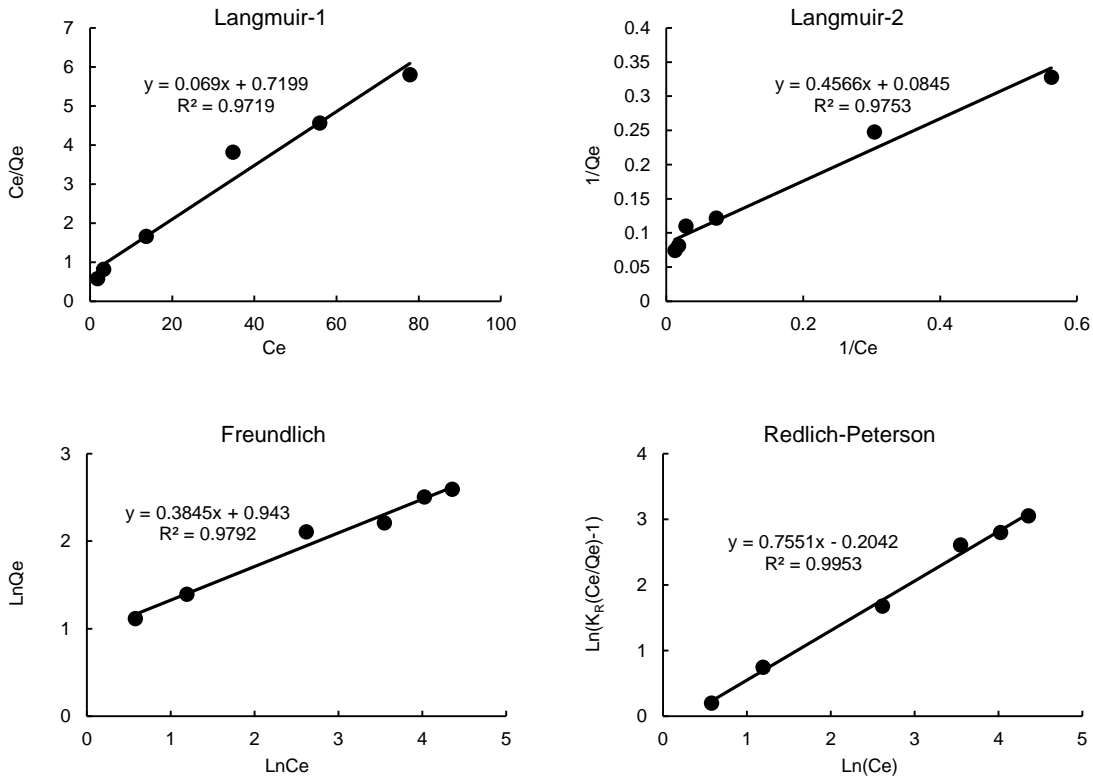
Figure A7:   Sorption of phenol on OrgBio @ 22°C
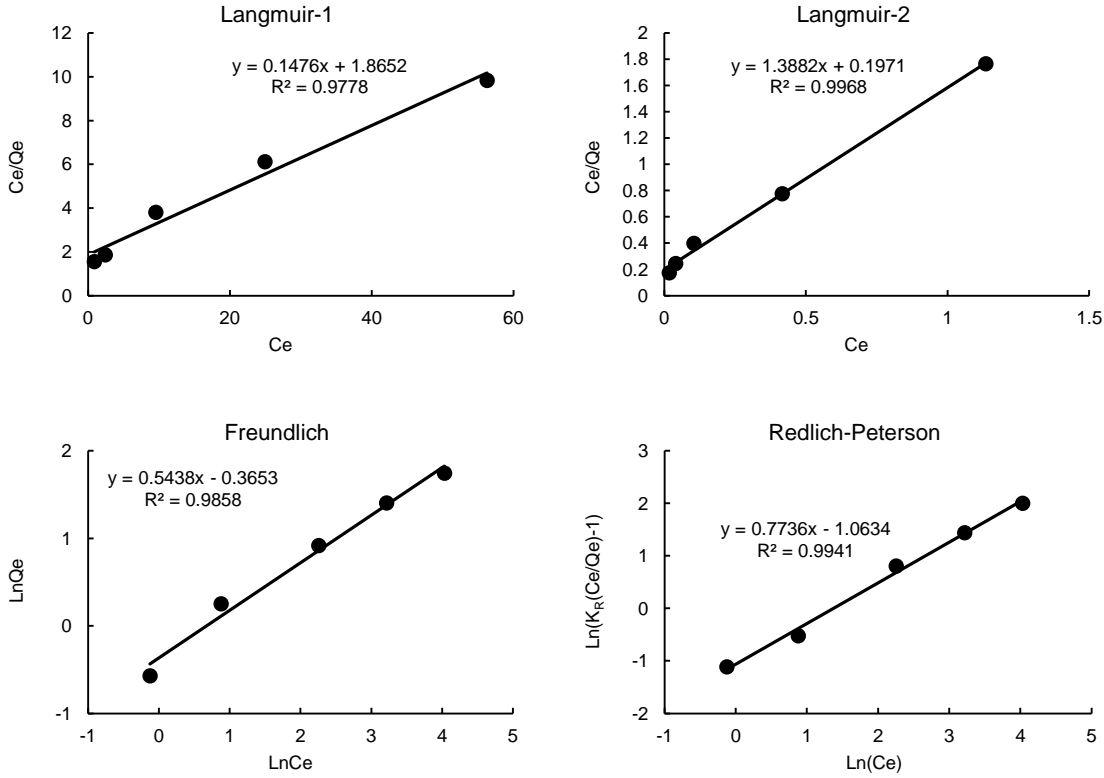
Figure A8:   Sorption of phenol on MOrgBio @ 22°C

A2 ISOTHERM MODEL PARAMETERS GENERATED USING ALL ERROR FUNCTIONS

Table A1: Sorption of phenol on CoAC @ 22°C

Model	Parameter	LTFM	CoD	HYB	MPSD	ARE	EABS	ERRSQ
	Q_m	231.15	222.40	209.17	190.11	230.96	225.21	219.15
	K_L	0.23	0.28	0.47	0.84	0.30	0.21	0.31
LANG	R^2	0.9854	0.9791	0.9524	0.9054	0.9766	0.9867	0.9757
	$1/n$	0.28	0.23	0.26	0.29	0.27	0.21	0.22
	K_F	63.71	77.80	68.80	60.96	63.72	85.03	80.29
FREU	R^2	0.9422	0.9620	0.9525	0.9404	0.9467	0.9684	0.9650
	K_R	433.25	206.06	286.49	381.17	408.95	433.03	209.54
	A_R	4.80	1.76	2.70	4.05	4.23	4.07	1.79
	β	0.80	0.86	0.84	0.81	0.82	0.84	0.86
RED-PET	R^2	0.9869	0.9977	0.9959	0.9904	0.9914	0.9941	0.9976
	Qo	-	272.96	278.13	288.29	278.74	272.96	272.96
	E	-	32.89	32.95	32.91	33.17	32.95	32.89
	b	-	3.42	3.30	3.12	3.25	3.41	3.42
DA	R^2	-	0.9996	0.9995	0.9990	0.9995	0.9996	0.9996
	Qo	-	272.97	278.14	288.31	274.79	272.64	272.88
	a	-	28.75	25.36	21.45	25.62	28.75	28.75
	b	-	3.42	3.30	3.12	3.34	3.42	3.42
PDM	R^2	-	0.9996	0.9995	0.9990	0.9995	0.9996	0.9996

Table A2: Sorption of phenol on MCoAC @ 22°C

Model	Parameter	LTFM	CoD	HYB	MPSD	ARE	EABS	ERRSQ
	Q_m	145.51	141.12	133.91	127.23	137.36	144.76	138.98
	K_L	0.10	0.13	0.21	0.29	0.18	0.10	0.14
LANG	R^2	0.9843	0.9770	0.9508	0.9252	0.9598	0.9863	0.9718
	$1/n$	0.27	0.23	0.25	0.28	0.27	0.24	0.22
	K_F	35.13	41.90	38.01	34.20	35.14	39.38	43.59
FREU	R^2	0.9533	0.9647	0.9593	0.9523	0.9557	0.9620	0.9671
	K_R	84.79	53.76	67.80	79.47	84.80	84.79	54.92
	A_R	1.54	0.79	1.09	1.40	1.51	1.54	0.81
	β	0.82	0.86	0.84	0.83	0.82	0.82	0.86
RED-PET	R^2	0.9920	0.9965	0.9955	0.9932	0.9926	0.9921	0.9964
	Qo	-	173.32	176.22	179.96	173.38	173.51	173.31
	E	-	30.68	30.77	30.79	30.91	30.91	30.70
	b	-	3.29	3.18	3.07	3.27	3.27	3.28
DA	R^2	-	0.9989	0.9989	0.9986	0.9989	0.9989	0.9989
	Qo	-	173.34	176.25	179.98	172.69	172.80	173.20
	a	-	31.80	28.07	25.00	30.77	31.80	31.80
	b	-	3.29	3.18	3.07	3.28	3.30	3.29
PDM	R^2	-	0.9989	0.9989	0.9986	0.9989	0.9989	0.9989

Table A3: Sorption of phenol on CoalAC @ 22°C

Model	Parameter	LTFM	CoD	HYB	MPSD	ARE	EABS	ERRSQ
	Q_m	207.62	204.90	190.10	169.71	203.70	205.35	201.90
	K_L	0.13	0.12	0.20	0.39	0.11	0.11	0.13
LANG	R^2	0.9830	0.9851	0.9538	0.8961	0.9874	0.9888	0.9819
	$1/n$	0.31	0.26	0.28	0.31	0.30	0.25	0.25
	K_F	46.31	56.89	50.59	45.23	46.32	58.07	58.80
FREU	R^2	0.9552	0.9696	0.9628	0.9546	0.9581	0.9711	0.9718
	K_R	192.62	90.11	137.00	178.39	192.63	86.64	94.18
	A_R	2.89	1.02	1.78	2.61	2.85	0.98	1.07
	β	0.77	0.84	0.81	0.78	0.78	0.83	0.83
RED-PET	R^2	0.9867	0.9944	0.9924	0.9882	0.9880	0.9947	0.9942
	Qo	-	265.10	279.21	295.70	265.31	265.09	265.21
	E	-	30.50	30.59	30.44	31.04	30.52	30.54
	b	-	3.11	2.86	2.67	3.01	3.11	3.10
DA	R^2	-	0.9974	0.9970	0.9961	0.9971	0.9974	0.9974
	Qo	-	265.12	279.26	295.76	254.43	265.10	265.27
	a	-	26.82	20.48	16.93	26.63	26.82	26.34
	b	-	3.11	2.86	2.67	3.17	3.11	3.10
PDM	R^2	-	0.9974	0.9970	0.9961	0.9965	0.9974	0.9974

Table A4:   Sorption of phenol on MCoalAC @ 22°C

Model	Parameter	LTFM	CoD	HYB	MPSD	ARE	EABS	ERRSQ	Average
	Q_m	131.52	128.30	119.64	113.03	124.11	131.89	125.37	124.84
	K_L	0.08	0.09	0.16	0.24	0.14	0.06	0.11	0.13
LANG	R^2	0.9761	0.9707	0.9335	0.9030	0.9447	0.9862	0.9618	0.9537
	$1/n$	0.27	0.24	0.26	0.28	0.26	0.25	0.24	0.26
	K_F	30.37	35.19	32.49	29.91	31.40	34.21	36.19	32.82
FREU	R^2	0.9702	0.9774	0.9740	0.9698	0.9729	0.9765	0.9787	0.9742
	K_R	70.87	49.71	60.90	68.44	70.87	70.87	50.88	63.22
	A_R	1.58	0.97	1.27	1.50	1.57	1.58	0.99	1.35
	β	0.80	0.83	0.82	0.81	0.81	0.80	0.83	0.81
RED-PET	R^2	0.9943	0.9962	0.9956	0.9947	0.9945	0.9943	0.9961	0.9951
	Q_o	-	171.91	175.15	177.37	172.40	171.93	171.91	173.44
	E	-	30.19	30.25	30.24	30.36	30.22	30.21	30.25
	b	-	2.78	2.70	2.65	2.72	2.77	2.78	2.73
DA	R^2	-	0.9989	0.9988	0.9988	0.9989	0.9989	0.9989	0.9989
	Q_o	-	171.93	175.20	177.37	171.92	171.16	171.96	173.26
	a	-	19.55	17.74	16.89	19.55	19.55	19.43	18.78
	b	-	2.78	2.70	2.65	2.78	2.79	2.78	2.75
PDM	R^2	-	0.9989	0.9988	0.9988	0.9989	0.9989	0.9989	0.9989

Table A5:   Sorption of phenol on Bio-1 @ 22°C

Model	Parameter	LTFM	CoD	HYB	MPSD	ARE	EABS	ERRSQ
	Q_m	25.21	25.02	21.99	20.06	21.31	24.73	24.31
	K_L	0.44	0.37	0.92	1.44	1.27	0.33	0.42
LANG	R^2	0.9717	0.9781	0.9358	0.9090	0.9172	0.9814	0.9731
	$1/n$	0.35	0.29	0.32	0.36	0.33	0.28	0.28
	K_F	7.36	8.57	7.73	7.07	7.52	8.77	8.67
FREU	R^2	0.9737	0.9856	0.9795	0.9719	0.9777	0.9865	0.9864
	K_R	61.26	49.65	55.09	59.03	61.26	53.88	50.055
	A_R	5.82	4.38	5.00	5.52	5.80	4.75	4.417
	β	0.77	0.792	0.784	0.775	0.773	0.792	0.792
RED-PET	R^2	0.9980	0.9988	0.9986	0.9983	0.9982	0.9987	0.9988
	Q_o	-	39.77	37.77	35.14	37.80	39.21	39.78
	E	-	32.50	32.65	32.93	32.51	32.46	32.51
	b	-	2.80	2.96	3.19	2.99	2.87	2.80
DA	R^2	-	0.9992	0.9991	0.9985	0.9991	0.9992	0.9992
	Q_o	-	39.78	37.77	35.15	37.39	40.40	39.74
	a	-	16.20	18.78	22.83	20.39	16.20	16.20
	b	-	2.80	2.96	3.19	3.04	2.78	2.80
PDM	R^2	-	0.9992	0.9991	0.9985	0.9991	0.9992	0.9992

Table A6:   Sorption of phenol on MBio-1 @ 22°C

Model	Parameter	LTFM	CoD	HYB	MPSD	ARE	EABS	ERRSQ
	Q_m	18.85	18.41	17.06	15.66	16.70	18.83	18.02
	K_L	0.34	0.34	0.58	0.90	0.77	0.23	0.38
LANG	R^2	0.9773	0.9772	0.9525	0.9232	0.9349	0.9871	0.9727
	$1/n$	0.33	0.28	0.31	0.34	0.31	0.28	0.28
	K_F	5.31	6.14	5.61	5.17	5.57	6.18	6.23
FREU	R^2	0.9745	0.9842	0.9794	0.9735	0.9791	0.9844	0.9851
	K_R	40.63	24.05	32.32	38.57	41.05	40.63	24.37
	A_R	5.64	2.83	4.14	5.26	5.73	5.64	2.87
	β	0.76	0.80	0.78	0.77	0.76	0.76	0.80
RED-PET	R^2	0.9956	0.9984	0.9976	0.9962	0.9954	0.9955	0.9983
	Q_o	-	27.97	28.32	28.45	28.62	28.40	27.97
	E	-	32.13	32.11	32.09	32.07	32.10	32.13
	b	-	2.93	2.89	2.87	2.87	2.89	2.93
DA	R^2	-	0.9997	0.9997	0.9997	0.9997	0.9997	0.9997
	Q_o	-	27.98	28.32	28.45	28.71	28.01	27.97
	a	-	19.06	18.28	18.04	17.89	19.06	19.06
	b	-	2.93	2.89	2.87	2.86	2.93	2.93
PDM	R^2	-	0.9997	0.9997	0.9997	0.9997	0.9997	0.9997

Table A7: Sorption of phenol on OrgBio @ 22°C

Model	Parameter	LTFM	CoD	HYB	MPSD	ARE	EABS	ERRSQ
	Q_m	14.49	14.44	13.01	12.42	12.86	14.47	13.77
	K_L	0.10	0.09	0.14	0.16	0.14	0.10	0.11
LANG	R^2	0.9486	0.9495	0.9339	0.9277	0.9342	0.9475	0.9433
	$1/n$	0.38	0.38	0.38	0.38	0.38	0.38	0.36
	K_F	2.57	2.66	2.63	2.55	2.56	2.56	2.76
FREU	R^2	0.9731	0.9736	0.9736	0.9731	0.9734	0.9733	0.9741
	K_R	3.82	5.02	4.75	4.43	3.83	3.83	5.69
	A_R	0.82	1.31	1.17	1.05	0.80	0.80	1.50
	β	0.76	0.70	0.72	0.73	0.75	0.75	0.71
RED-PET	R^2	0.9756	0.9766	0.9766	0.9764	0.9756	0.9756	0.9767
	Qo	-	42.76	33.26	28.13	42.76	42.74	44.39
	E	-	24.74	26.17	26.93	24.71	24.71	24.66
	b	-	1.90	2.18	2.45	1.91	1.91	1.81
DA	R^2	-	0.9753	0.9751	0.9745	0.9752	0.9752	0.9754
	Qo	-	44.79	33.48	28.30	44.73	45.69	41.69
	a	-	10.59	13.89	17.88	10.59	10.60	10.59
	b	-	1.85	2.17	2.44	1.84	1.84	1.88
PDM	R^2	-	0.9753	0.9751	0.9745	0.9753	0.9752	0.9754

Table A8: Sorption of phenol on MOrgBio @ 22°C

Model	Parameter	LTFM	CoD	HYB	MPSD	ARE	EABS	ERRSQ
	Q_m	6.78	7.39	6.41	5.55	5.29	6.78	7.25
	K_L	0.08	0.06	0.08	0.12	0.13	0.06	0.06
LANG	R^2	0.9783	0.9906	0.9755	0.9545	0.9460	0.9882	0.9896
	$1/n$	0.54	0.48	0.51	0.55	0.55	0.47	0.48
	K_F	0.69	0.83	0.75	0.68	0.70	0.84	0.83
FREU	R^2	0.9914	0.9958	0.9937	0.9909	0.9912	0.9963	0.9959
	K_R	0.85	1.30	1.16	1.00	0.87	0.76	1.31
	A_R	0.35	0.92	0.76	0.56	0.38	0.35	0.93
	β	0.77	0.63	0.65	0.69	0.74	0.72	0.63
RED-PET	R^2	0.9937	0.9991	0.9990	0.9984	0.9966	0.9981	0.9991
	Qo	-	22.38	18.39	13.79	22.53	22.38	22.47
	E	-	23.05	23.96	25.22	22.89	23.05	23.03
	b	-	2.15	2.39	2.80	2.23	2.15	2.14
DA	R^2	-	0.9991	0.9989	0.9976	0.9989	0.9991	0.9991
	Qo	-	22.56	18.45	13.81	22.06	22.56	22.49
	a	-	17.56	22.15	32.88	20.38	17.56	17.56
	b	-	2.14	2.38	2.80	2.25	2.14	2.14
PDM	R^2	-	0.9991	0.9989	0.9976	0.9989	0.9991	0.9991

Table A9: Sorption of phenol on CoAC @ 10°C

Model	Parameter	LTFM	CoD	HYB	MPSD	ARE	EABS	ERRSQ
	Q_m	223.32	215.86	198.39	174.23	206.28	223.31	211.13
	K_L	0.24	0.29	0.67	1.70	0.37	0.17	0.34
LANG	R^2	0.9791	0.9725	0.9242	0.8441	0.9621	0.9848	0.9660
	$1/n$	0.25	0.21	0.23	0.25	0.24	0.19	0.20
	K_F	69.29	80.71	73.49	67.74	69.29	85.64	82.37
FREU	R^2	0.9623	0.9755	0.9691	0.9616	0.9657	0.9794	0.9772
	K_R	1381.35	1381.37	941.36	1298.86	1381.35	1381.36	540.66
	A_R	16.32	14.97	10.20	15.24	16.21	14.88	5.29
	β	0.80	0.82	0.82	0.80	0.80	0.82	0.84
RED-PET	R^2	0.9864	0.9908	0.9919	0.9872	0.9873	0.9909	0.9943
	Qo	-	285.06	294.65	306.47	285.62	284.13	285.08
	E	-	33.09	33.17	33.06	33.58	32.92	33.11
	b	-	2.71	2.57	2.44	2.61	2.75	2.71
DA	R^2	-	0.9995	0.9993	0.9988	0.9993	0.9995	0.9995
	Qo	-	285.08	294.68	306.51	290.19	288.55	285.12
	a	-	14.15	12.23	10.88	12.23	14.18	14.10
	b	-	2.71	2.57	2.44	2.59	2.70	2.71
PDM	R^2	-	0.9995	0.9993	0.9988	0.9993	0.9995	0.9995

Table A10:   Sorption of phenol on MCoAC @ 10°C

Model	Parameter	LTFM	CoD	HYB	MPSD	ARE	EABS	ERRSQ
	Q_m	143.00	140.06	131.05	120.99	137.49	143.16	136.91
	K_L	0.12	0.13	0.26	0.48	0.22	0.09	0.16
LANG	R^2	0.9766	0.9717	0.9288	0.8735	0.9411	0.9866	0.9617
	$1/n$	0.25	0.22	0.23	0.25	0.23	0.24	0.21
	K_F	39.03	44.63	41.48	38.61	41.41	39.04	45.97
FREU	R^2	0.9649	0.9728	0.9692	0.9648	0.9688	0.9667	0.9745
	K_R	226.79	226.80	175.66	220.17	226.78	226.79	121.14
	A_R	4.52	4.23	3.25	4.37	4.48	4.20	2.03
	β	0.80	0.82	0.82	0.81	0.81	0.82	0.84
RED-PET	R^2	0.9861	0.9883	0.9892	0.9865	0.9867	0.9885	0.9907
	Q_o	-	182.50	191.74	201.63	187.33	182.49	182.53
	E	-	30.64	30.85	30.79	31.21	30.68	30.70
	b	-	2.74	2.51	2.34	2.52	2.74	2.73
DA	R^2	-	0.9972	0.9968	0.9960	0.9969	0.9972	0.9972
	Q_o	-	182.52	191.75	201.66	189.68	182.43	182.56
	a	-	17.88	13.87	11.69	13.75	17.88	17.60
	b	-	2.74	2.51	2.34	2.53	2.74	2.73
PDM	R^2	-	0.9972	0.9968	0.9960	0.9969	0.9972	0.9972

Table A11:   Sorption of phenol on Bio-1 @ 10°C

Model	Parameter	LTFM	CoD	HYB	MPSD	ARE	EABS	ERRSQ
	Q_m	25.02	24.35	21.72	19.52	21.37	24.65	23.44
	K_L	0.38	0.38	0.93	1.61	0.81	0.28	0.48
LANG	R^2	0.9683	0.9682	0.9232	0.8812	0.9315	0.9777	0.9585
	$1/n$	0.30	0.26	0.28	0.30	0.29	0.26	0.26
	K_F	7.91	8.74	8.20	7.79	8.10	8.73	8.80
FREU	R^2	0.9864	0.9920	0.9892	0.9859	0.9887	0.9920	0.9924
	K_R	143.21	84.01	113.70	137.08	143.24	143.28	84.88
	A_R	15.20	8.10	11.53	14.45	15.13	14.46	8.19
	β	0.76	0.78	0.77	0.76	0.76	0.77	0.78
RED-PET	R^2	0.9974	0.9990	0.9986	0.9977	0.9975	0.9984	0.9990
	Q_o	-	44.18	43.35	42.59	42.25	43.12	44.19
	E	-	31.18	31.26	31.35	31.40	31.32	31.18
	b	-	2.28	2.32	2.35	2.37	2.32	2.27
DA	R^2	-	0.9998	0.9998	0.9998	0.9998	0.9998	0.9998
	Q_o	-	44.21	43.37	42.60	44.25	44.03	44.19
	a	-	10.56	10.96	11.29	10.56	10.56	10.56
	b	-	2.27	2.32	2.35	2.27	2.28	2.27
PDM	R^2	-	0.9998	0.9998	0.9998	0.9998	0.9998	0.9998

Table A 12:   Sorption of phenol on MBio-1 @ 10°C

Model	Parameter	LTFM	CoD	HYB	MPSD	ARE	EABS	ERRSQ
	Q_m	18.45	17.72	16.40	14.96	16.08	17.82	17.20
	K_L	0.30	0.37	0.67	1.12	0.78	0.43	0.45
LANG	R^2	0.9686	0.9608	0.9276	0.8844	0.9166	0.9537	0.9517
	$1/n$	0.28	0.25	0.27	0.28	0.27	0.24	0.25
	K_F	5.85	6.39	6.06	5.78	6.07	6.69	6.44
FREU	R^2	0.9868	0.9911	0.9890	0.9865	0.9888	0.9925	0.9914
	K_R	75.26	50.18	63.66	72.85	71.67	75.28	51.04
	A_R	10.70	6.62	8.74	10.30	9.96	10.50	6.74
	β	0.77	0.79	0.78	0.77	0.78	0.78	0.79
RED-PET	R^2	0.9972	0.9981	0.9979	0.9973	0.9976	0.9975	0.9981
	Q_o	-	31.13	30.71	30.34	31.11	31.03	31.14
	E	-	31.26	31.32	31.38	31.22	31.24	31.28
	b	-	2.29	2.32	2.35	2.30	2.30	2.29
DA	R^2	-	0.9991	0.9991	0.9991	0.9991	0.9991	0.9991
	Q_o	-	31.22	30.73	30.35	31.09	31.55	31.17
	a	-	10.58	10.92	11.18	10.81	10.55	10.58
	b	-	2.28	2.32	2.34	2.30	2.27	2.28
PDM	R^2	-	0.9991	0.9991	0.9991	0.9991	0.9991	0.9991

A3 ISOTHERM FITTING PLOTS: NONLINEAR FITTING METHOD
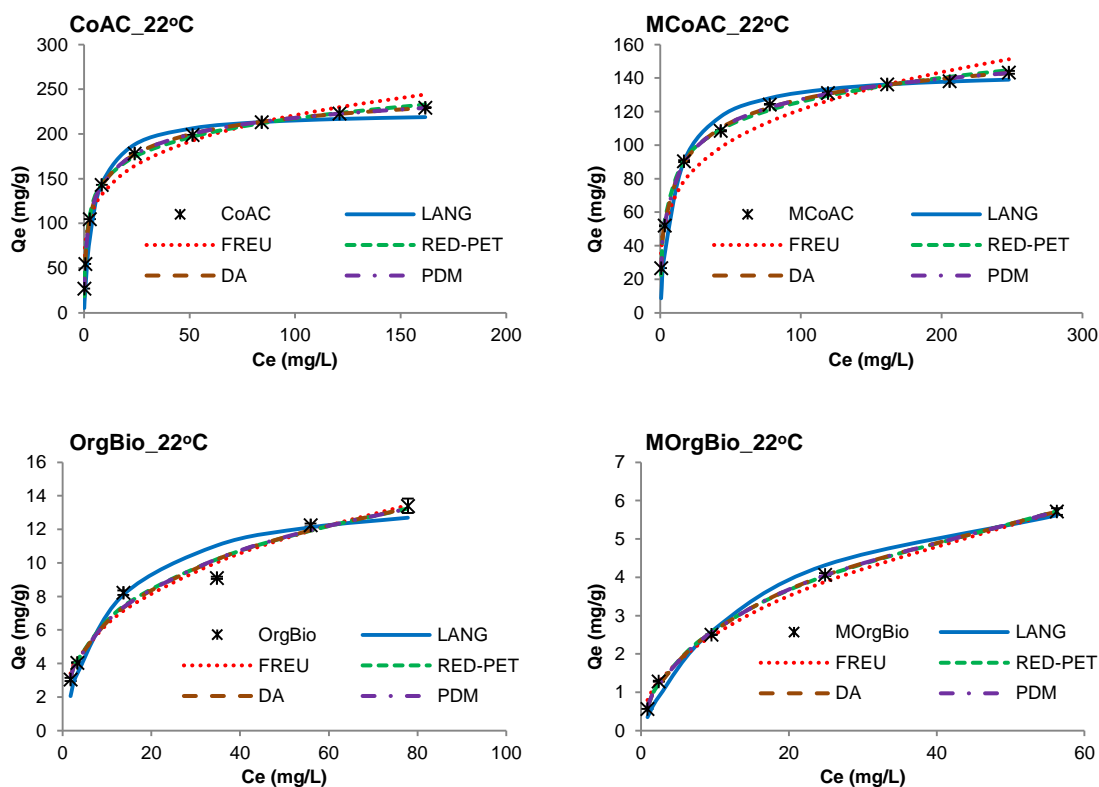

Figure A1:   Comparison of simulated and experimental isotherm plot for sorption of phenol @ 22°C

APPENDIX B: PHENOL SORPTION; RESULTS KINETICS MODELS FITTING

B1 KINETICS MODEL PARAMETERS GENERATED USING ALL ERROR FUNCTIONS

Table B1: Sorption kinetics of phenol on CoAC

Model	Parameter	LTFM	CoD	HYB	MPSD	ARE	EABS	ERSSQ
	Qe	78.54	194.95	167.71	162.01	155.06	190.08	173.52
	k1	1.54E-03	7.49E-02	1.63E-01	1.85E-01	1.59E-01	1.02E-01	1.42E-01
1st	R²	0.8247	0.7059	0.5358	0.5050	0.5419	0.6418	0.5678
	Qe	209.30	197.55	183.24	178.54	193.99	190.68	187.66
	k2	3.46E-04	7.45E-04	1.26E-03	1.46E-03	9.08E-04	9.23E-04	1.08E-03
2nd	R²	0.9023	0.8385	0.7994	0.7892	0.8224	0.8225	0.8099
	α	2656.12	2356.54	2466.69	2296.89	2187.54	2191.54	2656.12
	β	0.058	0.058	0.058	0.057	0.058	0.058	0.058
Elovich	R²	0.9849	0.9849	0.9849	0.9849	0.9849	0.9849	0.9849
	kid	98.16	98.85	98.93	97.83	96.29	100.58	100.07
	z	0.11	0.11	0.11	0.11	0.12	0.10	0.10
Intra-P	R²	0.9709	0.9712	0.9713	0.9709	0.9694	0.9717	0.9718

Table B2: Sorption kinetics of phenol on MCoAC

Model	Parameter	LTFM	CoD	HYB	MPSD	ARE	EABS	ERSSQ
	Qe	58.64	130.14	112.10	106.66	137.93	96.08	117.73
	k1	1.74E-03	5.37E-02	1.01E-01	1.18E-01	5.62E-03	1.41E-01	8.41E-02
1st	R²	0.7710	0.8170	0.7135	0.6844	0.9024	0.6475	0.7450
	Qe	139.12	133.04	125.00	121.02	132.91	133.18	128.59
	k2	4.58E-04	7.02E-04	1.00E-03	1.17E-03	8.77E-04	8.05E-04	8.58E-04
2nd	R²	0.9394	0.9174	0.8979	0.8894	0.9029	0.9085	0.9065
	α	183.07	151.82	147.91	121.07	137.42	143.84	183.07
	β	0.068	0.066	0.066	0.063	0.065	0.066	0.068
Elovich	R²	0.9653	0.9653	0.9653	0.9653	0.9653	0.9653	0.9653
	kid	49.20	50.81	50.61	48.17	47.72	58.64	53.11
	z	0.16	0.15	0.15	0.16	0.17	0.12	0.14
Intra-P	R²	0.9223	0.9246	0.9250	0.9216	0.9172	0.9348	0.9280

Table B3: Sorption kinetics of phenol on CoalAC

Model	Parameter	LTFM	CoD	HYB	MPSD	ARE	EABS	ERSSQ
	Qe	51.97	166.09	144.65	142.09	131.93	139.63	147.40
	k1	1.47E-03	1.04E-01	2.70E-01	2.93E-01	4.21E-01	3.54E-01	2.48E-01
1st	R²	0.8657	0.5588	0.3559	0.3410	0.2845	0.3087	0.3730
	Qe	175.44	166.66	154.92	152.57	153.29	163.74	157.24
	k2	5.42E-04	1.44E-03	2.83E-03	3.18E-03	2.65E-03	1.52E-03	2.52E-03
2nd	R²	0.8228	0.7297	0.6843	0.6781	0.6891	0.7266	0.6908
	α	1.21E+05	9.63E+04	1.25E+05	1.31E+05	1.18E+05	1.18E+05	1.21E+05
	β	0.095	0.093	0.095	0.096	0.095	0.095	0.095
Elovich	R²	0.9813	0.9813	0.9813	0.9813	0.9813	0.9813	0.9813
	kid	103.79	103.43	103.83	103.69	103.07	103.12	103.99
	z	0.07	0.07	0.07	0.07	0.07	0.07	0.07
Intra-P	R²	0.9817	0.9817	0.9817	0.9817	0.9817	0.9817	0.9817

Table B4:   Sorption kinetics of phenol on MCoalAC

Model	Parameter	LTFM	CoD	HYB	MPSD	ARE	EABS	ERSSQ
	Qe	29.42	108.03	100.36	99.26	109.60	99.40	101.50
	k1	1.30E-03	1.48E-01	2.59E-01	2.73E-01	6.63E-02	1.71E-01	2.44E-01
1st	**R²**	0.7549	0.6492	0.5196	0.5075	0.7869	0.6167	0.5329
	Qe	115.71	110.06	106.42	105.59	98.81	110.13	107.23
	k2	1.12E-03	3.05E-03	4.32E-03	4.60E-03	7.73E-03	3.02E-03	4.04E-03
2nd	**R²**	0.8948	0.8350	0.8186	0.8158	0.7972	0.8355	0.8214
	α	5.14E+05	3.34E+05	4.17E+05	3.35E+05	4.05E+05	3.25E+05	5.14E+05
	β	1.59E-01	1.54E-01	1.57E-01	1.54E-01	1.57E-01	1.55E-01	1.59E-01
Elovich	**R²**	0.9696	0.9696	0.9696	0.9696	0.9696	0.9696	0.9696
	kid	73.81	73.65	74.06	73.64	71.90	75.96	74.48
	z	0.06	0.07	0.06	0.07	0.07	0.06	0.06
Intra-P	**R²**	0.9563	0.9562	0.9566	0.9563	0.9548	0.9580	0.9568

Table B5:   Sorption kinetics of phenol on Bio-1

Model	Parameter	LTFM	CoD	HYB	MPSD	ARE	EABS	ERSSQ
	Qe	7.95	14.00	11.00	10.35	12.44	21.99	**11.86**
	k1	1.03E-03	3.57E-02	1.28E-01	1.65E-01	3.74E-02	2.32E-03	8.57E-02
1st	**R²**	0.8379	0.8127	0.5086	0.4594	0.8021	0.9086	0.6000
	Qe	14.77	13.83	12.33	11.74	12.55	14.58	12.90
	k2	2.70E-03	5.65E-03	1.23E-02	1.62E-02	9.56E-03	3.63E-03	9.12E-03
2nd	**R²**	0.9283	0.8590	0.7826	0.7583	0.8088	0.9016	0.8111
	α	24.57	24.44	25.08	25.44	24.92	24.97	24.57
	β	0.696	0.696	0.699	0.700	0.698	0.700	0.696
Elovich	**R²**	0.9991	0.9991	0.9991	0.9991	0.9991	0.9991	0.9991
	kid	5.38	5.50	5.45	5.36	5.58	5.72	5.53
	z	0.14	0.14	0.14	0.14	0.14	0.13	0.14
Intra-P	**R²**	0.9907	0.9914	0.9911	0.9907	0.9915	0.9921	0.9915

Table B6:   Sorption kinetics of phenol on MBio-1

Model	Parameter	LTFM	CoD	HYB	MPSD	ARE	EABS	ERSSQ
	Qe	6.68	11.27	8.85	8.22	11.91	9.87	9.67
	k1	1.08E-03	3.33E-02	1.11E-01	1.51E-01	3.78E-03	6.70E-02	7.04E-02
1st	**R²**	0.8482	0.8248	0.5363	0.4715	0.9310	0.6571	0.6448
	Qe	11.99	11.19	9.93	9.40	10.12	11.99	10.44
	k2	2.99E-03	6.18E-03	1.34E-02	1.82E-02	1.07E-02	3.92E-03	9.74E-03
2nd	**R²**	0.9324	0.8685	0.7924	0.7648	0.8166	0.9091	0.8236
	α	13.48	13.34	13.89	14.18	13.91	14.63	13.48
	β	0.826	0.825	0.831	0.834	0.829	0.843	0.826
Elovich	**R²**	0.9982	0.9982	0.9982	0.9982	0.9982	0.9982	0.9982
	kid	4.07	4.18	4.13	4.05	4.07	4.41	4.20
	z	0.15	0.15	0.15	0.15	0.15	0.14	0.14
Intra-P	**R²**	0.9905	0.9913	0.9910	0.9905	0.9906	0.9925	0.9914

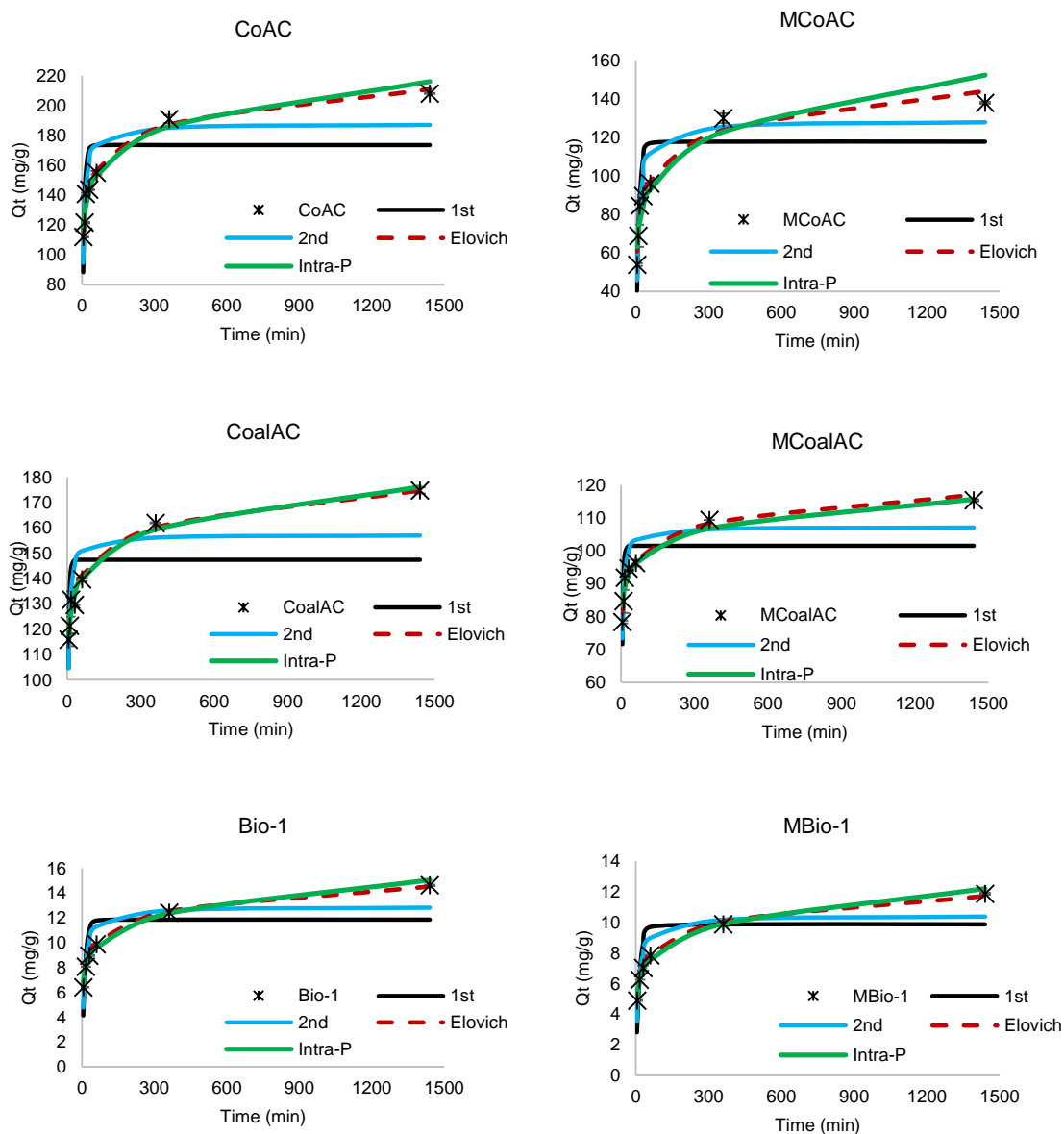## B2 KINETICS FITTING PLOTS: NONLINEAR FITTING METHOD

Figure B1: Comparison of simulated and experimental phenol sorption kinetics plot

APPENDIX C: BIOCHAR RETRIEVAL FROM AGRICULTURAL SOIL

C1   DESCRIPTION OF EXPERIMENT

A twice autoclaved soil (170 g) was mixed with 1.18% (w/w) magnetic biochar (2 g) in a 1 L beaker and 785 mL of autoclaved 0.01 M $CaCl_2$ solution was added such that the solid to liquid ratio was 22% (w/V). The setup was stirred adequately to ensure uniform dispersion of all materials. Triplicate treatment samples and two control samples (soil without MBC) were prepared in a similar manner. All samples were covered with a cling film and allowed to stand undisturbed for 12 days, with manual mixing every 3 days.
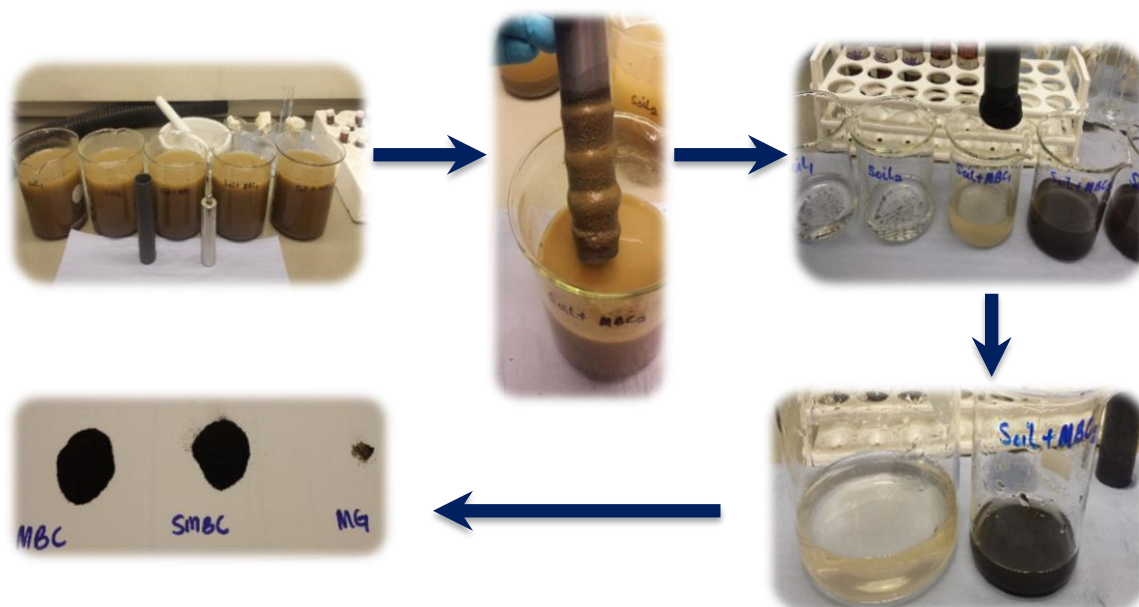

Figure C1: Retrieval of biochar from agricultural soil.

At the end of the contact period, each sample was stirred to re-suspend all the solids and enable the retrieval of the MBC or other magnetic materials using a specially prepared magnetic rod in a plastic sleeve as shown in figure C1. The recovered materials were then rinsed thoroughly with distilled water to remove silt and other nonmagnetic materials. They were then dried in an oven for 4 hours at 8 °C and the weight of the dry residue was recorded before being transferred into a 40 mL amber glass vial with a PTFE screw cap each. Two of the residue materials from the treatment samples were mixed with 30 mL acetone each, the third sample was mixed with 35 mL acetone in a 40 mL and then two of the

controls were mixed with 10 mL acetone each. All samples were then loaded on a shaker to shake at 200 rpm overnight at room temperature. In order to test for the recovery of MBC due to the cleaning with acetone, a control sample having 1 g of pristine MBC was also mixed with 20 mL acetone and run simultaneously with the other samples. All samples were then recovered from the vials using the magnetic rod and then washed three times with distilled water. The final residue was transferred into a 250 mL beaker and allowed to stand submerged in distilled water overnight. The supernatant was decanted carefully using pipettes and the remaining solids dried in an oven as stated previously. The final weights of the samples were recorded.

C2   RESULT

Substantial masses of magnetic materials were retrieved from all samples using magnetic separation. After washing with distilled water, there was about 0.608 g of strong magnetic materials retrieved from the control samples, while about 2.074 g of magnetic biochar related material were retrieved from the treatment sample. On average, there is about 0.062 g in excess of the added mass of the magnetic biochar due to other soil magnetic materials. Assuming the presence of an equal mass of non-biochar magnetic material in all samples, then about 72.38% of the magnetic biochar is retrieved. This compares closely to a similar result by (Han *et al.*, 2015a) where about 77% of magnetic biochar was recovered from amended sediments.

After the retrieved materials were washed with acetone, their masses dropped by 0.555 g and 0.041 g (about 91.20% and 1.97%) respectively for the non-biochar magnetic material and the magnetic biochar related materials respectively, see table C.1. Therefore, the mass of magnetic biochar retrieved less the mass of non-biochar magnetic material will be 1.979 g or about 98.97 %. However, when the solid to liquid ratio of the magnetic biochar related material was decreased during cleaning with acetone, the mass reduction increases by 0.89% and the magnetic biochar retrieved was 96.30% of the amount added to the soil. Consequently, a decrease in the mass of retrieved magnetic biochar related materials for a given volume of solvent would result in more compounds being released from the magnetic biochar. This suggests that the magnetic

biochar does not necessarily commingle with the same stuff as does the soil magnetic material and hence the recovery is between 72 to 98%. Furthermore, the process of regeneration resulted in the loss of about 14 mg per gram of pristine magnetic biochar material.

Table C1:   Biochar recovery

Sample	Mass recovered after washing with distilled water (g)	Vol of acetone for cleaning (mL)	Mass after cleaning with acetone (g)
Soil only	0.608	10	0.054
Soil + magnetic biochar	2.074	30	2.033
Soil + magnetic biochar*	2.038	35	1.979
Magnetic biochar	1.000	20	0.987

Magnetised activated carbon and biochar has been studied as potential sorbents in the removal of micropollutants from wastewater and contaminated soil. Substantial retrieval (72.38%) of magnetic biochar added as 1.2% to agricultural soil was recorded. This is regarded as a conservative estimate since the actual material that was retrieved is in the range of 98%. However, we could not ascertain the exact nature of stuff from the soil that got commingled with the added MBC. Furthermore, the magnetic material that was of soil origin showed outstanding loss in mass after washing with acetone compared to that recorded in the retrieved MBC. Therefore, it is more likely that the actual amount that can possibly retrieved is within the upper limit. This can be confirmed if the entire process is optimised and the composition of the retrieved MBC is thoroughly characterised.